Vol. 60 DECEMBER, 1956 No. 12

THE JOURNAL OF PHYSICAL CHEMISTRY

(Registered in U. S. Patent Office)

CONTENTS

John E. Benson and Takao Kwan: Kinetics and Mechanism of the Hydrogenation of Cyclopropane over a Nickel-Silica-Alumina Catalyst 1601

J. H. Singleton: Hydrogen Sorption and the Parahydrogen Conversion on Evaporated Nickel Films 1606

Thor A. Bak: A Minimum-Principle for Non-equilibrium Steady States. II 1611

Charles M. Huggins and George C. Pimentel: Systematics of the Infrared Spectral Properties of Hydrogen Bonding Systems: Frequency Shift, Half Width and Intensity 1615

Ignacio Tinoco, Jr., and William C. Hammerle: The Influence of an External Electric Field on the Optical Activity of Fluids 1619

Joseph A. Schufle and Carl D'Agostino, Jr.: The Stability of Thallium(I) Citrate Complex 1623

Joseph J. Jasper and T. Donald Wood: The Surface Pressure of Soluble Benzoic Acid Films at Water-Halobenzene Interfaces 1625

Prasom Sthapitanonda and John L. Margrave: Kinetics of Nitridation of Magnesium and Aluminum 1628

George I. Loeb and Harold A. Scheraga: Hydrodynamic and Thermodynamic Properties of Bovine Serum Albumin at Low *p*H 1633

Alfred P. Mills and Warren E. Becker: The Silicon-Bromine and Silicon-Carbon(Aryl) Bond Parachors and the Silicon-Bromine Bond Refraction 1644

Leroy E. Alexander and Elmer C. Sommer: Systematic Analysis of Carbon Black Structures 1646

Motoo Yasuda, Keinosuke Suzuki and Kazao Yamasaki: Stability of Copper and Nickel Chelates of Some Phthalic Acid Derivatives 1649

Robert R. Mod, Frank C. Magne and Evald L. Skau: Binary Freezing-Point Diagrams for Palmitic Acid with a Series of Substituted 2-Aminopyridines 1651

John S. Wollam and W. E. Wallace: A Comparison of Pycnometric and X-Ray Densities for the Sodium Chloride-Sodium Bromide and Potassium Chloride-Potassium Bromide Systems 1654

Marvin H. Winkler: An Experimental Investigation of Some Models for Optical Activity 1656

NOTES: **R. E. Rundle:** Methyl Compounds of the Elements 1659

Alvin W. Baker: Intermolecular Association of Carbonyl Compounds 1660

A. M. Armstrong, J. Halpern and W. C. E. Higginson: The Reaction between Mercury(I) and Thallium(III) in Aqueous Solution: Evidence for the Dismutation of Hg_2^{++} 1661

William F. Linke and Jerome A. Cooper: The System Sodium Sulfate-Sodium Molybdate-Water at 35 and 100° 1662

Arthur Lindenbaum and Jack Schubert: Binding of Organic Anions by Serum Albumin 1663

J. A. Magnuson and J. H. Wolfenden: Hydrogen Tri-iodide 1665

H. E. Moran, Jr.: System Lithium Chloride-Water 1666

Motoo Yasuda, Kozo Sone and Kazuo Yamasaki: Stability of Zinc and Cadmium Complexes with Some Methyl Derivatives of 1,10-Phenanthroline and 2,2′-Bipyridine 1667

F. H. Westheimer and Lloyd L. Ingraham: The Entropy of Chelation 1668

THE JOURNAL OF PHYSICAL CHEMISTRY

(Registered in U. S. Patent Office)

W. ALBERT NOYES, JR., EDITOR

ALLEN D. BLISS
ASSISTANT EDITORS
ARTHUR C. BOND

EDITORIAL BOARD

R. P. BELL
R. E. CONNICK
R. W. DODSON
PAUL M. DOTY
JOHN D. FERRY
G. D. HALSEY, JR.
J. W. KENNEDY
S. C. LIND
H. W. MELVILLE
E. A. MOELWYN-HUGHES
R. G. W. NORRISH

Published monthly by the American Chemical Society at 20th and Northampton Sts., Easton, Pa.

Entered as second-class matter at the Post Office at Easton, Pennsylvania.

The *Journal of Physical Chemistry* is devoted to the publication of selected symposia in the broad field of physical chemistry and to other contributed papers.

Manuscripts originating in the British Isles, Europe and Africa should be sent to F. C. Tompkins, The Faraday Society, 6 Gray's Inn Square, London W. C. 1, England.

Manuscripts originating elsewhere should be sent to W. Albert Noyes, Jr., Department of Chemistry, University of Rochester, Rochester 20, N. Y.

Correspondence regarding accepted copy, proofs and reprints should be directed to Assistant Editor, Allen D. Bliss, Department of Chemistry, Simmons College, 300 The Fenway, Boston 15, Mass.

Business Office: Alden H. Emery, Executive Secretary, American Chemical Society, 1155 Sixteenth St., N. W., Washington 6, D. C.

Advertising Office: Reinhold Publishing Corporation, 430 Park Avenue, New York 22, N. Y.

Articles must be submitted in duplicate, typed and double spaced. They should have at the beginning a brief Abstract, in no case exceeding 300 words. Original drawings should accompany the manuscript. Lettering at the sides of graphs (black on white or blue) may be pencilled in and will be typeset. Figures and tables should be held to a minimum consistent with adequate presentation of information. Photographs will not be printed on glossy paper except by special arrangement. All footnotes and references to the literature should be numbered consecutively and placed in the manuscript at the proper places. Initials of authors referred to in citations should be given. Nomenclature should conform to that used in *Chemical Abstracts*, mathematical characters marked for italic, Greek letters carefully made or annotated, and subscripts and superscripts clearly shown. Articles should be written as briefly as possible consistent with clarity and should avoid historical background unnecessary for specialists.

Notes describe fragmentary or less complete studies but do not otherwise differ fundamentally from Articles. They are subjected to the same editorial appraisal as are Articles. In their preparation particular attention should be paid to brevity and conciseness.

Communications to the Editor are designed to afford prompt preliminary publication of observations or discoveries whose value to science is so great that immediate publication is imperative. The appearance of related work from other laboratories is in itself not considered sufficient justification for the publication of a Communication, which must in addition meet special requirements of timeliness and significance. Their total length may in no case exceed 500 words or their equivalent. They differ from Articles and Notes in that their subject matter may be republished.

Symposium papers should be sent in all cases to Secretaries of Divisions sponsoring the symposium, who will be responsible for their transmittal to the Editor. The Secretary of the Division by agreement with the Editor will specify a time after which symposium papers cannot be accepted. The Editor reserves the right to refuse to publish symposium articles, for valid scientific reasons. Each symposium paper may not exceed four printed pages (about sixteen double spaced typewritten pages) in length except by prior arrangement with the Editor.

Remittances and orders for subscriptions and for single copies, notices of changes of address and new professional connections, and claims for missing numbers should be sent to the American Chemical Society, 1155 Sixteenth St., N. W., Washington 6, D. C. Changes of address for the *Journal of Physical Chemistry* must be received on or before the 30th of the preceding month.

Claims for missing numbers will not be allowed (1) if received more than sixty days from date of issue (because of delivery hazards, no claims can be honored from subscribers in Central Europe, Asia, or Pacific Islands other than Hawaii), (2) if loss was due to failure of notice of change of address to be received before the date specified in the preceding paragraph, or (3) if the reason for the claim is "missing from files."

Subscription Rates (1956): members of American Chemical Society, \$8.00 for 1 year; to non-members, \$16.00 for 1 year. Postage free to countries in the Pan American Union; Canada, \$0.40; all other countries, \$1.20. \$12.50 per volume, foreign postage \$1.20, Canadian postage \$0.40; special rates for A.C.S. members supplied on request. Single copies, current volume, \$1.35; foreign postage, \$0.15; Canadian postage \$0.05. Back issue rates (starting with Vol. 56): \$15.00 per volume, foreign postage \$1.20, Canadian, \$0.40; \$1.50 per issue, foreign postage \$0.15, Canadian postage \$0.05.

The American Chemical Society and the Editors of the *Journal of Physical Chemistry* assume no responsibility for the statements and opinions advanced by contributors to THIS JOURNAL.

The American Chemical Society also publishes *Journal of the American Chemical Society*, *Chemical Abstracts*, *Industrial and Engineering Chemistry*, *Chemical and Engineering News*, *Analytical Chemistry*, *Journal of Agricultural and Food Chemistry* and *Journal of Organic Chemistry*. Rates on request.

(Continued from first page of cover)

Bernard M. Mitzner: Infrared Absorption Cell for the Study of Heterogeneous Reactions 1670
Additions and Corrections 1671
Author Index 1675
Subject Index 1685

THE JOURNAL OF
PHYSICAL CHEMISTRY

(Registered in U. S. Patent Office) (© Copyright, 1957, by the American Chemical Society)

VOLUME 60 JANUARY 8, 1957 NUMBER 12

KINETICS AND MECHANISM OF THE HYDROGENATION OF CYCLOPROPANE OVER A NICKEL-SILICA-ALUMINA CATALYST

By John E. Benson[1] and Takao Kwan[2]

Frick Chemical Laboratory, Princeton University, Princeton, N. J.

Received April 5, 1956

The hydrogenation of cyclopropane has been investigated by a static method over a commercial nickel–silica–alumina isomerization catalyst between 56 and 100°. At 75° the rate expression for the reaction is $-dp/dt = kp_{C_3H_6}{}^{0.3}/p_{H_2}{}^{0.1}$, with an activation energy of 15.2 kcal./mole. Adsorption isotherms were determined for hydrogen between 0 and 400°, and for cyclopropane at 0 and 32.3°. By assuming the rate-determining step in the catalytic hydrogenation to be the reaction between adsorbed cyclopropane and an adsorbed hydrogen atom, the observed kinetic law has been interpreted in a manner consistent with the adsorption data. The reaction of the catalyst with carbon monoxide was investigated, and the chemical nature of the catalyst is discussed briefly.

Ciapetta and Hunter[3] found that silica–alumina containing *ca.* 5% nickel effectively catalyzes the isomerization of saturated hydrocarbons under high pressures (25 atm.) in the presence of hydrogen. It was suggested that the isomerization activity is due to compound formation between the nickel and hydrous aluminum silicate. However, hydrocracking is the primary reaction at atmospheric pressure, a result that suggests that the isomerization activity is due largely to the experimental circumstances. The present research was undertaken to investigate the nature of this commercial isomerization catalyst under laboratory conditions in order to compare its properties with those of other supported nickel catalysts. In this paper we report the kinetics and mechanism of the hydrogenation of cyclopropane and also some adsorption characteristics of this complex catalyst.

Experimental

Materials.—The catalyst used in this work was the one designated by Ciapetta and Hunter[3a] as SA-5N-VII-D and was supplied by The Atlantic Refining Company. Cylinder cyclopropane and propane from The Matheson Company were purified by pumping on the solid and subsequent fractional distillation. In the hydrogenation studies, cylinder hydrogen was purified by passage through charcoal, calcium chloride, palladized asbestos at 300°, ascarite, magnesium perchlorate and a liquid nitrogen trap. For the adsorption measurement, the hydrogen was further purified by diffusion through a palladium thimble. Oxygen and iron carbonyl were removed from cylinder carbon monoxide by passage over activated copper turnings at 400°; water and carbon dioxide were removed by magnesium perchlorate and ascarite, and a final drying was effected by a Dry Ice–acetone trap. The silica–alumina was from the Davison Chemical Co.

Apparatus and Procedure.—A U-type Vycor-glass tube connected with a buret, a mercury manometer and a high vacuum line was used for the adsorption measurements. A sample of the nickel–silica–alumina catalyst was placed in the middle of the U-tube and reduced by the standard activation technique used by Ciapetta and Hunter,[3a] *i.e.*, at 530° for 16 hours with a hydrogen flow rate of 6 liters/hour. After degassing the catalyst at 530° for 3 hours, a known volume of adsorbate was introduced into the catalyst vessel, which was kept at a desired temperature by means of an electric furnace or by a suitable constant temperature bath. The pressure of the gas in the adsorption vessel was read manometrically after a certain time of contact. The adsorbed amounts were determined from a knowledge of the dead space volume (approximately 60 cc.) for helium. A 10-g. sample of catalyst was used for hydrogen adsorption; in the cyclopropane adsorption work 3 g. of the catalyst that had been used for hydrogen adsorption were employed.

A cylindrical Pyrex reaction vessel of 211 cc. was used for the hydrogenation of cyclopropane. This reactor was connected with a capillary manometer and a high vacuum line and was equipped with a thermocouple well. The entire reaction volume could be enclosed by a removable jacket in which organic liquids were boiled to control the temperature. Mixtures of hydrogen and cyclopropane, prepared and mixed with a Töpler pump, were introduced into the reactor, and pressure readings were taken. The volume change due to hydrogenation was negligible compared with the total volume of the vessel. A 0.2-g. catalyst sample, reduced *in situ* by the standard technique, was found suitable for the measurement of the reaction rates under the experimental conditions.

---

[1] Department of Chemistry, The Pennsylvania State University, University Park, Penna.

[2] Research Institute for Catalysis, Hokkaido University, Sapporo, Japan.

[3] (a) F. G. Ciapetta and J. B. Hunter, *Ind. Eng. Chem.*, **45**, 147 (1953); (b) **45**, 155 (1953); (c) F. G. Ciapetta, *ibid.*, **45**, 159 (1953); (d) **45**, 162 (1953).

For the reaction of the catalyst with carbon monoxide a 1.90-g. catalyst sample, contained in a Pyrex tube equipped with a pre-heating coil, was reduced *in situ* by the standard technique and then treated with purified carbon monoxide at 50° for 84 hours. A flow rate of carbon monoxide of approximately 200 cc./min. was used. The resulting nickel carbonyl was decomposed at 300° in a weighed Pyrex tube equipped with a pre-heating coil and with standard taper joints to facilitate its removal.

The unreduced catalyst was analyzed for nickel by dissolving 0.5-g. samples in hydrofluoric acid and a few drops of sulfuric acid, evaporating to remove silica, complexing the aluminum as the tartrate, and precipitating nickel dimethylglyoxime.

Experimental Results

Adsorption of Hydrogen.—In order to see the extent of reduction, the catalyst, prepared by the standard activation technique, was allowed to contact with hydrogen for two weeks at 530° in a closed system. It was found that the pressure of hydrogen decreased slowly over this period. It was presumed that complete reduction was unattainable under the standard technique used, although the magnitude of the final static reduction indicated the catalyst was already more than 99% reduced. Regardless of the possibly incomplete reduction, the rate of hydrogen adsorption was immeasurably fast and reversible between 0 and 300°.

Adsorption isotherms were determined on this catalyst at 0, 100, 200 and 300° and at equilibrium pressures from a few mm. up to 800 mm. The results are shown in Fig. 1 by the solid lines.

After the above measurements the catalyst was reduced in hydrogen at 600° for 16 hours. No further static reduction could be detected in this case. Adsorption isotherms were also determined on this highly reduced catalyst at 0, 100, 200, 300 and 400° and at equilibrium pressures from a few mm. up to 900 mm. The results are shown in Fig. 1 by the dotted lines.

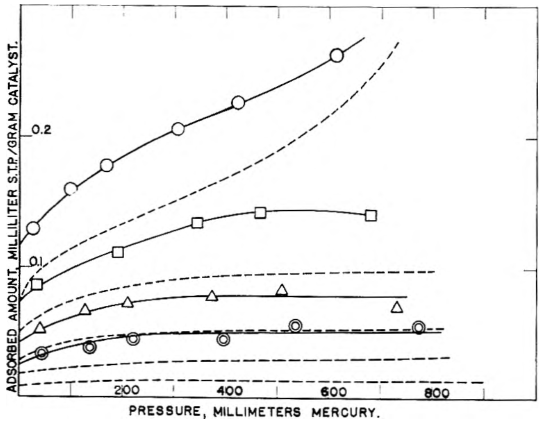

Fig. 1.—Adsorption isotherms of hydrogen on nickel–silica-alumina: full lines, catalyst reduced at 530°; ○, 0°; □, 100°; △, 200°; ◎, 300°; dotted lines: catalyst reduced at 600°.

The adsorption of hydrogen increased very slightly with increasing pressure except at 0°, where the isotherm was more or less concave upwards. The exponents of the pressure from the Freundlich equation, which approximately expressed all the isotherms, are given in Table I for the catalyst reduced at 530°, together with the corresponding exponents for reduced nickel[4] and for nickel–silica.[5]

The difference in adsorption activity for hydrogen between nickel–silica and nickel-silica–alumina would indicate a marked difference in these catalysts. Schuit and deBoer report that, at 100 mm. and −78°, nickel–silica adsorbs 27.5 cc. of hydrogen per gram of nickel, a value assumed to be near saturation. This corresponds to a Ni:H ratio of 7:1. On nickel–silica–alumina, saturation by hydrogen was not attained under the experimental conditions; however, for convenience the adsorbed amount at 760 mm. and 0° will be taken as the adsorption activity. This was only 7.5 cc. of hydrogen per gram of nickel, or a Ni:H ratio of 25:1. The large difference in adsorption activity indicates a poor dispersion of nickel in the nickel–silica–alumina catalyst.

It was difficult to obtain isosteric heat data over the entire range of coverage because of the flatness of the adsorption isotherms. However, a few numerical data are given in Table II. While the heat values do not differ from the current heat data for hydrogen adsorption on nickel, the decline of the heat of adsorption with adsorbed amounts seems more pronounced.

TABLE I

EXPONENTS FROM THE FREUNDLICH EQUATION (FOR HYDROGEN ADSORPTION)

Catalyst	Nickel–silica–alumina	Nickel[4]	Nickel–silica[5] (29.4% Ni–CLA 8281)
Equil. pressures, mm.	2–800	~1	10^{-1}–100
Temp., °C.			
0	0.22	..	0.02
100	.15	0.07	..
200	.16	.12	.13
300	.18	.24	...
400	..	..	.24

TABLE II

ISOSTERIC HEAT DATA

	Adsorbed amounts, cc. S.T.P./g. catalyst	Heat of adsorption, kcal./mole
530° Reduction	0.056	16
	.089	11
	.15	6
600° Reduction	.022	27
	.056	16
	.071	7

Adsorption of hydrogen presumably occurs on the silica–alumina support also, since Guenther[6] found that activated adsorption of hydrogen occurs on silica–alumina between 300 and 500° and since the carbonyl formation experiment indicates the nickel is not in chemical combination with the support (see later section).

Adsorption of Cyclopropane.—A 3-g. sample of the catalyst used for the hydrogen adsorption was oxidized in air and re-reduced under the standard activation technique. No static reduction was performed. Cyclopropane adsorption was measured at 0 and 32.3°. At these temperatures the

---

(4) T. Kwan, *J. Research Inst. Catalysis, Hokkaido Univ.*, **1**, 81 (1949).

(5) G. C. A. Schuit and N. H. deBoer, *Rec. trav. chim.* **72**, 909 (1953).

(6) H. W. Guenther, Ph.D. Thesis, Princeton University, 1946.

adsorption was quick and practically complete in 10 minutes, after which an extremely slow process occurred that was barely detectable after 30 minutes. At 100° this slow process occurred at an appreciable rate with the formation of no uncondensable gas at liquid nitrogen temperature. Mass spectrometric analysis of the gaseous products resulting from the adsorption of cyclopropane at 74° on a 2.3-g. sample of the silica–alumina support showed the presence of ethylene, propylene and benzene. Between 150 and 200° decomposition of cyclopropane set in.

Consequently, adsorption isotherms were determined at 0 and 32.3°. The pressure in the adsorption vessel after 10 minutes was taken as the equilibrium pressure. The data are given in Table III. Log-log plots of these data gave fairly good straight lines with the slopes given in Table IV. The slope at 75°, which will be used in the discussion, was obtained by assuming a linear relationship between the slope and $1/T$, a procedure generally accepted as valid.[7] The isosteric heat of adsorption ranged from 8.8 to 7.0 kcal./mole under the conditions investigated.

TABLE III

CYCLOPROPANE ADSORPTION DATA

Pressure, mm.	Adsorbed amounts, cc. S.T.P./g. catalyst	Pressure, mm.	Adsorbed amounts, cc. S.T.P./g. catalyst
Temp., 0°		Temp., 32.3°	
5	1.24	13.8	0.8
22	3.06	73.0	2.47
58	5.82	145	4.12
230	13.0	263	5.23
		413	7.8

TABLE IV

EXPONENTS FROM THE FREUNDLICH EQUATION (FOR CYCLOPROPANE ADSORPTION)

Temp., °C.	0	32.3	(75)
Slope	0.64	0.67	(0.70)

Hydrogenation of Cyclopropane.—Preliminary experiments indicated a slow poisoning of the catalyst during the hydrogenation experiments, and a reactivation technique, which consisted of cleaning the catalyst surface with hydrogen at 350° for one hour followed by pumping for one-half hour at the reaction temperature, was worked out. This schedule of pre-treatment was used between each run.

Propane was shown to be the only product of the reaction by a mass spectrometric analysis of the products from a run made at 74° in which the reaction was allowed to go to completion. A 2.3-g. sample of the silica–alumina support showed negligible hydrogenation activity at 74°.

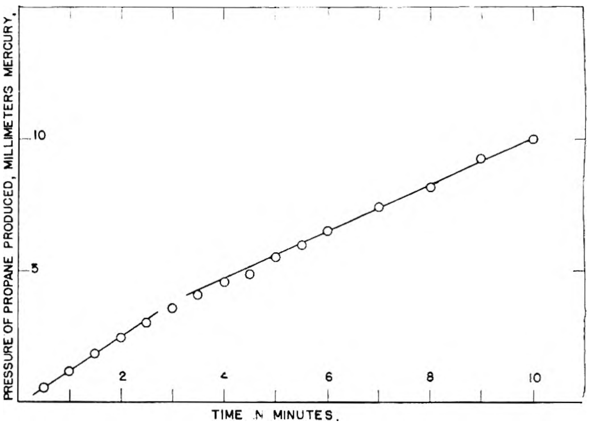

Fig. 2.—Typical rate of hydrogenation of cyclopropane on nickel–silica–alumina; temp., 75°.

The initially measured rates were complicated by the superposition of the rate of hydrogenation and of a secondary process. This is shown clearly in Fig. 2, an example of the type of data obtained. This secondary process was undoubtedly the same as the slow process observed after the initially very rapid adsorption of cyclopropane at 100° (see above) and involved adsorption of cyclopropane on the support. From plots similar to Fig. 2, however, it was shown that the effect of this process extended over only the first three or four minutes of a run, after which it could no longer be detected. The activation energy and kinetics were thus determined from slopes of pressure–time plots taken at 10 and 25% apparent reaction, respectively.

For the determination of the activation energy of the hydrogenation reaction equimolar mixtures of the reactants at about 200 mm. total pressure were used. The data, listed in Table V, gave an activation energy of 15.2 kcal./mole.

TABLE V

VARIATION OF REACTION VELOCITY, v, WITH TEMPERATURE

Total pressure, mm.	Temp., °C.	Log v (10%)
197.5	73.3	−0.155
207.1	56.0	− .682
236.7	100.0	+ .528
182.0	81.0	+ .053
200.0	73.5	− .167
199.8	64.8	− .398
196.4	91.5	+ .352
207.7	64.8	− .342

In Table VI are given the data for the determination of the kinetics. The small variation in the temperature was shown by calculation not to affect the reaction rates to a measurable extent. The rate equation

$$v = kp_C^f p_H^g$$

where the subscripts C and H refer to cyclopropane and hydrogen, respectively, was used to write a set of simultaneous equations

$$0 = \log k + f \log p_C + g \log p_H - \log v$$

that were then solved by the method of least squares[8] for the specific rate constant k and the exponents f and g. The resulting kinetic expression was

$$v = 0.327 p_C^{0.3} p_H^{-0.1} \qquad (1)$$

The sum of the residuals and the sum of the squares of the residuals were 0.000 and 0.004, respectively. Although the initial rates were difficult to analyze, a similar mathematical treatment indicated that f and g had values of 0.4 and -0.1, respectively. This tends to confirm the idea of initial cyclopropane adsorption expressed above.

---

[7] See, for example, E. Cremer, *Z. Elektrochem.*, **56**, 439 (1952), and T. Kwan, THIS JOURNAL, **59**, 285 (1955).

[8] See, for example, J. B. Scarborough, "Numerical Mathematical Analysis," The Johns Hopkins Press, Baltimore, 1930, p. 363.

Propane was found not to affect the rate of reaction by three experiments performed after the catalyst had been reactivated by the standard technique. Table VII shows the experimental conditions and the results of the experiments. The reaction rates were determined at 25% conversion.

Reaction of the Catalyst with Carbon Monoxide.—Two analyses of the catalyst gave results of 3.67 and 3.72% of nickel in the unreduced catalyst. The 1.90-g. sample of unreduced catalyst that reacted with carbon monoxide thus contained 0.070 g. of nickel. The nickel resulting from the decomposition of the carbonyl weighed 0.070 g. An analysis of the support after the carbon monoxide treatment showed no nickel remaining.

TABLE VI

DATA FOR THE DETERMINATION OF THE KINETICS

Initial pressure, mm. of Cyclopropane	Hydrogen	Rate (at 25% reaction), mm./min.
Temperature = 73.3-75.5°		
106.6	106.7	0.711
157.4	157.7	.748
45.2	45.2	.604
94.9	194.0	.626
57.0	116.4	.576
99.0	300.6	.622
51.1	155.2	.560
283.5	98.3	1.00
146.3	50.7	0.942
99.6	34.6	.900
199.8	199.8	.798
101.9	101.9	.666
134.9	134.9	.700
51.6	51.6	.597
299.1	147.0	.993
196.8	96.7	.929
100.8	49.5	.845

TABLE VII

DEPENDENCE OF REACTION RATE ON PROPANE PRESSURE

Initial pressure, mm., of Cyclopropane	Hydrogen	Propane	Rate (at 25% reaction), mm./min.
Temperature = 74.5-75.0°			
49.3	49.4	26.8	0.975
49.3	49.4	64.9	.988
49.1	49.1	116.0	.938

Because of the completeness of the removal of the nickel in the catalyst, we conclude that the nickel has a high accessibility to carbon monoxide, a fact found by Schuit and deBoer[9] to be characteristic of metallic impregnation catalysts. Furthermore, the complete removal of the nickel at the low temperature of 50°, that is, under conditions commonly used for the production of carbonyls from dispersed metals, suggests that the constitution of the catalyst does not involve any extensive amount of chemical bonding between the nickel and the support, as was suggested by Ciapetta and Hunter.[3a] This conclusion is supported by the isosteric heat data given above and by magnetic susceptibility measurements made by Selwood, who reports results characteristic of nickel metal.[10]

Discussion

We shall now investigate what mechanism of the hydrogenation of cyclopropane, consistent with the observed adsorption data, most suitably accounts for the observed kinetic law (eq. 1). We assume that the hydrogenation proceeds by the following consecutive elementary reactions

$$C_3H_6 \longrightarrow C_3H_6(a) \tag{i}$$

$$H_2 \longrightarrow 2H(a) \tag{ii}$$

$$C_3H_6(a) + H(a) \longrightarrow C_3H_7(a) \tag{iii}$$

$$C_3H_7(a) + H(a) \longrightarrow C_3H_8 \tag{iv}$$

where the suffix (a) refers to the adsorbed state and $C_3H_7(a)$ to the half-hydrogenated state of cyclopropane or to the n-propyl radical.

In view of the very fast adsorption rates of the reactants, steps (i) and (ii) may be excluded as the slowest step. The surface reaction of the adsorbed species thus seems to be rate-controlling. On the basis of the Langmuir–Hinshelwood scheme, the reaction rate is given by

$$\nu = k\theta_C\theta_H = k\,\frac{b_Cp_C\sqrt{b_Hp_H}}{(1 + b_Cp_C + \sqrt{b_Hp_H})^2} \tag{2}$$

if (iii) is assumed to be the slowest step in the overall reaction. From the adsorption data reported in this paper the values for b_C and b_H may be estimated from the Langmuir isotherm. At 75°, the temperature at which the kinetics were determined, $b_C \cong 0.002$ mm.$^{-1}$ and $b_H \cong 0.01$ mm.$^{-1}$. From these b values and the pressures given in Table VI it may be shown that the cross term, $b_Cp_C\sqrt{b_Hp_H}$, introduced in writing the approximation

$$\frac{1}{1 + b_Cp_C + \sqrt{b_Hp_H}} \cong \frac{1}{1 + b_Cp_C}\cdot\frac{1}{1 + \sqrt{b_Hp_H}} \tag{3}$$

averages 10% and is small enough not to introduce any significant error.

Most adsorption isotherms are approximately expressed by either the Langmuir or the Freundlich equation when the range of pressure is not large. This situation holds sufficiently for the present adsorption data that we may write

$$\frac{b_Cp_C}{1 + b_Cp_C} \cong (b_Cp_C)^m \tag{4 m}$$

$$\frac{\sqrt{b_Hp_H}}{1 + \sqrt{b_Hp_H}} \cong (b_Hp_H)^n \tag{4 n}$$

where $0 < m < 1$ and $0 < n < 1$. The values of m and n have already been given in Tables I and IV. At a temperature of 75°, where the kinetic law was obtained, m is 0.70 and n would be between 0.22 (0°) and 0.15 (100°). Consequently, we obtain the relations

$$\frac{1}{1 + b_Cp_C} = (b_Cp_C)^{m-1} = (b_Cp_C)^{-0.3} \tag{5}$$

$$\frac{1}{1 + \sqrt{b_Hp_H}} = (b_Hp_H)^{n-0.5} = (b_Hp_H)^{(-0.35)\sim(-0.3)} \tag{6}$$

From equations 2, 3, 5 and 6 it follows immediately that

---

[9] G. C. A. Schuit and N. H. deBoer, *J. chim. phys.*, **51**, 482 (1954).

[10] P. W. Selwood, private communication to Hugh Taylor.

$$\nu = k(b_{\mathrm{C}}p_{\mathrm{C}})^{0.4}(b_{\mathrm{H}}p_{\mathrm{H}})^{(-0.1)\sim(-0.2)} = k' \frac{p_{\mathrm{C}}^{0.4}}{p_{\mathrm{H}}^{0.1\sim0.2}} \quad (7)$$

Eq. 7 is very close to the observed kinetic law. A similar investigation of the kinetics with the assumption that (iv) is the slowest step results in a kinetic expression where the rate is proportional to $p_{\mathrm{C}}^{1}p_{\mathrm{H}}^{0.4}$, entirely different from eq. 1.

In studying the hydrocracking of ethane on fused iron catalysts Cimino, Boudart and Taylor[11] found a variety of reaction orders, depending on the amounts of potash added. It was shown, however, that these reaction orders could satisfactorily be summarized by the expression

$$v = kp^{n}{}_{\mathrm{C_2H_6}}p_{\mathrm{H}}{}^{\left(1 - n\frac{6-x}{2}\right)} \quad (8)$$

Equation 8 was obtained by assuming the slowest step to be the breaking of a C–C bond in an adsorbed dehydrogenated radical through an attack by molecular hydrogen, thus

$$\mathrm{C_2H}_x(\mathrm{a}) + \mathrm{H_2} \longrightarrow \mathrm{CH}_y + \mathrm{CH}_z$$

It is evident that the hydrogen exponent of eq. 8 depends on the variable parameter x and also on the form of the attacking hydrogen.

The application of eq. 8 to our system gives the observed kinetic law if x is taken as 2 or 3 and if atomic hydrogen is assumed to be the agent for breaking the C–C bond. Thus we have

$$v = kp_{\mathrm{C}}^{0.3}p_{\mathrm{H}}{}^{\left(0.5 - 0.3\frac{6-(2\sim3)}{2}\right)} = kp_{\mathrm{C}}^{0.3}p_{\mathrm{H}}{}^{+0.05\sim-0.1} \quad (9)$$

The present mechanism is consistent with that proposed by Bond and Turkevich[12] and by Bond and Sheridan,[13] who studied the same reaction with deuterium over pumice-supported Ni, Pd and Pt catalysts and suggested that a gaseous cyclopropane molecule in collision with an adsorbed deuterium atom may react to form either an adsorbed n-propyl radical or an adsorbed cyclopropyl radical and a molecule of HD. It should be noted, however, that the kinetic law on nickel–silica–alumina is different from that on the pumice-supported metals studied by Bond, *et al.*, in that the latter is first order with respect to cyclopropane and zero order with respect to hydrogen. This difference again might suggest that, in contrast with pumice-supported nickel, nickel–silica–alumina is a poor catalyst for adsorbing hydrogen. High pressures would be required to cover the entire active surface of the nickel–silica–alumina with hydrogen, and it is under these conditions that Ciapetta and Hunter[3a] find that hydrocarbons undergo isomerization rather than cracking.

It is interesting to note that the non-catalyzed isomerization of cyclopropane to form propylene, according to Slater,[14] is initiated when the vibrations of the molecule carry any hydrogen atom too near a carbon atom of another methylene group, followed by C–C bond rupture. We found that on the catalyzing surface the interaction of an adsorbed hydrogen atom with an adsorbed cyclopropane molecule is the most difficult step in the overall hydrogenation reaction. The readily occurring hydrogenation of propylene compared with cyclopropane on a nickel catalyst, as reported by Willstätter and Bruce[15] and also by Corner and Pease,[16] is thus readily understandable.

According to the absolute rate theory, the rate expression for a surface bimolecular reaction such as eq. 2 is given by[17]

$$v = \frac{kT}{h} G \frac{q^*}{q_{\mathrm{C}}q_{\mathrm{H}}} \frac{q_{\mathrm{C}}\dfrac{N_{\mathrm{C}}}{Q_{\mathrm{C}}}q_{\mathrm{H}}\sqrt{\dfrac{N_{\mathrm{H}}}{Q_{\mathrm{H}}}}}{\left(1 + q_{\mathrm{C}}\dfrac{N_{\mathrm{C}}}{Q_{\mathrm{C}}} + q_{\mathrm{H}}\sqrt{\dfrac{N_{\mathrm{H}}}{Q_{\mathrm{H}}}}\right)^2} \quad (1)$$

where G is the number of active sites per cm.², q_{C} and q_{H} the partition functions of the adsorbed species, q^* the partition function of the activated complex, Q_{C} and Q_{H} the partition functions of the gaseous molecules in unit volume, and N_{C} and N_{H} the concentrations of the gaseous molecules.

The conventional transformation of eq. 10 into power form, as has been performed by the Langmuir kinetics, yields

$$v = \frac{kT}{h} Ge^{-E/RT} \frac{(N_{\mathrm{C}}/Q_{0\mathrm{C}})^{0.4}}{(N_{\mathrm{H}}/Q_{0\mathrm{H}})^{0.1}} \quad (11)$$

where E is the activation energy for the reaction, 15.2 kcal./mole, and $Q_{0\mathrm{C}}$ and $Q_{0\mathrm{H}}$ the parts of the partition functions other than exponential terms, obtainable from the spectroscopic data.[18]

The observed rate is of the order of 10^{12} molecules/sec. cm.² at 75° and at a total pressure of 200 mm. for an equimolar mixture. The surface area value of 280 m.²/g., determined by the B.E.T. method for the similar catalyst SA-5N-VII,[3(a)] was used. The rate calculated from eq. 11 was found to be roughly 10^3 times larger than the observed one if we take $G = 10^{15}$. In the calculation, the entropy difference between the adsorbed state and the activated state was, as is usual, neglected. Since an adsorbed n-propyl radical is presumably adsorbed more tightly than adsorbed cyclopropane, it is to be expected that the activated state would be strongly adsorbed on the surface to a considerable extent. Thus a loss in entropy due to the formation of the activated complex would be anticipated. The discrepancy between the observed and calculated values should be ascribed to both G and the entropy factor.

Acknowledgments.—This work was a part of a program of research supported by the Office of Naval Research N6onr-27018 on Solid State Properties and Catalytic Activity. The advice and assistance of Dean Hugh Taylor and the helpful discussions with the other workers in the project are also gratefully acknowledged. One of us (T.K.) is grateful for the aid from the Fulbright/Smith-Mundt Program.

---

(11) A. Cimino, M. Boudart and H. S. Taylor, THIS JOURNAL, **58**, 796 (1954).

(12) G. C. Bond and J. Turkevich, *Trans. Faraday Soc.*, **50**, 1335 (1954).

(13) G. C. Bond and J. Sheridan, *ibid.*, **48**, 713 (1952).

(14) N. B. Slater, *Proc. Roy. Soc.* (*London*), **A218**, 224 (1953).

(15) R. Willstätter and J. Bruce, *Ber.*, **40**, 4456 (1907).

(16) E. S. Corner and R. N. Pease, *Ind. Eng. Chem., Anal. Ed.*, **17**, 564 (1945).

(17) See, for example, Horiuti, "Catalytic Chemistry," Asakura Book Co., Tokyo, 1953.

(18) G. Herzberg, "Infrared and Raman Spectra," D. Van Nostrand Co., New York, N. Y., 1945, pp. 352, 437.

HYDROGEN SORPTION AND THE PARAHYDROGEN CONVERSION ON EVAPORATED NICKEL FILMS[1]

BY J. H. SINGLETON[2]

Department of Chemistry, University of Washington, Seattle

Received May 8, 1956

The changes in electrical resistance of an evaporated nickel film, due to the ad- and absorption of hydrogen, have been studied at −78°. Three processes have been distinguished. Initially, hydrogen is irreversibly adsorbed causing a drop in resistance. This is followed by reversible adsorption over a pressure range from 10^{-5} to at least 600 mm., causing an increase in resistance; this adsorbed hydrogen is responsible for the parahydrogen conversion. A third type of sorption occurs rapidly at room temperature and to an appreciable extent at −78°, decreasing the resistance of the film and poisoning the catalyst with respect to the parahydrogen conversion. The limitations involved in obtaining evaporated metal films of reproducible properties are discussed.

Introduction

Despite the increasing trend toward studies of simpler heterogeneous catalytic processes no satisfactory, complete theory of any reaction has been achieved. The parahydrogen conversion is possibly the simplest reaction available for study and a large number of papers have been published on this subject.[3] The adsorption of hydrogen has similarly been widely investigated on wires and evaporated films.[3,4] Despite this concentration of effort it is still impossible to progress very far in any theoretical interpretation of the results. A basic reason for this difficulty is that one cannot apply results from, say, hydrogen adsorption on a tungsten film to the kinetics on a tungsten wire, without relative surface area measurements and the knowledge that both surfaces expose identical lattice spacings.

In this work it was originally hoped to carry out parallel investigations of adsorption and reaction kinetics on clean, evaporated metal films of known relative area, prepared under identical conditions. To this end nickel was selected as a catalyst since it was readily obtainable in very pure form and had previously been extensively studied.[3,4] Evaporated films were used because the temperature control is easier than for a wire and the larger area is much less sensitive to contamination.

Experimental

A conventional high vacuum system was employed. Precautions were taken to avoid contamination by air, mercury and stopcock grease. Parahydrogen was prepared immediately before each series of experiments. Nickel wire, 0.2 mm. diameter, was obtained from Johnson, Matthey & Company, England. It was stated to contain less than 0.01% impurity.

The Measurement of the Electrical Resistance of Nickel Films.—Nickel films were prepared by evaporation, from an electrically heated filament, on to the inside wall of a 20 mm. diameter Pyrex tube. This produced a uniform film across two platinum foil electrodes, sealed in the glass wall. The resistance of the film between these electrodes was measured on a sensitive Wheatstone bridge using a galvanometer for highest accuracy, or a millivoltmeter for rapid measurements. A d.c. potential of 1.5 volts was satisfactory for most films; the current flow was reversed to check for contact resistance and thermal e.m.f. errors, but no difficulties of this nature were detected. The limit of measurement of resistance was 0.001 ohms and the bridge was self-consistent down to this limit.

The cell was connected to a sensitive Pirani gage, for low pressure measurements, and also to the mercury manometer. The lower limit of pressure sensitivity of the Pirani gage was approximately 2×10^{-6} mm. for hydrogen. The nickel film was protected from mercury vapor and grease by a U-trap, packed with glass wool and cooled in liquid nitrogen.

Evaporation Procedure.—The system was carefully outgassed before preparation of a film. Evaporation was controlled by the heating current and took from 0.5–6 minutes. The walls of the cell were cooled to 0° during the evaporation. Films from 5 to 1000 ohms resistance were readily obtained. The resistance decreased rapidly after evaporation as the film annealed. This process was accelerated by warming to 80–90° for 10–20 minutes, followed by cycling between 80 and −195°. Annealing was assumed to be complete when the resistance remained constant, at 0°.

Pressure Dependence of Resistance.—The effect of hydrogen on film resistance was studied at −78°. Doses of gas, at known volume, temperature and pressure, were admitted to the film and the resistance changes recorded up to a pressure of approximately 10^{-4} mm. At higher pressures the variation of film resistance was observed without measurement of the volume of gas adsorbed.

The Kinetics of Parahydrogen Conversion.—Catalysts were prepared by the method described above. The reaction vessel was connected by 10 mm. bore tubing to an all-glass circulating pump of the type previously described.[5] The tubes immediately adjacent to the catalyst vessels were cooled to −195° and plugs of glass wool ensured thorough mixing of the gas stream and condensation of all traces of mercury and stopcock grease vapors. The gas stream was cooled to the reaction temperature by a long glass spiral before passing over the catalyst. The rate of circulation was shown to have no effect on the kinetics of the conversion. Three or four small gas samples were removed during each run and analyzed for p-hydrogen content in a thermal conductivity gage. The data were plotted using a first-order rate equation and gave good, straight lines.

Results

Adsorption of Hydrogen at Very Low Pressures.—The initial rate of adsorption of hydrogen, at −78°, was very rapid, with a residual pressure below 2×10^{-6} mm. of mercury. Successive additions of hydrogen produced a well-defined saturation point, at which a small pressure of hydrogen was detected. The volume of hydrogen adsorbed to this point, per milligram of catalyst, will be referred to as the "*saturation*" *volume* of the catalyst. When considerable care was exercised in reproducing the conditions of catalyst preparation, the "saturation" volume was constant to ±5%. Changing these conditions gave a variation up to ±10%. For example, seven films, between 10 and 24 mg., gave an average "saturation" volume, at −78°, of $(4.5 \pm 0.9) \times 10^{-3}$ ml. mg.$^{-1}$ at S.T.P. The subsequent experiments, on the changes of

---

(1) This research was supported by Contract No. AF 18 (600)-987 of the Air Research and Development Command, Baltimore.

(2) Westinghouse Research Laboratories, Beulah Road, Pittsburgh 35, Pennsylvania.

(3) D. D. Eley, *Advances in Catalysis*, **1**, 157 (1948).

(4) O. Beeck, *ibid.*, **2**, 151 (1950).

(5) J. H. Singleton, E. R. Roberts and E. R. S. Winter, *Trans. Faraday Soc.*, **47**, 1318 (1951).

electrical conductivity with annealing conditions, show that the above films could not have been completely annealed, possibly accounting for some of the variation in adsorption.

The measurement of the change in electrical resistance of evaporated films during the initial hydrogen adsorption gave the results shown in Fig. 1. Very thin films, weighing less than 1 mg. were used, in order to obtain resistances greater than 5 ohms for accurate measurement. Because of the low "saturation" volume of hydrogen, the number of gas inlets was small, producing uncertainty in the actual volume completely adsorbed. It is clear, however, that after the "saturation" volume of the adsorption was reached, a reversal occurred in the resistance change of the films. The initial rise in resistance, with the first inlet of gas, appeared to be due to a temperature increase caused by slow dissipation of the heat of adsorption of 30 kcal. mole^{-1} on a clean nickel surface.[4] It was greatest for the thinnest films (*i.e.*, those of highest resistance; Fig. 1a). This high resistance value decreased on standing for a few minutes; the following gas inlets produced stable resistance values. The resistance change during initial adsorption was completely irreversible by prolonged evacuation at −78°.

Hydrogen Uptake at Pressures Greater Than 10^{-5} mm.—As the hydrogen pressure was increased, the resistance of the film continued to rise. The primary change was very rapid and was immediately reversed on reducing the pressure. The hydrogen adsorbed in this way was therefore readily removed. In addition to the rapid adsorption a slow sorption of gas occurred, which decreased the film resistance. The curves in Fig. 2, which were obtained on a freshly sintered film, show the effects of the two processes. The arrows give the order in which the points were taken, over a total period of one hour. By taking measurements over short time intervals it was possible to observe the resistance variation caused by the adsorption while negligible change occurred in the slow sorption.

The extent and rate of the slow sorption varied considerably with the conditions of film preparation, but our results are not extensive enough for detailed analysis. On all catalysts the rate of the sorption became very low, at −78°, after one or two hours.

The upper curve in Fig. 3 was measured on a freshly evaporated film. After leaving in contact with hydrogen, for one hour, the middle curve was obtained. Finally, the film was warmed to room temperature, producing rapid sorption of hydrogen, and cooled again to −78°; the pressure dependence followed the lower curve of Fig. 3. From this and similar films, we conclude that the displacement of the pressure dependence curves to lower resistance is due to slow sorption of hydrogen.

The rapid adsorption process gives the same *form* of curve independent of the volume of sorbed gas. It was noted that the slope of the pressure dependence, at high pressures, was greatest on a new film. A similar difference may be present in other pressure regions, but the change is only readily observed for the almost linear portion of the curves. The change indicates that sorption decreases the coverage, or pressure dependence of coverage, by the rapidly adsorbed layer.

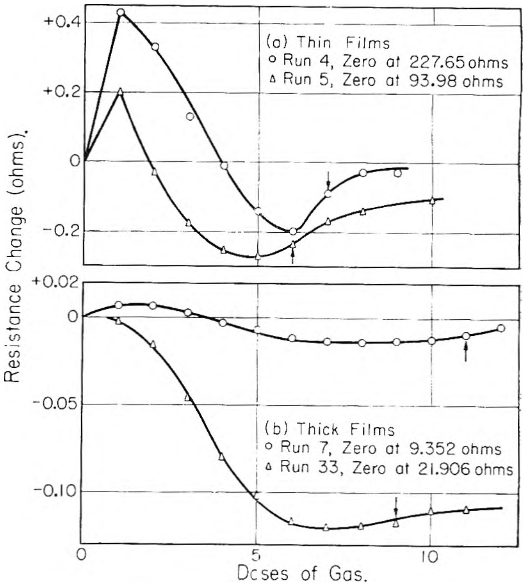

Fig. 1.—Change of film resistance with initial adsorption of hydrogen at −78°; the arrows indicate the point at which an equilibrium pressure was first detected (2×10^{-6} mm.).

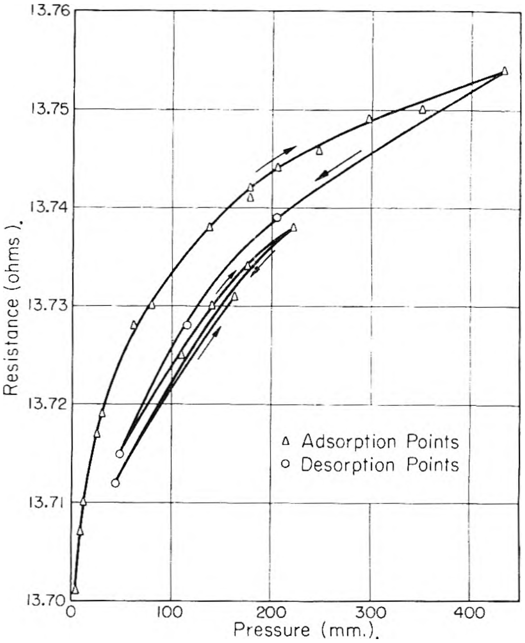

Fig. 2.—Resistance changes caused by adsorption and sorption on a freshly evaporated film at −78°.

The sorbed hydrogen was removed by evacuation at room temperature and also, at a very low rate, at −78°. Complete desorption was not attempted. The upper limit of the sorption was not investigated. A total resistance decrease of 16% was observed on one film before the process was arbitrarily stopped.

Comparison of Resistance Changes by the Three Types of Hydrogen Uptake.—The extent of these resistance changes is of interest in showing the magnitude of each phase. Results from some of

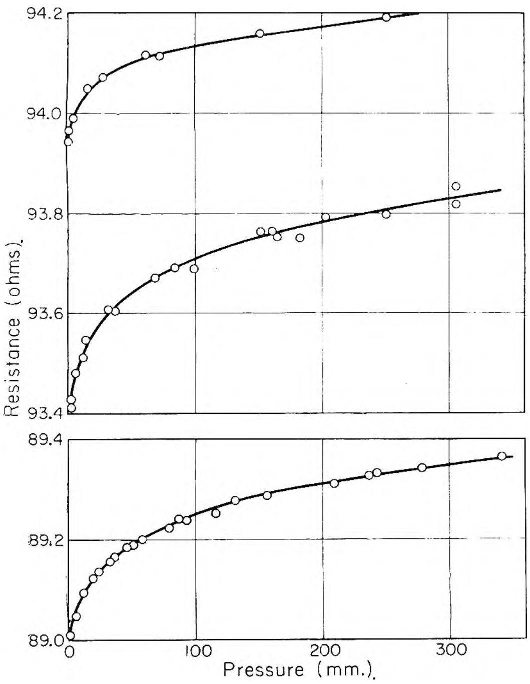

Fig. 3.—The effect of reversible adsorption of hydrogen on the film resistance, at −78°, for various degrees of hydrogen sorption. The points are adsorption and desorption measurements, taken at random.

the films are collected in Table I. The variation is shown as a percentage of the film resistance at −78° after sintering. The figures given are

A The change resulting during adsorption of the "saturation" vol.

B The resistance increment accompanying a pressure change from 100–200 ml., measured after appreciable sorption at 0°

C The resistance change due to sorption

The results in column A vary over a wide range, and thus the change in resistance is not related to the total resistance. In addition, neither the resistance *change* of column A, nor the absolute film resistance show any relation to the "saturation" volume of hydrogen adsorbed. The irregularity of the figures in column A suggests that this adsorption occurs on sites which are determined by the specific conditions of deposition of the film. The adsorption is not a simple function of the surface area.

Table I

Initial resistance (ohms)	"Saturation" vol. (ml. S.T.P.)	A	B	C
5.3	..	....	0.13	− 1.8
9.34	16.9	−0.1	.07	− 1.0
13.7	5.2	− .07	.09	− 7.0
21.8	16.9	− .6	.12	− 1.0
26.7	21.4	....	.10	− 0.4
66.1	5.7	− .4	.1	−16.0
93.8	11.3	− .25	.05	−12.0
967.2	9.0	....	.14	− 5.0

In contrast, the eight figures in column B have an average value of 0.1 and the individual deviations are relatively small, considering the 180-fold variation in absolute resistance. The reversible adsorption of hydrogen must therefore directly affect the electrical conductivity of the metal. Since the adsorption was rapid, readily reversible and occurred over a wide pressure range, it seems that for this type of adsorption, a considerable area of the metal was readily accessible to hydrogen.

It is obvious that no constant factor can be obtained in column C since the process was never continued to equilibrium. The figures show only the extent to which sorption was allowed to occur.

The Rate of Parahydrogen Conversion.—The films for resistance measurements were prepared using a wide range of evaporating conditions with the object of determining the effect of this on the various adsorption processes. By contrast, a fixed rate of evaporation was employed in each series of catalytic experiments, in order to give reproducible results. The data are collected in Table II. For runs 1 to 23 the "saturation" volume was measured at 0°, followed by sintering in the presence of hydrogen. These films contained much sorbed hydrogen when kinetic measurements were made. Catalysts 24 to 33 were sintered before measurement of the "saturation" volume and therefore were not in contact with high pressures of hydrogen prior to the kinetic runs. A different rate of film evaporation was used for the two groups of experiments.

Table II

Run	Hydrogen adsorbed (ml. S.T.P. × 10^3) 0°	−78°	Rate constant k_e (min.$^{-1}$)	Pressure (mm.)	R
1	2.1	2.4[a]	0.28	42.9	5.0
3	1.7	1.9[a]	.24	42.5	5.4
10	2.4	2.7[a]	.43	34.0	5.4
11	3.0	3.4[a]	.61	34.1	6.1
12	1.4	1.6[a]	.27	33.7	5.7
23	3.6	4.1[a]	2.05	30.0	15
24		5.4	3.76	30.3	21
25		4.1	2.72	30.0	20
26		1.8	1.04	30.0	17
27		2.3	1.48	30.2	20
33		1.7	0.90	35.0	19

[a] Calculated from measured value at 0°, using factor obtained in separate experiments.

Column 6 of Table II gives a factor R, equal to $k_e p/v$, where k_e is the initial experimental first-order rate constant, p the pressure of hydrogen and v the "saturation" volume, measured at −78°. Thus, R is proportional to the rate of reaction of hydrogen at the catalyst surface. Within the groups 1 to 12 and 24 to 33 the value of R is constant to 10%. Therefore, this method of comparison of the activity of several catalysts is satisfactory, provided standardized methods of catalyst evaporation are used. But a comparison of run 23 with the series 1 to 12 shows the great change of R for a different method of catalyst evaporation.

Runs 23 to 24 together give a comparison of the effect of hydrogen sorption on catalytic activity. Evaporated under identical condition, catalyst 24 contained little hydrogen, compared to 23, and had a higher activity. It was found that several hours exposure to hydrogen reduced the catalytic activity of all nickel catalysts by 50% or more. If such a deactivated film was outgassed at room temperature it regained a considerable portion of its catalytic efficiency.

To demonstrate that hydrogen sorption caused the loss in activity, simultaneous measurements were made of the electrical resistance change in catalysts and their activity in the parahydrogen conversion. During each kinetic measurement the resistance was measured at half-minute intervals. On a new film the initial high rate of sorption caused drift in the resistance values throughout the short period of a kinetic run. Therefore, these experiments were far from an equilibrium state and no reliance is placed on the results. After one or two runs the resistance remained constant within a half to one minute. Figure 4 shows the variation of film resistance and activity at increasing time intervals after film preparation. A standard pressure was used in these runs. Neglecting the initial non-equilibrium runs, the results show a loss of activity, paralleled by a drop in resistance, between runs 3 and 10. From the previously described experiments it is clear that slow hydrogen sorption occurred in this period.

Following experiment 10 the film was warmed to room temperature and further extensive sorption observed to occur. After cooling to $-78°$, runs 12 to 17 showed that a very considerable loss in catalytic activity accompanied the lower film resistance.

The pressure dependence of film resistance and the rate of the parahydrogen conversion were simultaneously measured on the nickel film referred to above and in Fig. 4. Runs 4 and 5 showed that the catalyst had reached an approximately constant activity and the pressure dependence of the reaction rate was determined at pressures from 10 to 120 mm. The results are plotted in Fig. 5a. The number of each run is given by the appropriate point. It is clear that some loss of activity occurred between runs 5 and 8, which were carried out using the standard procedure, but the approximate slope of the dependence is quite evident. The resistance of the films, measured simultaneously with the kinetic runs, is plotted in the upper curve of Fig. 5b. The curve exhibits the same general variation with hydrogen pressure as that for the reaction kinetics.

A further series of experiments was made on the catalyst containing a large volume of sorbed hydrogen. These runs are shown in the lower curves of Figs. 5a and 5b. It is clear that the absolute rate of reaction was very much lower and the pressure dependence was only one-tenth of that obtained when little sorbed gas was present. The resistance change also had a lower dependence on pressure, though not so marked as the rate of reaction plot. The spread of the points was much lower for both curves, compared with the previous experiments, because of the lower rate of sorption.

It is clearly not possible to draw any quantitative deductions from the curves of Fig. 5, because the experiments were not carried out under completely equilibrium conditions with respect to sorption. Also, no accurate zero can be defined for the resistance changes associated with the surface hydrogen adsorption, so the results do not permit of a quantitative comparison between the surface coverage by hydrogen and the change of resistance. In Figs. 6 and 7, a direct plot has been made between film resistance and reaction rate. The general trend is satisfactorily demonstrated in both cases.

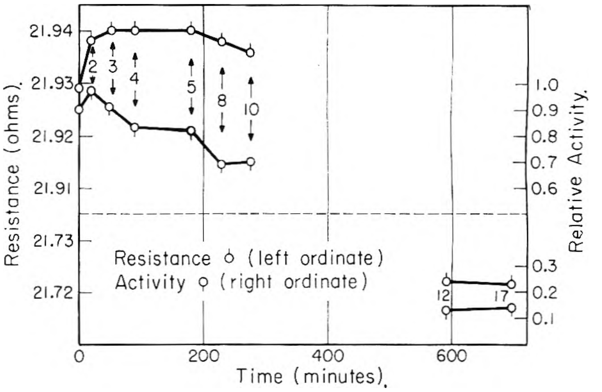

Fig. 4.—Change of catalytic activity and electrical resistance of a film with time of contact with hydrogen at $-78°$.

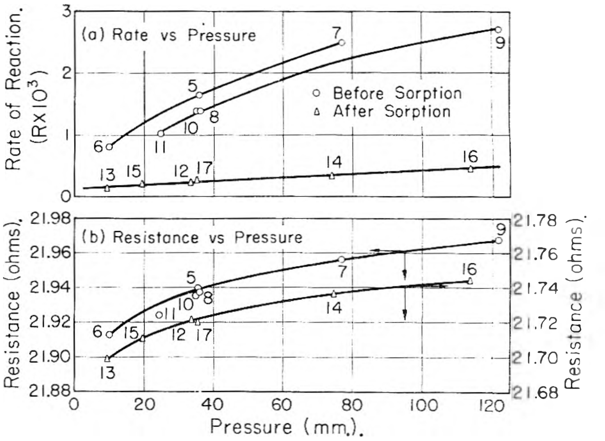

Fig. 5.—Variation of catalytic activity and electrical resistance of a film with the pressure of hydrogen, at $-78°$

Energy of Activation.—The energy of activation was determined on films containing sorbed hydrogen. In most cases the drift of activity caused by sorption, during the time taken to reach constant temperature, was too large and energies of activation could not be obtained. Only four satisfactory series of runs were achieved. Experiments in which over-all loss in activity was less than the experimental error of 5% are given in Table III. The four determinations give an average value of 1400 ± 50 cal. mole^{-1} for the energy of activation.

TABLE III

Catalyst	Hydrogen pressure (mm.)	Energy of activation (cal. mole^{-1})
1	44.0	1400
15	15.1	1380
15	34.6	1415
18	35.0	1310

Discussion

Characteristics of Evaporated Nickel Films.—Studies of evaporated films have previously emphasized a general linear relation between the weight of metal and properties such as surface area and catalytic activity. For the present system we have shown that this is true only when films are prepared under strictly comparable evaporation conditions (Table II). When the surface area is determined by the volume of hydrogen chemisorbed it will contain two terms: a volume which is irreversibly adsorbed, dependent on the method of film preparation and a volume which is reversibly adsorbed and which is active in catalysis. The two stages may not be completely independent. The films must also be annealed very thoroughly to produce an equilibrium state. The necessity for thorough annealing also has been observed by Suhrmann and Schultz[6a] and Hoffmann, Anders and Crittenden.[6b] The former workers evaporated nickel films on to glass surface at −183° and annealed the films for one hour at 110°, until the resistance decreased to a stable value. Hoffmann, *et al.*, measured the strain present in nickel films which had been evaporated on a mica backing at 70°. The films were annealed for half-hour periods at temperatures up to 300° and measurements were made of the decrease of strain in the metal. Complete annealing was not obtained until at least 200°. A decrease in resistance was observed during the process.

The actual changes occurring during annealing are not completely known. Hoffmann, *et al.*, suggest that the freshly evaporated film contains aggregates of lattice vacancies which collapse to form dislocation rings.[7] Because of the extreme conditions necessary to anneal evaporated films, it seems certain that many previous workers must have studied non-equilibrium surfaces. No data are available concerning the effect of this on adsorption and catalytic properties. The point requires investigation as a possible variable in the comparison of results of different workers.

Hydrogen Adsorption.—The adsorption at a very low pressure, up to the "saturation" point, is a distinct process from the subsequent, reversible uptake of hydrogen. The reversal of the resistance change at this point is well marked (Fig. 1). It should be noted that although Suhrmann and Schultz[6a] observed the initial decrease of film resistance, on hydrogen adsorption, they did not record any subsequent increase. It is not clear if their films were subjected to gas pressures much in excess of 10^{-3} mm., although the sorption of hydrogen at 0° is reported. One point of difference is that their work was carried out on transparent films of approximately 75 atoms thickness, compared with at least 1000 atoms in the present work.

The extent of the initial uptake of hydrogen on nickel appears to depend critically on the conditions of evaporation and therefore, probably on the defects in the metal (Table I). Such points in the lattice give rise to electron traps and, if filled by electron transfer from chemisorbed hydrogen, an increase in electrical conduction would occur.

The mechanism, by which the subsequent increase occurs, is not readily defined. There is evidence that, in the adsorption of hydrogen on a transition metal, the electron occupies a level in the d-band of the metal.[8] The relative atomic percentage of hydrogen, adsorbed by the metal, is small and would not be expected to produce any appreciable change in the number of available d-band levels. In the addition of a univalent metal to a transition metal, the electrical resistance increases with the addition of the solute, the change being associated with the increasing disorder of the alloy. While the adsorption of hydrogen by nickel also caused an increase in resistance, it is unlikely that any solid solution is involved, because of the rapid nature of ad- and desorption of the gas. It appears that the resistance changes we have measured are associated with the surface, rather than the bulk, of the metal.

A possible explanation of the resistance increase is that the contact resistance, between the metal crystallites, is varied by gas adsorption at such contacts. The results of Table I show that a given gas pressure produces the same percentage change of resistance for a wide range of film thickness. Therefore, if crystallite–crystallite contacts are the factor involved in resistance variation, we must make the unreasonable assumption that the formation of these contacts is independent of the conditions of evaporation and sintering of the film.

In measurements of the contact potential of a nickel film, Mignolet[9] observed the formation of two adsorbed hydrogen layers. These caused contact potential change of opposite sign and were ascribed to chemisorbed and van der Waals adsorbed layers. They have similar characteristics to the adsorbed layers we have described and are presumably identical with these. It is evident that the previous assumption of a single mechanism for hydrogen adsorption, from 0 to 0.1 mm. pressure, must be re-examined. Further, the distinct resistance changes indicate that the two types of chemisorption occur on different kinds of sites rather than one species having varying adsorption potential.

Because of the relatively slow change of hydrogen adsorption at pressures above 100 mm. it is extremely difficult to determine the area of nickel which is covered by chemisorption. The change of resistance is a method which possesses sufficient sensitivity to measure uptake of gas in the high pressure region.

The Sorption of Hydrogen.—Beeck[1] has described results which he interprets as showing the solution of hydrogen in nickel. These results have been discussed by Porter and Tompkins,[10] who conclude that they are explained on the basis of a single process for hydrogen uptake, occurring only on the surface. The resistance changes we have described confirm the existence of a slow sorption or solution, distinct from the reversible surface adsorption. The mechanism for the decrease in resistance caused by sorption cannot be determined from the present results. It is probable that sorption of hydrogen reduces the energy available for surface adsorption, since we have shown that the dependence of the electrical resistance of the film, on hydrogen pressure, is smaller after appreciable sorption of hydrogen by the film. The sorption of hydrogen on nickel apparently occurs by a process dif-

---

(6) (a) R. Suhrmann and K. Schultz, *Z. physik. Chem.*, **1**, 69 (1954); (b) R. W. Hoffmann, F. J. Anders and E. C. Crittenden, Jr., *J. Appl. Phys.*, **24**, 231 (1953).

(7) F. Seitz, *Advances in Physics*, **1**, 43 (1952).

(8) A. Couper and D. D. Eley, *Disc. Faraday Soc.*, **8**, 172 (1950).

(9) J. C. P. Mignolet, *ibid.*, **8**, 105 (1950).

(10) A. S. Porter and F. C. Tompkins, *Proc. Roy. Soc. (London)*, **A217**, 529, 544 (1953).

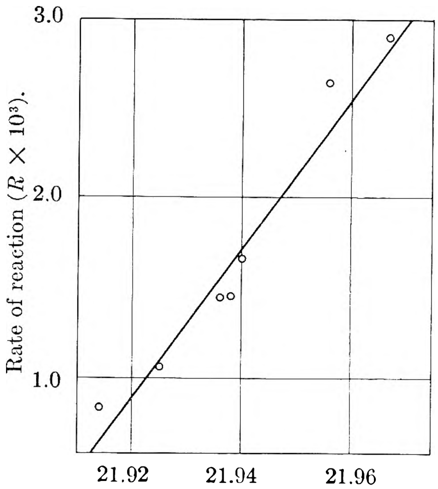

Fig. 6.—Relation between electrical resistance and catalytic activity of a film containing little sorbed hydrogen.

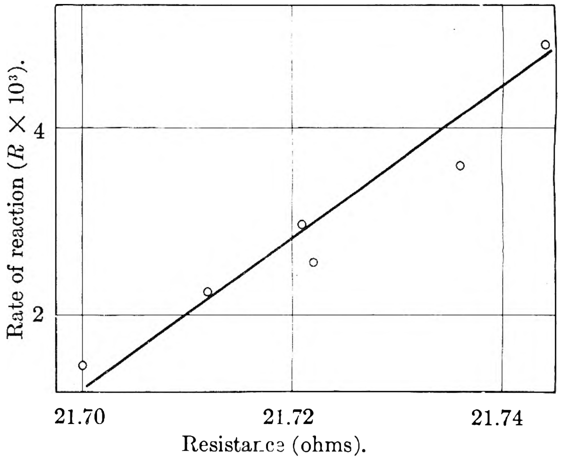

Fig. 7.—Relation between electrical resistance and catalytic activity of a film after sorbing hydrogen at room temperature.

ferent from the solution of hydrogen in palladium. For the latter system, the resistance is increased by solution of hydrogen.[8]

The Parahydrogen Conversion.—The parallel of changes of resistance and of the kinetics of conversion, with hydrogen pressure (Figs. 6, 7) is strong evidence that the same adsorbed hydrogen is responsible for both effects. Thus, the conversion proceeds through a readily desorbed layer, which is still incomplete at quite high pressures. The effect of gas pressure on the rate of conversion is to increase the concentration of hydrogen at the surface.

The results clearly show that the conversion occurs in a hydrogen layer which has a low heat of desorption. Hydrogen which is chemisorbed on the bare nickel surface with a high heat of adsorption[4] apparently does not have any direct part in the conversion. These facts are compatible with the Bonhoeffer–Farkas mechanism of parahydrogen conversion,[11] occurring on a considerable fraction of the surface and not confined to a restricted number of active sites.

The strong poisoning of the conversion by the sorption of hydrogen is similar to that previously described for palladium.[8] It appears that the poisoning mechanism is a simple reduction in the extent of surface adsorption, therefore reducing the concentration of reacting hydrogen.

Acknowledgment.—The author wishes to express his sincere thanks to Dr. G. D. Halsey, Jr., for many helpful discussions and suggestions during the course of this work.

(11) K. F. Bonhoeffer and A. Farkas, *Trans. Faraday Soc.*, **28**, 242 (1932).

A MINIMUM-PRINCIPLE FOR NON-EQUILIBRIUM STEADY STATES. II

BY THOR A. BAK*

Contribution from the Department of Chemistry, Columbia University, New York, N. Y.

Received June 15, 1956

The minimum-principle previously suggested is applied to reactions of arbitrary order and to diffusion in an external field. The connection between the function used in this principle and the dissipation function is discussed.

In a previous publication[1] the author introduced a minimum-principle for chemical reactions which can be considered a generalized formulation of Le Châtelier's principle. In this paper we shall examine this principle more closely and use it on more complicated physical situations.

It was shown previously that for one-dimensional diffusion the entropy production in the diffusion column between cross-sections at x_1 and x_2 is[2]

$$\sigma = -\frac{1}{RT}\int_{x_1}^{x_2} J\,d\mu = \int_{x_1}^{x_2}\frac{D}{c}\left(\frac{\partial c}{\partial x}\right)^2 dx = \int_{x_1}^{x_2}\frac{1}{Dc}J^2\,dx$$

in which the meaning of the symbols is

R is the gas constant
T is the temperature
J is the flow per unit cross-section of the diffusing species
μ is the chemical potential
D is the diffusion constant
c is the concentration

The entropy is measured in units of R, and the conversion from the first to the second integral can be performed, because

---

* Universitetets Fysisk–Kemiske Institut, Copenhagen, Denmark.

(1) Thor A. Bak, THIS JOURNAL, **59**, 665 (1955).

(2) In the first paper two of these expressions were given incorrectly.

$$\mu = RT \ln c + \text{const.}$$

We seek a variational principle which will characterize the time-independent state of this diffusion. Let us first consider the principle originally suggested by Prigogine: $\delta\sigma = 0$. The Euler equation is

$$-\frac{D}{c^2}\left(\frac{\partial c}{\partial x}\right)^2 - \frac{\mathrm{d}}{\mathrm{d}x}\left[2\frac{D}{c}\left(\frac{\partial c}{\partial x}\right)\right] = 0$$

or

$$-\frac{2}{c}\frac{\mathrm{d}}{\mathrm{d}x}\left[D(x)\frac{\partial c}{\partial x}\right] + D\left(\frac{1}{RT}\frac{\partial \mu}{\partial x}\right)^2 = 0$$

In order that this be the equation for time-independent diffusion, *viz.*

$$\frac{\mathrm{d}}{\mathrm{d}x}\left[D(x)\frac{\mathrm{d}c}{\mathrm{d}x}\right] = 0$$

we must have $\partial\mu/\partial x = 0$, that is, the diffusion process must have reached equilibrium.

For systems in which the time-independent state is not an equilibrium state (or very close to equilibrium) this variational principle cannot be used. However, Prigogine[3] showed that when the diffusion constant depends only on concentration, the variational principle

$$\delta\int_{x_1}^{x_2} J^2\,\mathrm{d}x = 0$$

will characterize the steady states.

It is easily verified that a similar principle also holds when the diffusion constant depends on geometrical coördinates only.[1] Here we shall investigate the case where it depends both on x and on c. When we are interested in diffusion *per se*, this is the most realistic point of view to take.

We have to construct a variational problem whose Euler equation is

$$\frac{\mathrm{d}}{\mathrm{d}x}\left[D(c,x)\frac{\mathrm{d}c}{\mathrm{d}x}\right] = 0$$

The left-hand side of this equation is not a linear differential operator operating on c, so that in general we cannot do much about it. If, however, we can write $D(c,\ x)$ as $D_1(x)\ D_2(c)$ we can introduce a new variable by

$$U = \int D_2(c)\mathrm{d}c$$

We now have to find a variational principle whose Euler equation is

$$\frac{\mathrm{d}}{\mathrm{d}x}\left[D_1(x)\frac{\mathrm{d}U}{\mathrm{d}x}\right] = 0$$

Accordingly, our variational principle reads

$$\delta\int D_1(x)\left(\frac{\mathrm{d}U}{\mathrm{d}x}\right)^2\mathrm{d}x = 0$$

Since

$$J = -D_1(x)\,D_2(c)\frac{\mathrm{d}c}{\mathrm{d}x} = D_1(x)\frac{\mathrm{d}U}{\mathrm{d}x}$$

this can also be written as

$$\delta\int D_1^{-1}(x)\,J^2\,\mathrm{d}x = 0$$

To say that $D(c,x)$ can be split into a product $D_1(x)\ D_2(c)$ implies that the dependence of the diffusion constant on concentration should be a common law for all substances in the diffusion column with only an adjustable factor $D_1(x)$.

This is certainly not generally true, but the result is nevertheless interesting because it indicates that in the case of chemical reactions—which we have previously compared to diffusion—we need not limit ourselves to considering monomolecular reactions.

It is interesting to note that the expression under the integral sign above has the form of "resistance" times flux squared, since $D_1^{-1}(x)$, the reciprocal of the geometrical factor in the diffusion constant, can be considered as a resistance against diffusion.

This resistance is a function of x, only if D depends on x. When D is constant or depends on c only, the resistance is a constant, and therefore it can be taken out of the integral in the variational principle.

Now we want to find a discrete analog to the continuous resistance $D^{-1}(x)$ as we did in the previous communication. We consider a system of chemical reactions between N species for which species i can only be converted directly into species i ± 1 (System II in the previous communication). We find the resistances R_i as the coefficients in the form

$$\Sigma R_i J_i^2$$

which makes it a minimum for stationary flux, that is, for

$$J_i = J \text{ (all i)}$$

In a simple system of first-order reactions the expressions for the fluxes are

$$J_i = w_{i,i+1}\,c_i - w_{i+1,i}\,c_{i+1}$$

Using this in the above written sum of squares and equating the derivatives with respect to c_i to zero we get

$$R_i = \frac{w_{21}w_{32}\cdot\cdot\cdot\cdot w_{i,i-1}}{w_{12}w_{23}\cdot\cdot\cdot\cdot w_{i-1,i}}\,\frac{1}{w_{i,i+1}}$$

except for an arbitrary positive factor. The R_i obtained in this way is to be compared to D^{-1} in the variational principle. Also we can see directly that it has the nature of a resistance. If we namely consider a system of discontinuous heat conduction using Newton's law of cooling we see the striking analogy to the above mentioned system of chemical reactions. And in the latter system the quantity that corresponds to R_i is the inverse of the i'th heat conductivity.[4]

We shall now consider a system of chemical reactions with arbitrary reaction orders. For the flux we may write

$$J_i = w_{i,i+1}\,c_i^{q_{i,i+1}} - w_{i+1,i}\,c_{i+1}^{q_{i+1,i}}$$

in which J_i is the flux from species i to species i + 1, the $w_{i,j}$'s are transition probabilities (or rate constants), c_i concentration and $q_{i,j}$ the power to which the concentration is raised in the kinetic equation. We now investigate whether all values of $q_{i,j}$ are permissible by forming a function

$$\sum_i r_i J_i^2$$

and requiring that this function be a minimum for the steady state, *i.e.*, for $J_i = J_{i+1}$ (all i). The derivatives of the function are

---

[3] I. Prigogine, *Bull. classe des Sci. Acad. roy. Belg.*, **40**, 471 (1954).

[4] B. O. Koopman, *J. Operations Res. Soc. Amer.*, **1**, 3 (1952).

$$\frac{\partial}{\partial c_i} \sum_i r_i J_i^2 = 2w_{i,i+1} q_{i,i+1} c_i^{q_{i,i+1}-1} r_i J_i - 2w_{i,i-1} q_{i,i-1} c_i^{q_{i,i-1}-1} r_{i-1} J_{i-1}$$

When we equate this to zero for $J_i = J_{i-1}$ we get the following recursion formula for r_i

$$r_i = \frac{w_{i,i-1}}{w_{i,i+1}} \frac{q_{i,i-1}}{q_{i,i+1}} c_i^{q_{i,i-1} - q_{i,i+1}} r_{i-1}$$

which for $q_{i,i-1} = q_{i,i+1}$ determines r_i to be equal to the above-mentioned R_i except for a constant factor. This shows that the power of c need only be the same for the forward and reverse reaction for each species separately.

From the point of view of chemical kinetics it is, however, not too important to consider the cases for which $q \neq 1$. Systems which reach steady or stationary states are mostly systems in which for each separate reaction all but two compounds are present in large, virtually constant, concentrations. A typical example of this is the mechanism proposed for nucleation

$$M_1 + M_1 \rightleftarrows M_2$$
$$M_2 + M_1 \rightleftarrows M_3$$
$$M_3 + M_1 \rightleftarrows M_4 \text{ etc.}$$

(M_i is a cluster of i molecules.) Here M_1 is necessarily constant, if we want a stationary state, and thus all the bimolecular steps appear as first-order reactions.

We could now generalize these results even further, for instance, to a set of reactions where transitions between any pair of the N species is possible. Since we have

$$\sigma = \frac{1}{RT} \sum_{i=1<j}^{N} \mu_{ij} J_{ij}$$

we have near equilibrium, as shown in reference 1

$$\sigma = \sum_{i=1<j}^{N} \frac{1}{c_j^{+} w_{ji}} J^2_{ij}$$

By the same reasoning as before we decide that in the form $\sum_{i<j} R_{ij} J^2_{ij}$ we shall take $R_{ij} = c_k^{+}/c_j^{+} w_{ji}$, in which c_k^{+} is some equilibrium concentration which we choose as reference state. It is, of course, a weakness that we have to choose one, but since the reactions in this case do not order the set of states, this is the only possible procedure if we do not want to take $\sum_i c_i^{+}$ as our reference. We shall not pursue generalizations of this kind further, since the results seem to be of little use.

Diffusion in an External Field.—Another possible generalization of the minimum-principle is to cases of diffusion in an external field. For this we have the equation[5]

$$\frac{\partial c}{\partial t} = \frac{\partial}{\partial x} \left[D(x) \frac{\partial c}{\partial x} + D(x)\, c \frac{\mathrm{d}F}{\mathrm{d}x} \right]$$

in which $F(x)$ is the potential energy divided by RT of one mole of the diffusing species at the point x. We seek a variational principle of the form $\delta \int RJ^2 \cdot \mathrm{d}x = 0$ for the time-independent state of this process. It is easily seen that the differential operator on the right-hand side of this diffusion equation is not self-adjoint. We can, however, make it self-adjoint by multiplying it by e^F.

It is probably more interesting, though, to resort to a physical argument. We consider diffusion as a random walk between potential minima spaced λ apart in a diffusion column of unit cross section. We have

$$J_{i,i+1} = w_{i,i+1}\, \lambda c_i - w_{i+1,i}\, \lambda c_{i+1}$$

and assuming that for vanishing field

$$w_{i,i+1} = w_{i+1,i} = w_i$$

we have for small λ, with the field $F(x)$

$$\frac{w_{i+1,i}}{w_{i,i+1}} = \exp\left[\left(\frac{\mathrm{d}F}{\mathrm{d}x}\right)_{x=x_{i+1}} \lambda \right] \cong 1 + \left(\frac{\mathrm{d}F}{\mathrm{d}x}\right)_{x=x_{i+1}} \lambda$$

Consequently

$$J_{i,i+1} = w_i\lambda(c_i - c_{i+1}) - w_i\lambda^2 \left(\frac{\mathrm{d}F}{\mathrm{d}x}\right)_{x_{i+1}} c_{i+1}$$
$$= w_i\lambda^2 \frac{\Delta_i c}{\lambda} - w_i\lambda^2 \left(\frac{\mathrm{d}F}{\mathrm{d}x}\right)_{x_{i+1}} c_{i+1}$$

or in the continuous case

$$J(x,t) = -D(x) \frac{\partial c(x,t)}{\partial x} - D(x) \frac{\mathrm{d}F}{\mathrm{d}x} c(x,t)$$

The resistance in the field free, discrete case is

$$R_i = \frac{\lambda w_1}{\lambda w_1} \cdots \frac{\lambda w_{i-1}}{\lambda w_{i-1}} \frac{1}{\lambda w_{i,i+1}} = \frac{1}{\lambda w_{i,i+1}}$$

Since what we want in the continuous case is the resistance per unit length, we take as the resistance in the continuous case[6]

$$R(x) = \lim_{\lambda \to 0} \frac{1}{\lambda^2 w_{i,i+1}} = D(x)^{-1}$$

When we repeat this procedure in the case of a field $F(x)$ we no longer have cancellations of all transition probabilities except one. We now have

$$R(x) = \lim_{\substack{\lambda \to 0 \\ k \to \infty}} \frac{1}{\lambda^2 w_{i,i+1}} \prod_{j=1}^{k} \frac{w_{j+1,j}}{w_{j,j+1}}$$

The logarithm of $R(x)$ can be evaluated as an integral and we get simply $R(x) = D^{-1}(x)e^{F(x)}$, so that the minimum-principle reads

$$\delta \int_{x_1}^{x_2} e^F D^{-1} J^2 \, \mathrm{d}x = 0$$

It can also be written

$$\delta \int_{x_1}^{x_2} De^{-F} \left[\frac{\mathrm{d}}{\mathrm{d}x} (ce^F) \right]^2 \mathrm{d}x = 0$$

In this way we can stress the similarity between this generalized principle and $\delta \int D\, (\mathrm{d}c/\mathrm{d}x)^2\, \mathrm{d}x = 0$ valid for diffusion without external field. The only change is that we now measure concentration in units equal to the equilibrium concentration at that point, *i.e.*, our unit of concentration is a function of x. Since we want J to be independent of this change in order to describe steady states in a simple way, Fick's first law requires that the proportionality factor between J and $\partial c/\partial x$ be De^{-F} rather than D.

Comparison with the Dissipation Function.—The function which occurs in the minimum-principle has the same form as the so-called dissipation function ϕ which was introduced in irreversible thermodynamics by Onsager.[7]

---

[5] See, for instance, M. Mason and W. Weaver, *Phys. Rev.*, **23**, 412 (1924).

[6] See, for instance, S. Glasstone, K. J. Laidler and H. Eyring, "The Theory of Rate Processes," McGraw-Hill Book Co., New York, N. Y., 1491, p. 519.

It is important to realize that this resemblance is purely formal and that the function we use should rather be considered a generalization of the entropy production. This is seen when we consider the nature of the dissipation function. The rational way of defining the dissipation function is as a function which, when differentiated with respect to the i'th flux gives the i'th force, *viz.*

$$\frac{\partial \phi}{\partial J_i} = X_i$$

From this we get near equilibrium where linear laws prevail

$$\phi = \frac{1}{2}\,\Sigma R_{ik} J_i J_k$$

where R_{ik} is the resistance matrix as used by Onsager.[7] Far from equilibrium in the absence of linear laws there will in general not exist such a function, and when it exists it will not have the simple form shown above. To show this we recall that the dissipation function for chemical reactions is introduced as

$$\mathrm{d}\phi = \sum_i X_i \mathrm{d}J_i = \sum_i \frac{\mu_i}{RT}\,\mathrm{d}J_i$$

We want to show that in general ϕ does not exist, *i.e.*, that $\mathrm{d}\phi$ is not integrable. We must therefore study a system with three or more independent variables. We will choose the triangular reaction originally considered by Onsager. The fluxes are

$$J_1 = w_{12}c_1 - w_{21}c_2$$

and analogously for J_2 and J_3.

The driving forces are $X_i = \mu_i/RT$, for example

$$X_1 = \frac{\mu_1}{RT} = \log \frac{w_{12}c_1}{w_{21}c_2}$$

taking the standard states to be those of equilibrium. We can now express $\Sigma X_i\ \mathrm{d}J_i$ in terms of c_1, c_2, c_3, and the rate constants. We get

$$\sum_i X_i\,\mathrm{d}J_i = \sum_i C_i\,\mathrm{d}c_i$$

in which

$$C_1 = w_{12} \log \frac{w_{12}c_1}{w_{21}c_2} - w_{13} \log \frac{w_{31}c_3}{w_{13}c_1}$$

Analogous expressions hold for C_2 and C_3. To show that this is not integrable we form

$$B = \sum_{i=1}^{3} C_i \left(\frac{\partial C_{i+1}}{\partial c_{i+2}} - \frac{\partial C_{i+2}}{\partial c_{i+1}}\right)$$

since $B \equiv 0$ is the necessary and sufficient condition for integrability.

Performing the differentiation one gets

$$B = \sum_{i=1}^{3} C_i \left(\frac{w_{i+2,i+1}}{c_{i+1}} - \frac{w_{i+1,i+2}}{c_{i+2}}\right)$$

We see that, except when we have detailed balance, $B \not\equiv 0$. When we have detailed balancing, the parenthesis vanishes, but since detailed balancing only occurs at equilibrium,[8] we have shown that in general ϕ does not exist outside equilibrium.

Although we have shown that ϕ does not exist in general, there may still be a number of reactions for which it does exist. The problem of classification of these reactions has recently been discussed by Prigogine and Balescu.[9]

Conclusion

The minimum-principle discussed in this and the previous paper does not give information which we do not have in advance. Its value is that it furnishes a general formulation of Le Châtelier's principle, *i.e.*, it gives a stability criterion for time-independent states. This is due to the fact that it is not a true variational principle in the same sense as Onsager's variational principle or Hamilton's principle, for which the varied states have no physical reality. The principle we have been discussing is, on the contrary, concerned with how deviations from the minimum value of $\Sigma\ RJ^2$ which occur in actual systems get smaller during the natural motion of the system and vanish for $t \rightarrow \infty$. It is therefore a statement about the stability of the system in a certain state rather than about its dynamics. For the same reason it is relatively insensitive to the transition from equilibrium to any time-independent state, whereas Onsager's variational principle ceases to be applicable for non-equilibrium states, because the dissipation function does not exist outside near-equilibrium states.

Acknowledgments.—The author wishes to gratefully acknowledge the grant of a Fellowship from the International Coöperation Administration which made his stay at Columbia University possible. Also he wishes to thank Professor Victor K. La Mer, Columbia University and Professor Laszlo Tisza, Massachusetts Institute of Technology, for many helpful discussions.

---

(7) L. Onsager, *Phys. Rev.*, **37**, 405 (1931); **38**, 2265 (1931).

(8) M. J. Klein, *ibid.*, **97**, 1446 (1955).

(9) I. Prigogine and R. Balescu, *Bull. classe des Sci. Acad. roy. Belg.*, **41**, 917 (1955).

SYSTEMATICS OF THE INFRARED SPECTRAL PROPERTIES OF HYDROGEN BONDING SYSTEMS: FREQUENCY SHIFT, HALF WIDTH AND INTENSITY[1]

BY CHARLES M. HUGGINS AND GEORGE C. PIMENTEL

Department of Chemistry and Chemical Engineering, University of California, Berkeley, California

Received June 20, 1956

Three spectral properties, frequency shift $\Delta\nu$, band width $\nu_{1/2}$ and integrated intensity B, have been measured for a variety of hydrogen bonding systems X–H···Y in solution. A linear relation is found between $\Delta\nu$ and $\nu_{1/2}$ which is applicable to a wide variety of systems: $\nu_{1/2} = 0.72\ \Delta\nu + 2.5$ cm.$^{-1}$. A simple monotonic relation is also found between $\Delta\nu$ and B. The intensity is discussed with reference to the intensities of X–H bending modes; polarization in the base molecule is suggested.

The infrared spectral region near 3μ reveals three types of perturbation when a compound R–X–H forms a hydrogen bond R–X–H···Y. The absorption band attributed to the X–H stretching mode usually displays a frequency shift $\Delta\nu$, the band has an enhanced band width $\nu_{1/2}$ (width at half intensity), and the integrated absorption B of the band increases. Although these perturbations have been known for almost two decades, relatively little is known about the systematics among these spectral changes. Some of the correlations which have been established relate $\Delta\nu$ with H-bond energy,[2] $\Delta\nu$ with X···Y distance in solids,[3] $\Delta\nu$ with chemical reactivities,[4] and B with ΔH of solution of $CDCl_3$ in a variety of bases.[5] A few quantitative intensity measurements have been made.[5-7] Barrow[7] studied the OH stretching modes of a series of alcohols and phenol in the solvents diethyl ether and triethylamine and he concluded "the intensity is greater, the more acidic is the alcohol and the more basic is the bonding agent." Tsubomura[8] studied this vibration for phenol in a variety of solvents and found a correlation between $\Delta\nu$ and B.

In these laboratories we have independently examined the systematics of the spectral changes accompanying hydrogen bonding. Although some of the systems we have selected duplicate some of those of Barrow[7] and of Tsubomura,[8] the variety of systems studied is broader and a more general picture of the hydrogen bond perturbation is obtained than is provided by the data of either Barrow or Tsubomura.

Experimental

All spectra were obtained using a Perkin–Elmer Model 21 Spectrophotometer with CaF_2 and/or NaCl optics. Unless specifically indicated, a CaF_2 prism was used, with a spectral slit width of 9 cm.$^{-1}$ at 3200 cm.$^{-1}$. The cell temperature was found to be 32 ± 2°. The frequency calibration was checked against the known spectra of CO, HBr, CO_2, NH_3, and/or H_2O. The zero and total transmissions were checked frequently to preclude instrument drift. Ascarite and silica gel placed in the spectrophotometer housing reduced atmospheric background absorptions. Sealed liquid cells of 0.019 and 0.095 cm. thickness were calibrated from their optical interference patterns. No evaporation of volatile solvents from these cells was noticed in periods as long as four hours.

All solutions of liquid solutes were prepared by delivering a volume of solute from a Misco micropipet into a suitable volumetric flask containing solvent. Concentration ranges were selected for optimum measurements of intensity in one of the two liquid cells.

The band intensities were determined by integration on a logarithmic scale over a frequency range of about three times the half-width. No correction for "wing" absorption was made and no attempt was made to extrapolate the apparent extinction coefficients to infinite dilution.

Standard "Reagent" or "C.P." grade chemicals were used. The infrared spectrum of each solvent was examined for spurious absorptions with particular attention to the spectral regions characteristic of O–H and C═O functional groups. For a few substances, special purification techniques were used.

Benzene.—Merck C.P. benzene was redistilled from anhydrous $CaCl_2$ in a thirty-plate, bubblecap column and a center fraction boiling at 81.1 ± 0.1° was chosen.

Carbon Tetrachloride.—J. T. Baker Analyzed carbon tetrachloride was redistilled from P_2O_5 in a single-stage still.

Phenol.—B and A Reagent-Grade phenol was heated at 100° overnight and stored over P_2O_5.

Triethylamine.—Eastman Kodak White Label triethylamine was redistilled from KOH in the same multiplate column and a center fraction boiling at 89.5 ± 0.1° was chosen.

Chloroform.—Merck Reagent-Grade chloroform was purified by the procedure given by Fieser[9] and in the final distillation a center fraction boiling at 61.4 ± 0.1° was taken.

Results

In discussing H-bonded systems X–H···Y, two classes are considered. In the first, the H-bonded complexes, Y is a base molecule which is different from the proton donor, X–H. In the second class, the H-bonded polymers, the base molecule Y is identical to the proton donor X–H. The systems of the second class provide data which are more difficult to interpret. Some of these form only dimers (*e.g.*, carboxylic acids and lactams) for which there may be angular constraints on the H-bond. Some of them form higher polymers, making it difficult to ascertain the species being studied and its concentration. Since the H-bonded complexes are more easily understood, they are considered first.

H-Bonded Complexes.—The X–H stretching frequencies and intensities of the compounds phenol, methanol and pyrrole were determined in some or all of the solvents carbon tetrachloride, benzene, diethyl ether and triethylamine. In every case, the concentration of the proton donor was sufficiently low that no significant amount of dimerization would occur. (This was indicated by the absence of absorption at the lower frequencies characteristic of the absorption of polymers.) The results are shown in Table I. The intensities are reported in terms of the "apparent absorption coefficients," B, since no attempt was made to correct for finite resolving power, to extrapolate to infinite dilution, or to estimate the fraction of solute not in H-bonded form.[10]

---

[1] Submitted in partial fulfillment of the requirements for the degree of Ph.D., by Charles M. Huggins, University of California, September, 1955.

[2] R. M. Badger and S. H. Bauer, *J. Chem. Phys.*, **5**, 839 (1937); R. M. Badger, *ibid.*, **8**, 288 (1940).

[3] R. E. Rundle and M. Parasol, *ibid.*, **20**, 1487 (1952); R. C. Lord and R. E. Merrifield, *ibid.*, **21**, 166 (1953); G. C. Pimentel and C. H. Sederholm, *ibid.*, **24**, 639 (1956); K. Nakamoto, M. Margoshes and R. E. Rundle, *J. Am. Chem. Soc.*, **77**, 6480 (1955).

[4] L. L. Ingraham, J. Corse, G. F. Bailey and F. Stitt, *ibid.*, **74**, 2297 (1952).

[5] C. M. Huggins and G. C. Pimentel, *J. Chem. Phys.*, **23**, 896 (1955).

[6] (a) S. A. Francis, *ibid.*, **19**, 505 (1951); (b) R. C. Lord, B. Nolin and H. D. Stidham, *J. Am. Chem. Soc.*, **77**, 1364 (1955).

[7] G. M. Barrow, THIS JOURNAL, **59**, 1129 (1955).

[8] H. Tsubomura, *J. Chem. Phys.*, **23**, 2130 (1955); **24**, 927 (1956).

[9] L. F. Fieser, "Experiments in Organic Chemistry," D. C. Heath and Co., Boston, Mass., 1941, pp. 265–266.

$$B = \frac{1}{CL}\int \log_e T^\circ/T \, d\nu$$

C = total concn., moles/l., of proton donor
L = cell length, cm.
T/T° = fraction of light transmitted
ν = frequency, cm.$^{-1}$

Frequencies are accurate to about ± 7 cm.$^{-1}$ and frequency differences to about 10 cm.$^{-1}$. Frequency shifts are listed as $\Delta\nu = (\nu_0 - \nu')$ where ν_0 and ν' are the frequencies of maximum absorption in a dilute solution in carbon tetrachloride and in the solvent listed, respectively. Of course $\Delta\nu$ is of particular interest in view of the known correlations with important properties of H-bonded systems.[2–4]

TABLE I

SPECTRAL PROPERTIES OF THE H-BONDED COMPLEXES

Acid	Solvent base	Acid concn. mole/l.)	ν (cm.$^{-1}$)	$\Delta\nu$ (cm.$^{-1}$)	$\nu_{1/2}$ (cm.$^{-1}$)	$B \times 10^{-3}$ (l. mole^{-1} cm.$^{-2}$)
Pyrrole	CCl_4	0.04	3495	..	22 ± 5	6.6
Pyrrole	Benzene	.1	3463	32	37 ± 5	11
Pyrrole	Ether[a]	.1	3354	141	81 ± 8	37
Pyrrole	t-e-amine[b]	.11	3200	295	225 ± 20	67
Methanol	CCl_4	.04	3640	..	33 ± 6	4.8
Methanol	Benzene	.04	3583	57	46 ± 15	15
Methanol	Ether[a]	.2	3507	133	88 ± 7	39
Methanol	t-e-amine[b]	.2	3246	394	275 ± 20	74
Phenol	CCl_4	.04	3614	..	25 ± 4	7.6
Phenol	Benzene	.02	3558	56	40 ± 5	16
Phenol	Ether[a]	.02	3344	210	143 ± 6	60

[a] Ether = diethyl ether. [b] t-e-amine = triethylamine.

Table II shows the qualitative correlation of each of the properties $\Delta\nu$, $\nu_{1/2}$ and B with base strength (assumed to increase in the order carbon tetrachloride, benzene, diethyl ether, triethylamine) and acid strength (assumed to increase in the order pyrrole, methanol, phenol). The earlier measurements for deuterochloroform[5,6b] are included although all of the spectral properties are influenced by the isotopic change.

TABLE II

CORRELATIONS OF $\Delta\nu$, $\nu_{1/2}$ AND B WITH BASE AND ACID STRENGTH

$\Delta\nu = \nu(CCl_4) - \nu(\text{base})$; B in liters moles^{-1} cm.$^{-2}$

Acid	Base	CCl_4	Benzene	Diethyl ether	Triethylamine
		...	...	...	...
$CDCl_3$	$\Delta\nu$	(0)[4]	5[4]	10[6]	84[3]
Pyrrole		(0)	32	141	295
Methanol		(0)	57	133	394
Phenol		(0)	56	210	...
$CDCl_3$	$\nu_{1/2}$	12	11	16	42
Pyrrole		22	37	81	225
Methanol		33	46	88	275
Phenol		25	40	143	...
$CDCl_3$	$B \times 10^{-3}$	0.12	0.71	0.58	4.1
Pyrrole		2.9	11	37	67
Methanol		1.9	15	39	74
Phenol		3.2	16	60	...

For each of the proton donors studied there is a systematic increase in $\Delta\nu$, $\nu_{1/2}$ and ΔB as base strength increases. On the other hand there are deviations from a simple progression for $\Delta\nu$, $\nu_{1/2}$ and ΔB as acid strength increases. This is in contrast to the conclusion of Barrow,[7] who compared only methanol and phenol in diethyl ether. Furthermore, Tsubomura's observation[8] of increasing intensity with increasing acidity for proton donors in an inert solvent is contradicted by the pyrrole–methanol comparison (although it is not clear that N–H and O–H intensities should be comparable).

In view of the absence of systematic dependence of any of these spectral changes with acid strength, we have sought correlations among the changes themselves. Figure 1 shows a plot of $\Delta\nu$ *vs.* $\nu_{1/2}$ and Fig. 2 shows a plot of $\Delta\nu$ *vs.* ΔB. The quantity ΔB, the intensity in the solvent base minus the intensity in CCl_4, seems to be a useful quantity to compare to $\Delta\nu$ (rather than B itself). The plot of Fig. 2 is in qualitative agreement with the correlation found by Tsubomura between ν and B for the single acid phenol. The results presented here, however, are striking in that the correlation exists among a wide variety of systems. All of the spectral properties are consistent despite the failure of the spectral properties to reflect the same relative acid strengths in different solvent bases. Thus methanol and phenol show about the same values of $\Delta\nu$, of $\nu_{1/2}$ and of ΔB in benzene and quite different values in diethyl ether. Pyrrole and methanol show similar spectral changes in ether and very different changes in either benzene or triethylamine. It would seem a reasonable conclusion that the spectral changes give a more direct and more reliable indication of the acid–base interaction than can be predicted from presumed acid strengths.

The data of Barrow and of Tsubomura are compared to the behaviors observed here in Figs. 3 and 4. Exact agreement is not expected for several reasons: H-bonding systems are notoriously sensitive to temperature change, the integrations of Barrow may extend over a different range of frequency; the assumption of Lorentzian band shape

---

(10) At infinite dilution the ratio of X–H present in H-bonded form to free X–H approaches the association equilibrium constant (in mole fraction units).[11] For large K, then, only a small error in B results from use of the total concentration. For some of the systems studied here, the constants may not be large compared to unity. To indicate the approximate magnitudes, we observe the following association constants (converted to mole fraction units): chloroform–triethylamine,[11,12] K = 3.0, K = 3.7; ethanol–triethylamine,[13] K = 30; phenol dimerization,[13] K = 14.5. For the present purposes we note that the true B will be higher than the calculated B by a factor $(K + 1/K)$ and the error is likely to be significant compared to experimental uncertainties only for the systems involving the weaker H-bonds.

(11) C. M. Huggins, G. C. Pimentel and J. N. Shoolery, *J. Chem. Phys.*, **23**, 1244 (1955).

(12) G. M. Barrow and E. A. Yerger, *J. Am. Chem. Soc.*, **76**, 5247 (1954).

(13) N. L. Coggeshall and E. L. Saier, *ibid.*, **73**, 5414 (1951).

TABLE III

SPECTRAL PROPERTIES OF THE H-BONDED POLYMERS

Compound	Polymer	Concn. (moles/l.)	ν (cm.$^{-1}$)	$\Delta\nu$ (cm.$^{-1}$)	$\nu_{1/2}$ (cm.$^{-1}$)	$B \times 10^{-3}$ (l. mole^{-1} cm.$^{-2}$)
Acetic acid[a]	Monomer	0.005	3529	..	......	2
Acetic acid[a]	Dimer	.028	3020	509	380 ± 40	74
γ-Butyrolactam	Monomer	.004	3453	..	......	2.9
γ-Butyrolactam	Dimer	.40	3221	232	150 ± 20	41
Phenol	Dimer	.08	3484	130	170 ± 30	30–40
Methanol	Dimer[b]	.10	3470	170	130 ± 10	30–60
Methanol	Polymer	.16	3355	285	210 ± 10	24
N-Ethylacetamide[a]	Monomer	.02	3471	..	....	2.3
N-Ethylacetamide[a]	Dimer	.04	3372	100	92 ± 15	28
N-Ethylacetamide[a]	Polymer	.16	3322	149	120 ± 15	44

[a] Studied using NaCl optics. [b] $CHCl_3$ solvent.

by Tsubomura is of doubtful validity; Tsubomura's use of base concentrations which require correction for free phenol introduces uncertainties in some of his points; internal consistency is more likely to exist within each of the three sets of data because of possible systematic errors (as introduced by cell length measurement, temperature differences, solvent impurities, etc.).

H-Bonded Polymers.—The data for the H-bonded polymers are listed in Table III and shown in Figs. 1 and 2. Frequencies in this table are accurate to about ±11 cm.$^{-1}$ and $\Delta\nu$ to ±15 cm.$^{-1}$ except for acetic acid dimer for which ν and $\Delta\nu$ are uncertain by 25 and 30 cm.$^{-1}$, respectively. Acetic acid and γ-butyrolactam are known to form only dimeric units.[14,15] Consequently, relatively reliable values for the spectral parameters of these compounds can be obtained. The data for these two substances are in reasonable concurrence with the correlations of the complexes as seen in Figs. 1 and 2. (Notice that all intensities are given *per X–H group* in this paper.)

Three substances were examined which form H-bonded polymers, phenol (in CCl_4), methanol (in chloroform) and N-ethylacetamide (in CCl_4). Each compound was studied at a concentration sufficiently low that no frequency change of the polymeric absorption occurred on further dilution. This absorption was considered to be associated with dimeric species. For phenol the equilibrium constants derived by Coggeshall and Saier[13] were used to calculate the fraction of the total phenol concentration present as dimer. For methanol and N-ethylacetamide the dimer concentration was calculated by subtraction of the monomer concentration appropriate to the integrated absorption area at the monomer frequency. This involves the assumption that the dimer does not also absorb at the monomeric frequency (*i.e.*, it is not an open dimer with one unbonded N–H group absorbing at the monomeric frequency). This assumption is inherent in the dimerization constants of Coggeshall and Saier also. If some or all of the dimers are open dimers, the actual concentration of dimers is in error but the number of H-bonded X–H groups is still approximately correct (exactly correct if the absorption coefficients of monomer and open dimer are equal).

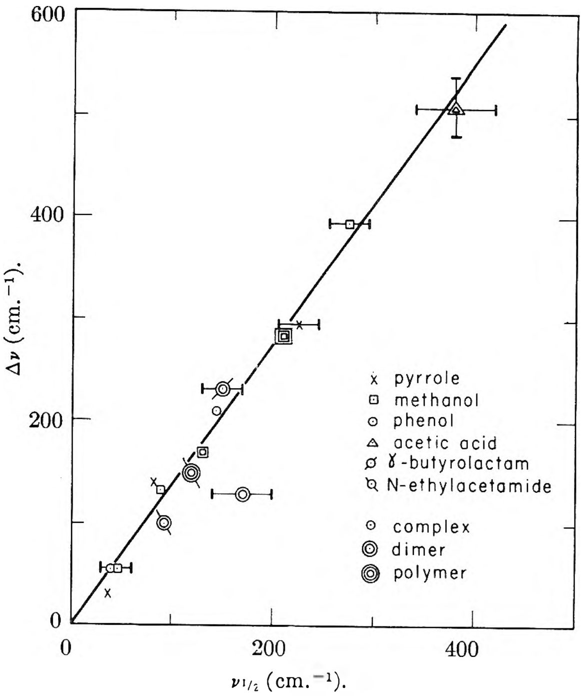

Fig. 1.—Frequency shift *vs.* half width for hydrogen bonded systems.

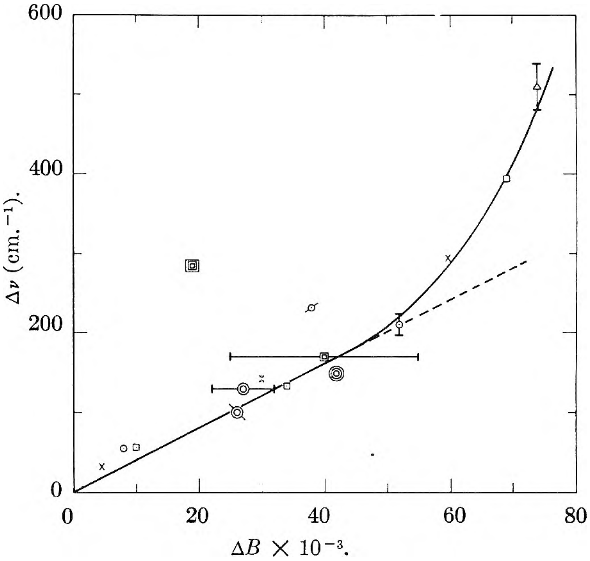

Fig. 2.—Frequency shift *vs.* intensity change for H-bonded systems; coded as on Fig. 1.

---

(14) R. E. Lundin, F. E. Harris and L. K. Nash, *ibid.*, **74**, 4654 (1952).

(15) W. Klemperer, M. W. Cronyn, A. H. Maki and G. C. Pimentel, *ibid.*, **76**, 5846 (1954).

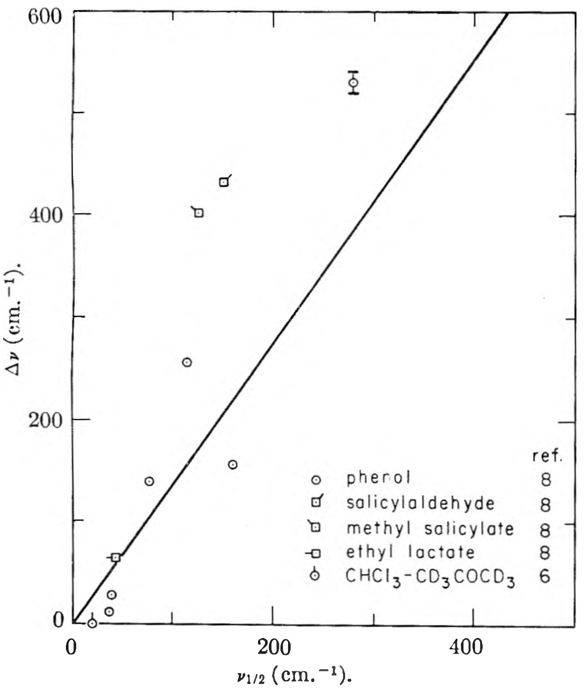

Fig. 3.—Frequency shift *vs.* half width; previously published data.

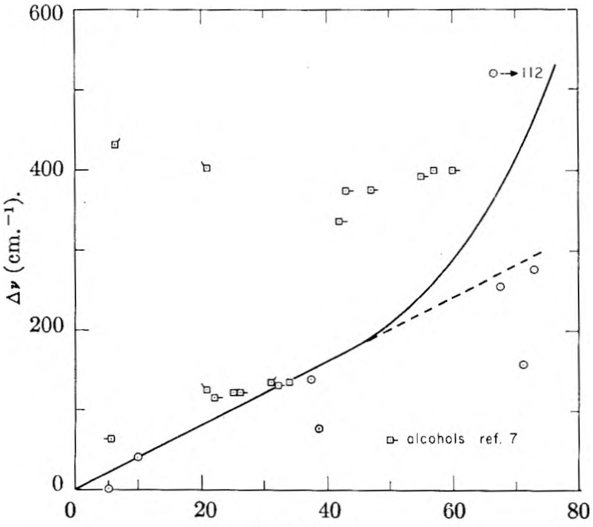

Fig. 4.—Frequency shift *vs.* intensity change; previously published data; coded as on Fig. 3 except as indicated.

Estimates were made of $\Delta\nu$, $\nu_{1/2}$ and B for polymeric species of methanol (in CCl_4) and N-ethylacetamide (in CCl_4). For methanol, the half-width was taken as twice the half-width on the low frequency side since overlap of dimer obscured the band shape on the high frequency side. Although it is not clear what species are represented, these data suggest that as the polymeric units increase in size, the increase in $\Delta\nu$ is accompanied by an increase in $\nu_{1/2}$.

Discussion

The correlation between $\Delta\nu$ and $\nu_{1/2}$ is surprisingly close to a linear relation. Using the data in Tables I and II, one obtains a least squares relation

$$\nu_{1/2} = 0.72\Delta\nu + 2.5 \text{ cm.}^{-1}$$

with a mean square deviation of 12 cm.⁻¹. (The datum for phenol dimer was omitted in the least squares calculation because it shows a deviation of six times the mean square deviation of all other data.) This simple relationship provides a critical test on any theory of the width of the H-bonded X–H stretching motion of species in solution. Perhaps the most interesting aspect of this correlation is its applicability to a wide variety of H-bonded species and its inapplicability to the intramolecular H-bonded compounds studied by Tsubomura, salicylaldehyde and methyl salicylate. It is suggested that a variety of molecular orientations (associated with bent H-bond configurations) is responsible for the band width. The intramolecular H-bond is restricted more and displays much narrower bands than an H-bond in an intermolecular complex. The existing theories of band width of H-bonded compounds will be discussed in a later paper describing other relevant data.

The intensities of the H-bonded complexes indicate again a relatively simple relationship between the enhancement of intensity and the frequency shift for a wide variety of systems. The H-bonded polymers seem in reasonable agreement in view of the greater uncertainty associated with these data. Nevertheless there seems to be no question that methanol polymer deviates very much from the behavior of the other systems. This is similar to Tsubomaru's observation that intramolecular H-bonded molecules deviate from the behavior of intermolecular H-bonded phenols. It is possible that non-linear H-bonds are indicated in those species which display abnormally low intensity increase on H-bonding.

The high intensities of H-bonded stretching modes have long been discussed in terms of "increased ionic character" of the X–H bond. This proposal is placed in explicit form by Barrow[7] and he attempts to evaluate the ratio of the coefficients of ionic and covalent components of the X–H bond. Tsubomaru[8] proposes that the intensity is associated with contribution of charge-transfer forms (of the form $X^- \cdots H\text{–}Y^+$). In the discussions of these models, apparently little notice has been given to the intensities of the O–H bending modes. In the simplest interpretation, the intensity of a bending mode is proportional to the bond dipole of the moving group. This dictates an intensification of bending modes roughly proportionate to the intensification of the stretching mode if the X–H bond has enhanced ionic character. On the other hand, the charge-transfer model seems to predict that such intensification will not be observed since it attributes no unusual charge properties to the proton itself. Thus it seems that these bending modes offer a significant test of these models. No doubt they have been largely ignored because of the absence of definitive identification. Thus Stuart and Sutherland[16] conclude after a thorough study of the spectra of a large number of alcohols that " . . . the effects of hydrogen bonding on the deformation motions of the O–H group are quite complex and . . . steric effects, rotational isomerization,

[16] A. V. Stuart and G. B. B. M. Sutherland, *J. Chem. Phys.*, **24**, 559 (1956).

and interaction with C–H deformation frequencies may all be involved . . ."

Nevertheless we feel that it is possible to conclude that the infrared spectra of H-bonded substances do not display spectacular changes in the spectral region 700–1500 cm.$^{-1}$ comparable to the changes found for the stretching modes. Quantitative intensity measurements of the bending mode of $CDCl_3$ in CCl_4 and in H-bonding solvents[5] have shown the absence of an intensity change. Measurements on the spectrum of H-bonded water show that the bending mode probably decreases in intensity upon hydrogen bonding.[17] These data permit a tentative generalization that the bending modes are not intensified on H-bond formation. Consequently, we suggest that polarization of the electrons in the base accounts for a significant part of the enhanced $d\mu/dr$ of the H-bonded stretching mode. Such polarization tends to decrease the intensity of this bending mode. As far as the "ionic character" and "charge-transfer" models are concerned, the latter is favored.

Conclusion

The empirical correlations among the spectral properties $\Delta\nu$, $\nu_{1/2}$ and ΔB are remarkable in their apparent applicability to a variety of acid-base systems which have in common *only* the H-bond interaction. Consequently, it is reasonable to use these correlations as a basis for construction of theoretical models for the H-bond. In particular, the linear relation between $\Delta\nu$ and $\nu_{1/2}$ provides a critical cornerstone for understanding the unusual band width behavior.

In an empirical way, the correlations described here potentially offer a norm of behavior for H-bonded systems. For example, the correlation between $\Delta\nu$ and ΔB substantiates the interpretation of the spectral behavior of chloroform in basic solvents in terms of H-bonding. When large discrepancy from this norm is observed (as for salicylaldehyde and methyl salicylate) it will be profitable to examine the possibility of an unusual bond, as exemplified by a non-linear H-bond. Conversely, the intensity behaviors described here are of crucial importance in the interpretation of infrared dichroic studies of H-bonded substances (even though the applicability to solid state systems has not yet been tested). On the one hand, the interpretation of the dichroism of stretching modes in terms of bond orientations is simplified for linear H-bonds because the enhanced intensity is caused by a dipole change along the bond. For a bent H-bond, however, the enhanced dipole change may well be parallel to the $H \cdots\cdot Y$ bond and not directly indicative of the X–H orientation. Since the dichroic data are of greatest interest when the linearity of the H-bond has not been established, the problem is a real one, indeed. Correlations of the type presented here may aid by giving a criterion of H-bond linearity.

---

[17] M. Van Thiel and G. C. Pimentel, to be published.

THE INFLUENCE OF AN EXTERNAL ELECTRIC FIELD ON THE OPTICAL ACTIVITY OF FLUIDS[1]

By Ignacio Tinoco, Jr.,[2] and William G. Hammerle

Sterling Chemistry Laboratory, Yale University, New Haven, Connecticut

Received June 25, 1956

In the presence of an external electric field, the optical activity of a fluid differs from its value when the field is absent. The change in activity is due to the partial orientation of the constituent molecules by the field. The optical activity of a molecule can be represented by a pseudo second-rank tensor. The activity of the fluid is obtained by averaging this tensor over all molecular orientations, which are weighted according to the angular orientation function produced by the electric field. This effect, which should be particularly apparent for macromolecules such as viruses, nucleic acids and proteins, can provide new structural information.

The optical activity of a fluid is determined by the optical activity of the constituent molecules, and by their orientations relative to the incident light. If no external field is acting on the fluid, all possible molecular orientations are equally probable, and the material is optically isotropic. The optical activity of an isotropic fluid has been investigated by Rosenfeld,[3a] Kirkwood[3b] and Condon.[3c] The activity is related to the transition probabilities of the electric and magnetic moments of the molecules.

If a static electric field is applied to the fluid, the molecular orientations are no longer random; certain configurations become more probable than others. As a result, the fluid acquires the optical properties of a uniaxial crystal with the optic axis parallel to the field.[4] One would expect the optical activity under these conditions to depend upon the direction of propagation of the incident light and upon its plane of polarization. This effect can be used to determine the optical activity along various directions in the molecule, and thus can provide new structural information.

In this paper, the change in the optical activity caused by an external field will be related to the properties of the constituent molecules. We shall consider the activity when the electric field is independent of the time, and also when the field is applied as a rectangular pulse. The time dependence of the optical activity upon application or removal of the field depends upon the rotary diffusion tensor of the molecules as well as their optical and electrical characteristics. This effect is important for solutions of macromolecules, because the diffusion tensor can provide information as to the size and shape of the molecules.

---

[1] Contribution No. 1378 from the Sterling Chemistry Laboratory, Yale University. This paper was presented at the 129th National ACS Meeting (April, 1956).

[2] Public Health Service Post-Doctoral Fellow of the National Cancer Institute. Present address: Chemistry Department University of California, Berkeley, California.

[3] (a) L. Rosenfeld, *Z. Physik*, **52**, 161 (1928); (b) J. G. Kirkwood, *J. Chem. Phys.*, **5**, 479 (1937); (c) E. U. Condon, *Rev. Mod. Phys.*, **9**, 432 (1937).

[4] F. A. Jenkins and H. E. White, "Fundamentals of Physical Optics," McGraw-Hill Book Co., Inc., New York, N. Y., 1950, p. 605.

The notation of Kirkwood's treatment of optical activity will be used.

Part I

A plain-polarized electromagnetic wave induces a dipole moment in the ground state of a molecule given by[2]

$$\mu_0 = [\boldsymbol{\alpha} + \boldsymbol{\gamma} - (2\pi i/\lambda)\mathbf{g}]\cdot\mathbf{F} \qquad (1)$$

F is the internal electric vector of the electromagnetic field; it has the form $\mathbf{F}_0 \exp[2\pi i(\nu t - \mathbf{R}\cdot\mathbf{a}/\lambda)]$. $\mathbf{F}_0$ is a constant vector and i is the $\sqrt{-1}$. The other parameters in **F** are ν, the frequency of the wave; t, the time; **R**, the position vector relative to some fixed coördinate system; **a**, the unit vector in the direction of the wave normal; and λ, the wave length. The tensors $\boldsymbol{\alpha}$, $\boldsymbol{\gamma}$ and g are given by

$$\boldsymbol{\alpha} = \frac{2}{h}\sum_n \frac{\nu_{n0}\boldsymbol{\mu}_{0n}\boldsymbol{\mu}_{n0}}{\nu_{n0}^2 - \nu^2} \qquad (2)$$

$$\boldsymbol{\gamma} = \frac{2e}{\lambda m h \nu}\sum_n \frac{\nu_{n0}\boldsymbol{\mu}_{0n}\mathbf{a}\cdot(\mathbf{rp})_{n0}}{\nu_{n0}^2 - \nu^2} \qquad (3)$$

$$\mathbf{g} = \frac{e}{\pi i m h}\sum_n \frac{\boldsymbol{\mu}_{0n}\mathbf{a}\cdot(\mathbf{rp})_{n0}}{\nu_{n0}^2 - \nu^2} \qquad (4)$$

The constants h, e and m are Planck's constant and the electronic charge and mass, respectively. The quantity $\boldsymbol{\mu}_{0n}$ is the matrix element of the electric moment of the molecule, *i.e.*, the transition dipole moment $\int\psi_0^*\mu\psi_n\mathrm{d}\tau$, where ψ_0 and ψ_n are the electronic wave functions of the molecule in states 0 and n. The vector μ is equal to $\sum\limits_s e\mathbf{r}_s$, where the sum is over all the electrons in the molecule. The tensor $(\mathbf{rp})_{n0}$ is equal to $\sum\limits_s(\mathbf{r}_s\mathbf{p}_s)_{n0}$; $\mathbf{r}_s$ is the position of electron s relative to the molecular center of gravity and $\mathbf{p}_s$ is its momentum operator. The parameter ν_{n0} is the spectroscopic frequency associated with the transition from state 0 to state n.

The tensor $\boldsymbol{\alpha}$ is the usual polarizability tensor; $\boldsymbol{\gamma}$ is a tensor characterizing the dipole moment induced by the magnetic vector of the electromagnetic wave and need not be considered further. The **g** tensor contains the terms characterizing the optical activity of the molecule.

Not all of **g** is necessary to describe the optical activity. The activity does not have an ohmic or dissipative character,[5] *i.e.*, it does not contribute to the electric energy density $(^1/_2)\mathbf{D}\cdot\mathbf{E}$, where **D** is the electric displacement vector and **E** is the electric intensity vector. This implies that only the part of **g** for which $\mathbf{F}\cdot\mathbf{g}\cdot\mathbf{F} = 0$ describes the optical activity of the molecule. If the **g** tensor is expanded in terms of components along an arbitrary, orthogonal set of unit vectors $\mathbf{i}_1'$, $\mathbf{i}_2'$, $\mathbf{i}_3'$ fixed in the molecule, we find that

$$\mathbf{g} = \frac{e}{\pi i m h}\sum_n \frac{1}{(\nu_{n0}^2 - \nu^2)} \sum_{\alpha,\beta,\gamma=1}^{3} a_\beta \mathcal{G}_{\alpha\beta\gamma}\mathbf{i}_\alpha{}'\mathbf{i}_\gamma{}'$$

where

$$\mathcal{G}_{\alpha\beta\gamma} = (\mu_\alpha)_{0n}\,(r_\beta p_\gamma)_{n0} \qquad (5)$$

$$a_\alpha = \mathbf{a}\cdot\mathbf{i}_\alpha{}',\ \mu_\alpha = \boldsymbol{\mu}\cdot\mathbf{i}_\alpha{}' \text{ etc.}$$

Only the part of $\mathcal{G}_{\alpha\beta\gamma}$ which is antisymmetric in the outer (first and third) indices contributes to the optical activity. The terms symmetric in the outer indices need not be considered further. It might be pointed out that Condon[3c] discards the terms symmetric in the second and third indices. Although this procedure gives the correct answer for isotropic materials, it is not in general correct.

If $\boldsymbol{\gamma}\cdot\mathbf{F}$ and the symmetric part of **g** are omitted from eq. 1 it can now be written in a slightly different form

$$\mu_0 = \boldsymbol{\alpha}\cdot\mathbf{F} - (2\pi i/\lambda)(\mathbf{a}\cdot\mathbf{G}) \times \mathbf{F} \qquad (6)$$

where

$$\mathbf{G} = \frac{-e}{2\pi i m h}\sum_n \frac{1}{(\nu_{n0}^2 - \nu^2)} \sum_{\alpha,\beta,\gamma=1}^{3} \mathcal{G}_{\alpha\beta\gamma}\mathbf{i}_\beta{}'(\mathbf{i}_\alpha{}' \times \mathbf{i}_\gamma{}')$$

We might note that **G** depends only upon the properties of the molecule and does not depend upon the vectors specifying the electromagnetic field. This equation is analogous to the equation derived by Born[6] in his treatment based on the classical theory of coupled oscillators.

The optical activity of a material may be expressed as the angle θ through which the plane of polarization of the electromagnetic wave is rotated for each centimeter traversed by the wave. If the material is isotropic and optically active, on a macroscopic scale we have

$$\mathbf{P} = \chi_e\mathbf{E} - (\rho/c)\partial\mathbf{B}/\partial t \qquad (7)$$

The electric polarization vector **P** is the dipole moment induced in a unit volume of the material by the electric vector **E** and the magnetic induction **B**. The parameters c, ρ and χ_e are the velocity of light *in vacuo*, the optical rotation coefficient and the electric susceptibility, respectively. Then θ is given by

$$\theta = 16\pi^3\rho/\lambda_0^2 \qquad (8)$$

In other words, the optical activity in an isotropic material is a measure of the dipole moment induced in the direction of $\partial B/\partial t$.

For a fluid under the influence of a static electric field, or for a crystal, eq. 7 is no longer valid. In its place is a macroscopic analog to eq. 6, which may be written as

$$\mathbf{P} = \boldsymbol{\chi}_e\cdot\mathbf{E} - (2\pi i/\lambda)(\mathbf{a}\cdot\boldsymbol{\Gamma}) \times \mathbf{E} \qquad (9)$$

with the tensors $\boldsymbol{\chi}_e$ and $\boldsymbol{\Gamma}$ characterizing the electric susceptibility and the optical activity. For an anisotropic medium, $\boldsymbol{\chi}_e\cdot\mathbf{E}$ may contribute to the component of **P** in the direction of $\partial\mathbf{B}/\partial t$. A description of the optical activity under these conditions is complicated because the plain-polarized wave not only rotates but also becomes elliptically polarized. Rather than consider all of the possible effects resulting from the introduction of eq. 9, we shall restrict ourselves to those cases where the electric susceptibility does not contribute to $\mathbf{P}\cdot(\partial\mathbf{B}/$

---

(5) A. Sommerfeld, "Optics," Academic Press, Inc., New York, N. Y., 1954, p. 158.

(6) M. Born, "Optik," Julius Springer, Berlin, 1933, p. 403.

∂t). This will be true if **a** is along an optic axis of the medium, or if both **a** and **E** are along principal axes of the dielectric susceptibility tensor.[7] A complete phenomenological treatment of the optical activity of crystals is given by Born.[6]

Along the directions in the anisotropic medium specified above, the optical activity characterizes the component of **P** in the direction of $\partial \mathbf{B}/\partial t$, just as for an isotropic material. We can therefore write eq. 9 in the form

$$\mathbf{P} = \chi_e\cdot\mathbf{E} - [\mathbf{a}\cdot\Gamma\cdot\mathbf{a}/c]\frac{\partial \mathbf{B}}{\partial t} \qquad (10)$$

Eq. 10 is obtained from one of Maxwell's equations

$$-(1/c)\partial\mathbf{B}/\partial t = \nabla \times \mathbf{E} = -(2\pi i/\lambda)\mathbf{a} \times \mathbf{E}$$

It is also necessary to use the fact that $\mathbf{a}\cdot\mathbf{E} = 0$, which is correct only if **a** is along an optic axis, or if both **a** and **E** are parallel to the axes of χ_e.[8] The rotation of the polarized light in radians per centimeter is given by

$$\theta = (16\pi^3/\lambda_0^2)\mathbf{a}\cdot\Gamma\cdot\mathbf{a} \qquad (11)$$

From the definition of **P**, it is possible to relate the observed, macroscopic optical activity to the activity of the individual molecules

$$\mathbf{a}\cdot\Gamma\cdot\mathbf{a} = (N/v)l < \mathbf{a}\cdot\mathbf{G}\cdot\mathbf{a}> \qquad (12)$$

The number of molecules per unit volume is designated by (N/v). The parameter l is defined by the equation $\mathbf{F} = l\mathbf{E}$; a good approximation to l is the Lorentz factor[2] $(n^2 + 2)/3$. The averaging process indicated by <> is the average over the appropriate distribution of molecule orientations. A more precise description of this average will be given in Section II.

From eq. 11 and 12 we can write

$$\theta = [16\pi^3(n^2 + 2)/3\lambda_0^2](N/v)g \qquad (13)$$

where

$$g = <\mathbf{a}\cdot G\cdot\mathbf{a}>$$

The derivation of the general relationship between θ and the properties of the molecules is now complete. Our main conclusions are: (1) the optical activity of a molecule (or a unit cell in a crystal) is characterized by the second-rank tensor **G**.[9] (2) If the direction of the wave normal and the electric vector are such that $\mathbf{a}\cdot\mathbf{E} = 0$, the optical activity depends only upon the direction of propagation of the light, and does not depend explicitly upon the direction of the electric or magnetic vectors.

Part II

The calculation of the optical activity of a fluid is now reduced to evaluation of <**a**·**G**·**a**>. For an isotropic fluid, the average is over all equally probable molecular orientations. For a fluid under the influence of a static electric field, the average must be weighted by the distribution function f produced by the field. If the molecules are rigid bodies

$$g = \int_0^{2\pi}\int_0^{2\pi}\int_0^{\pi} (\mathbf{a}\cdot\mathbf{G}\cdot\mathbf{a})f(\theta,\chi,\phi)\sin\theta d\theta d\chi d\phi \qquad (14)$$

The angles θ, χ and ϕ are the Eulerian angles of a molecule-fixed coördinate system with respect to a space-fixed system. For eq. 14 to be correct, the distribution function $f(\theta, \chi, \phi)$ must be normalized

$$\frac{1}{8\pi^2}\int_0^{2\pi}\int_0^{2\pi}\int_0^{\pi} f(\theta,\chi,\phi)\sin\theta d\theta d\chi d\phi = 1 \qquad (15)$$

In this section we shall obtain the distribution function for two cases: when a fluid is subjected to a static electric field, and when it is subjected to a rectangular electrical pulse, *i.e.*, the field is suddenly applied and suddenly removed.

Let us consider first a fluid composed of polar molecules each with permanent dipole moment $\boldsymbol{\mu}$ and polarizability tensor $\boldsymbol{\alpha}$, under the influence of a static effective electric field $\mathcal{E}$. The angular distribution function is proportional to $\exp(-V/kT)$, where k and T are Boltzmann's constant and the absolute temperature, respectively. The potential energy V of a molecule in the field is given by

$$-V = \mu\cdot\mathcal{E} + (1/2)\,\mathcal{E}\cdot\alpha\cdot\mathcal{E} \qquad (16)$$

This distribution function is used in the theory of Kerr effect.[10]

If the electric field is not too large, V is small compared with kT. We can then expand f in powers of $\mathcal{E}$, keeping only the terms up to $\mathcal{E}\lambda$. When f is normalized, this procedure gives

$$\begin{aligned}f(\theta,\chi) = 1 + (1/6)\mathcal{E}^2\{(p_1^2 + q_{11})[3(\mathbf{e}_1'\cdot\mathbf{k})^2 - 1]\\ + (p_2^2 + q_{22})[3(\mathbf{e}_2'\cdot\mathbf{k})^2 - 1] + (p_3^2 + q_{33})[3(\mathbf{e}_3'\cdot\mathbf{k})^2 - 1]\}\\ \mathcal{E} = \mathcal{E}\mathbf{k},\ q_{ii} = \varkappa_{ii}/kT,\ p_i = \mu_i/kT \qquad (17)\end{aligned}$$

We have introduced two new sets of orthogonal unit vectors; $\mathbf{e}_1'$, $\mathbf{e}_2'$, $\mathbf{e}_3'$ are the principal axes of the symmetric part of the molecular optical rotation tensor **G**, while **i**, **j**, **k** are a space-fixed coördinate system. The μ_i are the components of the permanent dipole along the principal axes of **G**, and α_{ii} are the corresponding components of the polarizability. The terms of f proportional to the first power of $\mathcal{E}$ do not contribute to the average of **a**·**G**·**a**, and have been left out of eq. 17.

For the second case, we are interested in the change in optical activity when the electric field is suddenly applied or suddenly removed. The required angular distribution function f has been used previously in the study of the dynamic electrical birefringence (Kerr effect).[11] Since the field depends upon the time, f is the solution of the diffusion equation[12]

$$\nabla\cdot\Theta\cdot\nabla_f - \frac{\partial f}{\partial t} = -\nabla\cdot\Theta\cdot\frac{f\nabla V}{kT} \qquad (18)$$

where V is the same potential as in eq. 16. Θ is the rotary diffusion tensor of the molecule.

We shall restrict the following calculations to a molecule having cylindrical symmetry. For a cylindrically symmetric rigid body with uniform electron density, α and Θ have colinear axes, with equal components along two of the axes. If $\mathbf{e}'_3$ is the axis of symmetry, then

$$\begin{aligned}\alpha &= \alpha_{11}(\mathbf{e}_1'\mathbf{e}_1' + \mathbf{e}_2'\mathbf{e}_2') + \alpha_{33}\mathbf{e}_3'\mathbf{e}_3'\\ \Theta &= \Theta_{11}(\mathbf{e}_1'\mathbf{e}_1' + \mathbf{e}_2'\mathbf{e}_2') + \Theta_{33}\mathbf{e}_3'\mathbf{e}_3' \qquad (19)\end{aligned}$$

While such a molecular model is not in general applicable to small molecules, it probably describes adequately macromolecules such as proteins or nucleic acids. In water, the macromolecules have an additional contribution to the polarizability[13] due to their mobile ions, *i.e.*, protons, or counter-ions from their ion atmosphere. The contribution of these ions to the polarizability does not change the colinearity of the tensors.

---

[7] A. Sommerfeld, ref. 5, p. 145.

[8] A. Sommerfeld, ref. 5, p. 134.

[9] To be precise, **G** is a pseudo second-rank tensor; it is a third-rank tensor which is antisymmetric in two indices.

[10] C. G. LeFevre and R. J. W. LeFevre, *Revs. Pure Appl. Chem.*, **5**, 261 (1955).

[11] I. Tinoco, Jr., *J. Am. Chem. Soc.*, **77**, 4486 (1955).

[12] J. G. Kirkwood and R. M. Fuoss, *J. Chem. Phys.*, **9**, 329 (1941).

The details of the solution of eq. 18 have been given previously.[11,14] If the electric field is suddenly applied

$$\mathcal{E} = \begin{cases} 0 & t < 0 \\ \mathcal{E}\boldsymbol{k} & t > 0 \end{cases}$$

$$f = 1 + (1/6)[3(\boldsymbol{e}_3'\cdot\boldsymbol{k})^2 - 1]\mathcal{E}^2 A$$

where

$$\begin{aligned} A = {} & p_3^2 + q_{33} - (p_1^2 + q_{11}) - (3/2)p_3^2 e^{-2\Theta_{11}t} \\ & + [6\Theta_{11}p_1^2/(5\Theta_{11} - \Theta_{33})]e^{-(\Theta_{11} + \Theta_{33})t} \\ & - [6\Theta_{11}p_1^2/(5\Theta_{11} - \Theta_{33}) - (p_3^2 + 2p_1^2)/2 + (q_{33} - q_{11})]e^{-6\Theta_{11}t} \end{aligned} \tag{20}$$

If the field has been applied for some time and is then removed

$$\mathcal{E} = \begin{cases} \mathcal{E}\mathbf{k} & t < 0 \\ 0 & t > 0 \end{cases}$$

$$f = 1 + (1/6)[3(\mathbf{e}_3'\cdot\mathbf{k})^2 - 1]\mathcal{E}^2 B \tag{21}$$

where

$$B = [p_3^2 + q_{33} - (p_1^2 + q_{11})]e^{-6\Theta_{11}t}$$

As in the static case, it has been assumed that V is small compared with kT; only terms up to $\mathcal{E}^2$ have been retained. Also, the terms in f which do not contribute to $\langle a\cdot G\cdot a\rangle$ have been discarded. We might note that the angular distribution function when $\mathcal{E}$ is a constant may be found by taking the limit of eq. 20 as the time approaches infinity, or by the value of eq. 21 at zero time. This result agrees with eq. 17 for $p_2 = p_1$ and $q_{22} = q_{11}$.

Part III

Using the distribution functions derived in the preceding section, we can now calculate the optical activity in the presence of the electric field. As only the symmetric part of the optical rotation tensor contributes to g, we can write $\mathbf{G}$ as $G_{11}\mathbf{e}_1'\mathbf{e}_1' + G_{22}\mathbf{e}_2'\mathbf{e}_2' + G_{33}\mathbf{e}_3'\mathbf{e}_3'$.

For the cylindrically symmetric macromolecules, G_{22} is equal to G_{11} as well.

For both the equilibrium and non-equilibrium electric field, there are two cases of interest. In section I, eq. 13 was shown to be correct where $\mathbf{a}\cdot\mathbf{E} = 0$. This requirement is satisfied if the incident light is parallel to the electric field ($\mathbf{a} \parallel \mathcal{E}$), or if the light is perpendicualr to the field ($\mathbf{a} \perp \mathcal{E}$). In the latter case, the electric vector $\mathbf{E}$ must be perpendicular or parallel to $\mathcal{E}$ (either position of the plane of polarization gives the same activity).

The following equations are obtained for a static field

$$\begin{aligned} a \parallel \mathcal{E} \quad & g = g_0 + (\mathcal{E}^2/45)C \\ a \perp \mathcal{E} \quad & g = g_0 - (\mathcal{E}^2/90)C \end{aligned} \tag{22}$$

where

$$\begin{aligned} C = {} & (p_1^2 + q_{11} - p_2^2 - q_{22})(G_{11} - G_{22}) + \\ & (p_2^2 + q_{22} - p_3^2 - q_{33})(G_{22} - G_{33}) \\ & + (p_3^2 + q_{33} - p_1^2 - q_{11})(G_{33} - G_{11}) \end{aligned}$$

and g_0 is $\langle a\cdot G\cdot a\rangle$ in the absence of the electric field. It is the value of $a\cdot G\cdot a$ averaged over a random distribution of molecules, and is one third the trace of $\mathbf{G}$

$$\begin{aligned} g_0 & = (1/3)(G_{11} + G_{22} + G_{33}) \\ & = \frac{e}{6\pi imh}\sum_n \frac{1}{(\nu_{n0}^2 - \nu^2)}[\mathcal{G}_{312} - \mathcal{G}_{213} + \mathcal{G}_{123} - \mathcal{G}_{321} + \mathcal{G}_{231} - \mathcal{G}_{13} \end{aligned} \tag{23}$$

By substituting $\mathbf{m}_{n0}$ for $(e/2mc)\sum_s(\mathbf{r}_s \times \mathbf{p}_s)_{n0}$, we can write g_0 in the form given previously[2]

$$g_0 = \frac{e}{3\pi ih}\sum_n \frac{\boldsymbol{\mu}_{n0}\cdot\mathbf{m}_{n0}}{(\nu_{n0}^2 - \nu^2)} \tag{24}$$

Lévy[15] has derived an equation similar to eq. 22 for the case when $\mathbf{a} \parallel \mathcal{E}$ and the permanent dipole moment is zero. However, his result is apparently incorrect due to improper antisymmetrization of $\mathcal{G}$.

For cylindrically symmetric macromolecules, when the dielectric field is suddenly applied we find that

$$\begin{aligned} \mathbf{a} \parallel \mathcal{E} \quad & g = g_0 + (2\mathcal{E}^2/45)(G_{33} - G_{11})A \\ \mathbf{a} \perp \mathcal{E} \quad & g = g_0 - (\mathcal{E}^2/45)(G_{33} - G_{11})A \end{aligned} \tag{25}$$

When the field is removed

$$\begin{aligned} \mathbf{a} \parallel \mathcal{E} \quad & g = g_0 + (2\mathcal{E}^2/45)(G_{33} - G_{11})B \\ \mathbf{a} \perp \mathcal{E} \quad & g = g_0 - (\mathcal{E}^2/45)(G_{33} - G_{11})B \end{aligned} \tag{26}$$

The optical rotation θ corresponding to each of the above results can be obtained by substituting g into eq. 13.

When the electric field is suddenly applied, the optical activity depends exponentially upon the time, with three time constants $2\Theta_{11}$, $\Theta_{11} + \Theta_{33}$ and $6\,\Theta_{11}$. If the field is removed the activity contains only the one time constant $6\Theta_{11}$. The latter case can be written more conveniently as

$$\Delta g/\Delta g_e = e^{-6\Theta_{11}t} \tag{27}$$

where $\Delta g = g - g_0$ and Δg_e is the value of $g - g_0$ at zero time. Such an equation is correct for either direction of incident light. The time constants are exactly the same as for the Kerr effect; the relative magnitudes of Θ_{11} and Θ_{33} for various molecular shapes have been discussed previously.

All of the equations for g in this section are correct only if the molecules are rigid. Relative motion of parts of the molecules may result in an optical activity somewhat different from that calculated here.

Part IV

By putting reasonable values of the various parameters into the equations derived in the previous section, we can estimate the magnitude of the change to be expected in the optical activity. For small molecules, let us assume the most favorable possible conditions for a large change in activity, *i.e.*, the optical activity tensor $\mathbf{G}$ is large along the axis of the permanent dipole and negligible in other directions ($p_1 = p_2 = G_{11} = G_{22} = 0$). If $\mathbf{a} \parallel \mathcal{E}$, it follows that

$$\theta/\theta_0 = g/g_0 = 1 + (2/15)\mathcal{E}^2 p_3^2 \tag{28}$$

For simplicity, the relatively small induced dipole orientation has been ignored ($q_{ii} = 0$) For a small molecule, a dipole moment of three debye is common; using eq. 28 we find that about one million practical volts/cm. is necessary to change the optical activity by 1%. Even if the dipole moment were 10 debye, the experimentally attainable field of 100,000 volts/cm. would produce only a 1% change. Experimental observation of the effect for small molecules would therefore be quite difficult.

---

[13] J. G. Kirkwood and J. B. Shumaker, *Proc. Natl. Acad. Sci.*, **38**, 855 (1952).

[14] J. G. Kirkwood, *J. Polymer Sci.*, **12**, 1 (1954).

[15] M. Lévy, *Compt. rend.*, **226**, 652 (1948). This article was kindly brought to our attention by Professor R. J. W. LeFevre.

Kunz and Babcock[16,17] attempted to measure the effect of an electric field on small molecules. Their results are inconclusive.

Macromolecules such as proteins, nucleic acids or viruses have apparent[18] dipole moments of the order of 10,000 debye in water solutions.[11,19] For desoxyribonucleic acid, which has an apparent dipole moment of about 20,000 debye, one can expect a 10% change in the optical rotation using only 500 volts/cm. For large molecules, it therefore appears feasible to measure the effect. One of the more interesting applications would be to macromolecules with an optical activity produced by an over-all helical structure as well as by the monomer units.[20,21] Experimental measurements of the effect on macromolecules would be possible with equipment designed for study of the Kerr effect.[22-24]

If the electric field is applied as a rectangular pulse, the equations giving the change in optical activity are completely analogous to the Kerr effect equations. The time dependence of the change thus gives the same information about size and shape of the molecules as has been discussed in previous articles.[11,22-24]

The influence of other types of orienting forces (hydrodynamic, magnetic, etc.) upon the optical activity can be derived in a fashion similar to that used for an electric field. The appropriate angular orientation functions have been derived previously.[25,26]

Acknowledgment.—We wish to thank Professor John G. Kirkwood for many valuable suggestions and discussions.

---

[16] J. Kunz and S. H. Babcock, *Phil. Mag.*, **22**, 616 (1936).

[17] J. Kunz and S. H. Babcock, *Nature*, **140**, 194 (1937).

[18] The word apparent is used because the mechanism of the orientational torque for these molecules is still in doubt. The orienting force may be due primarily to the polarizability of the molecule. Whatever the orienting mechanism, however, it can be characterized by an apparent dipole of the magnitude given.

[19] A. Jungner and I. Junger, *Acta Chem. Scand.*, **6**, 1391 (1952).

[20] W. E. Moffitt, *J. Chem. Phys.*, **25**, 467 (1956).

[21] D. D. Fitts and J. G. Kirkwood, *Proc. Natl. Acad. Sci., U. S.*, **42**, 33 (1956).

[22] H. Benoit, *Ann. Phys.*, **6**, 561 (1951).

[23] C. T. O'Konski and B. H. Zimm, *Science*, **111**, 113 (1950).

[24] I. Tinoco, Jr., *J. Am. Chem. Soc.*, **77**, 3476 (1955).

[25] A. Peterlin and H. A Stuart, *Hand und Jahrbuch chem. Physik*, **8**, 1 (1943).

[26] H. A. Scheraga, J. T. Edsall and J. O. Gadd, Jr., *J. Chem. Phys.*, **19**, 1101 (1951).

THE STABILITY OF THALLIUM(I) CITRATE COMPLEX

BY JOSEPH A. SCHUFLE AND CARL D'AGOSTINO, JR.

Department of Chemistry, New Mexico Institute of Mining & Technology, Socorro, N. Mex.

Received July 2, 1956

The thallium(I) citrate complex ion has been studied at ionic strengths of 0.1, 0.2, 0.3 and 0.5 by the equilibrium between solution and an ion-exchange resin. A value for the formation constant of 30 ± 3 l./mole at 25° and zero ionic strength was obtained by extrapolation.

The stability of the complex ions formed by thallium(I) ion with various anions has been reported by Bell and George.[1] In general these authors worked at ionic strengths of 0.005–0.1 (concentration units in moles per liter). They reported formation constants (K_f) for the reaction (1)

$$Tl^+ + A^{-x} = TlA^{(1-x)} \qquad (1)$$

to be in the range of 1 to 6 liters per mole for several monovalent anions ($x = 1$); 23 l./mole for a divalent anion (sulfate, $x = 2$); and 1700 l./mole for a quadrivalent anion (ferrocyanide, $x = 4$), at 25°.

The stability of the thallium(I) citrate complex has not been reported. It was of interest to study the complex with this trivalent anion because of the use of citrate solutions as eluting agents in ion-exchange methods of separation. It was proposed to determine the formation constant for the thallium(I) citrate complex at several ionic strengths and extrapolate the data to determine the value of the constant at zero ionic strength. The method of study was to use exchange equilibria on a cation-change resin, Amberlite IR-120 A.G., Rohm and Haas Co., Philadelphia, Pa. The data were analyzed by the method used by Schubert.[2] Conformity of the data with the theory shows that formation of polydentate complexes was negligible, and that no significant absorption of complexes on the resin occurred.

Experimental

The resin was prepared by equilibrating with a solution of sodium perchlorate of the particular ionic strength to be used, until the pH of fresh solution remained constant at 7.0 on prolonged standing in contact with the resin. The resin then was rinsed with distilled water and air-dried. The particle size of the resin was found to be between 28 and 65 mesh. All distribution coefficients

$$K_d = \frac{\%\ \text{Tl in resin}}{\%\ \text{Tl in soln.}} \times \frac{\text{vol. of soln.}}{\text{mass of resin}} \qquad (2)$$

were calculated on the basis of oven-dry resin. The resin had an exchange capacity of 3.9 meq. per gram of oven-dry resin.

Thallium-204 in the form of thallium(I) nitrate at a concentration of 10^{-6} mole per liter was used to determine the

---

[1] R. P. Bell and J. H. B. George, *Trans. Faraday Soc.*, **49**, 619 (1953).

[2] J. Schubert, E. R. Russell and L. S. Myers, Jr., *J. Biol. Chem.*, **185**, 387 (1950).

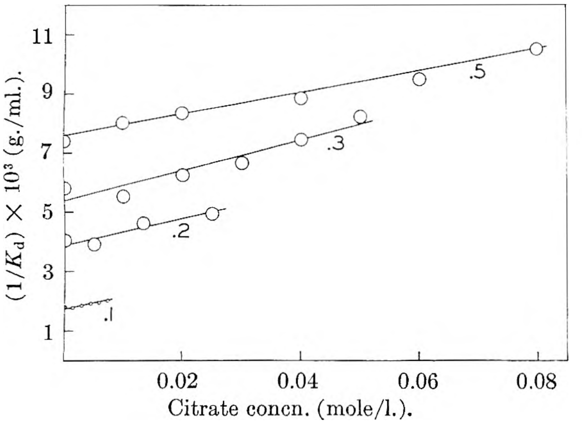

Fig. 1.

distribution coefficients. One-half gram of resin was equilibrated at 25° with 50 ml. of the thallium solution containing varying amounts of trisodium citrate and sufficient sodium perchlorate to bring the ionic strength to a constant value selected for a particular run. Samples of the solutions then were taken and analyzed by radiochemical method for thallium. The *p*H of the solutions was held at 7.0–7.5. The data are shown in Table I. The values of *b*, the intercept, and *m*, the slope, listed in Table I were obtained by the method of least squares. The data are plotted in Fig. 1.

Results

The data were treated according to the equation

$$1/K_d = 1/K_d^\circ + (K_f/K_d^\circ)(A) \qquad (3)$$

where (A) is the concentration of citrate, K_d is the distribution coefficient (2), K_d° the extrapolated value at zero concentration of citrate, and K_f the formation constant for the complex ion from eq. 1. Using the methods of least squares, the value of K_f was determined at four different ionic strengths, 0.1, 0.2, 0.3 and 0.5. The value of K_f° at zero ionic strength was obtained using an equation[3] derived from the Debye–Hückel equation extended to higher concentrations by the use of a "salting out" coefficient, C

$$\log K_f + 3.054\sqrt{\mu} = \log K_f^\circ - C\mu \qquad (4)$$

The coefficient $3.054 = (2^2 - 1^2 - 3^2)(0.509)$. The data are summarized in Table II.

TABLE I

Ionic strength	No. of samples	Citrate concn. (mole/l.)	$(1/K_d \times 10^3)$ (g./ml.)	$b \times 10^3$	$m \times 10^2$	K_f, (l./mole)
0.5	4	0	7.40	7.57	3.40	4.5
	4	0.01	8.02			
	4	.02	8.36			
	4	.04	8.86			
	4	.06	9.49			
	4	.08	10.5			
0.3	6	0	5.81	5.40	5.07	9.4
	6	0.01	5.53			
	6	.02	6.26			
	6	.03	6.68			
	6	.04	7.46			
	6	.05	8.22			
0.2	2	0	4.05	3.90	4.15	10.7
	2	0.005	3.91			
	2	.0167	4.61			
	2	.025	4.96			
0.1	2	0	1.82	1.73	1.90	11.0
	2	0.003	1.78			
	2	.006	1.85			
	2	.009	1.91			
	2	.012	1.95			
	2	.015	2.02			

TABLE II

μ	K_f (l./mole)	$(\log K_f + 3.054\sqrt{\mu})$
0.1	11.0 ± 0.4	2.006
.2	10.7 ± 1	2.394
.3	9.4 ± 1	2.646
.5	4.5 ± 0.8	2.814

A straight line was not obtained, and the data were found to fit the expression $\log K_f + 3.054\sqrt{\mu} = 1.482 + 5.92\,\mu - 6.80\,\mu^2$, from which $K_f = 30 \pm 3$ liters per mole. Comparison with the results of Bell and George[1] for other thallium(I) complexes at low ionic strength shows the value to be in reasonable agreement.

We wish to thank the Research Corporation for a grant in support of this work.

---

[3] S. Glasstone, "Thermodynamics for Chemists," D. Van Nostrand Co., Inc., New York, N. Y., 1947, p. 424.

THE SURFACE PRESSURE OF SOLUBLE BENZOIC ACID FILMS AT WATER-HALOBENZENE INTERFACES

BY JOSEPH J. JASPER AND T. DONALD WOOD

Department of Chemistry, Wayne University, Detroit, Michigan

Received July 16, 1956

The differential method, furnished by a vertical-pull film balance, was used to measure the interfacial surface pressures of soluble benzoic acid films which formed spontaneously between water and three halobenzenes. The pressures were varied by changing the concentrations and the temperatures of the two-phase liquid systems until a maximum and constant value was reached. A table is presented which gives the interfacial surface pressures and the interfacial tensions of the film-covered interfaces as a function of the concentration and temperature, and also the interfacial tension of the pure water-halobenzene systems as a function of the temperature.

A considerable body of data has been accumulated respecting surface films at water–air interfaces as a result of the extensive pioneering efforts of Harkins, Adam, Langmuir and others. The interpretation of the relations obtained when these data are expressed as functions of certain intensive and extensive properties, have furnished valuable knowledge concerning the nature and properties of surface films which has proved to be so useful in numerous aspects of theoretical and applied chemistry. Although a detailed knowledge of water–air interfacial films is now available, a careful review of the literature proved that very few studies of liquid–liquid interfacial films have ever been reported. The experimental difficulties attending accurate surface pressure measurements at liquid–liquid interfaces are considerable when the horizontal float-barrier film balance is used. Furthermore, this apparatus has limited application in liquid–liquid film studies by virtue of the requirement that the film-forming compound not only must be insoluble in both liquid phases, but must have a certain optimum work of adhesion with one of the liquids and a relatively small work of cohesion.[1] As a consequence of the experimental difficulties and the natural restriction on choice of film-forming compounds, little work has been carried out on films at liquid–liquid interfaces. Although the present knowledge of such films is extremely meager, such knowledge is potentially of great importance in a better understanding of certain biochemical processes, detergency, emulsification and other phenomena.

The purpose of the present investigation was to explore the applicability of the differential film balance in the study of the properties of films at liquid–liquid interfaces. This initial effort was directed to a study of the influence of groups of variable electronegativity on the film characteristics of benzoic acid at the interfaces between water and three halogenated benzenes. Since the vertical-pull film balance is applicable to both insoluble and soluble films, and measures the surface pressure directly,[2] this type of apparatus was adopted for use in the present investigation. No mechanism, equivalent to the barrier-float system, is required for varying the surface pressure. This variation is accomplished by additions of the surface active solute to either of the two mutually immiscible liquids, and by varying the temperature. The measurements were, accordingly, made at six temperatures over a range of 19 to 70°. The concentration of benzoic acid was varied at each temperature, and the surface pressure measured at each concentration.

Experimental

Purification of the Compounds.—The compounds used in this investigation were monochlorobenzene, monobromobenzene, monoiodobenzene and benzoic acid as the film-forming compound. The purest grades of the Eastman Kodak Company monohalogenated benzenes were obtained and further purified by vacuum fractionation. This was accomplished with the use of a 15-inch column packed with single-turn glass helices and equipped with a total reflux variable take-off head. The fractionations were carried out twice, each at a different pressure. In each case the middle third was collected for the next stage of the procedure. The refractive indexes of the purified compounds agreed with the values in the "International Critical Tables" to the fifth decimal. The benzoic acid was of reagent grade, and to ensure a high degree of purity, this compound was fractionally crystallized several times. Conductivity water was used for the water phase of the immiscible system. This was prepared in a Barnstead conductivity still by the procedure recommended by the manufacturer. The conductivity of the purified water was found to be of the order of 10^{-6} mho.

Description of the Apparatus.—The apparatus used in this investigation was a modification of the Wilhelmy balance adapted to the measurement of soluble films at liquid–liquid interfaces. A platinum slide plate, constructed in the shape of an inverted "T," carried a cross plate which served to stabilize the motion by damping lateral swinging as equilibrium conditions were approached. The dimensions of the vertical portion were 1 cm. wide, 2 cm. long and 0.25 mm. thick, and those of the horizontal cross plate approximately the same. The slide plate was attached to a gold chain which was suspended from the left arm of a Chainomatic balance. The chain passed through an opening in the base of the balance case at a point directly beneath the normal position of the center of the left pan. A fine platinum wire connected the plate to the chain. The cell designed for the measurements was constructed of Pyrex and had the shape of an oblate spheroid with a diameter of 8.5 cm. and a depth of about 5 cm. A 45/50 female standard joint was sealed in the upper flattened surface of the cell, and in the lower surface a hemi-spherical bubble was blown which was sufficient in diameter to freely accommodate the pendant slide with its horizontal cross plate. The effect was to deepen the cell without greatly increasing the total volume. The male portion of the standard joint was sealed shut about two inches above the ground surface and to this closed end was sealed two parallel glass tubes each 8 mm. in diameter. One of these tubes extended upward along the axis of the joint nearly to the bottom of the balance and served to guide the gold chain into the cell. The other tube was used to introduce solutions of the film-forming compound into the cell. When the ground glass joints were connected the cell was effectively closed to the surrounding water-bath and the chain to stray air currents which might disturb the freely hanging slide plate. A reference line, etched in the glass along the horizontal circumference of the cell, enabled the operator to maintain the interface at a constant level. Great care was taken to prevent the gold chain and platinum wire, which suspended the slide plate, from making contact with the walls of the tube. This was accomplished by careful levelling.

---

[1] N. K. Adam, "The Physics and Chemistry of Surfaces," Oxford Univ. Press, London, 3rd Edit., 1941, p. 99.

[2] W. D. Harkins and T. F. Anderson, *J. Am. Chem. Soc.*, **59**, 2189 (1937).

The thermostat bath consisted of a Pyrex cylinder of about 7.5-gallons capacity enclosed in a large plywood box. Viewing windows were built in the box on opposite sides of the cylinder and these were covered with sheets of Plexiglass to reduce thermal radiation through the windows. The top was covered with a sheet of 0.75 inch plywood. The space between the glass cylinder and the enclosing box was filled with expanded mica, and with this insulation it was possible to maintain the temperature constant to ±0.02° up to 70°. As an aid in maintaining the temperatures below ambient, a Frigidaire refrigeration unit was used to cool a buffer bath to about 10°. The cooling liquid was circulated through a coil in the main bath at such a rate that moderate additions of heat only were required to maintain the desired temperature. The temperatures were measured by means of a NBS certified Leeds and Northrup resistance thermometer used in conjunction with a NBS certified G-2 Mueller bridge made by the same company. The galvanometer used in the bridge circuit was an HS ballistic type with shielded leads. This instrument permitted readings accurate to 0.0001 ohm, but the temperatures were calculated only to 0.001°.

In the manipulation of a film balance such as described above, the force of the surface tension acting downward along the peripheral length of the slide, 2 (width + thickness), is measured directly by an analytical balance. The maintenance of zero contact angle in the organic phase is the most difficult, but extremely important, single requisite of the method. A model LCB Ainsworth Chainomatic balance was used for measuring the interfacial film pressures. The water-bath was mounted on a steel base and the balance on a steel shelf supported by steel framework welded to the base. To ensure minimum vibration, the entire apparatus was placed on steel-to-rubber vibration-damping mountings. The sensitivity of the balance was 0.05 mg. per scale division which is equivalent to 0.025 dyne per cm., for the surface pressure. In all cases it was experimentally possible to reproduce values to ±0.05 dyne per cm.

Experimental Procedure.—Since a zero contact angle between the slide plate and the organic phase only was desired, the surface of the platinum was first rendered clean and hydrophobic by heating it until nearly white hot and then cooling, while slowly rotating, in a smoky flame of benzene. In this way a uniform deposit of carbon black was obtained. The platinum wire, which connected the plate to the gold chain, was also made hydrophobic over the length which was immersed in the water phase. This obviated the necessity of corrections for surface tension effects of the wire. A few centimeters above the water surface the platinum wire was attached to the gold chain which was suspended from the beam of the balance.

The slide was next suspended inside of the measuring cell and the latter, in turn, clamped in position within the thermostat bath. Exactly 82 ml. each of the mutually saturated liquids were now introduced into the cell, first the halobenzene phase, to wet the slide, and then the water phase. When the slide was suspended in proper position it extended through the liquid–liquid interface and was, therefore, in contact with both liquid phases only one of which wet it. Any change in the interfacial surface energy was immediately reflected by a change in the position of the slide. Thus, if the interfacial tension is decreased by the formation of a film at the liquid–liquid interface, the downward pull on the slide will be decreased and it will rise accordingly. The weight on the balance beam is decreased, and this decrease will be proportional to the concentration of the molecular species which has accumulated at the interface.

The bath was brought to the desired temperature and weight added to the balance to raise the slide and to bring the balance pointer to zero position on the scale. At this point the system was tested by allowing it to stand immobile from one to two hours. During this time the position of the balance pointer was observed carefully to detect any changes. Any change in the equilibrium position or weight of the pendant slide was interpreted as being due to incomplete wetting of the plate by the organic liquid, or of the presence of surface active impurities. If such a change was observed the apparatus was disassembled and recleaned.

When the initial testing period was completed the weight was recorded and then small increments of a known aqueous solution of the film-forming benzoic acid were added at definite time intervals. After each addition the weight of the slide was carefully followed as a function of time until equilibrium was reached. The general slope of the curves thus obtained approximated exponential decay functions due possibly to the Doss effect,[3] and the time required to reach equilibrium was linearly dependent on the temperature. Since the addition of the aqueous benzoic acid solution to the system raised the liquid level of the water phase, the buoyancy of the platinum wire changed accordingly. This effect was counteracted to some extent by evaporation, which, in turn, was influenced by the temperature. A travelling microscope, mounted vertically, made it possible to measure concurrently changes in the levels of the two liquids. It was observed that the volume of the organic phase remained invariant while the upper phase increased in volume by 1 ml. for each 1.06×10^{-5} mole of benzoic added. Corrections in the calculations were made for these changes by subtracting, from the apparent film pressure, an amount equivalent to the weight of water displaced. To determine whether equilibrium data were being obtained, the benzoic acid was also added from a halobenzene solution. The results obtained were exactly the same as those from the aqueous solutions.

Results

Preliminary experiments proved that benzoic acid is capillary active in both the aqueous and the organic liquid phases. As a consequence there is established at the interface between these liquids, a positively adsorbed layer which behaves like, and has properties similar to, an insoluble monomolecular film. The theory that the monomolecular layer consists of oriented benzoic acid molecules[4] is justified on the basis of the decrease in the interfacial free surface energy accompanying the formation of the film. If the surface pressure equation[5] is applied to liquid–liquid interfacial films it is written as

$$P_s = \gamma_i - \gamma_f$$

where P_s is the interfacial surface pressure, γ_i the liquid–liquid interfacial tension, and γ_f the liquid–liquid interfacial tension with the film present. In a previous paper[6] empirical equations relating the interfacial tensions to the temperature for the three halobenzenes against water were reported for the temperature range 20 to 80°. With the aid of these equations and the measured interfacial film pressures, it was possible to calculate the effect of the surface layer of benzoic acid molecules on the interfacial free surface energy. The results of these calculations are shown in Table I. Each film pressure tabulated represents the equilibrium value, and time *versus* temperature curves (not shown) proved that the velocity of attainment of equilibrium was, in every case, a linear function of the temperature. A comparison of the interfacial tensions of the halobenzene–water systems, at the different temperatures, shows increasing values in the order chlorobenzene, bromobenzene and iodobenzene. The surface pressure also increases in this direction, and, in general, the decrease in the interfacial free surface energy attending the positive adsorption of benzoic acid in the interface is

---

[3] K. S. G. Doss, *Kolloid Z.*, **84**, 138 (1938); **86**, 205 (1939).

[4] W. D. Harkins, "The Physical Chemistry of Surface Films," Reinhold Publ. Corp., New York, N. Y., 1952, p. 35.

[5] Ref. 4, p. 121.

[6] J. J. Jasper and T. D. Wood, THIS JOURNAL, **59**, 541 (1955).

TABLE I

THE FILM PRESSURES AND INTERFACIAL TENSIONS AT THE LIQUID–LIQUID INTERFACES (ERGS./CM.^{2})

Temp., °C.	Moles of benzoic acid ($\times 10^{-6}$)	Chlorobenzene			Bromobenzene			Iodobenzene		
		P_s	γ_i	γ_i	P_s	γ_i	γ_f	P_s	γ_i	γ
19.457	1.63	0.70	38.12	37.42	3.15	39.33	36.18	6.50	41.54	35.04
	4.89	1.20		36.92	5.20		34.13	11.60		29.94
	8.15	1.60		36.52	6.35		32.98	14.10		27.44
	13.59	2.10		36.02	7.40		31.93	16.00		25.54
	19.02	2.15		35.97	7.75		31.58	16.15		25.39
	29.82				7.80		31.53			
29.558	1.63	0.60	37.74	37.14	3.00	38.70	35.70	6.00	40.88	34.88
	4.89	1.00		36.74	5.10		33.60	10.50		30.38
	8.15	1.50		36.24	6.20		32.50	12.45		28.43
	13.59	1.90		35.84	7.20		31.50	14.65		26.23
	19.02	2.05		35.69	7.30		31.40	14.85		26.03
	29.82				7.35		31.35			
39.582	1.63	0.40	37.25	36.85	2.80	37.99	35.19	5.50	40.15	34.65
	4.89	0.95		36.30	4.90		33.09	9.50		30.65
	8.15	1.30		35.95	6.05		31.94	11.80		28.35
	13.59	1.75		35.50	6.80		31.19	13.45		26.70
	19.02	1.95		35.30	6.90		31.09	13.60		26.55
49.607	1.63	0.45	36.60	36.15	2.70	37.20	34.50	4.00	39.34	35.34
	4.89	0.90		35.70	4.55		32.65	8.05		31.29
	8.15	1.25		35.35	5.60		31.60	10.30		29.04
	13.59	1.70		34.90	6.40		30.80	12.65		26.69
	19.02	1.90		34.70	6.50		30.70	12.90		26.44
59.691	1.63	0.40	35.82	35.42	2.55	36.34	33.79	3.75	38.45	34.70
	4.89	0.80		35.02	4.20		32.14	7.40		31.05
	8.15	1.20		34.62	5.10		31.24	9.60		28.85
	13.59	1.55		34.27	6.00		30.34	12.05		26.40
	19.02	1.80		34.02	6.15		29.19	12.55		25.90
	29.82	1.85		33.97						
69.568	1.63	0.35	33.22	32.87	2.45	35.40	32.95	3.20	37.51	34.31
	4.89	0.75		32.47	4.00		31.40	6.65		30.86
	8.15	1.10		32.12	4.80		30.60	9.05		28.46
	13.59	1.50		31.72	5.65		29.75	11.45		26.06
	19.02	1.75		31.47	5.90		29.50	12.25		25.26
	29.82	1.80		31.42						

greatest for the iodobenzene–water system. Three exceptions, however, are noted. For the systems involving the least benzoic acid at 49.607 and 59.691°, the value of γ_f for bromobenzene is slightly less than that for iodobenzene, while at 69.568° iodobenzene has the largest value. The reason for this deviation from general behavior is not clear since preliminary surface tension studies of solutions of benzoic acid in the three halobenzenes showed that positive adsorption of the acid was the greatest in iodobenzene over a concentration range whose smallest value was somewhat greater than the smallest one given in the table. Repeated trials gave the same results. The surface pressure increased with successive additions of benzoic acid to each of the halobenzene–water systems at all temperatures. This effect, however, decreased as the temperature was raised, due probably to the increased kinetic activity of the molecules in the interfacial region.

The highest value of the interfacial surface pressure recorded for each temperature represents the maximum attainable for the benzoic acid films which formed spontaneously at the interface between the given liquid solutions. Any further additions of benzoic acid merely extended the horizontal portion of the surface pressure isotherm, and this appears to justify the assumption that a degree of saturation was reached commensurate with the state of the film. Since both liquid solutions of the three systems described must contribute benzoic acid to the interfacial films, the concentration factor of the Gibbs equation is at present unknown. If the equilibrium concentrations of each liquid solution could be measured the surface concentration might be found from differences. The concentrations used in this investigation were, of a necessity, very small, and the experimental determinations of the equilibrium concentrations cannot be made by ordinary methods. It was not possible, therefore, to calculate the effective area of the benzoic acid molecule oriented in the interface, nor to describe the state of the interfacial films. Application of the Traube equation[7] may be justified for the smaller surface pressures and calculations for these pressures indicated that the films were gaseous.

---

[7] I. Langmuir, *Gen. Elect. Rev.*, **38**, 402 (1935).

KINETICS OF NITRIDATION OF MAGNESIUM AND ALUMINUM[1,2]

BY PRASOM STHAPITANONDA AND JOHN L. MARGRAVE

Department of Chemistry, University of Wisconsin, Madison, Wisconsin

Received July 23, 1956

The kinetics of nitridation of magnesium and aluminum has been studied as a function of time, temperature, pressure and surface preparation. A manometric apparatus was employed for all of the measurements. Nitridation of magnesium is quite appreciable at 415° and higher where the rate is found to follow a linear rate law closely. The relatively high vapor pressure of magnesium in the temperature range studied interferes with the measurements, and sets a high temperature limit at about 500°. The rate equation for the Mg–N system is $k(\text{mg./cm.}^2\text{-hr.}) = 2.2 \times 10^4\ e^{-22,300/RT}$ as compared to $k(\text{mg./cm.}^2\text{-hr.}) = 6.2 \times 10^{12}\ e^{-50,500/RT}$ for the Mg–O system. Studies of the initial nitridation period for magnesium from 300 to 400° show that the rate of nitridation is faster than that of oxidation in the low temperature range. The lower limit of temperature where the nitridation of magnesium begins is about 300°. The temperature where the rate constant for oxidation is equal to that for nitridation is about 460°; at higher temperatures, the rate of oxidation is faster than that of nitridation. Nitridation of aluminum has been studied over the temperature range 530 to 625°. The linear rate law is obeyed for low temperatures, up to 580°, while a parabolic rate law is more suitable for the interpretation at higher temperatures. The linear rate equation for the Al–N system is $k = 58e^{-17,900/RT}$ mg./cm.^{2}-hr. as compared to $k = 2.34 \times 10^{11}\ e^{-47,700/RT}$ mg./cm.^{2}-hr. for the Al–O system. The parabolic rate equation for the Al–O system has been reported as $k = 1.35 \times 10^3\ e^{-22,800/RT}$ mg.^{2}/cm.^{4}-hr., while in this work for the Al–N system, $k = 4.2 \times 10^{10}\ e^{-63,700/RT}$ mg.^{2}/cm.^{4}-hr. Studies of the initial nitridation period of aluminum at 400° and higher show that the rate of nitridation is much slower than the rate of oxidation at a given temperature.

Most of the work in the field of gas–solid kinetics at high temperatures has been concerned with the kinetics of oxidation of various metals and alloys. Since the air consists largely of nitrogen and since many stable nitrides are known, it is of considerable interest to study the kinetics of nitridation of metals, particularly of the active metals like magnesium and aluminum. There is probably no great difference in the chemical processes occurring and the theories which are applicable to oxidation reactions should hold for nitridation reactions as well. Similar experimental methods may also be used for studies of each.

Observations of the oxidation rates of metals and alloys now in the literature have been systematized on the basis of various "laws": the linear rate law, for which the weight gain or increase in film thickness depends directly on the time; the parabolic rate law, for which the square of the weight gain or film thickness depends directly on time; and the logarithmic rate law, for which there is an exponential relationship between weight gain or film thickness and time. These laws have been discussed in detail by Kubaschewski and Hopkins[3] and many earlier workers.

The temperature dependence of reaction rates can be considered on the basis of an Arrhenius-type equation

$$W = Ae^{-Q/RT}$$

where Q = energy of activation, W = reaction rate constant, A = constant, and R and T have their usual meanings. Gulbransen[4] has applied the absolute reaction rate theory and shown it to be applicable for several metal oxidations.

Previous Work on Mg–Gas, Al–Gas Systems

Reviews on the rates of oxidation and nitridation of metals may be found in the recent work of Kubaschewski and Hopkins.[3]

Magnesium.—Magnesium is known for its reactivity with oxygen at high temperature and has long been used as a getter in high vacuum systems. Very thin layers of MgO are protective as seen by the nearly parabolic rate of oxidation observed by Gulbransen[5] in the very early stages at temperatures lower than 475°. Thickening of the oxide film results in the loss of protective properties since the molar volume ratio of MgO is 0.81,[3] and a linear rate of oxidation is observed at higher temperatures.[5–8]

Values for the kinetic constants of this process were reported by Leontis and Rhines.[6] Further study of this reaction at temperatures higher than 575° is interrupted by the high rate of evaporation of magnesium. At still higher temperatures Mg ignites, as observed by Fassell, *et al.*,[9] at about 623° with 1 atm. pressure of oxygen.

Terem[10] has studied the rate of nitridation of Mg by a gravimetric method and reported very low rates at temperatures lower than 460°. The nitridation rate becomes appreciable at 480° and higher. A protective film was found at the end of 20 min. at 540° and after 5 min. at 560°. This is interesting since the molar volume ratio of Mg_3N_2 is 0.89,[2] and one would expect film cracking at higher temperatures as in the case of MgO. The reactivity of Mg_3N_2 to humidity and oxygen in air may have been responsible for this deviation. MgO or $Mg(OH)_2$ formed by the reaction of Mg_3N_2 and O_2 or H_2O may become protective. The results of Terem need to be checked in a dry atmosphere with continuous readings to avoid the possibility of contamination from the atmosphere.

Aluminum.—Up to 350°, Al and O_2 undergo interfacial reaction with initial film formation as reported by Gulbransen and Wysong.[11] The film

---

(1) Abstracted in part from the thesis presented by Prasom Sthapitanonda in partial fulfillment of the requirements for the degree of Doctor of Philosophy at the University of Wisconsin in March, 1955.

(2) Presented at the 129th Meeting of the American Chemical Society in Dallas, Texas, April 12, 1956.

(3) O. Kubaschewski and B. E. Hopkins, "Oxidation of Metals and Alloys," Academic Press, Inc., New York, N. Y., 1953.

(4) E. A. Gulbransen, *Trans. Electrochem. Soc.*, **83**, 301 (1943).

(5) E. A. Gulbransen, *ibid.*, **87**, 589 (1945).

(6) T. E. Leontis and F. N. Rhines, *Trans. Am. Inst. Mining Met. Engrs.*, **166**, 265 (1946).

(7) I. A. Makolkin, *Zh. prik. Khim.*, **24**, 460 (1951).

(8) H. N. Terem, *Rec. Fac. Sci. Univ. Istanbul*, **13A**, 147 (1948).

(9) W. M. Fassell, L. B. Gulbransen, J. R. Lewis and J. H. Hamilton, *J. Metals*, **3**, 522 (1951).

(10) H. N. Terem, *Rev. Fac. Sci. Univ. Istanbul*, **16A**, 81 (1951).

(11) E. A. Gulbransen and W. S. Wysong, THIS JOURNAL, **51**, 1087 (1947).

thickness then offers some resistance and results in a parabolic rate of oxidation for temperature from 350–475°. At higher temperatures than 475°, where film cracking takes place, the oxidation follows closely the linear rate as expected from the theory of Cabrera and Mott.[12] At room temperature, Cabrera and Hamon[13] have shown that there is a protective film about 20 Å. thick, but the rate of reaction failed to fit either the parabolic or the linear rates.

The rate of nitridation of Al has also been studied by Terem[10] for the temperature range 760–1050° in dry N_2. It was reported that the metal reacts easily with increasing activity at higher temperatures. The nitridation product, AlN, seemed to maintain its weight in a desiccator for 5 hr., whereas Mg_3N_2 and Be_3N_2 gained weight, possibly due to reaction with traces of moisture or O_2.

Since there are not sufficient data on the nitridation of Mg and Al, and the available data are only qualitatively reported,[10] this work was undertaken to obtain quantitative data on the kinetics of nitridation of these metals for comparison with the data on rates of oxidation which are available.

From the molar volume ratios for Mg_3N_2 and AlN (0.89 and 1.28), the rate of nitridation of Mg should be linear while that of Al should be parabolic, according to Pilling and Bedworth.[14] An appreciable amount of Mg_3N_2 is formed on heating the metal in a limited amount of air, indicating that the rate of nitridation of Mg may be fairly close to the rate of oxidation.

Experimental Apparatus and Procedure

Manometric Apparatus.—It was decided that the rates of nitridation of Mg and Al should be measured by the manometric method which is simple, and yet provides results of reasonable accuracy. For instance, see the works of Cubicciotti and co-workers.[15-18]

The apparatus was similar to that used by Campbell and Thomas[19] but modified for use at the higher temperatures of this work. Two Vycor glass bulbs of about 85-cc. capacity with two air-cooled standard taper 29/42 joints were connected to a Pyrex manometer and a high vacuum system. The Vycor bulbs were placed in an electric resistance heating furnace whose temperature was maintained constant to ±5°. The manometer fluid was Octoil, a low vapor pressure liquid used in oil diffusion pumps.

The volumes of the Vycor tubes were determined by filling with water of known density. The total volume of the manometric apparatus was also determined by this method. The capillary tube employed as the manometer was assumed to be uniform and the average diameter of the bore was measured by a microscope equipped with a calibrated-scale eyepiece. The two Vycor tubes were specially made to have volumes as close as possible (within 1%) so that the calculations of the weight-gain of the sample, which will be described later, may be done with ease. Apiezon-T high vacuum grease was used for all the joints in this system.

The reaction bulbs and the differential manometer were connected to the high vacuum system by a three-way stopcock which also led to a 5000-cc. gas reservoir. The pressure of the gas was measured by a mercury manometer. The gas reservoir was connected to a purification train consisting of a column of $Mg(ClO_4)_2$ and a column of hot reduced Cu. The high vacuum may be applied directly to the gas reservoir part, or to the manometric part, or both at the same time.

Furnace.—An electric resistance heating furnace was used for temperatures up to 1000°. It had a 3 in. diameter, a central cavity 9 in. deep, and was large enough to permit the insertion of the twin tubes of the manometric apparatus. Fiberfrax packing was used to fill up the space in the furnace core and two thermocouples were placed at the middle of the furnace. The furnace was insulated by asbestos packing and operated on the 115 volt a.c. lines.

The temperature was controlled by a Gardsman Model JP Indicating Pyrometric Proportioning Controller with a Pt/Pt–10% Rh thermocouple. Another thermocouple was used to read the temperature of the furnace directly with a potentiometer. The uncertainty in temperature control and measurement was about ±5°.

Sample Preparation.—Spectroscopically pure Mg and Al rods were obtained from Johnson, Matthey and Co., England. The Mg rods were 6.35 mm. in diameter and 10.15 cm. long, and spectrographic examination by the manufacturer showed the following impurities in the sample: 0.01% Fe, 0.005% Mn, 0.005% Al, 0.001% Si, 0.0001% Cu and less than 0.005% Pb. The Al rods were 6.25 mm. in diameter and 15.25 cm. long, and spectrographic examination by the manufacturer showed the following estimated amounts of impurities in the sample: 0.001% Mg, 0.001% Si, 0.0005% Cu and less than 0.005% Fe.

In addition, commercial Mg and Al of approximately 99% purity have been used with good results. Spectrographic analyses of these metals showed no pertinent lines except a few impurity lines at very low intensities.

The specimens were abraded and finished with No. 320 paper under purified kerosene to minimize formation of oxide films, cleaned and kept in a vacuum desiccator until used. The surface area of the specimen was determined by a combination of dimension and weight measurements with a known value of density of metal.

In cases where coating of the metal by a thin film of oxide was desired to reduce the rate of evaporation, it was accomplished by heating momentarily over a hot plate at about 300°. By heating in a furnace under an atmosphere of N_2 at about 400° for half an hour, Mg was given a nitride film.

Gas Purification.—The pre-purified nitrogen was passed over hot reduced Cu at 400° and a column of $Mg(ClO_4)_2$ to remove O_2 and H_2O. The effects of the purification were evaluated by mass spectrographic analyses of the gases.

Experimental Procedure.—A sample of metal of known area was placed in one bulb of the manometric apparatus while the other was left empty, and the whole system evacuated to about 10^{-4} to 10^{-6} mm. pressure. The out-gassing of the metal was then done at the same or a slightly lower temperature than that of the kinetics run. When the pressure in the system, cut off from the vacuum system, changed by less than 1 mm. per hour, the system was considered to be satisfactory.

Nitrogen was admitted into both bulbs and readings were taken on the manometer as the nitridation progressed. When the pressure difference between the bulbs reached about 5 mm., additional N_2 was bled into the bulb containing the sample so that the pressure of N_2 over the sample was constant (to ±5 mm.) during the reaction. The manometer readings could then be converted into the amount of N_2 consumed by a formula given by Campbell and Thomas.[19]

Calculations of weight gain could be made for two conditions, depending on which reaction tube was used for the sample. However, in most cases, the sample was placed in the left-hand tube. An additional correction factor is needed for gases other than oxygen.

The validity of the formulas has been checked by observing the amount of oxygen absorbed by a tantalum sheet (24 in.^{2} area) at various time intervals over a temperature range 400–500° where the oxidation is quite appreciable. The pressure change in the system caused by the oxidation was converted into weight gain by the formulas; then the system was evacuated and cooled, and the weight gain directly measured on an analytical balance. The results agreed to better than 10% in most cases.

---

[12] N. Cabrera and N. F. Mott, *Reports Prog. Phys.*, **12**, 163 (1949).

[13] N. Cabrera and J. Hamon, *Compt. rend.*, **224**, 1713 (1947).

[14] N. B. Pilling and R. F. Bedworth, *J. Inst. Metals*, **29**, 529 (1923).

[15] R. B. Bernstein and D. Cubicciotti, *J. Am. Chem. Soc.*, **73**, 4112 (1951).

[16] M. B. Brodsky and D. Cubicciotti, *ibid.*, **73**, 3497 (1951).

[17] D. Cubicciotti, *ibid.*, **72**, 2084 (1950); **72**, 4138 (1950); **74**, 557 (1952); **74**, 1079 (1952); **74**, 1200 (1952).

[18] P. Levesque and D. Cubicciotti, *ibid.*, **73**, 2028 (1951).

[19] W. E. Campbell and U. B. Thomas, *Trans. Electrochem. Soc.*, **91**, 623 (1947).

Discussion of Results

Nitridation of Magnesium.—Studies of this metal have been beset by one major difficulty: the relatively high vapor pressure of magnesium. Brewer[20] has given the vapor pressure of Mg at 382° as 10^{-6} atm., and at 516° as 10^{-4} atm. Since the vacuum employed in this work was generally better than 10^{-4} mm., the outgassing of Mg samples was done at much lower temperatures than the temperatures of kinetic studies, which were 300° and higher.

Some vaporization of Mg during the kinetics runs has been observed, and could not be absolutely avoided. This has set a higher limit on the temperature for this work. Experimental data at the higher temperatures are definitely less accurate. It was found that at higher temperatures than 500° Mg vaporizes to a black solid, and that reaction between the metal and nitrogen mostly occurs in the gas phase.

(a) **Time Effect.**—Figure 1 shows the time course of a typical kinetic run: the nitridation of Mg by dry, pre-purified N_2 at 465°. The course of reaction may generally be divided into 3 parts: initial nitridation, nitridation and evaporation, as indicated on the curve. The initial nitridation period is always observed, even at relatively low temperatures where the nitridation rate is slow. Evaporation of the sample has also been observed for all prolonged runs, and is the important factor which limits the temperature range of study. Most kinetic runs at temperatures higher than 500° show this deviation due to evaporation. The rate of nitridation of magnesium is determined from the center part of the curve where the rate follows closely a linear rate law.

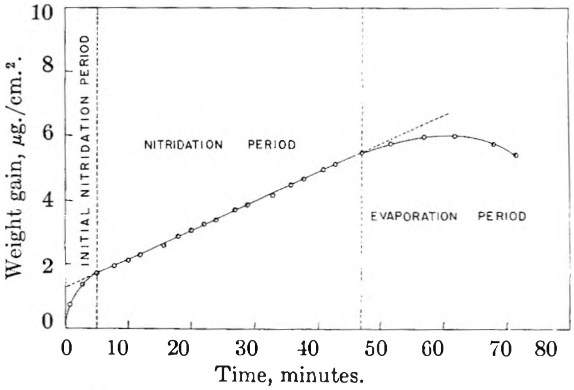

Fig. 1.—Nitridation of magnesium at 465° (P_{N_2} = 100 mm.).

The evaporation of Mg which affects the kinetic study has also been observed in the Mg–O system by Gulbransen[5] and Leontis and Rhines.[6] One must either study Mg at low temperatures or have a "protective film," but even a film is not fully protective, and as temperature is continually increased a film-cracking process has been observed as the result of evaporation.

(b) **Temperature Effect.**—The effect of temperature on the rate of nitridation of Mg over the temperature range 415 to 485° is shown in Fig. 2. The weight gain in micrograms per cm.² is plotted against the time in minutes. Assuming the ratio of the real to the measured area to be unity and the nitride to be Mg_3N_2, the thickness of the film in Å. is 1.331 times the weight gain in microgram per cm.². A scale of 1 Å. is marked on the curves.

Linear rate constants for the nitridation of Mg at various temperatures are listed in Table I together with one from the work of Leontis and Rhines.[6] The reproducibility of the measurements was such that three runs at the same experimental conditions gave k's that may agree within ±25%. The discrepancy may be due to errors in measurement of the dimensions of the samples, if the surface roughness from one sample to another is different. However, the uncertainty in log k is less than ±5% in most cases. The temperature uncertainty is about ±5° as previously mentioned.

TABLE I

LINEAR RATE CONSTANTS FOR THE NITRIDATION OF MAGNESIUM (P_{N_2} = 100 mm.)

t, °C.	T, °K.	$10^4/T$	k, (mg./cm.²-hr.)	−log k
415	688	14.535	1.84×10^{-3}	2.735
440	713	14.025	3.20×10^{-3}	2.468
450	723	13.831	4.00×10^{-3}	2.398
465	738	13.550	5.40×10^{-3}	2.268
473	746	13.405	6.20×10^{-3}	2.208
485	758	13.193	8.80×10^{-3}	2.055
550[a]	823	12.151	2.60×10^{-2}	1.585

[a] From Leontis and Rhines,[6] using 99% N_2.

Figure 3 shows a comparison of log k *vs.* $1/T$ plots for the Mg–O system previously reported and the Mg–N system as observed in this work. The uncertainty in the rate constants and the temperatures is indicated by the lines drawn through the points located on the curve. A straight line may be drawn through the 6 experimental points by the method of least squares, and the rate equation may be calculated. For N_2, k(mg./cm.²-hr.) = $2.2 \times 10^4\ e^{-22{,}300/RT}$ as compared with k(mg./cm.²-hr.) = $6.2 \times 10^{12}\ e^{-50{,}500\ RT}$ previously reported for O_2.

A rate constant observed by Leontis and Rhines[6] falls on the extrapolated curve from the data even though they used 99% pure N_2 as a gas supply while in this work the N_2 was found to be about 99.99% pure. This indicates that the absolute rate of oxidation at that temperature, *i.e.*, 550°, may not be too greatly different from that of nitrogen.

Since the activation energy of the Mg–O system is 50,500 cal./mole as compared to 22,300 cal./mole for the Mg–N system, the two curves cross at a certain temperature where the rate of nitridation is equal to that of oxidation; at lower temperatures the rate of nitridation is greater than the rate of oxidation. Studies at very low temperatures of reactions of N_2 and O_2 with Mg have confirmed this prediction, and will be discussed in a later section dealing with initial nitridation period.

(c) **Pressure Effect.**—The effect of pressure on the reaction at 465° is shown in Fig. 4. The pressure was varied from the standard 100 mm. to 200 and 20 mm. The effect is, however, not great enough to indicate that the rate depends largely on the pressure. At low pressures, the study was made with difficulty. Fluctuation of the rate data is generally found in this type of measurement with manometric apparatus for extremely low or high pressures. The pressure 100 mm. was selected because it generally produced satisfactory rate data.

---

[20] L. Brewer, "The Thermodynamic and Physical Properties of the Elements," in L. L. Quill, "The Chemistry and Metallurgy of Miscellaneous Materials: Thermodynamics," McGraw-Hill Book Co., New York, N. Y., 1950.

No simple relationship with the pressure has been determined, and the effect of pressure on the reaction rate is small. The rate constant changes about 10% for pressure change from 100 to 200 mm. and about 20% for pressure change from 100 to 20 mm. The standard runs at the pressure 100 mm. with an uncertainty of ±5 mm. were independent of pressure fluctuation during the runs.

(d) **Effect of Abrasion.**—There was no significant effect on the rate constant when either abraded or unabraded samples were used, but the abraded sample reacted much faster at the beginning of the run than the unabraded one. After nitridation Mg samples show thin films, white or light yellow in color, depending on the length of nitridation and the temperature of the system.

(e) **Initial Nitridation Period.**—As previously mentioned, the rate of nitridation of Mg may be faster than that of the oxidation at relatively low temperatures. Some studies have been carried out at low temperatures for the reactions of Mg with N_2, O_2 and air. The gas pressures were set at 100 mm. for all runs.

Table II shows the results of such studies. Assuming the ratio of the real to the measured area to be unity and the reaction products to be Mg_3N_2, MgO, or a mixture of these two compounds directly proportional to the N_2:O_2 ratio in the air, the thickness may be calculated by employing the conversion factors: 1.331, 0.703 and 1.205 Å./μg./cm.^{2} for N_2, O_2 and air, respectively. The system was evacuated while the temperature was raised, and then new gas was bled in to start a new run at the new temperature.

TABLE II

INITIAL FILM THICKNESSES

Temp., °C.	Film thickness, A. Nitrogen	Oxygen	Air
325	3.15		
330		No reaction	
345	5.37	No reaction	
365	6.26	0.40	
385		.79	
405	6.94		2.70
415	10.63		
425			3.50
430			4.88
445	15.22		
455			6.44
465			8.97

The results obtained here are significant in two ways: (1) they show that the rate of nitridation is really faster than that of oxidation in the low temperature range. At 345° where oxidation is not yet detectable, nitridation is already well under way. (2) The lower limit of temperature where the nitridation begins is about 300° and this tends to invalidate the conclusion of Terem[10] who used a less accurate gravimetric method to study this same problem.

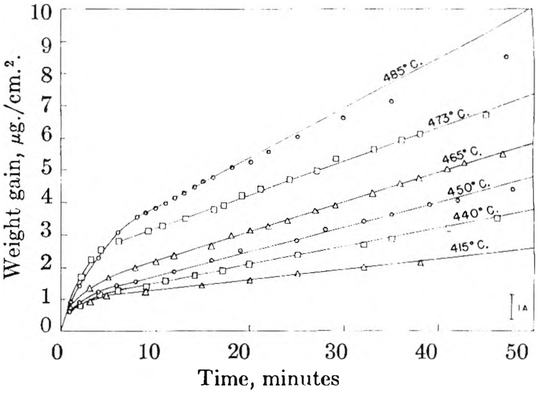

Fig. 2.—Nitridation of magnesium: effect of temperature (P_{N_2} = 100 mm.).

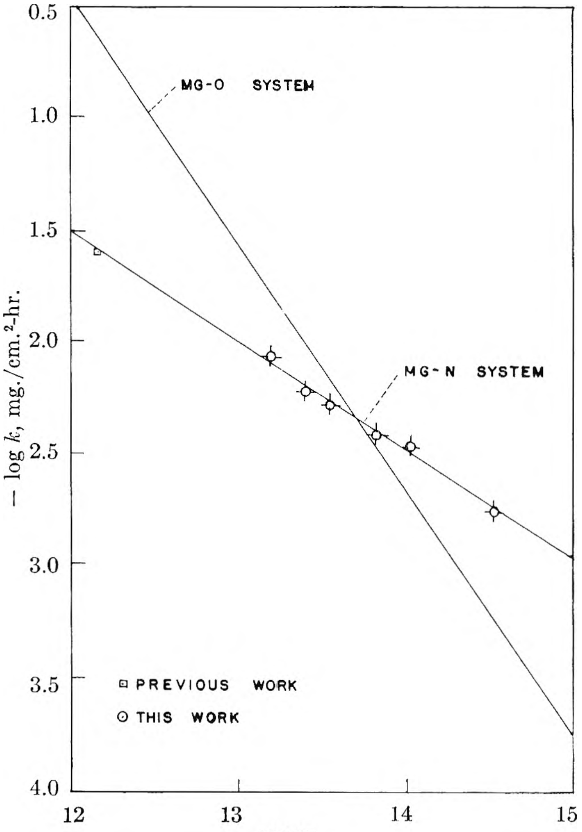

Fig. 3.—Nitridation of magnesium: a comparison of log K *vs.* $1/T$ plots for the Mg–O and Mg–N systems.

Even though magnesium starts to react with nitrogen at low temperatures, the reaction is only of the film-forming type and is almost completely stopped after a certain film thickness has been formed. Therefore, at any temperature lower than 415° where the nitridation period itself becomes appreciable, one may neglect the reaction as a source of corrosion as compared to other reactions. For example, rapid oxidation in a humid atmosphere is noted by other workers.[6,10] However, $Mg(OH)_2$ formed under such conditions will also act as a protective coating as it has a high molar volume ratio, *i.e.*, 1.74.[3]

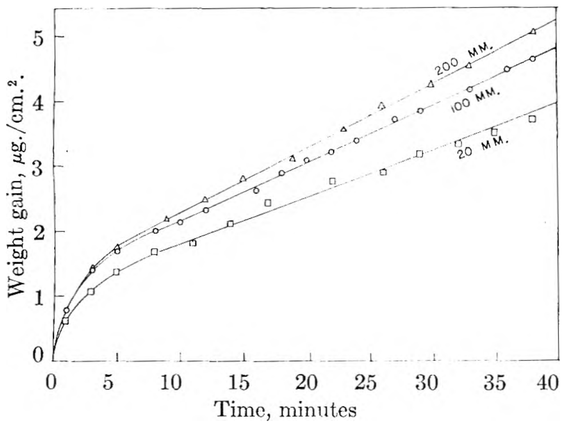

Fig. 4.—Pressure effect on nitridation of magnesium at 465°.

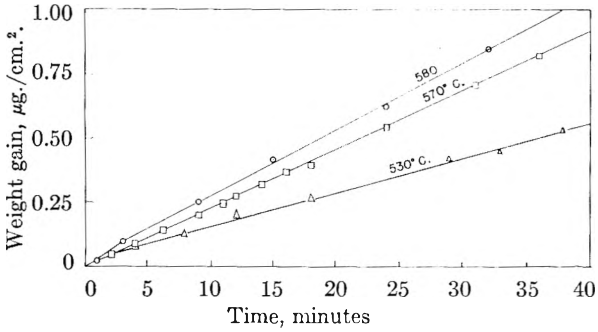

Fig. 5.—Nitridation of aluminum: effect of temperature (P_{N_2} = 100 mm.).

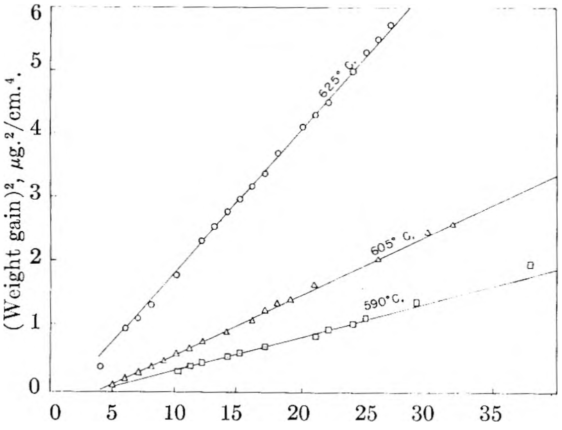

Fig. 6.—Nitridation of aluminum: effect of temperature (R_{N_2} = 100 mm.).

Nitridation of Aluminum.—Nitridation studies on aluminum have not been complicated by any difficulty due to its vapor pressure since the pressure is relatively low in the temperature range of interest. Brewer[20] has given the vapor pressure of Al at about 1000° as 10^{-6} atm. However, these studies were limited by the melting point of Al to temperatures below 932°K.

(a) **Time and Temperature Effects.**—Nitridation of Al in the temperature range studied, 530 to 625°, does not follow exclusively either the linear law or the parabolic law; it starts off with a linear rate which turns into a parabolic rate at still higher temperatures. The temperature where the change from the linear to parabolic rate takes place is around 580 to 590° and the rate measurements in that region may be interpreted in either way. The run at 590° tends to follow close to a parabolic law while the run at 580° tends to follow close to a linear rate law. Figure 5 shows the rates of nitridation of Al in the temperature range 530 to 580° and Fig. 6 shows the rates from 590 to 625°.

The linear rate constants for the nitridation of Al at various temperatures are tabulated in Table III and the parabolic rate constants are tabulated in Table IV. The reproducibility of these measurements was slightly better than in the case of magnesium. Runs under the same experimental conditions varied about ±15% for values of the rate constants. The method of least squares was used to obtain the rate equations. In the linear region, the results for N_2 give $k = 58e^{-17,900/RT}$ mg./cm.^{2}-hr. as compared to $k = 2.34 \times 10^{11} e^{-47,700/RT}$ mg./cm.^{2}-hr. previously reported for O_2.[21] From 590 to 625°, where the parabolic rate has been observed, $k = 4.2 \times 10^{10} e^{-23,700/RT}$ mg.^{2}/cm.^{4}-hr. for nitridation as compared to $k = 1.35 \times 10^3 e^{-22,800/RT}$ mg.^{2}/cm.^{4}-hr. for parabolic oxidation as reported by Gulbransen and Wysong.[11] Both rates of oxidation are much more rapid than the rates of nitridation, and corrosion of Al due to nitridation is nearly negligible.

TABLE III

LINEAR RATE CONSTANTS FOR THE NITRIDATION OF ALUMINUM (P_{N_2} = 100 MM.)

t, °C.	T, °K.	$10^4/T$	k, (mg./cm.^{2}-hr.)	−log k
530	803	12.453	8.0×10^{-4}	3.097
570	843	11.862	1.35×10^{-3}	2.870
580	853	11.723	1.55×10^{-3}	2.810

TABLE IV

PARABOLIC RATE CONSTANTS FOR THE NITRIDATION OF ALUMINUM (P_{N_2} = 100 MM.)

t, °C.	T, °K.	$10^4/T$	k (mg.^{2}/cm.^{4}-hr.)	−log k
590	863	11.587	3.15×10^{-6}	5.502
605	878	11.389	5.58×10^{-6}	5.253
625	898	11.136	1.33×10^{-5}	4.876

(b) **Pressure Effect and Effect of Abrasion.**—The effect of pressure on the nitridation of Al is very small and within the limit of other sources of experimental errors. The same difficulty of fluctuation of rate data at extremely low and high pressures has been observed in this case, as for magnesium. Thus the 100 mm. gas pressure was adopted for the standard gas pressure to be used throughout the experiments since it gave the least fluctuation. The rate constants change less than 10% for pressure change of 2- to 5-fold. The rate measurements at constant pressure with ±5 mm. uncertainty should be independent of pressure.

Abrasion is the cause of a great difference in the initial nitridation period, probably because of the removal of the thin oxide film usually covering the metal. The rate constant, as a whole, fails to show any significant change beyond the experimental errors. The rate measurements, however, in this work were done on abraded samples with shiny surfaces. The nitrided Al sample showed interference

---

(21) W. J. Moore, *J. Electrochem. Soc.*, **100**, 302 (1953).

colors ranging from gold to blue or purple, depending on the thickness of the nitride film formed.

(c) **Initial Nitridation Period.**—Studies were carried out to find the lowest temperature where nitridation may be observed with the sensitivity of this apparatus. At 450° there was no reaction at all for nitridation, whereas oxidation, as observed in this work and as previously reported, has already taken place in a significant amount, *i.e.*, at the end of 30 minutes the gain in weight is 3.5 μg./cm.^{2}. The results of these studies are shown in Table V and are compared with those reported by Gulbransen and Wysong on the oxidation.[11]

TABLE V

INITIAL NITRIDATION PERIOD OF ALUMINUM; COMPARISON OF NITRIDATION WITH OXIDATION OF ALUMINUM IN THE SAME TEMPERATURE REGION

t, °C.	Gas	Wt. gain at the end of 30 min., μg./cm.^{2}
400	O_2	2.90
450	O_2	3.50
450	N_2	No reaction
475	O_2	6.80
475	N_2	0.10
500	O_2	8.80
515	N_2	0.25

Al does not show any significant reaction with N_2 until the temperature is raised to 530° where an appreciable amount of nitridation has been observed. This is to be contrasted with the report by Terem[10] that the nitridation begins at 760°. As in the case of Mg, Terem's technique was probably not sensitive enough to observe the reaction taking place at lower temperatures.

Acknowledgment.—This research was in part conducted under Contract No. AF 33(616)-338 with the United States Air Force, the sponsoring agency being the Aeronautical Research Laboratory of the Wright Air Development Center, Air Research and Development Command.

HYDRODYNAMIC AND THERMODYNAMIC PROPERTIES OF BOVINE SERUM ALBUMIN AT LOW pH[1]

BY GEORGE I. LOEB AND HAROLD A. SCHERAGA

Department of Chemistry, Cornell University, Ithaca, New York

Received July 27, 1956

Hydrodynamic measurements (sedimentation and viscosity) have been carried out on bovine serum albumin at pH 4.0 and 5.13 in 0.5 M KCl in order to assess the influence of the molecular configuration on the apparently anomalous ionization behavior of the carboxyl groups. From the sedimentation–diffusion molecular weight and the computed hydrodynamic parameter β it is concluded that the hydrodynamic properties of bovine serum albumin can be interpreted in terms of an equivalent sphere at *both* pH 4.0 and 5.13, the volume at pH 4.0 being only about 11% greater than that at pH 5.13. This increase in volume at the lower pH can account for only a small part of the anomalous reactivity insofar as it influences the electrostatic contribution to the free energy of ionization. To circumvent this difficulty Tanford and co-workers have introduced a discontinuity into the description of the molecular model by allowing for penetration of ions at low pH but not above pH 4.3. Even with this discontinuity, the analysis of Tanford and co-workers accounts only for the slopes but not the absolute values of the pH dependence of the thermodynamic parameters. On the other hand, with the use of a reasonable empirical electrostatic contribution (*i.e.*, wZ *vs.* pH curve), both the slopes and absolute values can be accounted for by expanding on a previous suggestion of reversible formation and breakage of internal hydrogen bonds. Calculations on this basis are reported here to show that the anomalous behavior can be understood if it is assumed that *some* of the carboxyl groups are involved in carboxyl–carboxyl acetic acid dimer type hydrogen bonds. Upon ionization, carboxylate ion groups form hydrogen bonds with hydroxyl donors. The reversible formation and breakage of these internal hydrogen bonds is presumably accompanied by some penetration of solvent into the molecular domain to give rise to the 11% difference in volume at the two pH's. The calculations of the effects of hydrogen bonding thus account for both the hydrodynamic and thermodynamic properties of bovine serum albumin at low pH. At the same time they provide some details of the changes taking place on specific groups within the albumin molecule, and provide a basis for the so-called configurational adaptability of the albumin molecule.

Introduction

The free energy change for such reactions as the binding of small ions by proteins contains an electrostatic contribution which depends upon several factors including the net charge Z of the protein and an electrostatic interaction factor w, the latter depending on the size and shape of the protein molecule.[2-4] For example, the standard free energy of ionization $\Delta F°$ and the pK, respectively, of a particular group on a protein are

$$\Delta F° = (\Delta F°)° - 2RTwZ \qquad (1)$$

and

$$pK = pK° - \frac{2wZ}{2.303} \qquad (2)$$

if the ionizing group is influenced only by electrostatic effects (*e.g.*, if the group is not involved in a hydrogen bond). In these equations, R is the gas constant, T is the absolute temperature, $(\Delta F°)°$ is the value of $\Delta F°$ when $Z = 0$, and K and $K°$ are the ionization constants corresponding to $\Delta F°$ and $(\Delta F°)°$, respectively. The quantity w is given by the following formula for an impenetrable sphere with uniform surface charge

$$w = \frac{N\epsilon^2}{2DRT}\left(\frac{1}{b} - \frac{\kappa}{1 + \kappa a}\right) \qquad (3)$$

where N is Avogadro's number, ϵ is the electronic charge, D is the dielectric constant, κ is the inverse of the radius of the ionic atmosphere, and b and a are the hypothetical radii of the molecule and of exclusion, respectively. Whereas Z varies with pH, w (and, therefore, the size and shape of the molecule) is usually found to be constant over a considerable part of the pH range.[5] However, recent studies of the binding of protons[5,6] and other low molecular weight ions and molecules[7] by bovine serum albumin (BSA) show that the thermodynamics of such reactions cannot be accounted for adequately if only Z, but not w, is assumed to vary with pH. In other words, eqs. 1 and 2, with w assumed constant with changing pH, fail to apply in these cases. In the case of BSA this anomalous behavior manifests itself at low pH by an abnormal steepening of the titration curve in the region where carboxyl groups are ionizing, *i.e.*, whereas eq. 2 would predict a *given* increase in the observed pK as the pH rises (or as Z decreases), the experimental titration curve is excessively steep because the pK of the carboxyl groups increases less rapidly than the simple electrostatic theory requires if both w and pK° remain constant. Also, the experimental pK° is found[6] to be lower than expected. These effects, which make the carboxyl groups appear more acidic than normal, are illustrated in Fig. 1.

---

[1] This work was supported by the Office of Naval Research (Contract N6-onr 26414), by the National Science Foundation (Grant G-507), and by Eli Lilly and Co. Reproduction in whole or in part is permitted for any purpose of the United States Government.

[2] K. Linderstrøm-Lang, *Compt. rend. trav. lab. Carlsberg*, **15**, No. 7 (1924).

[3] G. Scatchard, *Ann. N. Y. Acad. Sci.*, **51**, 660 (1949).

[4] T. L. Hill, *Arch. Biochem. Biophys.*, **57**, 229 (1955).

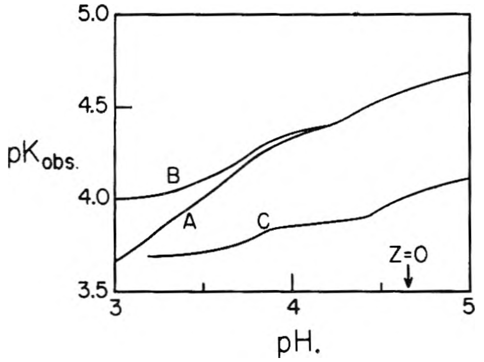

Fig. 1.—Variation of pK_{obsd} with pH for the carboxyl groups of BSA: curve A, expected behavior (eq. 2) assuming w constant (0.023) and $pK^\circ = 4.6$; curve B, same as curve A except that w was assumed to vary slightly with pH according to the hydrodynamic behavior; curve C, experimental curve[6] at ionic strength 0.15.

Curve A represents the *expected* variation in pK_{obsd} assuming the carboxyl groups of BSA to be normal ($pK^0 = 4.6$) and w to have the value 0.023, independent of pH. In order to obtain this curve, the Z *vs.* pH data were taken from Tanford, *et al.*,[8] and w was assumed equal to the value found in the neutral pH region[6] (evaluated from titration data[6] using eq. 2 in the neighborhood of the isoionic point). Curve B was computed on the same basis as curve A except that the slight variation of w with pH (due to a small pH dependence of b to be discussed below) was taken into account (eq. 3). Curve C is the experimental curve at ionic strength 0.15 (see Fig. 4 of reference 6). It should be noted that the slope of curve C is smaller than that of curve A or B, and also that curve C lies lower than curves A and B.

Two explanations have been proposed to account for the abnormal ionization behavior of the carboxyl groups in BSA. The first of these[5,6,8] can account for the slope of the pK *vs.* pH curve in terms of electrostatic effects by suggesting that the molecular weight remains unchanged but that the molecular configuration changes with pH[5,6,8-10] giving rise to a pH-dependent w factor. However, this explanation cannot account for the magnitude of pK°. The second explanation accounts for the slope partly in terms of electrostatic effects, and the magnitude in terms of an additional factor over and above those included in eqs. 1 and 2. Specifically, the abnormal steepness of the titration curve at low pH may be due to an additional pH dependence of the observed pK's of the groups being titrated because of the reversible formation and rupture of carboxyl–carboxyl hydrogen bonds of the acetic acid dimer type.[11] It is also possible that both effects are present, *i.e.*, reversible changes in size or shape may accompany the change in the hydrogen bonding between the side chain polar R groups of the protein

This investigation of the effect of pH on the hydrodynamic properties of BSA was undertaken in order to learn about the extent to which configurational changes occur as the pH region of anomalous reactivity is approached. Thus, we should be able to decide whether phenomena other than configurational changes must be considered in order to account for the reactivity. Similar investigations,[8,10,12-15] making use of hydrodynamic methods, have been carried out on human and bovine serum albumin but most of them involve the measurement of only one hydrodynamic quantity, *e.g.*, viscosity. Since two independent quantities are required,[16] some of the previous investigations have substituted an arbitrary assumption about the shape in order to deduce the size from the measurement of only one quantity.[17] By coincidence this arbitrary assumption, that the molecule is essentially spherical, is compatible with the results obtained in this investigation.

While it would have been desirable to apply the hydrodynamic method[16] over a wide pH range, it is unfortunate that albumin does not remain homogeneous at low and high pH[9,18-20] where most of the

---

(5) C. Tanford, *Proc. Iowa Acad. Sci.*, **59**, 206 (1952).

(6) C. Tanford, S. A. Swanson and W. S. Shore, *J. Am. Chem. Soc.*, **77**, 6414 (1955). We are indebted to Dr. Tanford for sending us the manuscripts for references 6 and 8 in advance of publicaton.

(7) I. M. Klotz and J. Ayers, *Disc. Faraday Soc.*, **13**, 189 (1953).

(8) C. Tanford, J. G. Buzzell, D. G. Rands and S. A. Swanson, *J. Am. Chem. Soc.*, **77**, 6421 (1955).

(9) M. E. Reichmann and P. A. Charlwood, *Can. J. Chem.*, **32**, 1092 (1954).

(10) J. T. Yang and J. F. Foster, *J. Am. Chem. Soc.*, **76**, 1588 (1954).

(11) M. Laskowski, Jr., and H. A. Scheraga, *ibid.*, **76**, 6305 (1954).

(12) C. Tanford and J. G. Buzzell, This Journal, **60**, 225 (1956).

(13) J. M. Creeth, *Biochem. J.*, **51**, 10 (1952).

(14) P. A. Charlwood, *ibid.*, **56**, 259 (1954).

(15) J. R. Colvin, *Can. J. Chem.*, **31**, 734 (1953).

(16) H. A. Scheraga and L. Mandelkern, *J. Am. Chem. Soc.*, **75**, 179 (1953).

(17) K. O. Pedersen, *Disc. Faraday Soc.*, **13**, 49 (1953), has also called attention to the danger of drawing conclusions from a single measurement.

(18) H. A. Saroff, G. I. Loeb and H. A. Scheraga, *J. Am. Chem. Soc.*, **77**, 2908 (1955).

(19) P. Bro, S. J. Singer and J. M. Sturtevant, *ibid.*, **77**, 4924 (1955).

(20) M. J. Kronman, M. D. Stern and S. N. Timasheff, This Journal, **60**, 829 (1956).

anomalies in the reactivity occur. Since the interpretation of hydrodynamic data is not unambiguous for polydispersed systems,[21] this investigation has been confined to the isoionic point (*p*H 5.13) and to an acid *p*H (4.0) in 0.5 *M* KCl where the protein is still homogeneous in the ultracentrifuge and where some of the titration anomalies (*e.g.*, the abnormally high reactivity of carboxyl groups) become apparent. Some previous interpretations of hydrodynamic data in the acid *p*H range have not taken cognizance of this heterogeneity.

It is worth noting that, in the *p*H range investigated here, a reversible reaction has been detected calorimetrically,[22] and anomalies have been found in the behavior of the depolarization of fluorescence[23]; also studies of chloride and thiocyanate binding by human serum albumin revealed[24] that the binding sites had to be considered as divided into two non-equivalent sets if the data were to be explained by electrostatic effects only.

Experimental

Materials and Solutions.—Armour crystallized bovine serum albumin (lot No. N67009) was dissolved in 0.5 *M* KCl to a concentration of about 10 g./100 cc. and dialyzed for 24 hours against this same salt solution in a rocking dialyzer at 2°. The *p*H of this solution was 5.13. Solutions to be used at *p*H 4.0 were then acidified; the amount of HCl required to lower the *p*H did not contribute appreciably to the ionic strength. These stock solutions were diluted with the corresponding solvents (*i.e.*, the outside solution from the dialysis) to obtain more dilute protein solutions. The concentrations of the stock solutions were determined by dry weight measurements (heating to 105°), using the solvent as a tare. The estimated amount of bound chloride was taken into account in computing the concentration.

The ionic strength was maintained at 0.5 in order to eliminate the Donnan effect. At lower ionic strengths at *p*H's away from the isoelectric point the net charge and attendant Donnan effect are sufficiently high so that the solvent in the protein solution contains unequal amounts of low molecular weight positive and negative ions; the viscosity of this solvent, η_0, is therefore undefined. This problem was circumvented in computations of specific viscosity ($\eta_{sp} = (\eta - \eta_0)/\eta_0$ where η is the viscosity of the protein solution) by using 0.5 *M* KCl.

The solutions used for viscosity measurements were clarified by centrifugation at 1600 × *g*. In a check experiment the solutions were filtered through Pyrex fine-grade sintered glass funnels; both clarification procedures yielded identical viscosity results. Solutions used for sedimentation measurements were naturally clarified during the acceleration period of the ultracentrifuge.

All non-protein materials were Mallinckrodt analytical reagents, aqueous solutions being made up with conductivity water. The Beckman model G *p*H meter, standardized at *p*H 4 and 7 with Beckman buffers, was used for *p*H measurements.

Viscosity.—Since the intrinsic viscosity $[\eta]$ of dilute solutions of BSA is very small ($\sim$0.04 for concentration expressed in g./100 cc.) good precision in measurements of *specific* viscosity can be obtained only by using viscometers with very long flow times, *e.g.*, for a 1% solution an error of 0.1 sec. in flow time corresponds to an error in specific viscosity of 5% for a flow time of 100 sec. and 0.8% for a flow time of 10 min. Ostwald viscometers with a 15-cm. hydrostatic head were used. The capillary portion of the viscometer was 90 cm. long with a bore diameter of about 0.6 mm. and was coiled for compactness. The flow time of water in these viscometers was about 10 min. With such long flow times, the kinetic energy correction was negligible. The viscosity measurements were carried out at 25.00°, the bath temperature being constant to ±0.003°. The viscosity data were expressed in terms of the flow times t_0 and t of solvent and solution, respectively, and plotted as $(t - t_0)/t_0c$ *vs.* *c*. Spring-driven stopwatches were used rather than electrical timers because the fluctuations in the electric power line frequency were large enough to lead to significant errors.

Calculations carried out with Booth's equation[25] indicate that, at an ionic strength of 0.5, the viscosity of the protein solution is not affected by the charge of the protein at *p*H 4.0.

Sedimentation.—Sedimentation constants *s* were used, in conjunction with diffusion data obtained on the same samples of BSA,[26] to compute molecular weights *M*; also the values of *s*, together with $[\eta]$ and *M*, permitted the hydrodynamic parameter β to be calculated.[16]

Sedimentation measurements were made with the Spinco Model E ultracentrifuge. In order to encompass a wide range of protein concentrations, cells with light paths of 3, 12 and 30 mm., respectively, were used. The runs were carried out at 59,780 r.p.m. except when the 30 mm. cell was used, the speed in the latter case being 50,740 r.p.m. All runs were made at room temperature. The reversible cooling on acceleration observed by Waugh and Yphantis[27] and by Biancheria and Kegeles[28] was taken into account by subtracting 0.9 and 0.7° from the interpolated temperatures at 59,780 and 50,740 r.p.m., respectively. The optics were focused according to the procedure recommended by Kegeles and Gutter[29] in order to obtain a set of symmetrical fringes on both sides of the peak, making it easier to measure its position. The photographs were read with a projection comparator previously described[26] with a precision corresponding to a distance of 5 μ movement of the boundary in the ultracentrifuge cell.

The sedimentation constants were corrected to 25° in 0.5 *M* KCl in the usual manner. Calculations similar to those made by Bro, Singer and Sturtevant[19] indicate that at this ionic strength the sedimentation constant depends on charge at *p*H 4.0 to the extent of only 0.5% which is about the limit of experimental error.

The partial specific volume was taken[30] as $\bar{v} = 0.734$ at 25° at both *p*H 4.0 and 5.13.

The concentration dependence of s is expressed in a plot of *s* *vs.* *c*.

Results

At both *p*H 4.0 and 5.13 there was no time dependence of the viscosity or sedimentation behavior within 5 hr. after the solutions were brought from 2° to room temperature. Aging at room temperature apparently produces changes in the viscosity[8] at *p*H values below 4. Aging for several days at *p*H values of 4 and above at 2° produces no apparent change in the viscosity or sedimentation behavior. Since all measurements reported here were completed within the 5 hr. period at room temperature, the subsequent reaction of BSA was of no concern.

In assessing the sedimentation patterns for evidence of polydispersity it was estimated that about 2 to 3% of a faster sedimenting component was present at *p*H 4.0 and 5.13. Typical sedimentation patterns are shown in Fig. 2. If the *p*H were lower than 4, the more extensive polydispersity previously reported[18–20] is evident. This poly-

---

[21] Except for homologous polymers of known molecular weight distribution, as discussed by E. V. Gouinlock, P. J. Flory and H. A. Scheraga, *J. Polymer Sci.*, **16**, 383 (1955).

[22] H. Gutfreund and J. M. Sturtevant, *J. Am. Chem. Soc.*, **75**, 5447 (1953).

[23] G. Weber, *Biochem. J.*, **51**, 155 (1952); *Disc. Faraday Soc.*, **13**, 33 (1953).

[24] G. Scatchard, I. H. Scheinberg and S. H. Armstrong, *J. Am. Chem. Soc.*, **72**, 535, 540 (1950).

[25] F. Booth, *Proc. Roy. Soc. (London)*, **A203**, 533 (1950).

[26] M. L. Wagner and H. A. Scheraga, THIS JOURNAL, **60**, 1066 (1956).

[27] D. F. Waugh and D. A. Yphantis, *Rev. Sci. Instr.*, **23**, 609 (1952).

[28] A. Biancheria and G. Kegeles, *J. Am. Chem. Soc.*, **76**, 3737 (1954).

[29] G. Kegeles and F. J. Gutter, *ibid.*, **73**, 3770 (1951).

[30] M. O. Dayhoff, G. E. Perlmann and D. A. MacInnes, *ibid.*, **74**, 2515 (1952).

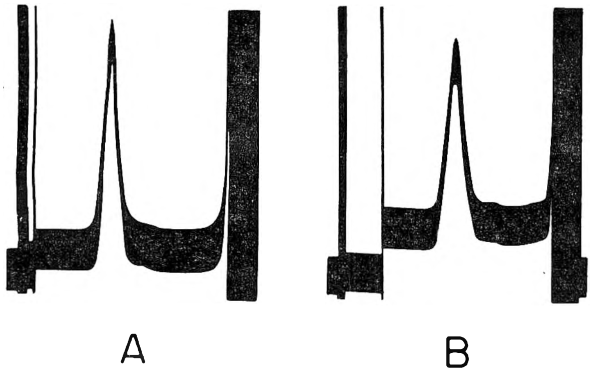

Fig. 2.—Typical sedimentation patterns of BSA in 0.5 M KCl at room temperature: A, pH 4.00, 6 g./100 cc.; B, pH 5.13, 2 g./100 cc.

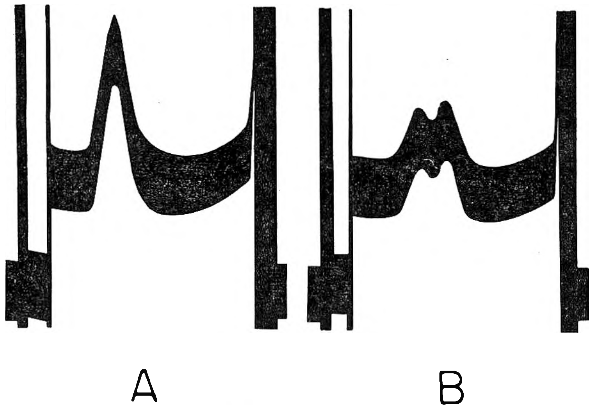

Fig. 3.—Sedimentation evidence for polydispersity in 0.5 M KCl at pH 3.6: A, BSA stored at 2°, but run at room temperature; B, solution A after more than 5 hours storage at room temperature.

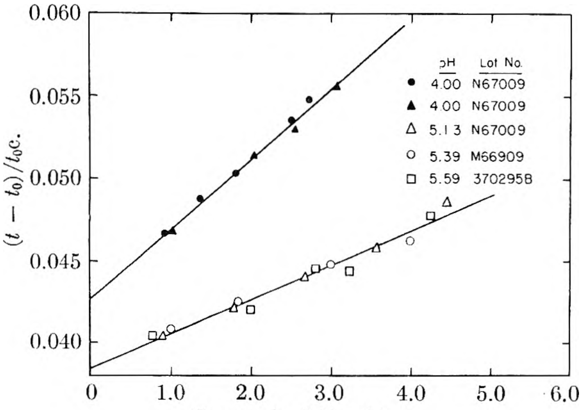

Fig. 4.—Viscosity data for BSA in 0.5 M KCl at 25°.

dispersity casts doubt on previous interpretations of low pH studies of BSA which have been based only on viscosity measurements. Examples of this polydispersity are shown in Fig. 3 in which Fig. 3A indicates the relative stability of BSA even after aging for several days at pH 3.6 at 2°. If the same solution stands at room temperature, then the polydispersity evident in Fig. 3B develops within a few hr. The sedimentation constants could not be determined for the solutions which were stable at pH 3.6 at 2° because of the inability to maintain adequate temperature control in the ultracentrifuge at low temperatures.[31] By keeping the temperature at 2°, it should be possible to make diffusion, sedimentation and viscosity measurements at lower pH's where the magnitude of the aforementioned anomalies in the reactivity increases at 25°.

Having indicated that the solutions at pH 4.0 and 5.13 are essentially monodispersed within the first 5 hours at room temperature we present the data obtained under these conditions. The viscosity and sedimentation data are shown in Figs. 4 and 5, respectively. In both figures the various lines shown were obtained by the method of least squares enabling extrapolations to be carried out to zero protein concentration. It may be noted that the sedimentation curves in Fig. 5 cross. This is simply a reflection of the fact that the concentration dependence of s is greater for the sample with the larger s_0 value as has often been noted previously, for example for polyisobutylene[32] and cellulose trinitrate.[33] This behavior illustrates that a comparison of s values at some *finite* concentration, say 1 g./100 cc., would not provide information about relative configurations.

The intercepts of the $(t - t_0)/t_0c$ *vs.* c plots are not the true intrinsic viscosities, but the limiting kinematic viscosities. To account for the difference in density between the pure solvent and the protein solution the term $(1 - \bar{v}_2\rho_0)/100\rho_0$ must be added.[34] In this term, which has the value 0.0025 for our data, the quantity ρ_0 represents the solvent density and $\bar{v}_2$ the partial specific volume of the protein. The corrected values, representing the intrinsic viscosities, are shown in Table I.

Table I

Viscosity and Sedimentation Data of BSA in 0.5 M KCl at 25°

	pH 4.00	pH 5.13
$[\eta]$, 100 cc./g.	0.0457 ± 0.0004	0.0413 ± 0.0004
s_0, Svedberg units at 25° in 0.5 M KCl	4.43 ± 0.03	4.59 ± 0.04

The limits of error are the standard deviations of the intercepts. It may be noted from Fig. 4 that the viscosity data are independent of the albumin lot. Preliminary studies not reported here indicate that this is not true of sedimentation and diffusion data. The sedimentation data presented here, and diffusion data,[26] pertain to lot No. N67009.

The sedimentation constants, extrapolated to zero concentration are given in Table I in terms of Svedberg units (1 Svedberg unit = 10^{-13} sec.). It may be noted that aging of the solution at pH 4.0 for 2 days at 2°, the ultracentrifuge runs being completed within 5 hours after warming to room temperature, had no appreciable effect on the sedimentation data.

Discussion

Comparison with Literature Values.—The values of $[\eta]$ reported in the literature for isoionic BSA show some scatter (see Table II). As noted above, differences in lot in our own work do not appear to affect the viscosity. It does not seem probable that differences in ionic strength are altogether responsible for these discrepancies. It may, however, be noted that measurements reported in the literature were carried out with viscometers having 100–200 sec. flow times. In contrast, our flow times were about 10 min., giving better precision in $t - t_0$. This difference in procedure need not of itself account for the discrepancies.

---

[31] A temperature control and temperature measuring device has recently been developed by Spinco for the model E ultracentrifuge. This auxiliary equipment has not been installed on our ultracentrifuge.

[32] L. Mandelkern, W. R. Krigbaum, H. A. Scheraga and P. J. Flory, *J. Chem. Phys.*, **20**, 1392 (1952).

[33] M. L. Hunt, S. Newman, H. A. Scheraga and P. J. Flory, This Journal, **60**, 1278 (1956).

[34] C. Tanford, *ibid.*, **59**, 798 (1955).

TABLE II

INTRINSIC VISCOSITIES OF ISOIONIC BSA

Ionic strength	$[\eta]$	Ref.
0.03, 0.15	0.037	8, 12
(0), (0.1)	.038[a]	10
.2	.041	35
.2	.042[b]	36
.5	.0413	This work

[a] This value includes the kinetic energy and density corrections estimated by Tanford, *et al.*[8] [b] This value was obtained at pH 7.

The sedimentation constant at pH 5.13 is compared with literature values in Table III. For this purpose our value given in Table I has been corrected to 20° in water in the usual manner, using the same correction data reported elsewhere.[26]

TABLE III

SEDIMENTATION CONSTANTS OF ISOIONIC BSA CORRECTED TO 20° IN WATER

$s_{20,w}$[a]	$s_{20,w}$[b]	Ref.
4.32	4.41	Taylor (see ref. 37)
4.30	4.39	Miller and Golder (see ref. 37)
4.31	4.40	Creeth (see ref. 37)
4.29	4.38	37
..	4.40	36
4.29[c]	4.34[c]	29
4.40	4.49	35
..	4.41	This work

[a] As reported in literature. [b] This column is obtained by multiplying the data in the previous column by 1.02 (ref. 37) to account for the Waugh-Yphantis or Biancheria-Kegeles effect. The value of Kegeles and Gutter[29] is multiplied by 1.01 since they took the correction into account but used only one-half the correct value. [c] The value of Kegeles and Gutter[29] is slightly lower than the others. This is probably due to the fact that their value corresponds to pH 4.4. As can be seen from Table I, the sedimentation constant decreases with decreasing pH in the pH range 5.13 to 4.0 in the presence of chloride where no cations except hydrogen ion are bound.

Molecular Weight and Configuration.—We may use the data of Table I to compute a sedimentation-diffusion molecular weight M for BSA and also the hydrodynamic parameter[16] β. In such calculations we must take account of the presence of about 3% of the faster sedimenting component (see Fig. 2). If we use hydrodynamic data which pertain to the whole albumin sample, then we will have computed average values of M and β. On the other hand, if we use data which pertain to the major component, which represents 97% of the total protein, then the computed values of M and β will pertain to this component alone. While it is of interest to have information about the major component, it should be emphasized that our primary interest in the configuration of BSA arises from the desire to account for its anomalous reactivity. Since the titration data[6] were obtained on the whole albumin sample (lot No. N67009, as in our work) we are also interested in the average values of M and β. We shall, therefore, carry out the computations in both ways, recognizing that the differences in the results will be small since the impurity is estimated to be present only to the extent of about 3%.

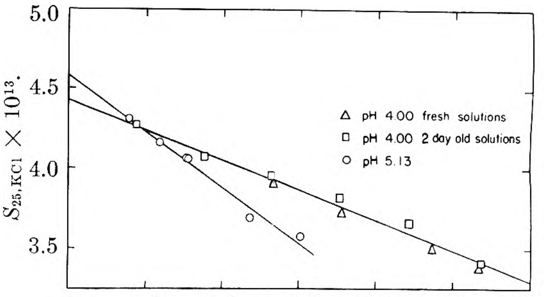

Fig. 5.—Sedimentation data for BSA (Lot No. N67009) in 0.5 M KCl at 25°.

The measured values of $[\eta]$ and D are average values for the whole sample, while the value of s pertains to a particular component. With this in mind we shall calculate first the molecular weight of the major component. For this purpose we use the value of $s_{20,w} = 4.41 \times 10^{-13}$ sec. reported in Table III for the major component at pH 5.13. Diffusion data on the same samples, reported elsewhere,[26] give $D_{20,w} = 5.90 \times 10^{-7}$ cm.^{2}/sec. for the major component. This value was computed[26] from the observed average diffusion coefficient on the basis that the major component represents 97% of the total protein, and that the ratio of the diffusion coefficients of the major and minor components is 1.5. Both of these assumptions are compatible with a heterogeneity analysis carried out on the diffusion data,[26] while the 3% value is, in addition, in agreement with the appearance of the sedimentation patterns of Fig. 2. The literature value[30] of $\bar{v} = 0.734$ at 25° may be corrected to 0.730 at 20° using the generalized temperature coefficient for $\bar{v}$ for proteins.[38] The density of water at 20° is 0.9982 g./cc. Using these data in the Svedberg equation

$$M = \frac{sRT}{D(1 - \bar{v}\rho)} \qquad (4)$$

we obtain for the major component the value M = 67,000 ± 3000 g./mole. We shall assume that the molecular weight of the major component, as well as the average molecular weight to be computed below, is the same at pH 4.0 as the value calculated above from data at pH 5.13. This seems justified in light of previously reported light scattering data.[8–10]

In order to compute the average molecular weight we use the observed average value[26] of the diffusion coefficient at pH 5.13. $D_{20,w} = 5.81 \times 10^{-7}$

---

[35] V. L. Koenig and J. D. Perrings, *Arch. Biochem. Biophys.*, **41**, 367 (1952).

[36] P. A. Charlwood, *Can. J. Chem.*, **33**, 1043 (1955).

[37] S. Shulman, *Arch. Biochem. Biophys.*, **44**, 230 (1953).

[38] T. Svedberg and K. O. Pedersen, "The Ultracentrifuge," Appendix II, Oxford, 1940.

cm.²/sec. The average sedimentation constant is computed as follows. The sedimentation constant of the faster, minor component is about 6.6×10^{-13} sec., this value being subject to a large experimental error since the concentration of this component is very small. However, since the faster component is present to the extent of only 3%, such a large error will not seriously affect the final result. The average value of s is taken as $[(0.97)\cdot(4.41) + (0.03)(6.6)] \times 10^{-13}$ or 4.48×10^{-13} sec. We thus obtain from equation 4 a value of M = 69,200 g./mole as an average molecular weight of the albumin sample.

We can now compute the hydrodynamic parameter β defined by the equation[16]

$$\beta = \frac{Ns[\eta]^{1/3}\eta_0}{M^{2/3}(1 - \bar{v}\rho)} \qquad (5)$$

Since the measured value of $[\eta]$ is an average for the whole protein, we shall first compute an average value of β using the $[\eta]$ data of Table I, the average values $s = 4.50 \times 10^{-13}$ sec. and 4.63×10^{-13} sec. for 0.5 M KCl at 25° at pH 4.0 and 5.13, respectively, and values of $\bar{v}$, ρ and η_0 pertaining to 0.5 M KCl at 25°. The results obtained are given in Table IV.

TABLE IV

VALUES[a] OF β FOR THE MAJOR COMPONENT OF BSA AND FOR THE WHOLE PROTEIN AT 25° IN 0.5 M KCl

	M	pH 4.0	pH 5.13
Major component	67,000	2.05×10^6	2.05×10^6
Whole protein	69,200	2.04	2.04

[a] The standard deviation in β is $\pm 0.06 \times 10^6$. This includes an estimate of the error in the diffusion coefficient. In this connection it may be mentioned that variations in D for BSA in the literature are approximately 5%. This may be due, in part, to the observation made in this Laboratory[26] that D varies with the albumin sample. Further, the standard deviation cited above is believed to be a minimum value which would be augmented by determinate errors in any of the measured values from which β was computed. For example, the intrinsic viscosity may be slightly in error because of an uncertainty in c arising from an unknown amount of bound chloride ion.

In order to compute β for the major component we must know the value of $[\eta]$ for this species. We can make the following reasonable assumptions to show that the measured value of $[\eta]$ for the whole protein is, within the experimental error of the determination of $[\eta]$, equal to $[\eta]$ for the major component. The intrinsic viscosity is

$$[\eta] = (N\nu/100)(V_e/M) \qquad (6)$$

where ν is a shape factor[39] and V_e is the effective hydrodynamic volume.[16] If we assume that $V_e \sim M$, then the ratio V_e/M for both components is the same, irrespective of the values of ν. Neglecting protein–protein interaction, we can write, as a consequence of eq. 6, the following equation for the observed value of the intrinsic viscosity.

$$[\eta] = [0.97\nu_1 + 0.03\nu_2](N/100)(V_e/M) \qquad (7)$$

If both components were spherical ν_1 would equal ν_2 and the observed intrinsic viscosity would be equal to that of *either component* separately. If the major component were spherical and component 2 were an aggregate of 2 spheres we could take ν_1 = 2.5, the value for a sphere, and ν_2 = 2.91, the value for a prolate ellipsoid of revolution of axial ratio 2. In such a case the observed intrinsic viscosity would be 2.51/2.50 times the value for the major component. Since this difference in $[\eta]$ is well within the experimental error, and since this error is further reduced by the fact that we take the cube root of $[\eta]$ in computing β from eq. 5, we are justified in assigning the measured value of $[\eta]$ to the major component.

Using then the measured values of $[\eta]$ and the values of s for the major component, as given in Table I, we obtain the values of β for the major component which are given in Table IV. From the data shown in Table IV it can be seen that the presence of about 3% of the faster sedimenting component has no significant effect on the resulting value of β even though it increases the average molecular weight by 3%.

The values obtained for β indicate[16] that an effective hydrodynamic sphere[40] will account *for all of the measurements of* BSA, *i.e.*, sedimentation, diffusion and viscosity, without any arbitrary assumption about the density or hydration of the molecule. Further, from the similar values[42] of β at both pH's we see that the shape is independent of pH in the pH region encompassed by the measurements reported here. The different viscosities are thus to be accounted for in terms of a greater hydrodynamic volume at pH 4.0 compared to pH 5.13. Similarly, the different sedimentation constants at these pH's reflect the different hydrodynamic radii. The ratio of the radius at pH 4.0 to that at pH 5.13 is

$$\frac{(f)_{p\text{H}4.0}}{(f)_{p\text{H}5.13}} = \frac{(s)_{p\text{H}5.13}}{(s)_{p\text{H}4.0}} = \frac{4.59}{4.43} = 1.04 \qquad (8)$$

where f is the translational frictional coefficient. If this value is cubed, we obtain for the ratio of the volumes at the two pH's a value of 1.12. This value is in excellent agreement with the ratio of the intrinsic viscosities 0.0457/0.0413 or 1.11. Thus, the configuration of the albumin molecule is presumably such that its volume is 11% greater at pH 4.0 than at pH 5.13. The agreement between the ratios obtained from f and $[\eta]$ is compatible with the spherical model for albumin. Further, the molecule presumably possesses sufficient flexibility to allow for this increase in volume, *i.e.*, the volume change is envisaged as arising from the entrance of solvent between the peptide helices.

It is of interest to emphasize a point made previously,[16] that while hydrodynamic measurements are carried out in order to ascertain sizes and

---

(39) R. Simha, THIS JOURNAL, **44**, 25 (1940).

(40) When the β value is near 2.1×10^6 the distinction between a sphere and an oblate ellipsoid cannot be made from β alone.[16] As discussed elsewhere[41] the absence of flow birefringence suggests the absence of high asymmetry for BSA. However, for molecules as small as BSA the results of flow birefringence are not very reliable. We shall, therefore, interpret the data in terms of a sphere. In view of the errors in the measured hydrodynamic quantities, and also in light of the comments in footnote *a* of Table IV, the deviation of the experimental β values from the minimum theoretical[16] value of 2.12×10^6 should not be regarded as a failure of the theory.

(41) H. A. Scheraga, W. R. Carroll, L. F. Nims, E. Sutton, J. K. Backus and J. M. Saunders, *J. Polymer Sci.*, **14**, 427 (1954).

(42) This comparison of β values at two pH's is essentially a comparison of the values of $s[\eta]^{1/3}$. Hence, since errors in D and M do not affect this quantity, this comparison is more precise than an individual β value.

shapes of protein molecules in dilute solution, it does not follow that the *hydrodynamic* volume is identical with the *particle* volume. This erroneous identification of the two volumes is embodied in eq. 7 of reference 12.[43] If the two volumes were identical, then Stokes' law would hold for *small* spherical particles, *i.e.*, for macromolecules. However, it is precisely because Stokes' law does not always hold for spherical macromolecules[47] (and correspondingly, Perrin's equation for ellipsoidal macromolecules) that the procedure of reference 16 used the concept of the *effective* hydrodynamic volume. It is thus impossible at present to relate the hydrodynamic volume to the partial specific volume, as equation 7 of reference 12 tries to do. Further, the claim[12] that the hydrodynamic properties of BSA cannot be represented by the theory previously cited[16] is based on the departure of β from the minimum value of 2.12×10^6. When experimental errors are taken in account this discrepancy becomes insignificant.[40,43] Further support for this point of view has been provided by Charlwood.[14] It is thus worthwhile to re-emphasize that hydrodynamic measurements (a) give sizes and shapes of effective hydrodynamic particles, not real particles and (b) that hydrodynamic methods are not very sensitive to changes in shape. This insensitivity is a characteristic feature of hydrodynamic methods. While a *single* hydrodynamic property, such as viscosity or sedimentation, is highly sensitive to changes in shape, it is unfortunate, as shown previously,[16] that a *single* hydrodynamic property does not lead to a unique size or shape. Rather, a *pair* of quantities is required, and the *combination* of two hydrodynamic quantities is not very sensitive to particle shape.[48] If one has carried out measurements of two hydrodynamic quantities, then the procedure of reference 16 will provide the size and shape without requiring arbitrary assumptions about the shape (or hydration). This procedure has been applied above in the evaluation of β for BSA at pH 4.0 and 5.13.

Reactivity (in Terms of Varying w).—We may now consider the question of the anomalous carboxyl ionization, first from the point of view that w may vary with pH, to see if the 11% increase in hydrodynamic volume at pH 4.0 (interpreted to mean an increase in the volume of the solvated protein molecule) will account for the steepness of the titration curve[49] at low pH.

We have seen from equation 8 that the ratio of the radius at pH 4.0 to that at pH 5.13 is 1.04. Such a ratio of radii corresponds to a *very small* ratio of w values (see eq. 3) for the impenetrable sphere model. The viscosity data[8] at ionic strength 0.15 correspond to a slightly greater expansion. If the titration data on BSA[6] are interpreted in terms of a variation in w with pH, the experimental variation[8] in w is in excess by several orders of magnitude of that computed from eq. 3 using the value 1.04 for the ratio of radii. We may thus conclude that the anomalous reactivity of the carboxyl groups of BSA cannot be accounted for by a changing molecular size (in terms of the impenetrable sphere model).

To circumvent this conclusion, but still preserving the concept of a varying w, Tanford, *et al.*,[8] ignoring the heterogeneity previously cited,[18–20] have interpreted the configurational changes over a wide, *acid* pH range in terms of an alternative model in which the salt ions penetrate some distance into the interior of the protein ion (with the protein fixed charges remaining on the "surface"). They then change the model, above pH 4.3, to that of an impenetrable sphere. In view of the fact that there is an 11% volume expansion at low pH there is certainly justification for assuming penetration of the protein ion by low molecular weight species. However, one may question, without being able to show conclusively, whether the discontinuity in the model at pH 4.3 represents a realistic description of the configurational changes of BSA. Whereas the impenetrable sphere model leads to equation 3, the penetrable sphere model leads to an alternative expression[8] for w. By using these two different models (the penetrable sphere at pH 4.0 and the impenetrable sphere at pH 5.13), the ratio of radii becomes 1.03, in reasonable agreement with the value 1.04 of eq. 8. This better agreement arises because the variation in w with pH, ascribed to variation in protein size in the impenetrable sphere model, is attributed to penetration by ions in the penetrable sphere model at pH 4.0. However, the assumption of a discontinuity in the model at pH 4.3 does not appear realistic. As stated in footnote

---

(43) Essentially this same error is committed by Harrington, Johnson and Ottewill[44] who attempt to correlate hydrodynamic volume with $\bar{v}$. Further, these authors criticize the procedure of Scheraga and Mandelkern[16] by stating that "for axial ratios smaller than 20 an approximate form of the Simha equation has to be used." This statement is incorrect since the exact Simha equation is available[39] and its solution has been given in connection with numerical viscosity calculations[45] for axial ratios from 1 to 300, as well as by Mehl, Oncley and Simha.[46] Further, Scheraga and Mandelkern used the *exact* Simha equation in the evaluation of their β function. Thus the contention of Harrington, Johnson and Ottewill that the Simha or Perrin equations do not hold accurately for nearly spherical particles is unfounded. We suggest here that the difficulties of Harrington, Johnson and Ottewill could be circumvented by a precision analysis of their β-values, as carried out here.[40] The same remarks about reliability and precision of hydrodynamic data apply to their calculations of β for southern bean mosaic virus and tobacco mosaic virus.

(44) W. F. Harrington, P. Johnson and R. H. Ottewill, *Biochem. J.*, **62**, 569 (1956).

(45) H. A. Scheraga, *J. Chem. Phys.*, **23**, 1526 (1955).

(46) J. W. Mehl, J. L. Oncley and R. Simha, *Science*, **92**, 132 (1940).

(47) The well-known failure of Stokes' law for macromolecules was taken into account in the treatment of Scheraga and Mandelkern.[16] The failure of Stokes' law for molecules has again been discussed recently by A. Spernol, THIS JOURNAL, **60**, 703 (1956).

(48) For example, the large change in intrinsic viscosity with particle shape at constant volume might seem to provide a sensitive tool for measurement of shape changes (a change from a sphere to a prolate ellipsoid of axial ratio 4 leads to an 85% change in $[\eta]$ *if* the volume stays constant). Unfortunately, however, we have no way of knowing whether a change in viscosity is due to a change in shape, or volume, or both. In order to determine which factor is responsible, another measurement, *e.g.*, sedimentation, is needed. The β function which isolates the shape factor's effects is a function of both s and $[\eta]$. Now, if $[\eta]$ increases, s will decrease (both are associated with increased frictional effects), and thus there is internal compensation in the function of s and $[\eta]$ (as indeed there must be to eliminate size effects) which makes the β function comparatively insensitive. *Any* method of separating the shape and size effects will suffer from such internal compensation. The combined function will only undergo a change of 4% as against 85% for viscosity alone in the example cited.

(49) Whereas the titration data[6] were obtained at several ionic strengths, the highest being 0.15, we shall assume that the conclusions reached about *changes* in particle shape from hydrodynamic data at ionic strength 0.5 may be applied to the titration data at ionic strength 0.15.

26 of reference 8, neither the penetrable nor the impenetrable sphere models are individually adequate to account for the thermodynamic and hydrodynamic properties without switching the model at pH 4.3. Further, even with this discontinuity in the model, the explanation of reference 8 can account only for the slope of the pK *vs.* pH curve but not for the difference in pK° values (*i.e.*, an "observed" pK° value of 4.0 compared to the "normal" value of 4.6), as pointed out in the Introduction in the discussion of Fig. 1. We therefore propose an alternative explanation below.

Reactivity (in Terms of Hydrogen Bonding).—The alternative explanation discussed here is concerned with the effects of hydrogen bonds[11] between un-ionized carboxyl groups, and of hydrogen bonds between ionized carboxyl groups and the OH groups of tyrosine, serine and threonine.

Considering first the tyrosyl ionization, if the tyrosyl residues are assumed to be involved in heterologous single hydrogen bonds with ionized carboxyl groups, then according to eq. I-38 of reference 11 the observed standard free energy change for the tyrosyl ionization is

$$\Delta F^\circ_{\text{obsd}} = \Delta F^\circ_1 + RT \ln (1 + K_{\text{ij}}) \qquad (9)$$

in the pH region of tyrosyl ionization. In this equation ΔF°_1 corresponds to the normal, non-hydrogen bonded tyrosyl group, and K_{ij} is a hydrogen bonding equilibrium constant previously defined.[11] In order to make $\Delta F^\circ_{\text{obsd}}$ agree with the experimental value[6] of 14.1 kcal./mole (assuming $\Delta F^\circ_1 =$ 13.1 kcal./mole[6]), K_{ij} must have the value[50] 4 according to eq. 9. The calculated values of $\Delta H^\circ_{\text{obsd}}$ and $\Delta S^\circ_{\text{obsd}}$ are then 11 kcal./mole and -10 e.u., respectively, which agree very well with the observed[6] values of 11.5 kcal./mole and -9 e.u., respectively. Such hydrogen bonding accounts for the thermodynamic parameters of the tyrosyl ionization.[11,51]

We now consider the ionization of the carboxyl groups. Since there are only 18 or 19 tyrosyl groups, only at most 18 or 19 ionized carboxyl groups can be hydrogen bonded to tyrosyls. However, we may postulate that the 57 seryl and threonyl hydroxyl groups may also hydrogen bond with ionized carboxyl groups.[52] We thus have available a total of 76 donors for hydrogen bonding with ionized carboxyl groups. Since there are at least 90 carboxyl groups, *it is implied that some of them are not hydrogen bonded in the ionized form.* When the carboxyl groups are un-ionized it is postulated that some of them are involved in COOH–HOOC acetic acid dimer type bonds[11] and some of them are not hydrogen bonded at all. The treatment given below considers the possible fates of the hydrogen bonded COOH groups upon ionization. While a direct test of such hydrogen bonding phenomena is not yet feasible for the carboxyl ionization, we may investigate the various possibilities to see whether the results so obtained can be correlated with the experimentally determined thermodynamic parameters. It must be recognized, however, that the following discussion is essentially qualitative because the hydrogen bonding theory[11] to be used applies only in cases where the polar R groups involved are attached to polypeptide chains which are rigidly fixed in position relative to each other. This is not true in the case of BSA in the acid region since the molecule has been shown to expand. The effect of such expansion on the hydrogen bonding between the polar R groups would not be expected to be negligible since the equilibrium constants for the formation of such hydrogen bonds are strongly dependent upon the distance between the polar groups concerned.[11] However, the expansion is small so that we may expect our results to be qualitatively correct.

In the following treatment we shall deal with three plausible models. These are not the only possibilities but they cover a wide range of values of the thermodynamic parameters. In all of these models the un-ionized COOH groups are doubly hydrogen bonded and the ionized COO^- groups are potentially capable of functioning as hydrogen bonding acceptors. If all these types of hydrogen bonding situations were present it is doubtful whether present methods of interpreting titration curves could distinguish between the various kinds of carboxyl groups.

In all the models those un-ionized COOH groups which are hydrogen bonded are assumed to be involved in acetic acid dimer type bonds. The models differ according to the behavior of the carboxyl group *after* ionization. In formulating these models we shall distinguish between the left and right carboxyl groups in the hydrogen bond and compute the expected thermodynamic parameters for the ionization of either the left or right carboxyl. In model A we allow only the left but not the right carboxyl group to form a heterologous single hydrogen bond with an OH donor when the carboxyl group is ionized. For this model we shall consider separately the ionization behavior of both the left and right carboxyl groups. In model B we consider that the ionized carboxyl groups can form coöperative hydrogen bonds (two OH donor groups to each COO^- group). Finally, in model C we assume that the ionized carboxyl groups are not hydrogen bonded. This model was considered previously.[11] In models B and C we shall consider the ionization of the left COOH group, but the same equations would be derived if the ionization of the right COOH group were considered.

Since the method of computing the thermodynamic parameters is the same for all the models, we shall illustrate the details for model B and merely state the results for the other, simpler cases.[53]

The ionization process may be generalized as

$$\text{I} \rightleftarrows \text{H}^+ + \text{II} \qquad (10)$$

In the case of model B, the symbol I represents species A-D, whereas II represents species E-J (see

---

[50] A revision[6] in the values of ΔF°_1 and $\Delta F^\circ_{\text{obsd}}$ leads to the value of 4 for K_{ij}, rather than 2.5 as reported previously.[11]

[51] As noted previously,[11] tyrosyl groups may be involved in a coöperative hydrogen bonding situation. If such is the case, the values of K_{ij} would have to be revised. In any event, the previous estimate[11] that K_{ij} is of the order of unity seems reasonable.

[52] It may be, however, that such hydrogen bonds are not as readily formed as tyrosyl hydrogen bonds since the acid pK's of seryl and threonyl hydroxyl groups are quite high.

[53] In all the models we shall make the simplifying and justifiable approximation that two COOH groups can be bonded only when two not one, hydrogen bonds are formed.

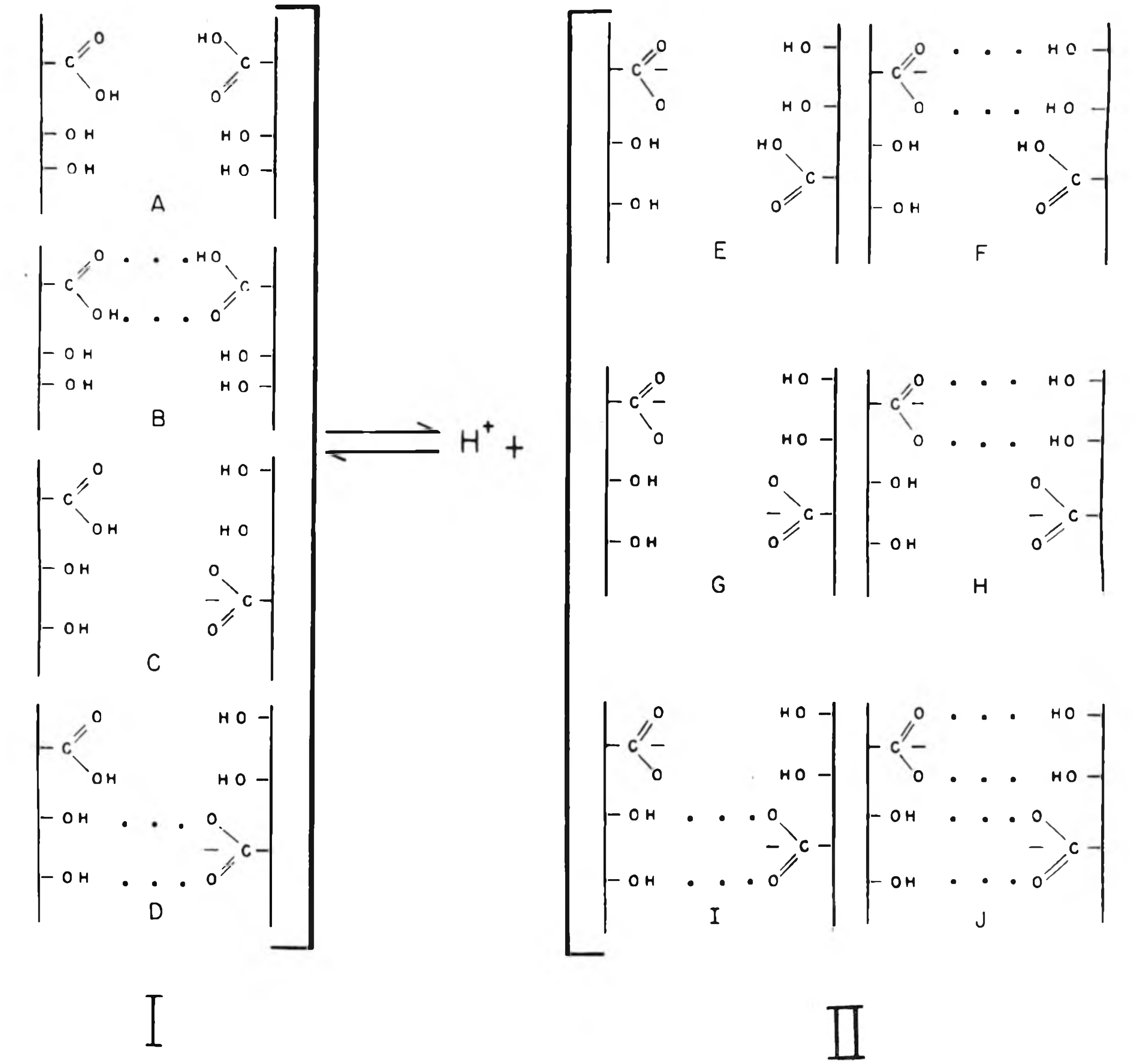

Fig. 6.—Species designated as I and II in model B (see eq. 10).

Fig. 6). The observed ionization constant K_{obsd} for the left carboxyl group in model B can be computed by the method of Appendix I of reference 11. The *relative* concentrations n_i of the various species are listed below, where K_{ij}, K_{lm} and K_{rs} are hydrogen bonding equilibrium constants defined in reference 11. The normal value for the ionization constant of a non-hydrogen bonded COOH group in a protein of charge Z is K_2.

Species	n_i
A	1
B	K_{lm}
C	$K_2/[H^+]$
D	$K_{rs}K_2/[H^+]$
E	$K_2/[H^+]$
F	$K_{rs}K_2/[H^+]$
G	$(K_2/[H^+])^2$
H	$K_{rs}(K_2/[H^+])^2$
I	$K_{rs}(K_2/[H^+])^2$
J	$(K_{rs}K_2/[H^+])^2$

From these we obtain

$$K_{obsd} = \frac{[H^+](n_E + n_F + n_G + n_H + n_I + n_J)}{(n_A + n_B + n_C + n_D)} \qquad (11)$$

where $[H^+]$ is the hydrogen ion activity. Substitution for the n's gives

$$K_{obsd} = \frac{K_2(1 + K_{rs})[1 + (1 + K_{rs})K_2/[H^+]]}{1 + K_{lm} + (1 + K_{rs})K_2/[H^+]} \qquad (12)$$

By the usual thermodynamic procedures we can obtain ΔF°_{obsd}, ΔS°_{obsd} and ΔH°_{obsd} from eq. 12. The relation for ΔF°_{obsd} is

$$\begin{aligned}\Delta F^\circ_{obsd} &= -RT \ln K_{obsd} \\ &= \Delta F^\circ_2 - \\ &RT \ln \frac{(1 + K_{rs})[1 + (1 + K_{rs})K_2/[H^+]]}{1 + K_{lm} + (1 + K_{rs})K_2/[H^+]} \qquad (13)\end{aligned}$$

The equations for ΔS°_{obsd} and ΔH°_{obsd} are somewhat cumbersome. However, they can be simplified if we recall that $\Delta H^\circ_2 \approx 0$ for carboxyl groups. The simplified equations are then

$$\begin{aligned}\Delta H^\circ{}_{\text{obsd}} &= RT^2\left(\frac{\partial \ln K_{\text{obsd}}}{\partial T}\right)_{P,\,[\mathrm{H}^+]} \\ &= \left[\frac{K_{\text{rs}}}{1+K_{\text{rs}}} + \frac{K_{\text{rs}}K_2/[\mathrm{H}^+]}{1+(1+K_{\text{rs}})K_2/[\mathrm{H}^+]} - \right. \\ &\left. \frac{K_{\text{rs}}K_2/[\mathrm{H}^+]}{1+K_{\text{lm}}+(1+K_{\text{rs}})K_2/[\mathrm{H}^+]}\right]\Delta H^\circ{}_{\text{rs}} - \\ &\left[\frac{K_{\text{lm}}}{1+K_{\text{lm}}+(1+K_{\text{rs}})K_2/[\mathrm{H}^+]}\right]\Delta H^\circ{}_{\text{lm}}\end{aligned} \qquad (14)$$

and

$$\Delta S^\circ{}_{\text{obsd}} = (\Delta H^\circ{}_{\text{obsd}} - \Delta F^\circ{}_{\text{obsd}})/T \qquad (15)$$

Similar considerations applied to the other models give

Model A_L (*i.e.*, ionization of left carboxyl)

$$K_{\text{obsd}} = \frac{K_2(1+K_{\text{ij}})(1+K_2/[\mathrm{H}^+])}{1+K_{\text{lm}}+K_2/[\mathrm{H}^+]} \qquad (16)$$

$$\Delta H^\circ{}_{\text{obsd}} = \frac{K_{\text{ij}}}{1+K_{\text{ij}}}\Delta H^\circ{}_{\text{ij}} - \frac{K_{\text{lm}}}{1+K_{\text{lm}}+K_2/[\mathrm{H}^+]}\Delta H^\circ{}_{\text{lm}} \qquad (17)$$

Model A_R (*i.e.* ionization of right carboxyl)

$$K_{\text{obsd}} = \frac{K_2[1+(1+K_{\text{ij}})K_2/[\mathrm{H}^+]]}{1+K_{\text{lm}}+(1+K_{\text{ij}})K_2/[\mathrm{H}^+]} \qquad (18)$$

$$\begin{aligned}\Delta H^\circ{}_{\text{obsd}} &= \left[\frac{K_{\text{ij}}K_2/[\mathrm{H}^+]}{1+(1+K_{\text{ij}})K_2/[\mathrm{H}^+]} - \right. \\ &\left. \frac{K_{\text{ij}}K_2/[\mathrm{H}^+]}{1+K_{\text{lm}}+(1+K_{\text{ij}})K_2/[\mathrm{H}^+]}\right]\Delta H^\circ{}_{\text{ij}} - \\ &\frac{K_{\text{lm}}}{1+K_{\text{lm}}+(1+K_{\text{ij}})K_2/[\mathrm{H}^+]}\Delta H^\circ{}_{\text{lm}}\end{aligned} \qquad (19)$$

Model C

$$K_{\text{obsd}} = \frac{K_2(1+K_2/[\mathrm{H}^+])}{1+K_{\text{lm}}+K_2/[\mathrm{H}^+]} \qquad (20)$$

$$\Delta H^\circ{}_{\text{obsd}} = \frac{-K_{\text{lm}}}{1+K_{\text{lm}}+K_2/[\mathrm{H}^+]}\Delta H^\circ{}_{\text{lm}} \qquad (21)$$

The expressions for $\Delta F^\circ{}_{\text{obsd}}$ and $\Delta S^\circ{}_{\text{obsd}}$ follow readily from those given, and have therefore been omitted.

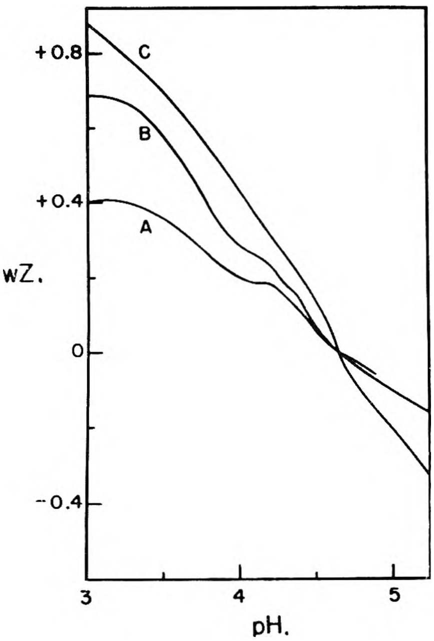

Fig. 7.—Dependence of wZ on pH: curve A, penetrable model; curve B, impenetrable model; curve C, empirical.

The experimental thermodynamic parameters[6] lie between curves calculated from the above equations for the various models using the values $K_{\text{ij}} = 4$, $K_{\text{lm}} = 100$, $K_{\text{rs}} = 40$, $K^\circ{}_2 = 2.5 \times 10^{-5}$, w *vs.* pH data from the hydrodynamic behavior, and Z *vs.* pH data from Tanford, *et al.*[8] However, the slopes of the resulting ΔF° *vs.* pH curves do not match the experimental slopes. On the other hand, it must be kept in mind, as stated in reference 6, that the Z *vs.* pH data have been estimated on the basis of measurements of chloride binding at one or two pH's, and assumptions about potassium binding. Thus, there is considerable uncertainty in the Z *vs.* pH data for BSA, and *consequently in the w vs. pH data.* We have, therefore, introduced an *empirical* wZ *vs.* pH dependence, chosen so that the slopes of the ΔF^0 *vs.* pH curves (computed from the above models) would be compatible with the experimental ones. This empirical curve is compared in Fig. 7 with theoretical curves computed from the Z *vs.* pH data postulated by Tanford, *et al.*,[8] and from w *vs.* pH data using the impenetrable and penetrable models.[54] It is also of interest to examine the pH dependence of the *empirical* charge, Z_{emp}, computed from the empirical wZ *vs.* pH curve of Fig. 7, using the impenetrable model for w. The resultant curve is compared with that postulated[55] by Tanford, *et al.*,[8] in Fig. 8. We do not feel that sufficient data are available at present to provide an accurate wZ *vs.* pH curve. If we use the empirical wZ *vs.*

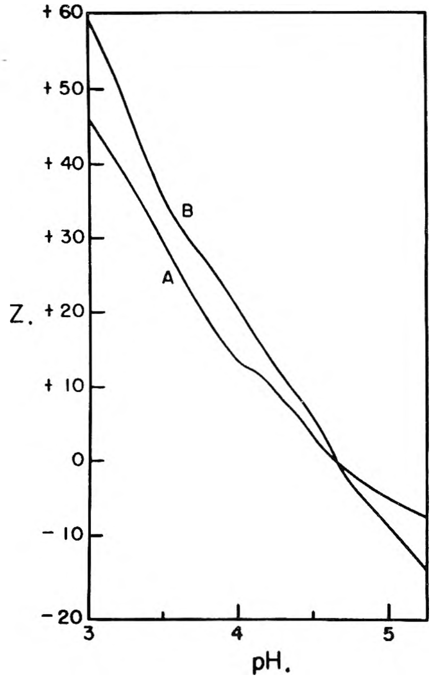

Fig. 8.—Dependence of Z on pH: curve A, values assumed by Tanford, *et al.*[8]; curve B, values computed from Fig. 7, using the impenetrable model for w (allowing for the small expansion at low pH).

(54) The empirical wZ *vs.* pH curve could be inaccurate at the low pH end since the hydrogen bonding theory,[11] on which it is based, does not hold rigorously because of the molecular expansion.

(55) It is obvious that there is a need for a complete study on BSA of the simultaneous binding of Cl^-, K^+ and H^+ in order to obtain Z at any pH. Such studies are being carried out by Saroff (private communication) with the aid of perm-selective membranes.

pH curve we can account not only for the slope of $\Delta F°$ vs. pH curves, but also for the $\Delta H°$ and $\Delta S°$ parameters[56] and resolve the anomaly of the carboxyl ionization. Thus, the curves of Figs. 9, 10, and 11 were computed using this empirical wZ vs. pH curve and the above values of K_{ij}, K_{lm}, K_{rs} and $K°_2$. It can be seen that the experimental curves lie between the theoretical curves for the models chosen, both with respect to absolute values and slopes. Thus, the experimental curve may be considered as representing some average among these models plus a few possibly normal COOH groups. This average cannot be evaluated quantitatively because the theory of reference 11 assumes that the helices are maintained in fixed positions with respect to each other, whereas the small expansion deduced from the hydrodynamic data suggests that solvent may force the helices apart.[57] Nevertheless, we can see qualitatively that the hydrogen bonding picture is plausible and accounts for the thermodynamic behavior of the carboxyl groups of BSA (*i.e.*, both the slopes and absolute values of the thermodynamic parameters).[58]

Further, in view of the possibility of making and breaking various kinds of hydrogen bonds reversibly, permitting expansion as the charge on the molecule increases, we can see how the configurational adaptability commonly ascribed to the albumin molecule can arise.

Thus, the foregoing analysis provides a compatible picture to account for both the hydrodynamic and thermodynamic data on BSA at low pH. As the pH rises the hydrogen bonds between OH groups and COO$^-$ groups may bring the peptide helices closer together, squeeze solvent out of the molecular domain, and account for the decrease in volume in going from pH 4.0 to pH 5.3. No change in configuration then occurs until high pH where tyrosyl groups ionize.

Finally, we should emphasize the limited range of conditions under which our conclusions apply. First of all, they apply to fresh solutions (less than 5 hours at room temperature), and not to older solutions which at the lower pH exhibit the time-dependent phenomena observed by Tanford and coworkers.[8] The titration data[6] were obtained with fresh solutions and, therefore, are comparable to our hydrodynamic data. Secondly, because of the

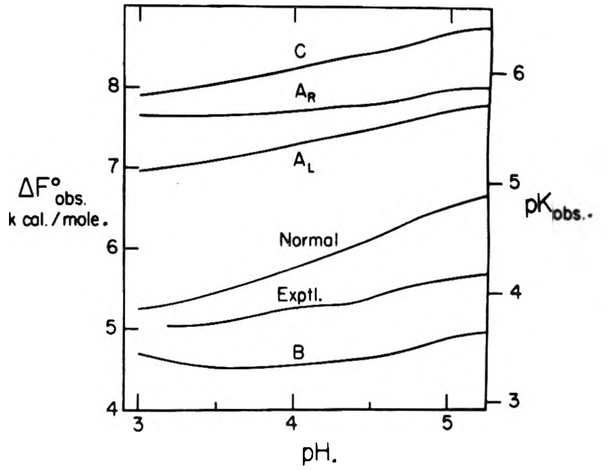

Fig. 9.—Dependence of $\Delta F°_{\rm obsd}$ on pH. Curves A$_R$, A$_L$, B, C correspond to the hydrogen bonded models given in the text. The normal curve was computed using $pK° = 4.6$ and the empirical wZ vs. pH data of Fig. 7. The experimental curve[6] is also shown.

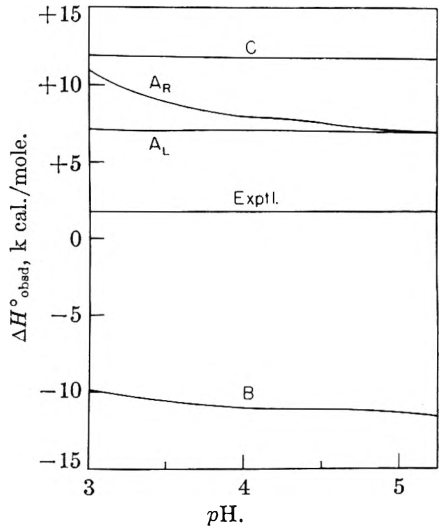

Fig. 10.—Dependence of $\Delta H°_{\rm obsd}$ on pH. The curves correspond to those of Fig. 9.

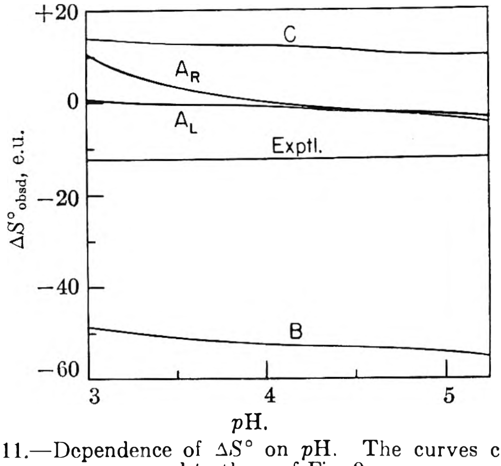

Fig. 11.—Dependence of $\Delta S°$ on pH. The curves correspond to those of Fig. 9.

[56] It should be noted that the empirical wZ vs. pH relation is not required to give the proper range of $\Delta F°$, $\Delta H°$ and $\Delta S°$; it was chosen only to make the slopes of the $\Delta F°$ curves agree with experiment. The range of values of these parameters, obtained from the several hydrogen bonding models, is sufficient to account for the experimental data even with the wZ vs. pH data of Tanford, *et al.*[8]

[57] It should be noted that contributions to the observed free energy of ionization due to configurational changes (*e.g.*, the volume change accompanying the shifting of helices relative to each other) have been neglected in this treatment.

[58] It may be mentioned that the experimental curve lies between the normal curve and curve B in Fig. 9 whereas in Figs. 10 and 11 it lies between the normal curves (not shown in the Figures) and curve A$_L$. This shift, however, corresponds to relatively small changes in the parameters K_{ij}, K_{rs}, K_{lm} and in the values selected for $\Delta H°_2$, $\Delta H°_{ij}$, $\Delta H°_{rs}$, $\Delta H°_{lm}$. For example, if $\Delta H°_2$ were not zero as assumed, there would be errors in $\Delta H°_{\rm obsd}$ arising not only from the nonzero value of $\Delta H°_2$ but also from the differentiation process of eq. 14, carried out at *constant* [H$^+$]. (It should be noted that $\Delta H°_{\rm obsd}$ of eq. 14 corresponds to constant [H$^+$] whereas the experimental value usually corresponds to constant r). Finally, since an error of 2 kcal. in the enthalpy would correspond to an error of about 7 e.u. in the entropy, such errors in $\Delta H°_{\rm obsd}$ will also appear in $\Delta S°_{\rm obsd}$. Hence, the change in the sequence of the curves as calculated is not outside the expected range of uncertainty inherent in these calculations, especially since the averaging procedure is different for the different thermodynamic parameters.

heterogeneity[18–20] at low pH our investigation was confined to the homogeneous region at $p\text{H} \geqq 4.0$. Thus, the conclusions of previous investigators,[8,10] based on hydrodynamic data, are open to question. For this reason, also, we cannot confirm or deny the idea of an α–β transformation at pH's below 4 proposed by Yang and Foster,[10] and discussed recently by Hill.[59] It may be pointed out that the heterogeneous sedimentation patterns of Fig. 3 are compatible with the existence of two forms. However, our sedimentation observations are too meager to identify these as α- and β-forms. It is our opinion that the nature of the configurational changes *below* pH 4 is still an unsettled matter. However, insofar as these changes already manifest themselves to a small extent as the pH is lowered from 5.13 to 4.0, we may conjecture at this time that the combined effects of reversible formation and breakage of hydrogen bonds between side chain polar R groups of BSA, and the concomitant penetration of solvent into the molecular domain (*i.e.*, swelling), will account for the abnormal steepening of the titration curve in the pH region of the ionization of carboxyl groups. However, it must be emphasized that, without a determination of β for each species present below pH 4, we have no assurance that a sphere is a good model at the low pH. Therefore, conclusions drawn from only one hydrodynamic quantity (*i.e.*, viscosity) plus the assumption of spherical symmetry[8,10,60] could be erroneous. It is quite conceivable that the changes taking place below pH 4 would require the use of *asymmetrical* equivalent ellipsoids to account for the hydrodynamic properties of BSA. In fact recent experiments of Harrington, Johnson and Ottewill[44] indicate that such may be the case.

---

(59) T. L. Hill, THIS JOURNAL, **60**, 358 (1956).

(60) The lack of flow birefringence in a molecule as small as BSA is no guarantee of spherical symmetry.

THE SILICON-BROMINE AND SILICON-CARBON(ARYL) BOND PARACHORS AND THE SILICON-BROMINE BOND REFRACTION[1]

BY ALFRED P. MILLS AND WARREN E. BECKER

Contribution from the Department of Chemistry, University of Miami, Coral Gables, Florida

Received July 27, 1956

Trimethylphenylsilane, dimethyldiphenylsilane, trimethylbromosilane, dimethylphenylbromosilane, dimethyldibromosilane and methyldiethylbromosilane were prepared and purified and their refractive indices, densities, surface tensions and viscosities were measured. Using the bond parachor system of Mills and MacKenzie as a basis, values of 74.1 and 1.8 were derived for the silicon–bromine and silicon–carbon(aryl) bond parachors, respectively. Using the system of Vogel and coworkers as a basis, a new value of 10.24 was derived for the silicon–bromine bond refraction from data on 14 compounds. For the six compounds listed above, values of Trouton's constant were found to range from 21.1 to 25.5 and the ratio $\Delta E_{\text{vap}}/\Delta E_{\text{vis}}$ ranged from 2.96 to 3.86.

The organosilicon bond parachor system developed by Mills and MacKenzie[2] did not contain a value for the Si–Br bond and the value for the Si–C-(aryl) bond was based on a high temperature measurement of only one compound. Since most parachors change slightly with temperature it was considered desirable to obtain a new value based on measurements made at 25°.

The Si–Br bond refraction in Vogel's system[3] was based on only three compounds. A new value was obtained by also considering the molar refractions of four compounds measured in this research and eight compounds measured by McCusker and Reilly.[4]

Experimental

Materials.—Trimethylphenylsilane and dimethyldiphenylsilane were prepared by the addition of phenylmagnesium bromide to trimethylchlorosilane and dimethyldichlorosilane, respectively. The silicon–phenyl bonds were then cleaved with bromine by the method of McBride and Beachell[5] to form trimethylbromosilane, dimethylphenylbromosilane and dimethyldibromosilane. Methyldiethylbromosilane was prepared by the addition of appropriate quantities of ethylmagnesium bromide and p-tolylmagnesium bromide to methyltrichlorosilane to form methyldiethyl-p-tolylsilane (b.p. 132° at 20 mm. and 143° at 30 mm.) which was then cleaved with bromine. All of the above compounds were purified by reduced pressure fractionation[6] using a column packed with glass helices and having about 15 theoretical plates.

Density.—The densities were determined in stoppered density bulbs by the method of MacKenzie, Mills and Scott,[7] a cathetometer being used for the measurements.

Refractive Index.—The refractive indices were measured with an Abbe refractometer. Measurements were made rapidly in order to minimize errors due to oxidation and hydrolysis.

Surface Tension.—The surface tensions were determined by the capillary rise method in the double capillary type of apparatus, the two capillaries having internal diameters of 0.3 and 0.55 mm., respectively. A cathetometer was used to measure the capillary rise.

Viscosity.—The viscosities were measured with a Drucker viscometer.

The experimental data are listed in Table I.

Results and Discussion

Bond Parachors.—Using the bond parachor

---

(1) Presented in part at the Meeting-in-Miniature of the Florida Section of the American Chemical Society, Orlando, Florida, May, 1955. Abstracted in part from the M.S. Thesis of Warren E. Becker, University of Miami, May, 1955.

(2) A. P. Mills and C. A. MacKenzie, *J. Am. Chem. Soc.*, **76**, 2673 (1954).

(3) A. I. Vogel, W. T. Cresswell and J. Leicester, THIS JOURNAL, **58**, 177 (1954).

(4) P. A. McCusker and E. L. Reilly, *J. Am. Chem. Soc.*, **75**, 1583 (1953).

(5) J. J. McBride, Jr., and H. C. Beachell, *ibid.*, **74**, 5247 (1952).

(6) We wish to thank Louis H. Dunlop (McKeesport High School, McKeesport, Pa.) Future Scientists of America Summer Fellow, for his help with some of the fractionations.

(7) C. A. MacKenzie, A. P. Mills and J. M. Scott, *J. Am. Chem. Soc.*, **72**, 2032 (1950).

TABLE I

PHYSICAL PROPERTIES OF BROMO- AND PHENYLSILANES

Compound	B.p. °C.	B.p. Mm.	n^t_D	t, °C.	d^{25}_4	d^{35}_4	d^{45}_4
Me_3SiPh	67.3	20	1.4879	25.0	0.8646	0.8561	0.8474
Me_2SiPh_2	137	9	1.5644	20.0	0.9880	0.9797	0.9719
Me_3SiBr	40.5	200	1.4228	28.6	1.1805	1.1656	1.1507
$Me_2PhSiBr$[a]	102.2	20	1.5294	25.0	1.2666	1.2558	1.2449
Me_2SiBr_2	51.9	100	1.4713	25.0	1.7177	1.6992	1.6807
$MeEt_2SiBr$[a]	41.0	20	1.4464	25.0	1.1515	1.1397	1.1277

Compound	γ (dynes/cm.) 25°	γ 35°	γ 45°	Viscosity (m.p.) 25°	Viscosity 35°	Viscosity 45°	MR_D Obsd.	MR_D Calcd.[b]	Br, % Obsd.	Br, % Calcd.
Me_3SiPh	24.29	23.49	22.72	8.55	7.42	6.53	50.07	50.08		
Me_2SiPh_2	32.47	31.59	30.71	35.72	27.80	22.35	69.65	67.97		
Me_3SiBr	19.87	18.75	17.73	5.60	5.00	4.55	33.16	32.72	50.8	52.2
$Me_2PhSiBr$[a]	28.30	27.59	26.88	17.64	14.74	12.55	52.43	52.61	36.9	37.2
Me_2SiBr_2	24.57	23.63	22.80	8.83	7.96	7.14	35.49	35.26	73.6	73.4
$MeEt_2SiBr$[a]	23.55	22.71	21.87	7.86	6.93	6.13	41.99	42.02	44.5	44.1

[a] Previously unpurified compounds. [b] System of Vogel and co-workers.[3]

systems of Mills and MacKenzie[2] and Vogel[8] as a basis, the following bond parachors (ml./mole) were derived: Si–Br 74.1, Si–C(aryl) 1.8. This latter, when used with Vogel's[8] values of 17.85 for C–H and 16.5 for C_{ar}–C_{ar} gives a value of 190.0 for the Si–Ph bond-group. The parachors used in deriving these values are listed in Table II. The probable 50% deviation based on these six observed parachors is 0.72%.

TABLE II

PARACHORS USED IN DERIVING Si–Br AND Si–Ph BOND PARACHORS

Compound	P Obsd.	P Calcd.	Dev., %
Me_3SiPh	385.9	386.1	+0.05
Me_2SiPh_2	513.1	510.7	−0.47
Me_3SiBr	275.9	272.6	−1.19
$Me_2PhSiBr$	391.8	396.4	+1.17
Me_2SiBr_2	282.6	280.5	−0.74
$MeEt_2SiBr$	346.6	350.0	+0.98

Bond Refraction.—Using the bond refraction system of Vogel and co-workers[3] as a basis, a value of 10.24 was derived for the Si–Br bond refraction. The molar refractions used in deriving this value are listed in Table III. The probable 50% deviation based on these 14 observed molar refractions is 0.38%.

TABLE III

MOLAR REFRACTIONS USED IN DERIVING THE Si–Br BOND REFRACTION

Compound	Observer	MR_D Obsd.	MR_D Calcd.	Dev., %
Me_3SiBr	a	33.16	32.88	−0.84
Me_2SiBr_2	a	35.49	35.58	+ .25
$MeEt_2SiBr$	a	41.99	42.18	+ .45
$Me_2PhSiBr$	a	52.43	52.77	+ .65
$MeSiBr_3$	b	38.56	38.27	− .75
$EtSiBr_3$	b	43.35	42.92	− .99
Et_2SiBr_2	b	44.72	44.87	+ .34
$PhSiBr_3$	b	58.10	58.16	+ .10
$PhSiHBr_2$	b	51.04	51.09	+ .10
$PhSiH_2Br$	b	44.09	44.02	− .16
Et_3SiBr	b	46.67	46.83	+ .34
Ph_2SiBr_2	b	75.52	75.36	− .21
$Et_2(ClCH_2CH_2)SiBr$	c	51.37	51.66	+ .56
$SiBr_4$	d	40.74	40.96	+ .54

[a] This research. [b] See ref. 4. [c] D. L. Bailey, L. H. Sommer and F. C. Whitmore, *J. Am. Chem. Soc.*, **70**, 436 (1948). [d] E. L. Warrick, *ibid.*, 68, 2455 (1956).

Vapor Pressure and Viscosity.—The normal boiling points of the six compounds used in this research were obtained by a critical evaluation of literature data. Values of ΔH_{vap} were then calculated from these normal boiling points and the reduced pressure boiling points measured in this research. The Trouton's constants were found to range from 21.1 to 25.5. Values of ΔE_{vis} were calculated from the viscosity data and the ratio $\Delta E_{vap}/\Delta E_{vis}$ was calculated using the approximation, $\Delta E_{vap} = \Delta H_{vap} - RT$. The latter ratio ranged from 2.96 to 3.86, which is quite reasonable for this type of compound. These results are summarized in Table IV.

TABLE IV

VAPOR PRESSURE AND VISCOSITY RELATIONSHIPS

Compound	B.p., °C. (760 mm.)	ΔH_{vap} (kcal./mole)	$\Delta H_{vap}/T_b$ (cal./mole deg.)	ΔE_{vis} (kcal./mole)	$\Delta E_{vap}/\Delta E_{vis}$
Me_3SiPh	171.3	10.49	23.6	2.54	3.82
Me_2SiPh_2	277.4	14.03	25.5	4.42	2.96
Me_3SiBr	79.9	7.46	21.1	1.95	3.48
$Me_2PhSiBr$	215	11.77	24.1	3.21	3.40
Me_2SiBr_2	111.6	8.45	22.0	2.00	3.86
$MeEt_2SiBr$	139.5	9.51	23.1	2.34	3.75

---

(8) A. I. Vogel, W. T. Cresswell, G. J. Jeffery and J. Leicester, *J. Chem. Soc.*, 531 (1952).

SYSTEMATIC ANALYSIS OF CARBON BLACK STRUCTURES[1]

BY LEROY E. ALEXANDER AND ELMER C. SOMMER

Department of Research in Chemical Physics, Mellon Institute, Pittsburgh 13, Pennsylvania

Received July 30, 1956

Diffractometric intensities from carbon blacks were subjected to a precise, systematic analysis in order to disclose both major and minor differences in the structural parameters characterizing the pseudo-crystals, or parallel-layer groups. The method yields the pseudo-crystal dimensions, L_a and L_c, the fraction of disorganized material, the proportion of single (unassociated) layers, and a rather precise choice of the distribution of numbers of layers constituting the pseudo-crystals. Results are given for three representative blacks: Acetylene, Furnex and Micronex.

Introduction

In a previous report[2] a condensed account was given of an X-ray study of four reinforcing carbon blacks wherein a photographic procedure was employed, which, of course, placed a definite limitation on the accuracy of the intensity measurements. In addition, the use of Debye–Scherrer geometry unavoidably introduced some instrumental broadening into certain features of the diffraction pattern. These deficiencies precluded any attempt to evaluate minor differences in the structural parameters.

When subsequently the need arose to measure systematically the structural features of a much larger number of blacks, improved experimental techniques were employed in order to disclose differences of both primary and secondary magnitude. However, time and cost factors required a compromise between the ultimate in accuracy on the one hand and routineness of the method on the other. It was decided that these requirements would be satisfied by employing a parafocusing Geiger-counter diffractometer together with flat specimens of sufficient thickness to yield maximum diffracted energy over the entire range of Bragg angles involved.[3] Geometrical considerations, confirmed experimentally, showed that the use of such thick specimens did not appreciably alter the shapes and breadths of the diffraction lines studied, which are inherently very broad.

As in the previous study, a curve-fitting interpretative method similar to that of Franklin[4] has been followed, but the (002) and (10), rather than (002) and (11), line profiles have been analyzed. In addition to the parameters measured in the earlier investigation, it has been found possible to derive additional information: the fraction of single (unassociated) layers and the fractions of the layers that are associated in groups of 2, 3, 4 and so on. In the present paper attention is focused on the experimental technique and the interpretation of the data obtained, and the results for three carbon blacks are presented for purposes of illustration. No attempt has been made to assess the chemical significance of the structural data or to propose correlations with other physical characteristics. A full account of these properties for all the specimens included in the larger study is to be published later by the Research Laboratories of Columbian Carbon Company. For the information of the general reader it must be emphasized that the present investigation embraces only carbons whose structures are based upon the random-layer lattice, that is, turbostratic structures.[5]

Experimental

The carbon black samples were packed manually in a rectangular cavity of dimensions 1 × 2 × 0.4 cm. in a flat aluminum holder and analyzed with a Norelco wide-range diffractometer using Cu$K\alpha$ radiation. An X-ray beam monitor with auxiliary synchronized counting and timing circuits was employed to compensate for variations in the intensity of the X-ray source.[6] Counts were recorded over the angular range $2\theta = 16–70°$ and corrected for the dead time loss of the Geiger tube.[7] Because of the small sensitivity of the Geiger counter to the shorter wave lengths the contribution of the general radiation could be determined with sufficient accuracy by remeasuring the intensity over the range 16–70° with a 0.035-cm. aluminum filter in the path of the diffracted ray. This eliminated the $K\alpha$ component but permitted about 70% of the general radiation to pass, assuming an effective wave length of 0.5 Å. After subtraction of the general radiation contribution, the approximately monochromatic intensities were corrected for polarization, giving the experimental curve A (see Fig. 1) in arbitrary units.

The usual method of normalizing the experimental curve to electron units consists in matching it to the theoretical independent scattering curve B, at large values of $(\sin \theta)/\lambda$. This approach was not applicable in the present study because of the use of a relatively long wave length ($\lambda = 1.5418$ Å.) as well as the need for restricting the measurements to the narrow angular range $(\sin \theta)/\lambda = 0.08$ to 0.34. However, an analysis of photographic intensity data for four blacks[2] taken over a large angular range showed that the integrated intensity from 0.08 to 0.34 bore a very nearly constant relationship to the intensity of the range 0.56 to 0.90, which had been employed for normalizing the photographic data to electron units. Thus a numerical constant was derived which, when multiplied by the ratio of the integrated intensities of the B and A curves in the range 0.08–0.34, yielded a factor for converting the A intensities to electron units.

In the above normalization procedure the carbon scattering factors of McWeeny[8] were used rather than those of James and Brindley[9] in order to avoid systematic errors arising from an anomaly in the James and Brindley data at lower values of $(\sin \theta)/\lambda$.[4,8] The incoherent scattering[10] was next subtracted to give the coherent scattering curve, A − C, which was then divided by the independent coherent scattering curve E (Fig. 1) point by point to yield a "reduced" intensity curve $I = (A - C)/E$. This curve is suitable for mathematical analysis of the structural parameters.

---

[1] This investigation was sponsored by the Research Laboratories of Columbian Carbon Company.

[2] L. E. Alexander and S. R. Darin, *J. Chem. Phys.*, **23**, 594 (1955); **24**, 1118 (1956).

[3] H. P. Klug and L. E. Alexander, "X-Ray Diffraction Procedures," John Wiley and Sons, New York, N. Y., 1954, pp. 252, 297.

[4] R. E. Franklin, *Acta Cryst.*, **3**, 107 (1950).

[5] B. E. Warren, *Phys. Rev.*, **59**, 693 (1941).

[6] L. E. Alexander, S. Ohlberg and G. R. Taylor, *J. Appl. Phys.*, **26**, 1068 (1955).

[7] Reference 3, pp. 281–290.

[8] R. McWeeny, *Acta Cryst.*, **4**, 513 (1951).

[9] R. W. James and G. W. Brindley, *Phil. Mag.*, **12**, 104 (1931).

[10] A. H. Compton and S. K. Allison, "X-Rays in Theory and Experiment," D. Van Nostrand Co., New York, N. Y., 1935, pp. 780–782.

TABLE I

CALCULATION OF THE (002) INTENSITY PROFILE OF MICRONEX AND COMPARISON WITH THE OBSERVED PROFILE

P'_M	M	Intensity values as a function of Δs							P_M
		$\Delta s = 0$	0.02	0.04	0.06	0.08	0.10	0.12	
0	1								0.07
0.362	2	0.725	0.69	0.59	0.45	0.29	0.145	0.045	.34
.245	3	.735	.65	.41	.17	.03	.00	.05	.23
.147	4	.59	.455	.20	.025	.005	.04	.025	.14
.123	5	.615	.405	.09	.00	.035	.01	.00	.11
.098	6	.59	.315	.02	.025	.02	.00	.015	.09
.025	7	.175	.07	.00	.01	.00	.00	.00	.02
Calcd. intensity		3.43	2.585	1.31	0.68	0.38	0.195	0.135	
Calcd. intensity × 0.860		2.95	2.22	1.13	.58	.33	.17	.12	
M_1 background		0.07	0.07	0.07	.07	.07	.07	.07	
Total calcd. intensity		3.02	2.29	1.20	.65	.40	.24	.19	
Mean obsd. intensity		3.02	2.29	1.18	.68	.41	.26	.19	
Discrepancy		0	0	+0.02	− .03	− .01	− .02	0	

Note: $s_{\max} = 0.283_5$ for Micronex and corresponds to the point $\Delta s = 0$ in the table.

Interpretation of the Data

From the theory of the simple diffraction grating the pattern of an (00*l*) reflection sequence in reduced intensity units can be calculated from the expression[4,11]

$$I = \frac{0.0606}{s^2} \sum \frac{P_M \sin^2 (\pi M d_{M}s)}{M \sin^2 (\pi d_{M}s)} \qquad (1)$$

wherein d_M is the interlayer spacing for a parallel-layer group consisting of M layers, P_M is the fraction of all the layers associated in groups of M layers, and $s = 2(\sin\theta)/\lambda$. A maximum in the summation, being symmetrical, can be conveniently matched with the experimental line profile, I_{002}, after the latter has first been converted to the equivalent symmetrical form by modifying it as[4]

$$I' = \frac{s^2}{0.0606} \times \frac{I - D}{1 - D} \qquad (2)$$

This expression is very sensitive to the proper choice of D, the fraction of disorganized matter in the specimen, which is the first parameter to be determined. The optimum value of D is that which makes the I' profile most symmetrical. Figure 2 illustrates the effects on the I' profile of choosing a value of D that is (a) too small, (c) too large and (b) optimum for Micronex. A "best" value of the interlayer spacing is determined from the maximum point on the (002) line profile as follows. From eq. 1 the first observable maximum occurs when $d_{M}s = 1$, which is equivalent to the second-order reflection in terms of the graphite unit cell. Hence

$$d_M = 1/s_{\max} \qquad (3)$$

For Micronex $s_{\max} = 0.283_5$, so that $d_M = 3.53$ Å.

The next interpretative step is to match the experimental I' profile with a theoretical profile deduced from expression 2. It has been found possible to arrive at a very precise fit by testing a considerable number of M distributions. Figure 3 shows theoretical (002) profiles for several discrete values of M. The diffraction ripples characterizing these pure profiles tend to disappear when the line shape is synthesized from the contributions of various M's. Figure 4 shows the good agreement effected by matching the experimental I'_{002} profile of Micronex with a distribution of M values ranging from 1 to 7 as given in Table III. The mean thickness of a parallel-layer group in a direction normal to the layers, L_c, is given by $\Sigma P_M M d_M$, which for Micronex is found to be equal to 12.1 Å. The quantity $\Sigma P_M M$ may be regarded as the effective number of layers, M_e, per parallel-layer group. For Micronex the computed value of M_e is 3.43.

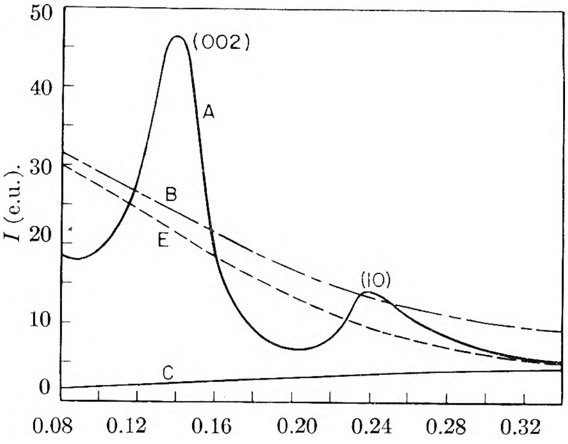

Fig. 1.—(A) Experimental scattering curve of Micronex: theoretical (E) coherent, (C) incoherent, and (B) total independent scattering curves of carbon.

It is important to note that an appreciable proportion (7%) of the layers are unassociated ($M = 1$). These layers contribute to the background of Fig. 4. This background also includes a contribution from the (00*l*) sequence, which does not drop to zero intensity between maxima, as can be seen from the same figure.

The calculation of I' profiles for various distributions of M's is a very tedious process if the precise value of d_M as measured experimentally for each carbon black is substituted in expression 1. Acceptable accuracy is retained, however, and the computations are greatly speeded, if a fixed value of d_{002}, such as 3.54 Å., is employed to compute in advance a complete set of theoretical profiles for M ranging from 2 to 10 or more. It is then a straightforward matter to rapidly compute I' profiles for a variety of distributions of M. The only significant inaccuracy entailed is in the $s_{\max}$ position of

---

[11] R. W. James, "The Crystalline State, Vol. II. The Optical Principles of the Diffraction of X-Rays," G. Bell and Sons, London, 1948, pp. 1–4.

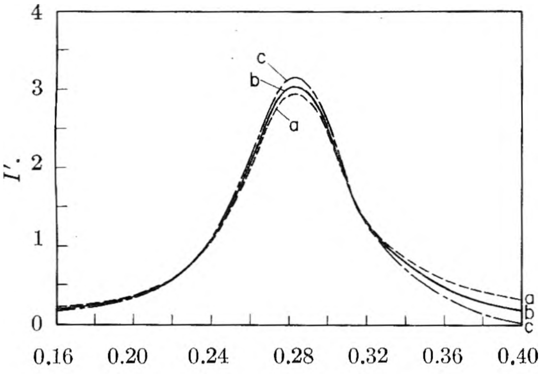

Fig. 2.—Illustration of the proper choice of the parameter D using the (002) profile of Micronex: (a) $D = 0.155$; (b) $D = 0.205$ (best value); (c) $D = 0.255$.

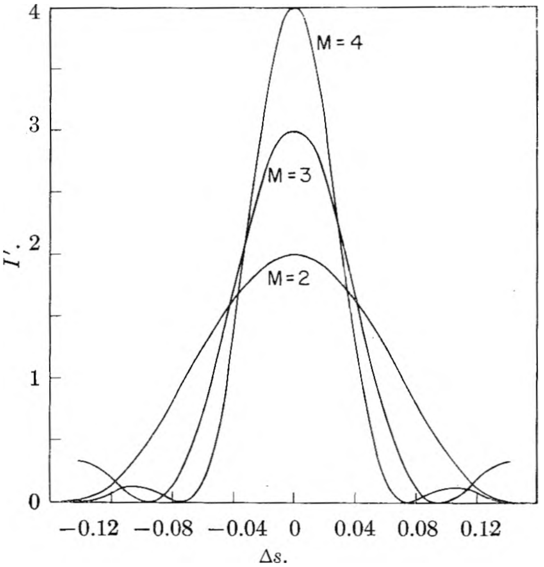

Fig. 3.—Theoretical (002) profiles for three discrete values of M.

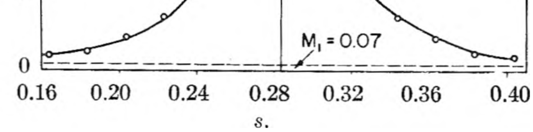

Fig. 4.—Agreement between the experimental (002) profile of Micronex (solid line) and a theoretical profile based on a distribution of M values (small circles).

the computed profile, but this is of no practical concern.

Table I illustrates the (002) calculations by means of the Micronex data. The first stage of the calculations involves choosing a trial distribution of P'_M values such that an approximate fit is simultaneously obtained at $\Delta s = 0$ and at an intermediate value, say 0.04 or 0.06. (The P'_M values are fractions which add up to unity without the inclusion of the $M = 1$ fraction). It is to be emphasized that the P'_M values are selected with a view to matching the line shape rather than the peak intensity, and an arbitrary normalizing factor is deduced to put the calculated line profile on the same intensity scale as that of the observed profile (0.860 for Micronex). In practice the $M = 1$ fraction is initially estimated and a preliminary distribution of P'_M's is arrived at which gives approximate overall agreement. The $M = 1$ fraction is then refined, followed by refinement of the P'_M values, this cyclic process being continued until a stationary state is reached. Finally the P'_M values may be converted to P_M values (last column of Table I) by including the $M = 1$ fraction ($M_1 = 0.07$ for Micronex), which is accomplished by multiplying P'_M values by $1 - M_1$.

The final step in the interpretation of the pattern is to determine L_a, the dimension of a pseudo-crystal in the plane of the layers, by matching the (10) line profile. Franklin has written Warren's equation for the intense low-angle portion of an (hk) profile in the form

$$I = \frac{mF^2}{2\sqrt{2}\pi n A_a}\left(\frac{L_a}{\sqrt{\pi}}\right)^{1/2} s^{-3/2} F(a) \qquad (5)$$

The shape of the broad high-angle portion of the profile has also been described by Warren, but it need not be considered in the present simplified scheme of analysis. Warren[4] has tabulated numerical values of the function $F(a)$, which is given by

$$F(a) = \int_0^{\infty} \exp\left[-(x^2 - a)^2\right]dx \qquad (6)$$

wherein $a = \sqrt{\pi}L_a(s - s_0)$. The various symbols in these expressions have been defined by Franklin.[4] For the (10) reflection the appropriate numerical quantities are: $F = 1$, $m = 12$, $n = 2$, $A_a = 5.25$ Å.^{2}, $s_0 = 0.4703$. The analysis of a carbon specimen is greatly facilitated by calculating in advance the intensities at the peak of the (10) line for all L_a values likely to be encountered. Table II gives the intensities as calculated with the aid of eq. 5 for L_a between 10 and 30 Å.

The choice of L_a can be made simply and directly from the peak intensity alone as follows (where we illustrate the procedure by means of the Micronex data). At $s = 0.48$ the (10) profile is approximately at its peak, the over-all intensity reaching a maximum value of $I_{\max} = 1.10$. In addition to the (10) line the following three contributions to the total intensity must be reckoned with at $s = 0.48$

Disorganized matter, D		0.205
(00) profile	$(00) \times 0.795 \times 0.07 =$	0.012
$(00l)$ profile	$(00l) \times 0.795 \times 0.86 =$	0.058
		0.275

The (00) contribution in the above is calculated using Franklin's eq. 6

$$I = 0.0606s^{-2}$$

it being borne in mind that only the unassociated layers ($M_1 = 0.07$) are involved. The layers associated into groups (M_2, M_3, M_4, etc.) contribute

TABLE II

COMPUTED PEAK INTENSITY OF THE (10) LINE AS A FUNCTION OF L_a

L_a (Å.)	I_{max}	L_a (Å.)	I_{max}
10	0.94	19	1.33
12	1.04	20	1.37
13	1.08	21	1.41
14	1.13	22	1.45
15	1.17	24	1.52
16	1.21	26	1.58
17	1.25	28	1.65
18	1.29	30	1.70

to the (00*l*) sequence, which is given by expression 1. The (00*l*) computation must also take into account the arbitrary normalizing factor (0.86) required to put the calculated and observed intensities on a common basis, and both the (00) and (00*l*) profiles are weakened by the disorganized fraction, 0.205. Subtracting the total intensity, 0.275, due to *D*, (00), and (00*l*), from 1.10, we find 0.825 as the observed intensity due to (10) alone. However, this quantity, as measured, is also weakened by the disorganized fraction, so that we find for the equivalent theoretical (10) intensity of Micronex in the absence of disorganized material

$$I_{10} = 0.825/0.795 = 1.04$$

Reference to Table II shows the appropriate value of L_a to be 12 Å. It is important to notice that in the present analytical scheme no use is made of the breadth of the (10) reflection, as is the rule in the usual rapid procedures for determining crystallite dimensions from experimental line breadths.

Experimental Results

Table III presents the experimental findings for three representative blacks: Micronex—a Columbian channel black, Furnex—a Columbian furnace black, Acetylene—a Shawinigan black made by thermal decomposition of acetylene. The estimated precision of the analytical results is indicated for most of the parameters in the form of probable deviations. It may be noted that Acetylene black shows the greatest growth in both the L_a and L_c dimensions, whereas Micronex shows the least. Conversely, Acetylene contains the least disorganized carbon and Micronex the most.

TABLE III

STRUCTURAL PARAMETERS OF THREE CARBON BLACKS

Parameter	Estimated precision (probable deviation)	Micronex	Furnex	Acetylene
D	0.02	0.205	0.09	0
L_a (Å.)	1.0	12.0	15.0	21.9
L_c (Å.)	0.3	12.0	13.6	19.0
d_M (Å.)	.01	3.53	3.55	3.55
M_e	.15	3.40	3.83	5.34
Distribution of M values				
1	0.015	0.07	0.06	0.05
2	.025	.34	.29	.215
3	.02	.23	.20	.12
4	.02	.135	.14	.105
5	.015	.115	.12	.09
6	.015	.09	.095	.09
7	.01	.02	.07	.08
8	.01		.025	.08
9	.01			.07
10	.01			.07
11	.01			.02
12	.01			.01

Acknowledgment.—The authors are grateful to Dr. C. W. Sweitzer of Columbian Carbon Company for supplying the specimens and for his continued interest during the investigation. They acknowledge with thanks the assistance of Mr. D. T. Pitman with the experimental measurements.

STABILITY OF COPPER AND NICKEL CHELATES OF SOME PHTHALIC ACID DERIVATIVES*

By MOTOO YASUDA, KEINOSUKE SUZUKI AND KAZUO YAMASAKI

Chemical Institute, Nagoya University, Nagoya, Japan

Received July 30, 1956

The stability constants have been measured in aqueous solutions at 25° for the complex $M + XC_6H_3(COO)_2 = XC_6H_3(COO)_2M$, with X equal to H, 3-$NO_2$, 4-$NO_2$, 3-Cl, 3-Br, 4-Br, 4-$OCH_3$ and 4-OC_2H_5, and M equal to Cu and Ni. Compared with phthalic acid, log k_1 and pK_2 of Br, Cl and NO_2 derivatives are smaller, while those of OCH_3 and OC_2H_5 are larger.

There is considerable work available concerning the dissociation constants of metal chelates of dicarboxylic acids. For example, Cannan and Kibrick,[1] and Topp and Davies[2] determined the dissociation constants of dicarboxylates of bivalent metals such as Zn, Mg, Ca and Ba and found that the dissociation constants of the salts formed by a particular metal increased on passing along the series oxalate to adipate. Peacock and James[3] also determined the dissociation constants of dicarboxylates of bivalent metals and came to a similar conclusion. Further, the result obtained by Riley[4] revealed the influences of alkyl substitution on the dissociation constant. But most of these results were confined to zinc and alkaline earth metals.

---

* Presented at the XV International Congress of Pure and Applied Chemistry (Analytical Chemistry) held at Lisbon in September, 1956.

(1) R. K. Cannan and A. Kibrick, *J. Am. Chem. Soc.*, **60**, 2314 (1938).

(2) N. E. Topp and C. W. Davies, *J. Chem. Soc.*, 87 (1940).

(3) J. M. Peacock and J. C. James, *ibid.*, 2233 (1951).

(4) H. L. Riley, *ibid.*, 1642 (1930).

In the present study the stability constants of copper and nickel chelates of phthalic acid and its 3- and 4-substituted derivatives are determined by pH method and the effects of substitution on the stability are examined.

Experimental

Reagents.—All the reagents used, including copper and nickel nitrates, sodium hydroxide and potassium biphthalate were chemicals of analytical grade. 3-Nitro- and 4-nitrophthalic acids, were prepared by nitration of phthalic acid. 3-Bromo- and 4-bromophthalic acids were synthesized by the method of Stephens,[5] and 3-chlorophthalic acid was prepared by diazotization of 3-aminophthalic acid.[6] 4-Methoxy- and 4-ethoxyphthalic acids were the products prepared by Katayama & Co., Osaka.

Measurement of pH.—Measurements of pH were made at 25° by a glass electrode combined with an electronic amplifier made by Mitamura & Co., Tokyo. Standardization of the apparatus was effected by suitable buffer solutions. Potassium nitrate was added to the solution to maintain the ionic strength at 0.1. More concentrated solutions for nickel than for copper were used for the measurements and it was difficult to make measurements at a constant ionic strength. In this condition for nickel, therefore, the ionic strength was maintained at about 0.1 by nickel nitrate itself without adding neutral salt, as the concentration of nickel ion participating in the chelate formation is very low.

To convert the hydrogen ion activity into the concentration the value 0.83 suggested by Kielland[7] was used.

Results

1. Acid Dissociation Constants.—If phthalic acid and its derivatives are represented by H_2A, the acid dissociation constants to be determined are

$$K_1 = \frac{[H^+][HA^-]}{[H_2A]} \tag{1}$$

and

$$K_2 = \frac{[H^+][A^{--}]}{[HA^-]} \tag{2}$$

where [ ] expresses concentration in mole/l. The dissociation constants were determined by titration with alkali and the values obtained are given in Table I.

The first dissociation constants of 3-nitro, 4-nitro and 3-chloro derivatives are considerably larger than the constant of phthalic acid and their accurate values were not determined by pH measurement. Therefore, the dissociation of the first step of these three compounds was assumed to be complete in a pH range larger than 4 and the stabilities of the chelates formed by these ligands were determined in the same pH range.

TABLE I

	Ligand	pK_1	pK_2
1	Phthalic acid[a]	2.76	4.92
2	3-Nitrophthalic acid	<2	3.93
3	4-Nitrophthalic acid	<2	4.12
4	3-Bromophthalic acid	2.27	4.35
5	4-Bromophthalic acid	2.50	4.60
6	3-Chlorophthalic acid	<2	4.49
7	4-Methoxyphthalic acid	2.67	5.16
8	4-Ethoxyphthalic acid	2.74	5.12

[a] Maxwell and Partington obtained values 2.98 and 5.28 for pK_1 and pK_2, respectively, at an ionic strength of 0.03 (*Trans. Faraday Soc.*, **33**, 670 (1937)).

2. Stability Constants.—Phthalic acid and its derivatives can form two chelates with metals, *i.e.*

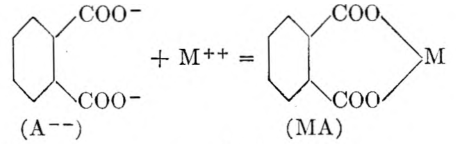

(3)

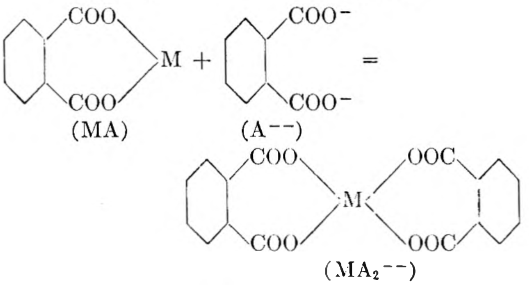

(4)

$$k_1 = \frac{[MA]}{[M^{++}][A^{--}]} \tag{5}$$

$$k_2 = \frac{[MA_2^{--}]}{[MA][A^{--}]} \tag{6}$$

According to Peacock and James,[3] the values of k_2 found for dicarboxylic acids are much smaller than k_1, *i.e.*, the concentration of MA_2^{--} may be neglected in dilute solutions of chelating agents having comparatively low pH. Therefore, in the present experiments in which the following concentrations are used: Cu^{++}, $0.8\text{–}3.8 \times 10^{-3}$, ligands, 1.0×10^{-3} mole/l.; Ni^{++}, $3.3\text{–}3.5 \times 10^{-2}$, ligands, 1.0×10^{-2} mole/l., the species present in the solutions are H^+, M^{++}, MA, A^{--}, HA^-, H_2A and OH^- not including the alkali and nitrate ions added as the neutral salt. Then the following relations exist between concentrations of these species, C_H, C_A and C_M used to express total concentrations of H, ligand and metal, respectively. The concentration of OH^- is negligible in acidic solutions. Thus

$$C_H = [H^+] + [HA^-] + 2[H_2A] \tag{7}$$

$$C_A = [A^{--}] + [HA^-] + [H_2A] + [MA] \tag{8}$$

$$C_M = [M^{++}] + [MA] \tag{9}$$

By substituting (1) and (2) into (7), one obtains

$$C_H - [H^+] = \frac{[A^{--}][H^+]}{K_2} + \frac{2[A^{--}][H^+]^2}{K_1K_2} \tag{10}$$

From the pH measurements of the solutions $[H^+]$ was calculated. By substituting $[H^+]$ into (10), $[A^{--}]$ was found and then [MA] and $[M^{++}]$ were obtained from (8) and (9) combined with (1) and (2) and finally $k_1 = [MA]/([M^{++}][A^{--}])$ was found.[8] The values of stability constant k_1 thus obtained are given in Table II

As shown in Table II the chelates of copper are more stable than those of nickel.

The relationship between basic strength of ligands and stability of chelates was first pointed out

---

(5) H. N. Stephens, *J. Am. Chem. Soc.*, **43**, 1951 (1921).

(6) 4-Chlorophthalic acid was not obtained in pure state.

(7) J. Kielland, *J. Am. Chem. Soc.*, **59**, 1675 (1937).

(8) Experiments were carried out in a more concentrated solution of ligands to find log k_2, stability constant of copper chelate having two moles of phthalate, but the values obtained were less than 1 and were not in good agreement.

TABLE II

	Ligand	log k_1 Cu chelate	Ni chelate
1	Phthalic acid	3.10	2.14
2	3-Nitrophthalic acid	2.42	1.72
3	4-Nitrophthalic acid	2.42	1.65
4	3-Bromophthalic acid	2.95	2.10
5	4-Bromophthalic acid	2.84	2.05
6	3-Chlorophthalic acid	2.86	2.02
7	4-Methoxyphthalic acid	3.32	2.27
8	4-Ethoxyphthalic acid	3.25	2.18

by Calvin and Wilson[9] in connection with cupric chelates of a number of enolic substances.

Similar relations are also found in the derivatives of phthalic acid. An approximate linear relationship between log k_1 and pK_2 is found for copper and nickel chelates, respectively, although the values of 3-bromophthalate deviate from the straight line (Fig. 1).

The stability decreases as the acid dissociation constant K_2 of ligands increases, that is, as pK_2 decreases. The effect is most remarkable first for the substitution of a nitro group, and next for Cl and Br atoms. The effects of methoxy and ethoxy groups are opposite to other groups, that is, the stability increases as the pK_2 increases. These results are shown in Fig. 1.

Peacock and James[3] obtained 8.6 × 10^{-5} for the thermodynamic dissociation constant of copper phthalate, Davies' empirical formula[10] being used to calculate the activity coefficient of copper and phthalate. The equation proposed by Davies for the mean ionic activity coefficient of an electrolyte in water at 25° is

$$-\log f \pm = 0.50Z_1Z_2\left\{\frac{\sqrt{I}}{1+\sqrt{I}} - 0.20I\right\}$$

where Z_1, Z_2 are the valencies of the ions and I is the ionic strength. If our value for copper phthalate is recalculated in the same way, the value $10^{3.98}$ for the thermodynamic stability constant is obtained which agrees well with $10^{4.07}$, the reciprocal of 8.6 × 10^{-5} of Peacock and James' value.

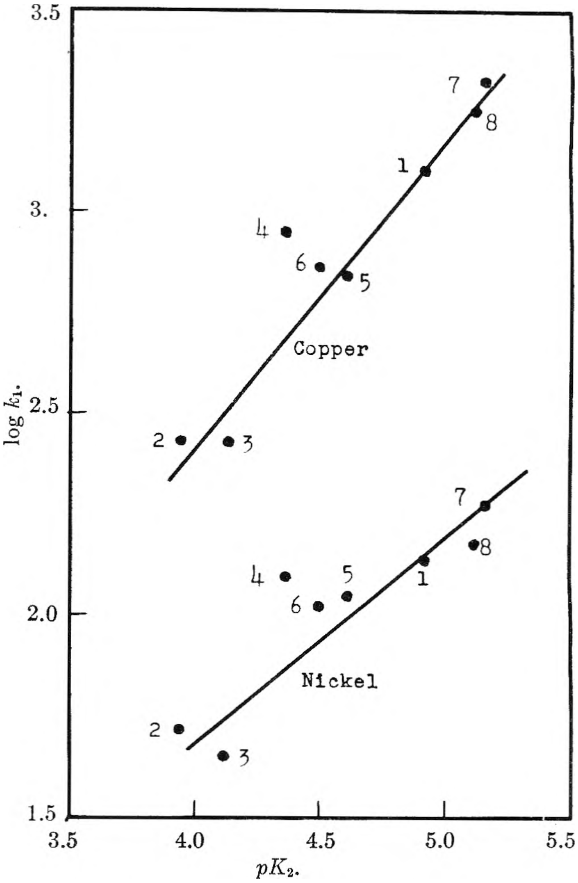

Fig. 1.—Relations between log k_1 and pK_2 of copper and nickel chelates: (1) phthalic acid, (2) 3-nitro-, (3) 4-nitro, (4) 3-bromo-, (5) 4-bromo-, (6) 3-chloro-, (7) 4-methoxy-, (8) 4-ethoxyphthalic acid.

[9] M. Calvin and K. W. Wilson, *J. Am. Chem. Soc.*, **67**, 2003 (1945).

[10] C. W. Davies, *J. Chem. Soc.*, 2093 (1938).

BINARY FREEZING POINT DIAGRAMS FOR PALMITIC ACID WITH A SERIES OF SUBSTITUTED 2-AMINOPYRIDINES

BY ROBERT R. MOD, FRANK C. MAGNE AND EVALD L. SKAU

Southern Regional Research Laboratory,[1] *New Orleans, Louisiana*

Received July 30, 1956

Binary freezing point data have been obtained for palmitic acid with each of the following 2-aminopyridine derivatives: 2-amino-3-methylpyridine, 2-amino-4-methylpyridine, 2-amino-5-methylpyridine, 2-amino-6-methylpyridine, 2-amino-4,6-dimethylpyridine and 2,2′-dipyridylamine. The binary freezing point diagrams show that each of these amines forms an equimolecular compound with palmitic acid and, in addition, the 2-amino-3-methylpyridine forms a 2:1 (2 acid:1 amine) compound. The freezing points of these molecular compounds and a number of metastable polymorphic modifications have been determined.

In a recent publication from this Laboratory[2] it was shown by binary freezing point measurements that 2-aminopyridine forms congruently melting, crystalline molecular compounds with long-chain fatty acids—an equimolecular compound and a compound consisting of 2 or 4 molecules of acid per mole of amine, respectively, depending upon whether the acid is unsaturated or saturated. It was pointed out that all of these compounds might play a part in procedures such as that described by Ramsay and Patterson,[3] in

[1] One of the laboratories of the Southern Utilization Research Branch, Agricultural Research Service, U. S. Department of Agriculture.

[2] R. R. Mod and E. L. Skau, THIS JOURNAL, **60**, 963 (1956).

[3] L. L. Ramsay and W. I. Patterson, *J. Assoc. Off. Agr. Chemists*, **31**, 139 (1948).

which this amine is used in the separation of homologous fatty acids by partition chromatography. Similar freezing point data have now been obtained for binary systems of palmitic acid with various derivatives of 2-aminopyridine including the four isomeric 2-amino-methylpyridines, 2-amino-4,6-dimethylpyridine and 2,2′-dipyridylamine.

Experimental

Practical grades of the amines, obtained from Reilly Tar and Chemical Corporation,[4] were purified as described below. All recrystallizations were performed from concentrated solutions in centrifugal filtration tubes.[5] Special precautions to exclude moisture were necessary in weighing the 2-amino-3-methylpyridine and the 2-amino-6-methylpyridine into the composition tubes.

The 2-amino-3-methylpyridine was recrystallized 3 times from benzene. Most of the residual benzene was removed from the crystals over paraffin wax in an evacuated desiccator. The amine was then transferred to a separatory funnel containing dry nitrogen and sodium hydroxide pellets. After standing in the liquid state with periodic shaking for 3 hours, it was transferred under a nitrogen blanket to a specially designed acuum distilling flask, refluxed gently under a slow sweeping current of dry nitrogen to drive off any residual solvent, and distilled. The foreruns were rejected and then the desired amounts of the pure amine (f.p. 33.17°) were distilled under vacuum directly into composition tubes containing weighed portions of pure palmitic acid. The exact composition was obtained by difference from the weight of the sample tube after sealing.

The 2-amino-6-methylpyridine was recrystallized 3 times from acetone and the residual solvent was removed *in vacuo* at about 45°. The rest of the procedure for preparing the pure amine (f.p. 44.22°) and making up the binary mixtures from 0 to 60.39 mole % of acid was the same as that described for the 2-amino-3-methylpyridine. Except for the 60.39% sample all of the mixtures containing more than 50% of acid were made up by weighing out the proper amounts of the acid and the 1:1 compound. The 1:1 compound (f.p. 65.31°; N, 7.74%, theory, 7.68%) was prepared by repeated recrystallization of an equimolecular mixture of palmitic acid and the crude 2-amino-6-methylpyridine.

The pure 2-amino-5-methylpyridine (f.p. 76.54°) and 2,2′-dipyridylamine (f.p. 95.09°) were obtained by repeated recrystallization from acetone, the 2-amino-4-methylpyridine (f.p. 99.21°) from a 2 to 1 mixture of benzene and acetone by volume, and the 2-amino-4,6-dimethylpyridine (f.p. 68.36°) from benzene. All the binary composition tubes were filled with dry nitrogen and then sealed off in vacuum.

The palmitic acid (f.p. 62.51°) was a recrystallized sample obtained through the usual fractional vacuum distillation of the methyl ester.

The freezing points were determined by the thermostatic, sealed-tube method previously described,[6] which gives the true equilibrium temperature between the crystals and the liquid mixture of the given composition with an accuracy of ±0.2° after correction for thermometer calibration and emergent stem.

Results and Discussion

Binary freezing point data for palmitic acid with the various amines are given in Table I and represented graphically in Figs. 1 and 2. A congruently melting 1:1 compound forms in all of these binary systems. In the 2-amino-3-methylpyridine system there is an additional molecular compound, also melting congruently, made up of two molecules of acid and one of amine.

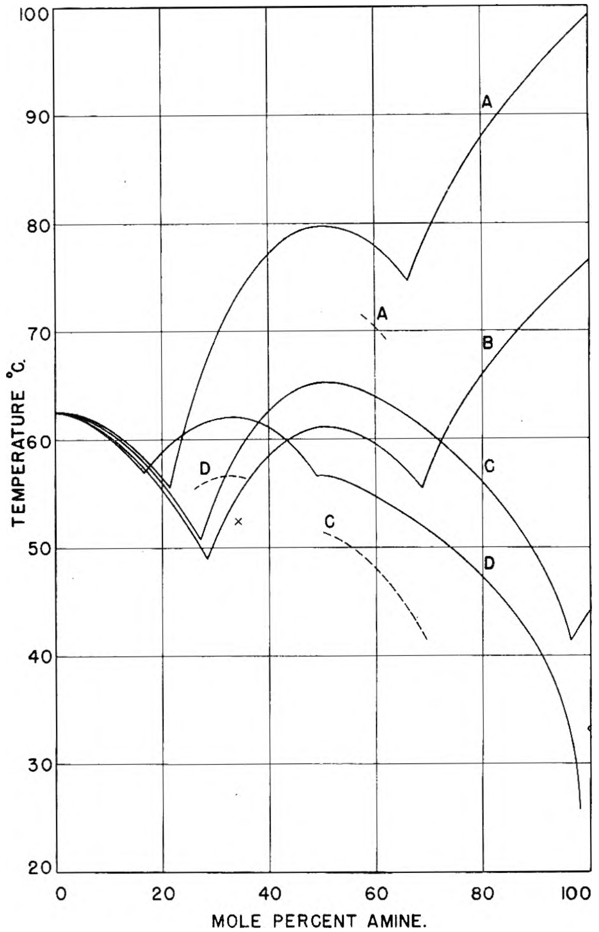

Fig. 1.—Binary freezing point diagrams for palmitic acid with: A, 2-amino-4-methylpyridine; B, 2-amino-5-methylpyridine; C, 2-amino-6-methylpyridine; D, 2-amino-3-methylpyridine. Cross (system C) and broken lines represent metastable equilibria.

In the compound region of the diagrams two freezing points were sometimes obtainable. The full lines represent the temperatures at which the various liquid compositions are in equilibrium with the stable polymorphic form of the molecular compound. The broken lines represent the corresponding metastable equilibria between the liquid and the lower-melting modification. The higher freezing point was almost always obtained on the initial melting of the samples. Heating the samples some degrees above this temperature resulted in the destruction of the crystal nuclei of the stable modification, and the solid which formed on slow cooling gave freezing points which tended to fall on the lower, broken curves. More than one attempt was usually necessary to obtain the low-melting form and its freezing point could not always be measured with the same precision. The higher freezing point could practically always be obtained again by shock-chilling the molten sample in a Dry Ice–alcohol mixture. In some instances, spontaneous transformation to the high melting modification took place during the freezing point measurement of the low-melting form.

---

(4) The mention of names of firms or trade products does not imply that they are endorsed by the Department of Agriculture over other firms or similar products not mentioned.

(5) E. L. Skau, This Journal, **33**, 951 (1929); E. L. Skau and W. Bergmann, *J. Org. Chem.*, **3**, 166 (1938); E. L. Skau and H. Wakeham, "Melting and Freezing Temperatures," in Weissberger, "Physical Methods of Organic Chemistry," 2nd ed., Vol. I, Part I, Interscience Publishers, New York, N. Y., 1949, pp. 99-100.

(6) F. C. Magne and E. L. Skau, *J. Am. Chem. Soc.*, **74**, 2628 (1952).

An attempt was made to obtain the metastable equilibrium points for all compositions in the compound regions. Only in the 2-amino-4,6-dimethylpyridine system, however, was it possible to delineate the curve for the metastable form over a wide range of compositions—as shown by the broken line in Fig. 2. In the other systems only a few points on the curve were obtainable: 3 points for the 2:1 compound with 2-amino-3-methylpyridine, one point for the 1:1 compound with 2-amino-4-methylpyridine, and 4 points in the 2-amino-6-methylpyridine for either a 1:1 or a 2:1 compound. One of these 4 points, represented by the cross in Fig. 1, seems to be inconsistent with the other 3 points. These delineate the broken line which is more or less parallel to the upper curve for the 1:1 compound. The solid phase at the 4th point could be a second metastable modification of the 1:1 compound or, less likely, a metastable 2:1 com-

TABLE I

FREEZING POINT DATA FOR BINARY MIXTURES OF PALMITIC ACID WITH SUBSTITUTED 2-AMINOPYRIDINES

Mole % amine[a]	F.p., °C.[a,d]		Mole % amine[a]	F.p., °C.[a,d]	
		2-Amino-3-methylpyridine			
0.00	62.51		47.74	57.6	
11.67	59.6		(49.1)[b]	(56.7)[b]	
16.28	57.3		(50.00)[c]	(56.7)[c]	
(16.8)[b]	(57.1)[b]		50.13	56.7	
16.94	57.2		54.72	56.1	
21.33	59.4		66.68	52.7	
21.65	59.4		80.53	44.9	
24.23	60.6		83.43	45.4	
26.92	61.5,	*55.8*[d]	90.19	40.8	
29.99	61.9,	*56.4*	94.61	36.0	
(33.33)[c]	(62.2),[c]	*(56.7)*[c]	97.62	29.2	
34.42	62.2,	*56.6*	98.16	26.3	
38.32	61.7		100.00	33.17	
45.87	58.8				
		2-Amino-4-methylpyridine			
0.00	62.51		(50.00)[c]	(79.8),[c]	*(72–73)*[c]
14.08	59.5		50.49	79.7	
(21.5)[b]	(55.6)[b]		56.01	79.2	
22.73	58.2		60.18	77.9,	*70.3*
25.21	62.8		(66.2)[b]	(74.7)[b]	
29.55	68.6		69.22	78.2	
40.45	77.4		80.02	88.1	
45.51	79.3		89.66	94.0	
			100.00	99.21	
		2-Amino-5-methylpyridine			
0.00	62.51		(50.00)[c]	(61.2)[c]	
11.77	59.8		50.12	61.2	
16.52	57.5		55.69	60.8	
19.31	55.8		59.95	59.7	
27.11	50.3		(68.8)[b]	(55.5)[b]	
(28.5)[b]	(49.0)[b]		69.85	56.8	
30.35	51.2		79.93	66.0	
39.76	58.4		90.00	71.7	
			100.00	76.54	
		2-Amino-6-methylpyridine			
0.00	62.51		50.00[c]	65.3,[c]	*51.4*[c]
14.72	59.0		56.54	64.9	
18.96	56.8		58.86	64.3,	*47.5*
20.85	55.7		69.82	60.7,	*41.5*
24.33	53.2		78.05	57.2	
(27.2)[b]	(50.8)[b]		89.89	49.4	
29.64	54.0		94.15	44.9	
34.11	58.6,	*52.5*	(96.4)[b]	(41.5)[b]	
38.62	61.8		97.70	42.5	
39.61	63.2		100.00	44.22	
43.42	64.0				
		2-Amino-4,6-dimethylpyridine			
0.00	62.51		49.26	73.3	
10.96	60.1		(50.00)[c]	(73.3),[c]	*(64.2)*[c]
19.12	56.2		54.47	72.8,	*64.2*
20.91	55.0		60.23	71.4,	*63.0*
(23.8)[b]	(52.9)[b]		69.30	67.5,	*62.5*
25.35	55.1		73.97	65.2	
28.02	57.6		75.65	64.2,	*61.6*
29.57	.. ,	*58.6*	79.66	60.3	
29.96	.. ,	*58.9*	81.97	59.4	
34.37	64.8,	*61.1*	(84.3)[b]	(57.1)[b]	
35.80	66.5,	*61.5*	84.85	57.8	
40.09	70.2,	*61.9*	89.42	61.5	
46.82	72.6		100.00	68.36	
		2,2′-Dipyridylamine			
0.00	62.51		49.82	60.9	
10.78	60.7		(50.00)[c]	(61.0)[c]	
18.83	58.7		55.29	60.0	
20.34	58.3		(59.2)[b]	(58.3)[b]	
26.87	56.1		60.59	61.2	
(30.0)[b]	(54.9)[b]		69.64	75.3	
30.21	55.0		79.48	83.7	
33.81	56.7		89.38	89.7	
40.32	59.3		100.00	95.09	
45.47	60.6				

[a] The values in parentheses were obtained by graphical interpolation. [b] Eutectic. [c] Freezing point of compound. [d] Values in italics are for metastable equilibria.

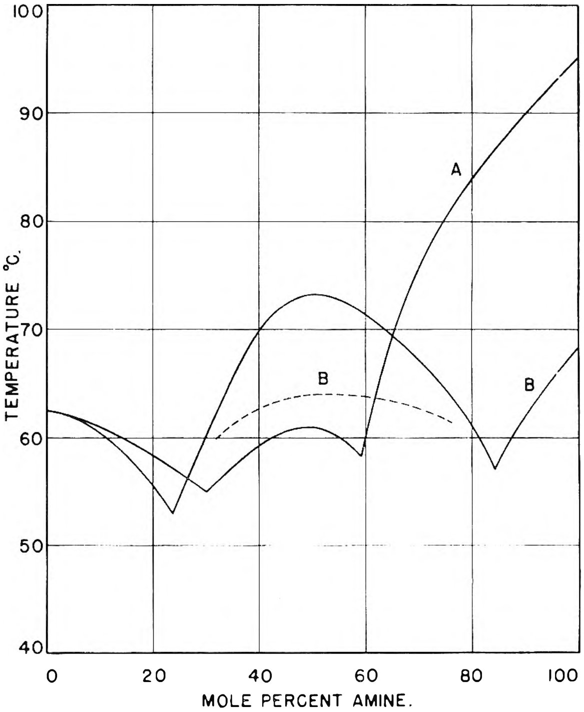

Fig. 2.—Binary freezing point diagrams for palmitic acid with: A, 2,2′-dipyridylamine; B, 2-amino-4,6-dimethylpyridine. Broken lines represent metastable equilibria.

pound. No evidence was found of the existence of a metastable modification of the 1:1 compound of either 2-amino-3-methylpyridine, 2-amino-5-methylpyridine or 2,2′-dipyridylamine.

Comparison of the present results with those for the corresponding binary system between 2-aminopyridine and palmitic acid[2] shows that the introduction of a methyl group in the various positions in the pyridine ring does not prevent the formation of a 1:1 compound. It does, however, interfere with the formation of crystalline compounds richer in palmitic acid. The binary freezing point diagrams show that the unsubstituted 2-aminopyridine forms a 4:1 compound (4 moles of acid to one of the amine). The 3-methyl derivative of 2-aminopyridine, on the other hand, gives only a 2:1 compound in addition to the equimolecular composition and the other derivatives give only the 1:1 compound.

The melting point of the low-melting modification of the equimolecular compound of 2-amino-4-methylpyridine and palmitic acid was not determined experimentally but from Fig. 1 it was estimated to be about 72–73°. Though the data do not permit the estimation of the exact eutectic on the amine side of the 2-amino-3-methylpyridine system it obviously lies at a composition just above 98% of amine.

The relative degrees of dissociation of the acid–amine compounds can be deduced tentatively from the freezing point data. The ideal freezing point curve for palmitic acid calculated from its heat of fusion and freezing point would fall above all the curves on the palmitic acid side of Figs. 1 and 2. That is, over the range of concentrations in which the acid is the solid phase, the experimental freezing points fall below the ideal (calculated) values. If the deviation is assumed to be caused wholly by compound formation in the liquid state the data show that, at the given temperature, the proportion of free acid in the molten acid–amine compound is greatest for the 2,2′-dipyridylamine and decreases in the order 4-methyl-, 6-methyl-, 4,6-dimethyl-, 5-methyl- and 3-methyl-2-aminopyridine. The data for unsubstituted 2-aminopyridine[2] on this basis indicate that its acid-amine compound dissociates to about the same extent as the 2-amino-5-methylpyridine compound.

A COMPARISON OF PYCNOMETRIC AND X-RAY DENSITIES FOR THE SODIUM CHLORIDE–SODIUM BROMIDE AND POTASSIUM CHLORIDE–POTASSIUM BROMIDE SYSTEMS[1,2]

BY JOHN S. WOLLAM AND W. E. WALLACE

Department of Chemistry, University of Pittsburgh, Pittsburgh 13, Penna.

Received August 9, 1956

Pycnometric and X-ray densities are presented for seven NaCl–NaBr and two KCl–KBr solid solutions, and for NaCl, NaBr and KCl. Discrepancies found were in general smaller than had been found in earlier comparisons of X-ray and directly determined densities of alkali halide solid solutions. The discrepancies for the solid solutions are, however, in almost all cases larger than for the pure salts suggesting the existence of a greater number of lattice defects in the solutions than in the pure components.

Introduction

Studies of NaCl–KCl solid solutions conducted in this Laboratory several years ago showed[3] that the densities, when measured by a flotation technique, were for some compositions significantly lower than the values calculated from the lattice parameters. If the density deficiency were ascribed to Schottky defects, a comparison of the measured and computed densities showed for some compositions, a vacancy concentration of up to 1.1%. These large values, found in the solutions rich in NaCl, exceeded by a factor of about 100 the number of unoccupied sites[4] in the pure salts at room temperature.

This unexpected finding prompted immediate consultation of the literature with respect to the densities of other alkali halides systems. Wallace and Flinn,[5] using density data by Tammann and Krings[6] and unit cell dimensions by Oberlies,[7] found density discrepancies for the KCl–KBr system which indicated that it too contained Schottky defects of the order of 1%, with a maximum for the KCl-rich solutions. The idea was then advanced that strains arising from the distribution of components of unequal size over a given set of lattice sites could be relieved if an occasional site were left vacant. As a corollary, it of course follows that strains and therefore defect concentrations will be greatest where larger ions try to fit themselves into a smaller lattice, *i.e.*, at low mole fractions of the larger component.

On this basis, it would seem that as a first approximation the vacancy concentration at any given composition should depend on the difference in lattice parameter of the compounds. With regard to the two systems KCl–NaCl and KCl–KBr this did not appear to be the case, since KCl–NaCl, with 11.5% difference in component lattice con-

---

[1] From a thesis submitted by John S. Wollam to the Graduate School of the University of Pittsburgh in partial fulfillment of the requirements for the M.S. degree, June, 1956.

[2] This work was assisted by the U. S. Atomic Energy Commission.

[3] W. T. Barrett and W. E. Wallace, *J. Am. Chem. Soc.*, **76**, 366 (1954).

[4] W. Shockley, *et al.*, "Imperfections in Nearly Perfect Crystals," John Wiley and Sons, New York, N. Y., 1952, p. 31.

[5] W. E. Wallace and R. A. Flinn, *Nature*, **72**, 681 (1953).

[6] G. Tammann and W. Krings, *Z. anorg. Chem.*, **130**, 229 (1923).

[7] F. Oberlies, *Ann. Physik*, **87**, 238 (1928).

stant showed a maximum density discrepancy of 1.1% at 70% NaCl, while KCl–KBr, with only 4.7% parameter difference had a 1.2% density difference at 70% KCl and a maximum of 1.9% at 80% KCl. An obvious first step in the resolution of this apparent paradox was the comparison of density and X-ray data for a third system. The NaCl–NaBr system was chosen for this purpose. The results of this comparison, given below, made it desirable to extend the work to include a partial reexamination of the KCl–KBr system.

Experimental

The NaCl used was J. T. Baker Analyzed Reagent 99.99% pure, while the NaBr, KCl and KBr were Fisher Certified Reagents containing 99.75% NaBr with 0.25% NaCl, 99.99% KCl and 99.68% KBr with 0.32% KCl, respectively, by weight. The solid solutions were prepared and their concentrations determined using methods previously employed in this Laboratory.[3]

The macroscopic densities were measured by placing the crystals in pycnometer bottles with toluene as the confining liquid. To minimize errors due to occluded air, the bottle containing the small crystals of salt was pumped on in a vacuum desiccator and the toluene added to it while still under vacuum. A water-bath, held at 24.995°, was used as a thermostat.

The X-ray data for the calculation of microscopic densities were obtained by conventional X-ray powder diffraction techniques. The samples, in 0.5 mm. Vycor tubes, were placed in a Debye camera of 114 mm. diameter with a one-mm. pinhole and exposed to Cu $K\alpha$ radiation for 12 hours during which time the temperature was held at 25 ± 1°. The back reflection lines on the resulting photographs were indexed and the lattice parameter was determined using the Bradley and Jay[8] method of extrapolation. The average weight of the contents of unit cell was divided by the volume of the unit cell, as calculated from the lattice parameter, to find its density.

Results

In Table I the data obtained for the NaCl–NaBr system by the procedures described above are collected and compared. It will be seen that the expected difference in density of 1% or more was not found. Therefore, even if the entire difference in density is assumed to be due to Schottky defects, the concentration of vacancies is considerably less than 1%. It is to be noted, however, that the differences in densities for the solid solutions in six out of seven cases exceed the values for the pure salts. The differences found at 30, 40 and 50% NaBr are more than twice the differences found in the pure salts and suggest the possibility that some depopulation of lattice sites has occurred. Additional support of a qualitative nature is provided by the observation that the solid solutions discolor in the X-ray beam much more readily than the pure salts. The discoloration undoubtedly originates with color centers, which are generally regarded as resulting from the trapping of electrons in vacant lattice sites.

The density difference of 0.22% found at 80% NaBr is of considerable interest. If vacancies originating with strains are responsible for this difference, it may be that the strains arise from the very considerable disparity between the anion–cation distance in this solution and the sum of the ionic radii of sodium and chlorine. Electrostatic forces work to establish the Na^+–Cl^- distance in the solution as the sum of the ionic radii, but this entails considerable local distortion and straining of the lattice, possibly giving rise to the formation of vacancies to relieve these strains. However, other effects may be responsible for the density difference such as a short range phase segregation, giving a crystal composed of clumps of a dozen or so ions of each component with strains and therefore vacancies along their borders. A long range phase segregation is not responsible since all the X-ray photographs, including the one for this composition, showed the crystals to consist of a single homogeneous phase.

TABLE I

DENSITIES OF NaCl–NaBr SOLID SOLUTIONS BY PYCNOMETRIC AND X-RAY MEASUREMENTS AT 25°

Mole % NaBr	Pycnometric densities, g./cm.^{3} Individual values	Pycnometric densities, g./cm.^{3} Mean value	X-Ray densities, g./cm.^{3}	% Difference
0.000	2.1612 2.1618 2.1616	2.1615	2.163_0	0.07
10.00_0	2.2826 2.2831 2.2829	2.2829	2.284_8	.08
19.97_7	2.3970 2.3971	2.3971	2.398_7	.07
29.96_3	2.5069 2.5069	2.5069	2.512_3	.22
39.91_2	2.6171 2.6172 2.6164	2.6169	2.622_0	.20
49.93_1	2.7203 2.7204	2.7203	2.724_4	.15
59.91_3	2.8256 2.8247 2.8263	2.8255	2.828_4	.10
79.87_2	3.0163 3.0162 3.0159 3.0157	3.0160	3.022_8	.22
99.56_2	3.1979 3.1981	3.1980	3.199_2	.04

When it became apparent that the NaCl–NaBr system did not contain the expected numbers of Schottky defects, the reality of the vacancy concentrations thought to exist in the KCl–KBr system became questionable. The sets of data used in the previous comparison,[5] while each reliable in itself, were obtained by different workers using different samples so that conclusions drawn from their comparison are not completely satisfactory. Therefore, the KCl–KBr system was re-examined at those concentrations most likely to contain the largest numbers of vacancies, and both macroscopic densities were determined from the same sample. The resulting data, shown in Table II, indicate that while some Schottky defects may be present, the concentration is at least an order of magnitude less than had been supposed.

In Table III the data collected in the present investigation are shown together with values found by other workers. For the NaCl–NaBr system, the previously determined X-ray densities are

---

[8] A. J. Bradley and A. H. Jay, *Proc. Phys. Soc. (London)*, **44**, 563 (1932).

TABLE II

DENSITIES OF KCl–KBr SOLID SOLUTIONS BY PYCNOMETRIC AND X-RAY MEASUREMENTS AT 25°

Mole % KBr	Pycnometric densities, g./cm.³ Individual values	Pycnometric densities, g./cm.³ Mean value	X-Ray densities, g./cm.³	% Difference
0.000	1.9868	1.9868	1.9862	−0.03
	1.9868			
20.00	2.1557	2.1558	2.1602	.20
	2.1555			
	2.1561			
30.00	2.2379	2.2377	2.2386	.04
	2.2374			
	2.2377			

TABLE III

DENSITIES OF NaCl–NaBr AND KCl–KBr SOLID SOLUTIONS AT 25°

Mole % bromide	X-Ray densities, g./cm.³ Present work	X-Ray densities, g./cm.³ Previous work	Directly determined densities, g./cm.³ Present work	Directly determined densities, g./cm.³ Previous work
		NaCl–NaBr System		
0.00	2.163	2.164[a]	2.162	2.170[b]
10.0	2.285	2.286[a]	2.283	
20.0	2.399	2.403[a]	2.397	
30.0	2.512	2.515[a]	2.507	2.427[b]
40.0	2.622	2.624[a]	2.617	
50.0	2.724	2.728[a]	2.720	2.611[b]
60.0	2.828	2.831[a]	2.826	2.711[b]
80.0	3.023	3.024[a]	3.016	2.911[b]
100	3.199	3.202[a]	3.198	3.179[b]
		KCl–KBr System		
0.00	1.986	1.988[c]	1.987	1.988[c]
		1.994[d]		1.994[e]
20.00	2.160	2.166[d]	2.156	2.124[e]
30.00	2.239	2.247[d]	2.238	2.214[e]

[a] Nickels, Fineman and Wallace, ref. 9. [b] Bellanca, ref. 10. [c] Barrett and Wallace, ref. 3. [d] Oberlies, ref. 7. [e] Tammann and Krings, ref. 6.

by Nickels, Fineman and Wallace[9] and the directly determined densities are by Bellanca.[10] He used a flotation method with a methylene iodide and benzene mixture as his buoyant liquid, the density of which was in turn measured with a Westphal balance. For the KCl–KBr system the previous X-ray data are by Barrett and Wallace[3] and by Oberlies[7] and the direct measurements by Barrett and Wallace[3] and by Tammann and Krings.[6]

The X-ray densities are in fairly good agreement in view of the difficulty in the estimation and control of sample temperature. The directly determined densities observed in the present work are generally greater than those previously found. It would seem that this difference is mainly due to the precautions taken in the present case for the removal of occluded air from the crystals.

[9] J. E. Nickels, M. A. Fineman and W. E. Wallace, THIS JOURNAL, **53**, 625 (1949).

[10] A. Bellanca, *Periodico mineral*, **10**, (1939).

AN EXPERIMENTAL INVESTIGATION OF SOME MODELS FOR OPTICAL ACTIVITY

BY MARVIN H. WINKLER*

Contribution from the Nichols Laboratory, Department of Chemistry, New York University, New York, N. Y.

Received August 9, 1956

Karl F. Lindman[1–5] investigated the interaction of several different models, with a beam of microwaves. He obtained data which, according to his interpretation, showed that his models affected plane polarized microwaves in a manner analogous to the way in which optically active molecules affect plane polarized light. These models have been generally accepted in the literature as valid models for optical activity. The present author has obtained results with helical models which duplicate those obtained by Lindman; however, efforts to repeat Lindman's work on irregular tetrahedra were not successful. The "rotations" of these asymmetric models were found to be a function of the position of the model. Further investigation showed that a symmetric unit placed asymmetrically was capable of giving the same results, indicating that no rotation of the plane of polarization is involved. An alternate theory based on the diffraction by a single sphere is offered to explain the data.

Introduction

During the early part of this century, K. F. Lindman published the results of a series of experiments dealing with model systems which seemed to have the power of rotating the plane of polarization of linearly polarized microwaves.[1–5] These systems, copper helices or asymmetric spatial distributions of copper spheres which had diameters ranging from several millimeters to several centimeters, were studied with electromagnetic radiation in the 3 to 20 cm. wave length region of the spectrum. Absorption spectra and rotatory dispersion curves were reported which strongly resembled the Cotton curve characteristic of optically active molecular systems. The microwaves were generated by a high frequency spark and the desired wave length selected by tuning the radiating (polarizing) antenna. The power picked up by a rotatable receiving antenna after the radiation had passed through a model was measured by means of a thermocouple. The readings of this thermocouple were compared with those of another coupled to an indicating antenna which was positioned to sample a portion of the beam which did not pass through the model and therefore was assumed to give readings proportional to the total power emitted without reference to any possible influence

---

* Roswell Park Memorial Institute, Buffalo 3, New York.

[1] K. F. Lindman, *Ann. Physik*, **38**, 523 (1912).

[2] K. F. Lindman, *ibid.*, **63**, 621 (1920).

[3] K. F. Lindman, *ibid.*, **69**, 270 (1922).

[4] K. F. Lindman, *ibid.*, [4] **74**, 541 (1924).

[5] K. F. Lindman, *ibid.*, **77**, 337 (1925).

which may have been exerted by the model. The purpose of work reported here was to determine to what extent the experimental results obtained with these model systems could be used to interpret the optical activity of molecules.

Experimental

Apparatus.—Two microwave generators were designed to operate in the 3 and 10 to 20 cm. regions of the spectrum. A detailed description of both instruments has been given elsewhere[6] and therefore only those features essential to the ensuing discussion will be noted here. The 10 to 20 cm. radiation was generated by a 2C40 tube in a tunable lighthouse cavity. The 3 cm. waves were produced by a 723/A Klystron and its associated wave guide components. The receiving antennae for both spectral regions and the transmitting antenna for the longer wave lengths were slotted dipoles[7] modified so that different wings could be screwed in as the wave length was changed. Reflections were kept at a minimum in the 10 to 20 cm. region by operating out of doors well away from any metal structure. At 3 cm. a tuned absorber was found to be adequate for reducing interfering radiation.

The receiving antennae were rotated synchronously with the chart drive of a Brown recorder which continuously plotted energy intercepted against the angular position of the antenna. Once during each revolution, a cam rotating with the dipole closed a fixed micro switch, momentarily deflecting the recorder pen, and thus defining the angular position of the antenna with respect to the chart. Maximum power is received by a dipole when its plane is parallel to the plane of polarization of the intercepted radiation, therefore, the linear chart distance between the pen deflection, and the center of a power peak, defines a plane of polarization, assuming a uniform symmetrical field. A change in this chart distance can be interpreted as an optical rotation. The centers of the peaks are found by drawing several tie lines in the vicinity of the half power points and then constructing the best perpendicular bisector for all lines. The charts obtained could be read reproducibly to 0.65°.

It was considered advisable to confirm the results of K. F. Lindman as a prelude to extending them. To this end the investigations of the interaction of plane polarized microwaves and systems of copper helices were repeated. Some modifications of Lindman's procedures were undertaken, consequently the methods used by the present author will be described in full.

A cylindrical cardboard container, 25 cm. in diameter and 30 cm. deep, was suspended from Nylon threads in the center of a cubic wood framework 1.8 m. on edge. The forward edge of the container was 20 cm. from the sending antenna. Three plots of power *versus* angular position of the receiving antenna were obtained with the container empty. The container was then filled with 200 copper helices, having the same screw sense, made from eighteen gage copper wire. The helices were of two and a half turns, one centimeter in diameter with 7 mm. between turns. Helices having a right-hand screw sense will be called plus and those having a left hand screw sense will be called minus. Each helix was individually wrapped in absorbent cotton before packing into the box. Three more curves were obtained with the empty container in the optical path after which the opposite helices were packed into the box. After recording another three curves, the box was rotated 180° about the perpendicular bisector to its long axis and the above process repeated. Counter-clockwise rotations at a wave length of 18 cm. of approximately 12° for the minus helices and clockwise rotations of approximately 12° for the plus helices were obtained. These data are in very good agreement with the results obtained by K. F. Lindman.

The next step was to obtain a rotatory dispersion curve for a set of helices. The minus helices were arbitrarily chosen and the results are plotted in Fig. 1.

After completing the work outlined above, an irregular tetrahedral distribution of spheres in space was investigated. For this portion of the work the 3 cm. generator was used and Lindman's model scaled-down proportionally.

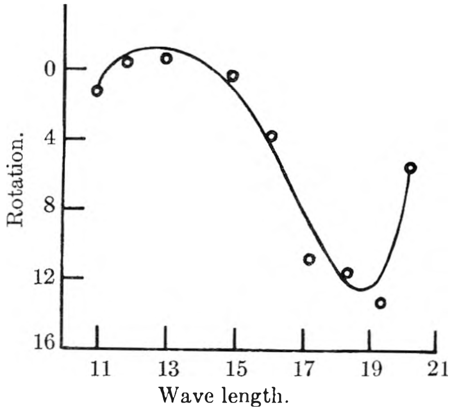

Fig. 1.—The rotation of a beam of plane polarized microwaves, due to the interposition of 200 copper helices in the optical path, plotted as a function of wave length.

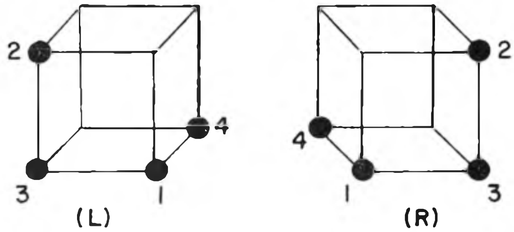

Fig. 2.—Two enantiomorphic tetrahedral distributions of conducting spheres, showing their relation to the cubes from which they were derived.

The scaled-down model derived from a cube with the spheres at the corners (Fig. 2), was constructed of aluminum spheres 6 mm. in radius with a distance between the centers of spheres lying along any edge of the cube of 1.5 cm. This model failed to show a rotation for any position having an edge of the cube parallel to the plane of polarization when placed midway between the receiving and sending antennae. It was thought that perhaps the rotation of one model was too small to be observed, therefore, an array of forty-five models was constructed by stretching a number of nylon threads, parallel to each other and perpendicular to the direction of wave propagation, on which brass spheres were mounted in the fashion of wooden balls on an abacus. The models were arranged in five layers containing nine tetrahedra each, so disposed as to cover the radiation field as uniformly as possible. All models had the same orientation with respect to the plane of polarization, and no two models came within less than 3 cm. of each other. This array also failed to show any rotation.

We next returned to a single model and tried the one orientation that Lindman reported to give no rotation, that is with the plane of polarization bisecting the angle 1,3,2 (Figure 2). This orientation produced the first rotations observed with a tetrahedral model; however, the magnitude and sometimes the sign of the rotation proved to be a function of the position of the model. Table I shows the effect of varying the distance between the sending antenna and the center of the face formed by spheres 1, 2 and 3 (Fig. 2). Following this determination, different combinations of the spheres constituting the model were removed from the radiation field and the "rotatory power" of those remaining was tested. The results are discussed in the next section.

Discussion

The experiments performed with the helical models seemed in large measure to confirm Lindman's results. There was, however, no absorption observed in models which rotated the plane of polarization. On the contrary, an increase in the intensity of the transmitted beam was generally noted. This increase was found to be a function of the position of the model with respect to the antennae, indicating that in these experiments as well

---

(6) M. H. Winkler, University Microfilms Publication 11959.

(7) S. Silver, "Microwave Antenna Theory and Design," McGraw-Hill Book Co., New York, N. Y., 1949, p. 246.

as the experiments performed with tetrahedral models the observed effects were due to diffraction.[8]

For tetrahedral models, the deviations from Lindman's work were more striking. The one orientation of the model which Lindman found to be optically inactive, *i.e.*, with the plane of polarization bisecting the angle 1,3,2 and the radiation falling perpendicularly on face 1,3,2 (Fig. 2), gave consistent apparent rotations in the current investigation. (Fig. 2L) was found to give a rotation opposite to that of (Fig. 2R), providing the line joining the centers of the antennae passed perpendicularly through the center of the 1,3,2 face of the model. For (L), with the 1,3,2 face at a distance of 2.5 cm. from the transmitting antenna, a counter-clockwise rotation of 3° was noted, while for (R), at a distance of 2.4 cm. a clockwise rotation of 5° was observed. However, if (R), was raised so that ball 4 was now above the line joining the centers of the antennae, then the rotation changed from 5° clockwise to 5° counter-clockwise, that is, the rotation obtained with (R) was now in the same direction as that obtained with its enantiomorph. When the model is raised, only ball 4 changes position without a corresponding change in a mirror plane bisecting the angle 1,3,2. Ball 3 moves along the vertical axis, and balls 1 and 2 fall an equal distance to either side of the vertical, remaining in the same horizontal plane. This suggested the possibility that ball 4 may be entirely responsible for the observed rotation of the complete model. The model was therefore partially disassembled, and the rotations of the various combinations of spheres, in the positions they occupied in the complete model, were measured. It was found that balls 2 and 3 showed an apparent counter-clockwise rotation regardless of the position of the assembly with respect to the center of the horn antenna, or of its distance from the horn. As would be expected from symmetry considerations, spheres 1 and 3 showed the opposite rotation. The complete face, 1,3,2, showed no rotation. Ball 4, studied alone, showed an apparent rotation having the same magnitude and direction as that measured for the entire model. Upon this evidence, it was concluded that there was no interaction between the balls, 1,3,2 and ball 4, and that ball 4 alone was responsible for the observed effects. Further, if a plane perpendicular to the direction of propagation of the wave and containing ball 4 is divided into quadrants by a perpendicular and horizontal with their intersection on the line of centers joining antennae, the direction of rotation is determined by the quadrant containing ball 4. This would explain the fact, mentioned above, that raising the model changes the sign of the rotation, since raising the model sufficiently would change ball 4 to another quadrant. At this point, it was thought that perhaps what was taken for a rotation of the plane of polarization was not that at all, but rather an unsymmetrical intensification of the radiation field in the plane of the receiving antenna, due to the presence of ball 4. It can be easily seen that such a local intensification could lead to an apparent rotation of the plane of polarization. For a linear resonator, such as a dipole antenna, the powder absorbed is a function of the field intensity, E, about the antenna, and the cosine of the angle θ between $\vec{E}$ and the dipole. Ordinarily we assume $\vec{E}$ to be constant over the area swept out by the receiving antenna. When that is the case a plot of angle *versus* power results in the familiar cosine square curve with a maximum at θ equals 0. If, however, $\vec{E}$ is not constant over the area swept out by the antenna, a plot of θ against power will not be a cosine square curve and, depending on how E varies with θ, may show several maxima or may show a displaced maximum.

TABLE I

THE APPARENT ROTATION OF THE PLANE OF POLARIZATION OF 3 CM. MICROWAVES BY A TETRAHEDRAL MODEL AT VARIOUS DISTANCES FROM THE RADIATING HORN ANTENNA

Model to antenna, cm.	Apparent rotation, °	Model to antenna, cm.	Apparent rotation, °
0.5	0.98	2.1	0.39
.9	1.6	2.5	.3
1.3	0.48	2.9	.29
1.7	.00	3.3	1.6

The reason for obtaining no rotation with an array of forty-five models now becomes clear. The models were arranged in several planes perpendicular to the line of propagation in such fashion that all quadrants were about equally populated with spheres, thereby cancelling any asymmetric effect. Also, the observed increase in power at the receiving antenna can be explained if the directivity of the sphere at the proper distance from the transmitting antenna toward the receiving antenna is assumed to be greater than any scattering which may take place.

Since the size of the lobes of the radiation pattern of a sphere excited by an antenna is a periodic function of the distance between the sphere and the antenna, the apparent rotation of a tetrahedral model should also be a periodic function of the model to antenna distance, if the above reasoning is correct. Table I gives the results for the rotation at various separations of model and antenna, and indeed the rotation goes through zero at approximately a half wave length interval. A single sphere occupying the position of ball 4 at the zero rotation model to antenna distance shows neither intensification nor apparent rotation.

Two balls lying in a plane perpendicular to the direction of propagation and having the line joining their centers at an angle to the plane of polarization, also showed an apparent rotation of the plane of polarization. In this case, however, the quadrant or quadrants in which the system lies does not change the sense of the rotation so long as the angle made with the plane of polarization remains constant. It can be inferred, then, that it is the interaction of the two spheres which causes the rotation in this case. Rotation of the two spheres by 90° in a plane perpendicular to the direction of propagation about their common center of gravity results in an opposite rotation of the plane of polari-

---

(8) G. C. Southworth, "Principles and Applications of Waveguide Transmission," D. Van Nostrand Co., Inc., New York, N. Y., 1950, p. 396.

zation. This result is most easily explained by reference to Fig. 3 where $\vec{E}$ is the electric vector of the incident radiation and S_1 and S_2 are the two spheres constituting the portion of the models presently under consideration. In principle, $\vec{E}$ can be resolved into two components, $\vec{E}'$ and $\vec{E}''$. Since $\vec{E}''$ lies along the line of centers of S_1 and S_2, S_1 and S_2 can be considered to be a capacitor which is charged by $\vec{E}''$. This implies a transfer of energy from $\vec{E}''$ to S_1 and S_2, which in turn means a scattering or attenuation of $\vec{E}''$ in the direction of propagation leaving E' dominant in the transmitted beam. This would be equivalent to a rotation of the plane of polarization in the direction of E'. This phenomenon is to be distinguished from optical activity, however, since the sense of the rotation can be changed merely by twisting the model through 90°. In fact, the observed effect corresponds to linear dichroism which is caused by anisotropic true absorption or anisotropic scattering.[9]

On the basis of the preceding discussion, it seems likely that the results obtained by Lindman could be partly attributed to the exercise of insufficient care in centering the model and partly to an uncertainty in the plane of polarization of the microwaves. The apparent absorptions observed by Lindman but never observed by the present author probably were due to a local intensification of the radiation field, as a result of diffraction, at the indicating antenna used to measure the total power emitted from the generator. The model itself does not seem to be optically active even though theoretical considerations[10] suggest that it may be when the model is very close to the antenna. In this case, the wave front at the model is no longer planar, that is to say, the electric vector has a longitudinal component[11,12] and so the necessary coupling between spheres lying in different planes perpendicular to the direction of propagation could arise. However, since a single sphere yields data which are identical with those obtained for the complete model, it can be assumed that this coupling does not occur to any appreciable extent.

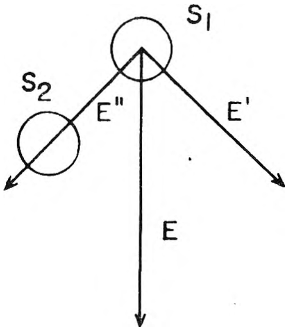

Fig. 3.—The origin of linear dichroism from a specific orientation of spheres.

Acknowledgment.—The author wishes to express his gratitude to Professor K. M. Mislow for the advice and aid which he gave during the course of this work.

---

[9] W. Heller, *Rev. Modern Phys.*, **14**, 406 (1942).

[10] B. Y. Oke, *Proc. Roy. Soc. (London)*, **A153**, 339 (1936).

[11] F. E. Terman, "Radio Engineers' Handbook," McGraw-Hill Book Co., New York, N. Y., 1943, p. 827.

[12] "Radar Electronics Fundamentals," Bureau of Ships, Navy Department, Washington, D. C., 1944, p. 412.

NOTES

METHYL COMPOUNDS OF THE ELEMENTS

By R. E. Rundle

Contribution No. 412 from the Department of Chemistry and Institute for Atomic Research, Iowa State College, Ames, Iowa[1]

Received December 16, 1955

From a novel and instructive approach to electronegativity,[2] Sanderson infers the net charge on a methyl group in simple compounds $M(CH_3)_n$, and he observes that there is a direct relation between the degree of "polymerization" and the methyl charge thus inferred.[3] He has suggested, moreover, that polarity arguments may lead to an explanation for electron deficient bonding in general.[2]

Unfortunately, in assembling his correlations Sanderson omitted tetramethylplatinum, which forms a tetramer of known structure.[4] A solid up to its decomposition point, tetramethylplatinum remains a tetramer in solution,[5] and is relatively unreactive with O_2, CO_2 and H_2O. Any reasonable electronegativity for platinum would put tetramethylplatinum far from the class of methyl compounds which polymerize according to Sanderson's observation.

For other reasons, too, Sanderson's correlation of polymerization with methyl charge seems fortuitous rather than fundamental. In going across the periodic table from groups I to IV electronegativity assuredly increases, but so does the number of methyls per metal atom. Surely, for example, trimethylaluminum is only a dimer while dimethylberyllium is a solid polymer[6] because, while both tend to form four bonds to methyl, the methyl-to-metal ratio is 3/1 in the former, 2/1 in the latter, and the methyl charge has little to do with the degree of "polymerization." It is easily seen that coördination number *vs.* methyl–metal ratio will explain most of Sanderson's table.

---

[1] Work was performed in the Ames Laboratory of the Atomic Energy Commission.

[2] R. T. Sanderson, *J. Chem. Ed.*, **29**, 539 (1952); **31**, 2, 238 (1954).

[3] R. T. Sanderson, *J. Am. Chem. Soc.*, **77**, 4531 (1955).

[4] R. E. Rundle and J. H. Sturdivant, *ibid.*, **69**, 1561 (1947).

[5] R. E. Rundle and E. J. Holman,, *ibid.*, **71**, 3264 (1949).

[6] A. I. Snow and R. E. Rundle, *Acta Cryst.*, **4**, 348 (1951).

For the least electronegative metals the metal-carbon bonding is no doubt so ionic as to justify using the ionic coördination numbers to explain the "polymerization." But even for dimethylberyllium and trimethylaluminum the structures in the solid state are not characteristic of ionic structures (large Madelung constants), and the coördination number for the metal is strictly equal to the number of low energy orbitals of the metal. (For group IVB metals and non-metals coördination number, number of electrons for bonding and number of low energy orbitals are all equal, so there is no polymerization problem.) A comparison of tetramethyllead and tetramethylplatinum illustrates the importance of the point.

The lead atom is larger than the platinum atom, as judged by its covalent radius, and probably has a lower electronegativity, yet experimentally the coördination number of lead for methyl is four, for platinum it is six. Lead IV has tetrahedral sp^3 orbitals for bond formation, platinum IV has octahedral d^2sp^3 orbitals for bond formation. In both cases all the bond orbitals are used, resulting in a monomer for tetramethyllead and a tetramer for tetramethylplatinum.

The principle that bond delocalization arises when atoms with more low energy orbitals than valence electrons (always metals) are combined with atoms or groups with no unshared electron pairs is easily justified by simple quantum mechanical arguments,[7] and leads naturally to the expectation that bonds will become more delocalized as the metal–non-metal ratio increases until the highly delocalized bonding in metals is reached. Surely polarity is not a necessary requirement for "polymerization" of this type.

[7] R. E. Rundle, *J. Am. Chem. Soc.*, **69**, 1327 (1947); *J. Chem. Phys.*, **17**, 671 (1949).

INTERMOLECULAR ASSOCIATION OF CARBONYL COMPOUNDS

By Alvin W. Baker

Research Department, Western Division The Dow Chemical Company, Pittsburg, California

Received February 7, 1956

Three recent publications[1–3] have discussed the Raman spectra of aliphatic and alicyclic ketones, and the authors have come to different conclusions regarding the causes affecting the broadening or splitting of the carbonyl band. Their data show that the splitting is of the order of eight[4] wave numbers (cm.$^{-1}$) for all ketones which were examined except for the larger splitting of 20 cm.$^{-1}$ in cyclopentanone.

Each of these theories ascribes the carbonyl doubling to hydrogen bonding, one[1] through the mechanism of enolization followed by hydrogen bonding to a second carbonyl group, and the other[2,3] to an activation of the α-hydrogens such that they become acidic enough to bond to a second carbonyl group, perhaps in a cyclic dimerization. On either basis, the bonded carbonyl gives rise to the lower frequency band and the free keto to the higher frequency band.

I have obtained additional information which I believe can best be interpreted by a dipole interaction of carbonyl groups rather than by either of the above hydrogen bonding theories. Infrared and Raman spectra[5] of cyclopentanone (I), cyclohexanone (II), and several straight-chain ketones were run in this Laboratory. The doubled carbonyl band of cyclopentanone is clearly resolved in the Raman spectrum and verifies the doublet separation of 20 cm.$^{-1}$. However, this band could not be resolved in the infrared spectrum although a slight shoulder was observed at less than 20 cm.$^{-1}$.

Upon dilution with a non-polar solvent such as carbon tetrachloride, the lower frequency carbonyl band of I decreases relative to the higher frequency band and disappears at a concentration of about 10%. On the other hand, the infrared frequency is only slightly affected by dilution, and is nearly identical in frequency to the higher frequency band in the Raman spectrum. It appears probable from this behavior that the vibrational selection rules for the dimer may be different from those for the monomer; if the dimer is symmetrical, the infrared frequency may correspond to the higher (asymmetric) and the Raman to the lower (symmetric) vibration. On this basis, one would therefore expect the infrared frequency to be very nearly equal to the monomeric frequency and little or no shift would be expected as concentraton is changed.

In pure I, association amounts to nearly 50% since the Raman carbonyl bands are of nearly equal intensity (ratio of free to bonded is 1.15). This rules out enolization as the cause of splitting because Ingold[6] reports an experimentally determined enol concentration in I of only 0.0048%. Furthermore, the enol content of II is 0.02% so that, if enolization was the cause, splitting should be greater in II than in I.

Hirschfelder and Courtauld molecular model construction of I and II indicates that there is probably small difference between steric or inductive effects involving activation of the α-hydrogens. If the extent of ring strain due to hydrogen–hydrogen repulsion is considered, the constellation theory of Brown and Borkowski[7] predicts 3–4 kcal./mole for I and less than 1–2 kcal./mole for II. This is due to the fact that the methylene groups are alternately staggered above and below the plane of the molecule in II while I is more nearly planar.

---

[1] E. Gray and M. M. Bottreau, *Compt. rend.*, **240**, 2134 (1955).

[2] W. Suetaka, *Gazz. chim. ital.*, **82**, 768 (1952).

[3] W. Suetaka, *J. Chem. Soc. Japan, Pure Chem. Sect.*, **74**, 318 (1953).

[4] *C. A.*, **12**, 962b (1955), incorrectly states 18 cm.$^{-1}$.

[5] Raman spectra were obtained with a Hilger recording Raman spectrometer.

[6] C. K. Ingold, "Structure and Mechanism in Organic Chemistry," Cornell University Press, Ithaca, N. Y., 1953, p. 566.

[7] H. C. Brown and M. Borkowski, *J. Am. Chem. Soc.*, **74**, 1894 (1952).

That I is not completely planar[8] is due to hydrogen–hydrogen repulsion of adjacent methylene groups. Hyperconjugation could reduce this strain by about one kcal./mole, but hardly enough to change the acidity of the α-hydrogens appreciably.

On the other hand, the models show that the carbonyl group of I is more exposed, and therefore capable of greater dipole overlap of interacting molecules than that of II or any aliphatic ketone. This is particularly evident if the ring bending frequencies are considered because this vibration produces much less motion in I than in II. The greater overlap naturally results in greater perturbation of the carbonyl frequency.

The Raman spectra of diethyl, ethylene and propylene carbonates (obtained here) disclose an even greater interaction for these compounds than for I. This gives additional confirmation to the theory of dipole interaction because in the carbonates, there are no hydrogens alpha to the carbonyl groups. Therefore, association or dimerization should be impossible by either of the above hydrogen bonding theories. Furthermore, it is quite unlikely that the β-CH_2 groups would be unusual in acidity. Both the strength of association and accessibility of the carbonyl groups are in the order diethyl carbonate < propylene carbonate < ethylene carbonate.

The Raman spectrum of diethyl carbonate[9] shows a doubled carbonyl band at 1730–1752 (doublet separation 22 cm.$^{-1}$) with the associated band being nearly three times as strong as the free band. In propylene and ethylene carbonate, the interaction is so strong that the free carbonyl is nearly undetectable.

In both the infrared and Raman effect, the carbonyl frequency of pure ethylene carbonate is doubled. This is a result of Fermi resonance[10] between the carbonyl stretching frequency and the first overtone of the very strong ring frequency at 893 cm.$^{-1}$. However, the frequency of the unassociated carbonyl is sufficiently higher than that of the bonded carbonyl (about 31–34 cm.$^{-1}$) that Fermi resonance does not occur in the monomer, and the frequency is single. In both of the cyclic carbonates, the relative intensity of the bonded carbonyl has been shown here to be a linear function of the concentration.

---

(8) Gunnar Erlandsson, *J. Chem. Phys.*, **22**, 563 (1954).

(9) Also run by W. G. Brown, *et al.*, *Anal. Chem.*, **22**, 1074 (1950).

(10) C. L. Angell, paper given June, 1956 at the Symposium on Molecular Structure and Spectroscopy, Ohio State University, Columbus, Ohio.

THE REACTION BETWEEN MERCURY(I) AND THALLIUM(III) IN AQUEOUS SOLUTION: EVIDENCE FOR THE DISMUTATION OF Hg_2^{++}

By A. M. Armstrong, J. Halpern and W. C. E. Higginson

The University of British Columbia, Vancouver, Canada
The University of Manchester, Manchester, England

Received July 23, 1956

We have examined the kinetics of the reaction between mercury(I) and thallium(III), *i.e.*

$$Hg_2^{++} + Tl^{+++} \longrightarrow 2Hg^{++} + Tl^{+} \qquad (1)$$

in aqueous perchloric acid solution. Most of the measurements were made at 25° and 3 *M* $HClO_4$, the initial solution composition being varied in the range 10^{-5} to 5×10^{-5} *M* $Hg_2(ClO_4)_2$, 10^{-5} to 10^{-3} *M* $Tl(ClO_4)_3$, 0–10^{-4} *M* $Hg(ClO_4)_2$ and 0–10^{-4} *M* $TlClO_4$. The reaction was followed spectrophotometrically,[1] using the Hg_2^{++} absorption peak at 236.5 mμ and correcting for the small absorption of the other ions at this wave length.

The rate was found to be first order in Hg_2^{++} and Tl^{+++} and inversely proportional to the concentration of Hg^{++}, suggesting that the reaction proceeds through the following mechanism

$$Hg_2^{++} \underset{k_{-1}}{\overset{k_1}{\rightleftarrows}} Hg^{++} + Hg \qquad (2)$$

$$Hg + Tl^{+++} \xrightarrow{k_2} Hg^{++} + Tl^{+} \qquad (3)$$

The dismutation equilibrium (step 2) is assumed to be rapidly established (and thus serves to determine the concentration of Hg atoms in solution) while the subsequent reaction between dissolved Hg and Tl^{+++} is rate controlling. The resulting rate law is

$$\frac{-d[Hg_2^{++}]}{dt} = \frac{k_1k_2}{k_{-1}}\frac{[Hg_2^{++}][Tl^{+++}]}{[Hg^{++}]} \qquad (4)$$

which becomes, on integration

$$\frac{[Hg^{++}]_0 + 2[Hg_2^{++}]_0}{[Tl^{+++}]_0 - [Hg_2^{++}]_0}\log\frac{[Hg_2^{++}]_0}{[Hg_2^{++}]} - \frac{[Hg^{++}]_0 + 2[Tl^{+++}]_0}{[Tl^{+++}]_0 - [Hg_2^{++}]_0}\log\frac{[Tl^{+++}]_0}{[Tl^{+++}]} = \frac{k_1k_2t}{2.303k_{-1}} \qquad (5)$$

where $[\ ]_0$ denotes the initial concentration and $[\ ]$ the concentration at time *t*.

In Fig. 1, the function corresponding to the left-hand side of equation 5 is plotted against *t*, for a number of experiments made with solutions of widely varying initial composition. In conformity with equation 5 all the points are seen to lie fairly close to a single straight line passing through the origin. The experimental results are thus considered to provide strong support for the proposed mechanism.

At 25° and 3 *M* $HClO_4$, the value of k_1k_2/k_{-1}, calculated from the slope of this plot by means of equation 5, is 2.7×10^{-3} min.$^{-1}$. The equilibrium constant of the Hg_2^{++} dismutation step (*i.e.*, k_1/k_{-1}) has been estimated[2] at about 10^{-9} mole liter^{-1}, suggesting that k_2 is of the order of 10^6 liter mole^{-1} min.$^{-1}$. It seems likely that reaction 3 involves a two-electron transfer between Hg and Tl^{+++}; the high value of the rate-constant for this process presumably reflects, at least in part, the fact that Hg is uncharged and hence is not repelled electrostatically by Tl^{+++}. The results of some preliminary experiments suggest that the rate of the reaction (and hence presumably k_2) increases as the $HClO_4$ concentration is lowered. The simplest interpretation of this is that hydrolyzed thallium(III) ions, such as $TlOH^{++}$, react more rapidly with Hg than does Tl^{+++}. This type of behavior

---

(1) W. C. E. Higginson, *J. Chem. Soc.*, 1438 (1951).

(2) N. V. Sidgwick, "The Chemical Elements and their Compounds," Vol. I, Oxford Univ. Press, New York, N. Y., 1950, pp. 285–92.

(3) R. J. Zwolinski, R. J. Marcus and H. Eyring, *Chem. Revs.*, **55** 157 (1955).

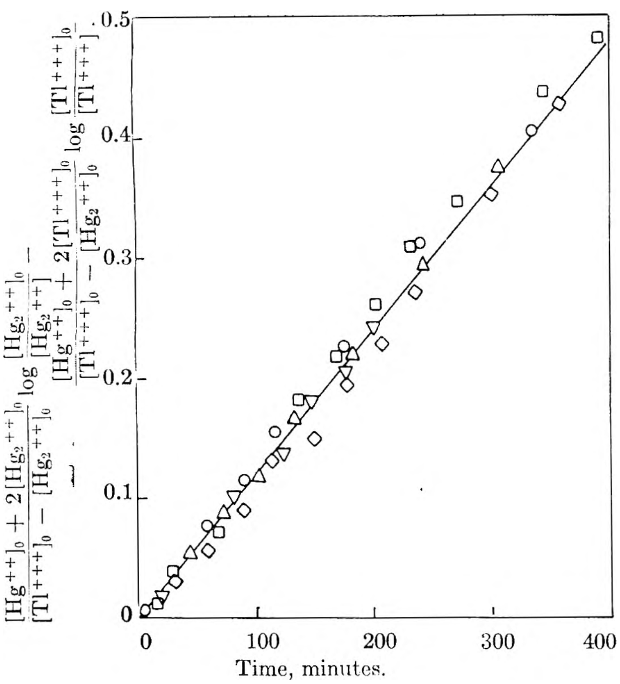

Fig. 1.—Rate plots for the reaction between mercury(I) and thallium(III) at 25°, 3 *M* $HClO_4$. Initial concentrations (× 10^5) in mole/l.: ○, 2.7 Hg_2^{++}, 5.3 Tl^{+++}; △, 2.7 Hg_2^{++}, 10.6 Tl^{+++}; □, 1.2 Hg_2^{++}, 2.6 Tl^{+++}; ▽, 2.7 Hg_2^{++}, 10.7 Tl^{+++}, 8.6 Tl^{+}; ◇, 2.7 Hg_2^{++}, 10.7 Tl^{+++}, 5.1 Hg^{++}.

is characteristic also of other electron transfer reactions.[3]

The kinetic results fail to provide an indication of any contribution from a rate-determining step involving the direct reaction of Hg_2^{++} with Tl^{+++}, although the concentration of Hg_2^{++} is much greater than that of Hg. From this it may be concluded that the rate constant for this process is probably less than 1 liter $mole^{-1}$ $min.^{-1}$ at 25°. Although this reaction (represented by equation 1) like that between Hg and Tl^{+++} can be considered formally as a two-electron transfer, its much lower rate is readily understandable in the light of the much greater repulsion between Tl^{+++} and Hg_2^{++}, resulting from the latter's charge, and of the Franck-Condon barrier to electron transfer[3] which probably results from its dimeric configuration.

The fact that Hg_2^{++} may undergo dismutation in aqueous solution according to equation 2, and that this equilibrium is rapidly established, has long been recognized. When reagents such as NH_3 and CN^-, which form stable mercuric complexes and thus decrease the concentration of free Hg^{++}, are added to a solution of a mercurous salt, they cause this equilibrium to be shifted to the right with the formation of metallic mercury.[2] Evidence for the existence of Hg atoms, in appreciable concentrations, in aqueous solutions has also been provided by direct measurements[4] of the solubility of metallic mercury in water (estimated to be about 10^{-7} mole/l. at 20°) and by spectroscopic observation[5] of the 2537 Å. absorption band of Hg in solution. Hg atoms also have been postulated as intermediates in at least two other reactions in aqueous solution, *i.e.*, (a) Wolfgang and Dodson[6] have suggested that the very rapid isotopic electron exchange between Hg^{++} and Hg_2^{++}, *i.e.*

$$Hg_2^{++} + \overset{*}{Hg}{}^{++} \longrightarrow \overset{*}{Hg}{}_2^{++} + Hg^{++} \qquad (6)$$

proceeds through the mechanism

$$Hg_2^{++} \longrightarrow Hg + Hg^{++} \qquad (7)$$

$$Hg + \overset{*}{Hg}{}^{++} \longrightarrow \overset{*}{Hg}{}_2^{++} \qquad (8)$$

Their results support the conclusion that the Hg_2^{++} dismutation equilibrium is established rapidly.

(b) The homogeneous reduction of mercuric salts in aqueous solution by molecular hydrogen, *i.e.*

$$2Hg^{++} + H_2 \longrightarrow Hg_2^{++} + 2H^+ \qquad (9)$$

has been postulated[7] to proceed through the mechanism

$$Hg^{++} + H_2 \longrightarrow Hg + 2H^+ \text{ (slow)} \qquad (10)$$
$$Hg + Hg^{++} \longrightarrow Hg_2^{++} \text{ (fast)} \qquad (11)$$

This sequence of steps is the reverse of that proposed for the reaction between Hg_2^{++} and Tl^{+++}.

Earlier measurements[1] on the ultraviolet absorption spectra of mercurous perchlorate solutions, revealed deviations from Beer's law at low concentrations ($<10^{-5}$ *M* Hg_2^{++}) which were attributed to the homolytic dissociation equilibrium

$$Hg_2^{++} \rightleftharpoons 2Hg^+ \qquad (12)$$

The spectroscopic data suggested that the equilibrium constant for this process was in the range 10^{-8} to 10^{-6} mole $liter^{-1}$. In the light of the considerations discussed in this paper, it seems more probable that these deviations arise from the dismutation reaction represented by equation 2. This suggestion is also in accord with our observations that the reactions of Hg_2^{++} with one-electron oxidizing agents such as Ce^{++++} are slower than with Tl^{+++}.

The portion of this research which was conducted at the University of British Columbia was supported through a grant from the National Research Council of Canada.

[4] A. Stock, *Z. anorg. Chem.*, **217**, 241 (1934).

[5] H. Reichardt and K. F. Bonhoeffer, *Z. Elektrochem.*, **36**, 753 (1930); *Z. physik.*, **67**, 780 (1931).

[6] R. L. Wolfgang and R. W. Dodson, THIS JOURNAL, **56**, 872 (1952).

[7] G. J. Korinek and J. Halpern, *ibid.*, **60**, 285 (1956).

THE SYSTEM SODIUM SULFATE–SODIUM MOLYBDATE–WATER AT 35 AND 100°

BY WILLIAM F. LINKE AND JEROME A. COOPER

The Wm. H. Nichols Laboratory, New York University, New York, N. Y.

Received June 25, 1956

The solid solutions in the system sodium sulfate–sodium molybdate–water have been studied at temperatures at which $Na_2SO_4 \cdot 10H_2O$, $Na_2MoO_4 \cdot 10H_2O$ and $Na_2MoO_4 \cdot 2H_2O$ are the saturating phases.[1–3] Although the extent of the decahydrated solid solutions diminishes with increasing

---

[1] J. E. Ricci and W. F. Linke, *J. Am. Chem. Soc.*, **73**, 3607 (1951).

[2] W. E. Cadbury, THIS JOURNAL, **59**, 257 (1955).

[3] W. F. Linke, unpublished work.

TABLE I

THE SYSTEM Na_2SO_4–Na_2MoO_4-H_2O

Complex, wt. %		Satd. soln., wt. %		Density	Algebraic extrapolation to composition of pure solid	Solid phase
Na_2SO_4	Na_2MoO_4	Na_2SO_4	Na_2MoO_4			
		Results at 35°				
...	...	32.90	0.0	1.319	...	S[a]
39.14	5.04	28.14	5.89	1.335	+0.32	S
34.01	11.99	21.66	14.15	1.359	+ .35	S
29.10	19.11	15.40	22.73	1.395	+ .40	S
25.12	25.15	10.50	30.00	1.435	+ .25	S
16.08	34.79	9.47	31.89	1.443	...	S + M2[b]
14.03	38.08	9.42	31.92	1.444	...	S + M2
10.02	40.15	9.46	31.90	1.447	...	S + M2
6.08	41.79	7.28	33.73	1.443	− .38	M2
3.47	43.15	3.88	36.65	1.435	+ .82	M2
...	...	0.0	39.90	1.434	...	M2
		Results at 100°				
28.71	17.49	14.57	21.45	...	−2.46	S
22.78	24.99	9.75	29.66	...	−2.63	S
20.05	32.00	5.57	38.02	...	−1.05	S
20.04	35.01	4.52	41.85	...	−0.23	S
14.96	39.76	4.60	41.91	...	...	S + M2
8.81	45.24	4.39	42.05	...	...	S + M2
3.02	48.72	3.83	41.79	...	−1.24	M2
...	...	0.0	45.47	...	...	M2

[a] S = Na_2SO_4. [b] M2 = $Na_2MoO_4 \cdot 2H_2O$.

temperature, the anhydrous salts form continuous solid solutions at their melting points,[4,5] and limited solid solutions below 212°.[4] We have therefore studied the aqueous system at 35 and 100°, where anhydrous Na_2SO_4 is a saturating phase, in order to determine the extent of the anhydrous solid solutions at comparatively low temperatures.

Materials and Methods.—Complexes of predetermined composition were prepared from C.P. Na_2SO_4, analyzed $Na_2MoO_4 \cdot 2H_2O$ and water. At 35° these were tumbled for up to 3 months in a water-bath held constant to ±0.05°. Equilibrium was ascertained by repeated analysis after varying periods of time. At 100°, the sealed mixtures were placed in a steam-bath (±0.1°) and stirred vigorously for from 3 to 6 hours. Analyses were made by determining (1) total solids by evaporation and heating at 110° to constant weight, and (2) molybdate by a modified Volhard procedure.

Results and Discussion.—The ternary data at 35 and 100° are given in Table I. Algebraic extrapolation of the tie-lines at each temperature indicates that Na_2MoO_4 does not dissolve in anhydrous Na_2SO_4 to any appreciable extent. The somewhat poorer extrapolations at 100° are probably attributable to experimental difficulties. Similarly, although the data are limited, no solid solution of Na_2SO_4 in dihydrated Na_2MoO_4 is indicated.

In order to determine whether the transition $Na_2MoO_4 \cdot 2H_2O \rightleftarrows Na_2MoO_4$ + aq. would occur below the normal boiling point of a saturated solution, the solubility of the salt in water was determined at 100° (45.47 wt. %), 104° (45.90%) and 107° (b.p.) (46.32%). The data lie on a smooth extension of the solubility curve of Funk,[6] and indicate that the dihydrate is the stable phase up to the boiling point. Hence, although solid solutions of Na_2SO_4 in anhydrous Na_2MoO_4 may (and probably do) exist in this temperature range,[7] they do not appear in the (stable) aqueous system at one atmosphere pressure.

---

(4) H. E. Boeke, *Z. anorg. Chem.*, **50**, 355 (1906).

(5) I. N. Balyaev and A. K. Doroshenko, *Zhur. Obshchei Khim.*, **24**, 427 (1954).

(6) R. Funk, *Ber.*, **33**, 3697 (1900).

(7) See H. E. Boeke, ref. 4.

BINDING OF ORGANIC ANIONS BY SERUM ALBUMIN

BY ARTHUR LINDENBAUM AND JACK SCHUBERT

Division of Biological and Medical Research, Argonne National Laboratory, Lemont, Illinois

Received July 23, 1956

Earlier studies have shown that the most effective compounds for reversing beryllium-induced inhibition of plasma alkaline phosphatase are characterized first, by possession of carboxyl and hydroxyl groups in the *ortho* position on a ring-type resonating nucleus such as benzene,[1] and second, by their ability to bind protein.[2] To further investigate the relative contribution of prosthetic groups and molecular size to protein binding we have made quantitative measurements of the binding of a well characterized protein, serum albumin, with a series of related organic compounds.

Experimental

Binding was measured on the basis of competition between methyl orange and the anion for albumin by the equilibrium dialysis technique of Klotz, *et al.*[3,4] Armour crystalline bovine serum albumin (molecular weight ≅ 69,000) was used at a concentration of 1.43×10^{-5} *M*. Dialysis was conducted at *p*H 6.87 (veronal buffer) for 72 hr. at 5–10°. In order to eliminate interference in the spectrophotometric determination of methyl orange by the highly colored aurintricarboxylic acid (ATA) the ATA was precipitated from solution after dialysis by reducing the *p*H to 1.4. Initial concentration of organic anion was 1×10^{-4} *M* for ATA and 1×10^{-3} *M* for all others.

---

(1) A. Lindenbaum, M. R. White and J. Schubert, *Arch. Biochem. Biophys.*, **52**, 110 (1954).

(2) J. Schubert and A. Lindenbaum, *J. Biol. Chem.*, **208**, 359 (1954).

Results

The binding constants (k_B) obtained by the equilibrium dialysis method are listed in Table I, along with previously obtained data on the ability of an excess of the test compound (concentration range 2×10^{-5} *M* to 1×10^{-4} *M*) to reverse the beryllium-induced inhibition of plasma alkaline phosphatase.[1] Deviation from the mean was less than 8% for each value reported.

TABLE I

BINDING CONSTANTS (k_B) OF ORGANIC IONS WITH BOVINE SERUM ALBUMIN AS MEASURED BY EQUILIBRIUM DIALYSIS TECHNIQUE USING METHYL ORANGE AS A COMPETING ION

*p*H = 6.87. Albumin concentration in Visking bag = 1.43×10^{-7} *M*. Methyl orange concentration varied between 1×10^{-4} and 4×10^{-6} *M*.

Source of anion	k_B	% reversal of Be inhibition of plasma alkaline phosphatase
ATA (ammonium salt)	48,000	100
5-*t*-Butylsalicylic acid	5,380	100
2,4-Dihydroxybenzoic acid (β-resorcylic acid)	2,990	71
2,5-Dihydroxybenzoic acid (gentisic acid)	2,120	47
Salicylic acid	1,920	79
p-Aminosalicylic acid	1,270	49
Sulfosalicylic acid	1,260	57
Phenol	94	0
Benzoic acid	950	0
m-Hydroxybenzoic acid	960	0
p-Hydroxybenzoic acid	780	7
Inositol	0	30
Catechol	0	48
Catechol disulfonic acid	640	71
dl-Mandelic acid	170	0

The greatest amount of protein binding was observed in those compounds containing *ortho*-hydroxyl, carboxyl groups on the benzene nucleus. In general the degree of protein binding follows the same trend as the reversal of enzymatic inhibition with some notable but anticipated exceptions. Examination of Table I brings out the importance of a number of factors involved, either alone or in combination, in protein–anion interactions.[5]

(1) **Interaction with the Water Solvent.**—The increased binding by albumin for salicylic acid (SA) over *m*- or *p*-hydroxybenzoic acids (Table I) is ascribed to the formation of an intramolecular hydrogen bond by SA, thus reducing the reactivity of the –OH groups with the aqueous solvent.

(2) **Ionization.**—The greater the degree of ionization of the anion the greater the electrostatic attraction for the cationic centers in albumin. Hence, undissociated molecules such as phenol, inositol, catechol and mandelic acid are bound weakly to albumin at the *p*H employed. The binding of catechol disulfonic acid is obviously induced by the negatively charged sulfonic acid groups.[6] The contribution of van der Waals forces to the binding potential of these small molecules is minor compared to the electrostatic effects; *e.g.*, compare phenol and benzoic acid.

(3) **Van der Waals Forces.**—These become an important factor with increasing molecular size of anion. The increased binding of *t*-butylsalicylic acid over SA may result from increased van der Waals forces as well as from reduced solubility due to the alkyl side chain. An even better example is ATA which consists of three molecules of SA bound by a methyl group and is bound to albumin 25 times more strongly than SA. The increased binding undoubtedly is due to the additional aromatic rings in the ATA molecule and to the probability that ATA exists in solution as a polymerized species.[6]

The capacity of ATA for strong protein binding is well correlated with its greater ability, compared with SA, to reverse the activity of Be-poisoned alkaline phosphatase *in vitro* (Table I) and with the smaller concentrations required to protect Be-poisoned mice, as well as with its more sustained protective effects.[7]

It will be noted that catechol, for example, has no binding affinity for serum albumin but is able to substantially reverse the beryllium-induced inhibition of alkaline phosphatase. The reason for its latter action is due to the ability of catechol to form a chelate with Be. Here then is an example of the ability of a metal ion to bring an organic molecule to a protein site to which it ordinarily would not be bound. This is akin to the well-known mediating action of metals demonstrated experimentally by Klotz[8] and confirmed by Malmström.[9]

Values obtained by the enzymatic method[2] for the binding of salicylic, sulfosalicylic (SSA) and aurintricarboxylic acids by beryllium-free rat plasma alkaline phosphatase—K_{AE} = 20, 60 and 850, respectively—give ratios which are reasonably close to those for the binding values of these compounds with bovine serum albumin. The small apparent discrepancy involving SA and SSA may be resolved by the fact that the alkaline phosphatase protein is associated with a metallic cation, Mg^{++}. The interaction of SSA for alkaline earth cations is substantially greater than SA because of the added electrostatic attraction imparted to SSA by the negatively charged $-SO_3^-$ group.[2,10,11]

---

(3) I. M. Klotz, F. M. Walker and R. B. Pivan, *J. Am. Chem. Soc.*, **68**, 1186 (1946).

(4) I. M. Klotz and J. M. Urquhart, THIS JOURNAL, **53**, 100 (1949).

(5) See chapter on Protein Interactions by I. M. Klotz in "The Proteins," ed. by H. Neurath and K. Bailey, Vol. 1, Part B, Academic Press, New York, N. Y., 1953, p. 727 ff; also, I. M. Klotz, *J. Am. Chem. Soc.*, **68**, 2299 (1946).

(6) T. Vickerstaff, "The Physical Chemistry of Dyeing," Interscience Publishers, New York, N. Y., 1950, pp. 171 ff.

(7) M. R. White and J. Schubert, *Arch. Biochem. Biophys.*, **52**, 133 (1954).

(8) I. M. Klotz and W. C. Loh Ming, *J. Am. Chem. Soc.* **76**, 805 (1954)

(9) B. G. Malmström, *Arch. Biochem. Biophys.*, **58**, 398 (1955).

(10) N. R. Joseph, *J. Biol. Chem.*, **164**, 529 (1946).

(11) J. Schubert, E. R. Russell and L. S. Myers, Jr., *ibid.*, **186**, 387 (1950).

HYDROGEN TRIIODIDE

By J. A. Magnuson and J. H. Wolfenden[1]

Department of Chemistry, Dartmouth College, Hanover, N. H.

Received July 25, 1956

Although the triiodides are a well-defined series of salts, the sporadic attempts to establish the existence of the parent acid, hydrogen triiodide, in molecular form have led to negative or ambiguous results.[2-5] An early comparison,[5] ancillary to another investigation, of the absorption spectra of mixtures of iodine and hydrogen iodide in cyclohexane solution with those of solutions of the two constituents is reported to have given no indication of compound formation. It seemed to us of interest to renew the enquiry by a spectrophotometric investigation of solutions of iodine and of hydrogen iodide in carbon tetrachloride and their mixtures.

Hydrogen iodide prepared by synthesis,[6] iodine resublimed from potassium iodide and carbon tetrachloride of A.R. grade, redistilled after drying over calcium chloride, were used. Rigorous exclusion of moisture was necessary to prevent the formation of a faint opalescence in solutions of hydrogen iodide and the preparation of mixtures and the filling of the stoppered silica cuvettes was carried out in a dry box. Absorbance measurements were made with a Beckman DU spectrophotometer with the temperature of the cuvettes controlled to within one degree of 25°.

Preliminary exploration was carried out in 10 mm. cuvettes over the range 3200 to 4400 Å. The absorbance of mixtures of equal volumes of solutions of hydrogen iodide (0.017–0.044 M) and of iodine (0.012–0.026 M) was compared with the sum of the absorbances of the individual solutions, separately diluted to halve their concentrations with pure solvent. Ten such comparisons were made and the absorbance of the mixture was invariably greater than the sum of the absorbances of the individual diluted solutions over the whole spectral range measured. Only at the short wave length end of the range was this "absorbance increment" small enough to be conceivably attributable to experimental error; it attained its maximum value (0.12 to 0.44 according to the composition of the mixture) at 3700 Å. and this wave length was accordingly selected for more detailed study.

The measurement of the equilibrium constant of the reaction in carbon tetrachloride solution from

$$HI + I_2 \rightleftharpoons HI_3$$

spectrophotometric measurements is simple enough in principle even though the molar extinction coefficient of hydrogen triiodide is unknown. Difficulties are to be anticipated, however, if its molar extinction coefficient is not very different from that of iodine, particularly if the equilibrium constant is not very high. The shallowness of the peak in a plot of absorbance increment against wave length suggested that this might be the case Quantitative study confirmed this expectation and it is only possible to make a rough estimate of the equilibrium constant and of the molar extinction coefficient of hydrogen triiodide in carbon tetrachloride solution.

The measurements directed to this end were carried out in stoppered 100 mm. silica cuvettes. Immediately after the absorbance of a given mixture had been measured, its composition was determined by titrating its water extract with alkali (potentiometrically using a glass electrode) and with thiosulfate. Twenty-eight mixtures were measured with hydrogen iodide concentrations ranging from 0.0034 to 0.0301 M and iodine concentrations ranging from 0.0033 to 0.0103 M; mixtures with excess of iodine were avoided to eliminate possible complications due to the formation of higher poly-iodides. The absorbances of the mixtures measured ranged from 0.256 to 1.256. As hydrogen iodide is effectively transparent at 3700 Å., the absorbance increment was calculated by deducting the absorbance due to titrated iodine (derived from a calibration curve obtained in the same cuvettes) from the absorbance of the mixture.

With both equilibrium constant and molar extinction coefficient of hydrogen triiodide unknown it is necessary to use the absorbance and concentration data for a pair of solutions; these can be substituted in the rather obvious quadratic equation derived by the combination of Beer's law and the law of mass action to give values of the two unknown quantities. Treatment of the experimental data in this way quickly discloses that, in sharp and unfortunate contrast to the triiodide ion in aqueous solution, the molar extinction coefficient of hydrogen triiodide in carbon tetrachloride is not much bigger than that of iodine.

A closer scrutiny of the quadratic equation with the added knowledge of the order of magnitude of its numerical coefficients shows that only a limited number of pairings of runs in any given set of measurements will be other than extravagantly sensitive to probable experimental errors (such as 0.005 in absorbance measurements and 1% in concentration measurements). It is, however, possible to grade all possible run-pairs beforehand in terms of their vulnerability to experimental error, using objective arithmetical criteria derived from the form of the equation. On this basis thirteen run-pairs were classified as favorable ("Grade I") and another nineteen as moderately favorable ("Grade II"). The study of the influence of experimental errors upon the equilibrium constant obtained also makes it clear that the geometric mean should be the most suitable way of averaging the values of the equilibrium constant. For this reason as well as because of the very approximate nature of the values obtained, the logarithm of the equilibrium constant is used in our estimate of the equilibrium constant and its probable error.

When our measurements are handled in this way, the values in Table I are obtained for the equilibrium constant, K, of the reaction in mole liter^{-1}

$$HI + I_2 \rightleftharpoons HI_3$$

units in carbon tetrachloride solution at 25° and for

---

(1) Department of Chemistry, Dartmouth College, Hanover, N. H. The authors are grateful to Research Corporation for the spectrophotometer used in the work.

(2) M. Trautz and F. A. Henglein, *Z. anorg. Chem.*, **110**, 279 (1920).

(3) C. K. Tinkler, *J. Chem. Soc.*, **91**, 996 (1907).

(4) A. Batley, *Trans. Faraday Soc.*, **24**, 438 (1928).

(5) R. H. Potterill and O. J. Walker, *ibid.*, **33**, 363 (1937).

(6) E. R. Caley and M. G. Burford, "Inorganic Syntheses," Vol. I, McGraw-Hill Book Co., New York, N. Y., 1939, p. 159.

the molar extinction coefficient (ϵ) of hydrogen triiodide in these solutions.

TABLE I

Group	No. of run-pairs	Arithmetic mean of $\log_{10} K$	Probable error	Arithmetic mean of ϵ	Probable error
Grade I	13	2.02	±0.38	19.1	±6.1
Grade II	19	2.04	±0.54	18.1	±6.4

The close agreement between the arithmetic means of the two groups of run-pairs is largely fortuitous as is shown by the magnitude of the probable error.

It seems reasonably certain that K lies somewhere between 25 and 400 liter mole^{-1} and that the molar extinction coefficient of hydrogen triiodide lies between 13 and 25 at 3700 Å. The similarity of this latter value to that of iodine (*ca.* 7) at the same wave length is the principal reason why these experiments afford such a crude estimate of the equilibrium constant governing the formation of hydrogen triiodide; the restriction imposed by the limited solubility of hydrogen iodide in carbon tetrachloride is also a contributing factor. There appears, however, no reason to doubt the existence of hydrogen triiodide in carbon tetrachloride solution.

SYSTEM LITHIUM CHLORIDE-WATER

By H. E. Moran, Jr.

U. S. Naval Research Laboratory, Washington, D. C.

Received July 26, 1956

Lithium chloride appears eminently suited for making nearly neutral, low-freezing solutions. In view of a current requirement for a non-freezing, inorganic liquid suitable for use at sub-Arctic temperatures, the solubility-temperature relationship of the system $LiCl-H_2O$ was investigated.

The transition temperature between anhydrous LiCl and the monohydrate has been reported as 100.5° by Hüttig and Steudemann,[1] 98° in the ICT[2] and 93.55° by Appleby and Cook.[3] The same sources report the transition temperature of monohydrate to dihydrate as 12.5, 12.5 and 19.1°, respectively. Hüttig and Steudemann place the transition temperature of dihydrate to trihydrate at −20°, the transition from trihydrate to pentahydrate at −68° and the binary eutectic at −80°. Voskrenskya and Yanet'eva[4] report the existence of a pentahydrate, and place its eutectic with water at −66°. Garrett and Woodruff[5] report the binary eutectic to contain 28.85% LiCl at a temperature of −73°. Other investigators[6,7] have indicated the eutectic to be below −96°.

Experimental

The data were obtained by thermal analysis.

Apparatus.—The freezing point apparatus used at sub-zero temperatures comprised a 25 × 150 mm. glass sample holder, an electrically heated phenolic-resin jacket for the sample holder, and a liquid nitrogen-cooled air-bath. A reciprocating spiral wire stirrer driven by a constant speed motor was used for agitation. A thermocouple well extended to within 2 cm. of the bottom. In making a test, LiCl solution to give 5 cm. depth was put in the sample holder. The current in the heater jacket was adjusted to give a uniform cooling rate between 0.1 to 1° per minute over the last 10°. Concordant results were obtained with cooling rates within this range. Liquid nitrogen consumption was moderate. Temperature was measured by a thermocouple which had been calibrated against a standardized resistance thermometer. The thermocouple potential was automatically plotted against time by a recording potentiometer. This arrangement was sensitive to 0.05°.

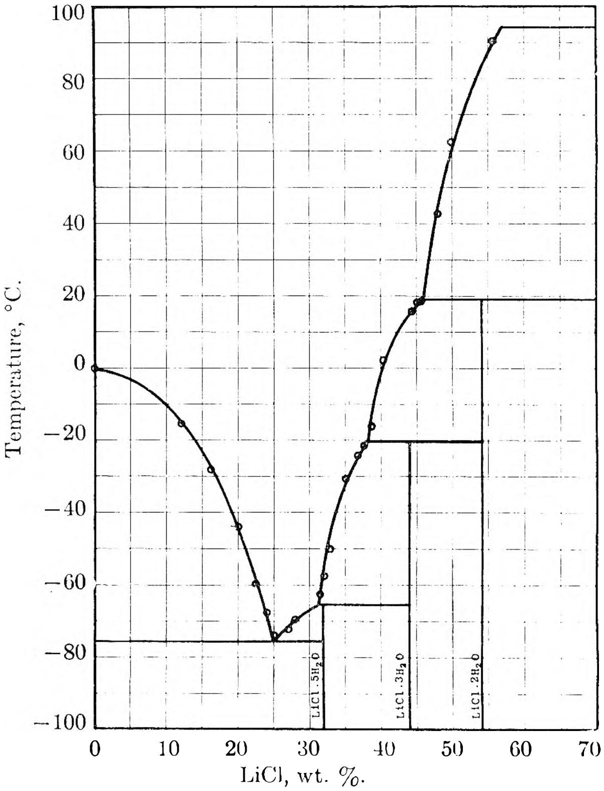

Fig. 1.—System $LiCl-H_2O$.

Supercooling caused a great deal of trouble through its persistence over a large temperature drop, although vigorous efforts were make to induce crystallization. Crystallization was not spontaneous, except at very low or very high concentrations of the salt. In fact, vitrification of solutions near the eutectic composition sometimes persisted for considerable periods of time even at liquid-nitrogen temperature. In successful runs, crystallization was induced after 2 to 5° supercooling either by shock seeding or by crystal seeding. In shock seeding, the solution was agitated by the tip of a 4 mm. diameter glass rod precooled with liquid nitrogen. Seed crystals were prepared in advance by wetting the tip of a glass rod with the solution being tested and holding it under liquid nitrogen until needed. The crystals so formed were scraped or knocked off the rod and into the solution. When repeated seeding produced an offset in the cooling curve, or when the supercooling exceeded 5°, the run was discarded.

The apparatus of Crawford and Harbourn[8] was used with solutions freezing above 0°. Crystallization sometimes was spontaneous in this region. When seeding was needed, a single small granule of the appropriate hydrate was sufficient.

---

[1] G. F. Hüttig and W. D. Steudemann, *Z. physik. Chem.*, **126**, 105 (1927).

[2] "International Critical Tables," McGraw-Hill Book Co., Inc., New York, N. Y., 1928.

[3] M. P. Appleby and R. P. Cook, *J. Chem. Soc.*, 547 (1938).

[4] N. K. Voskrenskya and O. K. Yanet'eva, *Bull. Acad. Sci. URSS, classe sci. nat. math., ser chim.*, 97 (1937).

[5] A. B. Garrett and S. A. Woodruff, *J. Phys. Colloid Chem.*, **55**, 477 (1951).

[6] Foster D. Snell, Inc., Report to the Navy Dept., Bureau of Aeronautics, Contract No. NOa(s) 10579.

[7] Dept. Chemical Engineering, University of Maryland Report on Contract DA 44-009eng1671, Engineer Research and Development Laboratories. June 15, 1954.

[8] Wm. Crawford and C. L. A. Harbourn, *Anal. Chem.*, **27**, 1449 (1955).

The average deviation of repeated determinations of points on the solubility curve was 0.3°; of transition temperatures, 0.1°.

Material.—Reagent grade LiCl was obtained and analyzed. Less than 0.03% impurities was found; of this, 0.02% was NaCl. The material was used without further treatment.

Results

The solubility data are presented graphically in Fig. 1. Transition temperatures and the binary eutectic temperature are given in Table I.

TABLE I

TRANSITION TEMPERATURES IN THE SYSTEM $LiCl-H_2O$, °C.

LiCl anhydrous $\rightleftarrows$ $LiCl \cdot H_2O$	94.0
$LiCl \cdot H_2O$ $\rightleftarrows$ $LiCl \cdot 2H_2O$	19.0
$LiCl \cdot 2H_2O$ $\rightleftarrows$ $LiCl \cdot 3H_2O$	−20.5
$LiCl \cdot 3H_2O$ $\rightleftarrows$ $LiCl \cdot 5H_2O$	−65.6
Eutectic	−75.9

The transition temperatures determined for LiCl (anhyd.) $\rightleftarrows$ $LiCl \cdot H_2O$ and $LiCl \cdot H_2O$ $\rightleftarrows$ $LiCl \cdot 2H_2O$ are in good agreement with those reported by Appleby and Cook. The temperature of the transition $LiCl \cdot 2H_2O \rightleftarrows LiCl \cdot 3H_2O$ is in good agreement with that reported by Hüttig and Steudemann. The transition temperature for $LiCl \cdot 3H_2O \rightleftarrows LiCl \cdot 5H_2O$ apparently is that reported as the eutectic by Voskrenskya and Yanat'eva. The eutectic composition, 25.0% is in excellent agreement with that reported by Garrett and Woodruff, although the temperature was found to be lower.

No evidence of a tetrahydrate was found.

Acknowledgment.—The author wishes to acknowledge the assistance of A. W. Bertschy and M. T. Lyons in carrying out this work.

STABILITY OF ZINC AND CADMIUM COMPLEXES WITH SOME METHYL DERIVATIVES OF 1,10-PHENANTHROLINE AND 2,2'-BIPYRIDINE

BY MOTOO YASUDA, KÔZÔ SONE AND KAZUO YAMASAKI

Contribution from Chemical Institute, Faculty of Science, Nagoya University, Nagoya, Japan

Received July 30, 1956

As the continuation of our former study[1] on the stability of zinc and cadmium complexes of 1,10-phenanthroline and 2,2'-bipyridine, stability constants of complexes with some methyl derivatives of these chelating agents[2] were determined using pH titration methods.

Experimental

Method and Apparatus.—The method and apparatus used in the present investigation were the same as in the previous study.[1] Acid dissociation constants of phenanthrolinium and bipyridinium ions were determined by means of potentiometric pH titration with standard nitric acid and sodium hydroxide at 25°. Potassium nitrate was added to keep the ionic strength of solutions at 0.1. Similar measurements were made on solutions which contained metal ion to be investigated together with the ligand and 0.1 M potassium nitrate.

Materials.—All chelating agents studied were the products prepared by G. F. Smith, Co., Columbus, Ohio, U.S.A. Nitrates of both metals were of analytical grade.

Results and Discussion

Acid dissociation constants of methyl-substituted 1,10-phenanthrolinium and 2,2'-bipyridinium ions determined are given in Table I, together with those reported by previous workers.

TABLE I

	pK_H	Author
1,10-Phenanthroline	4.92	Yamasaki, Yasuda[1]
2-Methyl-1,10-phenanthroline	5.42	Irving, *et al.*[2]
5-Methyl-1,10-phenanthroline	5.26	Present study
5-Methyl-1,10-phenanthroline	5.2	Brandt, *et al.*[2]
2,9-Dimethyl-1,10-phenanthroline	6.15	Present study
4,7-Dimethyl-1,10-phenanthroline	5.94	Present study
2,2'-Bipyridine	4.44	Yamasaki, Yasuda[1]
4,4'-Dimethyl-2,2'-bipyridine	5.32	Present study

Stability constants determined for zinc and cadmium complexes are given in Table II. First formation constants (k_1) of 5-methyl- and 4,7-dimethylphenanthroline complexes could not be determined by pH method because they were too large. Cadmium complexes of methyl-substituted phenanthrolines were found to be difficultly soluble in water, and in particular 4,7-dimethylphenanthroline complex was so easily precipitated from its solution that its stability constants could not be determined in aqueous media. Further, second and third formation constants of the 2,9-dimethylphenanthroline complexes were too small to be determined with sufficient accuracy.

As shown in Table I, all methyl-substituted derivatives have higher basicity than the parent chelating agents. This effect is easily understood because the well-known electron-releasing tendency of methyl group enhances the donor properties of these basic molecules. Dimethyl derivatives are more basic than monomethyl ones, just as observed actually in the case of 1,10-phenanthroline derivatives. As to the effect of substituent positions, pK_H value of 2-methyl-1,10-phenanthroline is greater than that of 5-methyl derivative, and also pK_H of 2,9-dimethyl-1,10-phenanthroline is greater than that of 4,7-dimethyl derivative. It is interesting to compare these results with the recent molecular orbital studies of Longuet-Higgins and Coulson[3] who showed that relative net charges on the 1,10-phenanthroline molecule are distributed as shown in Fig. 1.

From Fig. 1 it is clear that positive charges are most concentrated on 2,9- and then 4,7-positions, making these positions most active, that is, most susceptible to electron releasing effect of substituted methyl groups. It is to be noted that observed changes of pK_H with positions of methyl

---

(1) K. Yamasaki and M. Yasuda, *J. Am. Chem. Soc.*, **78**, 1324 (1956).

(2) Stability constants of ferrous complexes of similar ligands have been reported by W. W. Brandt and D. K. Gullstrom (*J. Am. Chem. Soc.*, **74**, 3532 (1952)) and by H. M. Irving, M. J. Cabell and D. H. Mellor (*J. Chem. Soc.*, 3417 (1953)).

(3) H. C. Longuet-Higgins and C. A. Coulson, *J. Chem. Soc.*, 971 (1949); *cf.* also W. H. McCurdy and C. F. Smith, *Analyst*, **77**, 846 (1952).

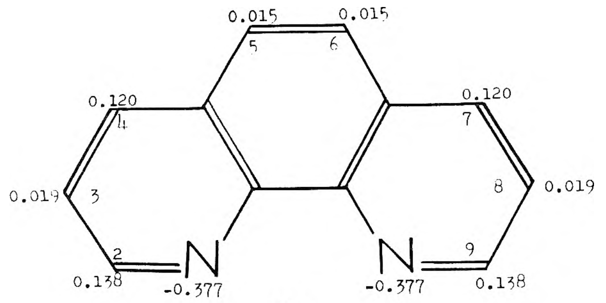

Fig. 1.

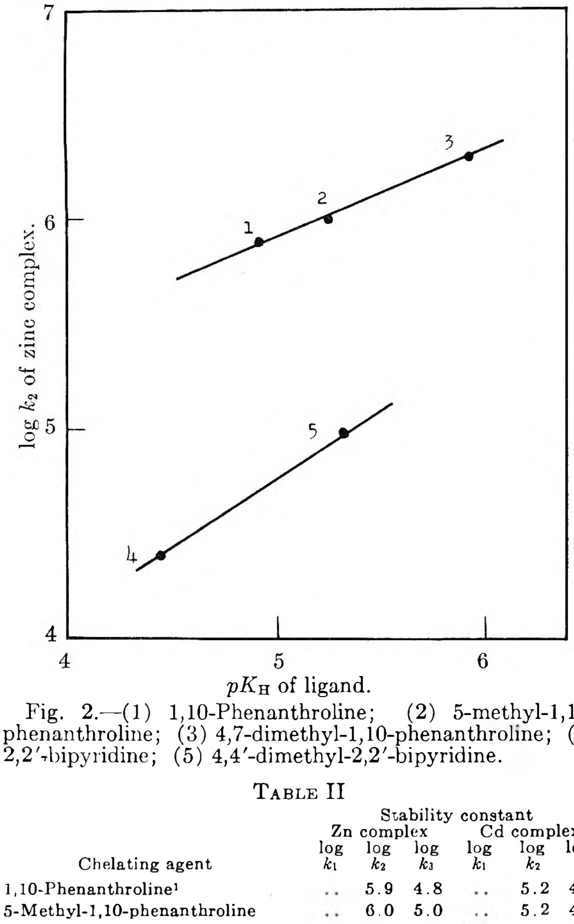

Fig. 2.—(1) 1,10-Phenanthroline; (2) 5-methyl-1,10-phenanthroline; (3) 4,7-dimethyl-1,10-phenanthroline; (4) 2,2′-bipyridine; (5) 4,4′-dimethyl-2,2′-bipyridine.

TABLE II

	Stability constant					
	Zn complex			Cd complex		
Chelating agent	log k_1	log k_2	log k_3	log k_1	log k_2	log k_3
1,10-Phenanthroline[1]	..	5.9	4.8	..	5.2	4.2
5-Methyl-1,10-phenanthroline	..	6.0	5.0	..	5.2	4.3
4,7-Dimethyl-1,10-phenanthroline	..	6.3	5.4	Ppt.	..	..
2,9-Dimethyl-1,10-phenanthroline	3.1	..	..	2.8	..	..
2,2′-Bipyridine[1]	5.4	4.4	3.5	4.5	3.5	2.5
4,4′-Dimethyl-2,2′-bipyridine	6.0	5.0	4.0	4.9	3.8	3.0

groups agree well with this theoretical expectation.[4]

The relationship between basic strength of ligands and stability of chelates was first pointed out by Calvin and Wilson[5] in connection with cupric chelates of a number of enolic substances. Similar relations were also found in the derivatives of 1,10-phenanthroline and 2,2′-bipyridine. In Fig. 2 values of log k_2 of zinc complexes are plotted against pK_H values of ligands. Values of log k_2 are chosen in this comparison because this constant is equal to the average stability constant, or third root of the over-all constant K, when the formation curve belongs to the symmetrical type. According to Bjerrum[6] k_2 is also equal to the reciprocal of the free ligand concentration where the degree of formation, $\bar{n}/N$, is equal to 0.5.

In Fig. 2, the three phenanthroline points and the two bipyridine points fall on two separate curves, the phenanthroline curve lying above the bipyridine curve. This means that complexes of phenanthroline derivatives are always more stable than those of bipyridine derivatives. The only exception is 2,9-dimethyl-1,10-phenanthroline for which the formation of complexes is strongly suppressed although it has the strongest basicity in all the ligands investigated. This peculiar phenomenon is probably due to the steric hindrance of two methyl groups which are located so near to the coordination center. In this connection it is interesting to note that this same substance does not show the familiar red coloration with ferrous ion, that is, the ability for $[Fe(phen)_3]^{+2}$ type complex formation is lacking for this ligand,[7] and that ferrous complex of 2-methyl-1,10-phenanthroline has been reported to be much less stable than that of unsubstituted phenanthroline.[2] Both phenomena have been explained on the basis of steric hindrance.

---

(4) In this connection, a similar relation was also observed in simpler heterocyclic compounds, methyl derivatives of pyridine: *cf.* E. A. Braude and F. C. Nachod, "Determination of Organic Structures by Physical Methods," Academic Press, New York, N. Y., 1955, pp. 597, 750.

(5) M. Calvin and K. W. Wilson, *J. Am. Chem. Soc.*, **67**, 2003 (1945).

(6) J. Bjerrum, "Metal Ammine Formation in Aqueous Solutions," P. Haase and Son, Copenhagen, 1941.

(7) J. Gillis, *Anal. Chim. Acta*, **8**, 97 (1953).

THE ENTROPY OF CHELATION

BY F. H. WESTHEIMER AND LLOYD L. INGRAHAM

Contribution from the Mallinckrodt Chemical Laboratory, Harvard University, Cambridge, Massachusetts

Received August 15, 1956

Schwartzenbach[1] measured the stabilities of metal chelates of ethylenediamine relative to those of metal complexes with ammonia, and postulated that the "chelate effect" was due to the more favorable entropy of formation for the latter compounds. He approximated the entropy effect by comparing the probability of ring closure as compared with the probability of reaction with molecules of a complexing agent free in solution. This type of calculation has recently been refined by Cotton and Harris.[2] Somewhat earlier, Calvin and Bailes[3] pointed out that the formation of $Ni(en)_3^{++}$ requires that four molecules combine to one, whereas the formation of $Ni(NH_3)_6^{++}$ requires that seven molecules combine to one; the added stability of the chelate may be ascribed to the smaller loss of translational entropy which accompanies its formation. (Here "en" is used to designate ethylenediamine.) But this explanation can scarcely be complete, since the change in translational entropy is so large as to account for the chelation effect several times over.

However, closing a ring is accompanied by a loss of internal rotation, and therefore by a considerable decrease in entropy. For example, the entropy of cyclohexane is 21 units less than that of its open chain isomer, hexene-1. The decrease in entropy on cyclization will in part compensate for the greater translational entropy of chelation as compared with complex formation. A semi-empirical method of estimating the chelation effect consists in considering the entropy change which accompanies the reaction shown in equation 1; here the extra molecule on the right-hand side of the equation supplies the additional translational entropy, and the cyclization of the hydrocarbon causes the decrease which accompanies ring closure.

---

(1) G. Schwartzenbach, *Helv. Chim. Acta*, **35**, 2344 (1952).

(2) F. A. Cotton and F. E. Harris, THIS JOURNAL, **59**, 1203 (1955); **60**, 1451 (1956).

(3) M. Calvin and R. Bailes, *J. Am. Chem. Soc.*, **68**, 949 (1946).

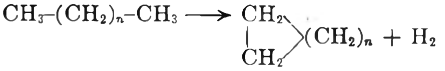

$$CH_3-(CH_2)_n-CH_3 \longrightarrow \begin{matrix} CH_2 \\ | \\ CH_2 \end{matrix} \rangle (CH_2)_n + H_2 \quad (1)$$

The over-all change in entropy may be expected to approximate the difference between the $\Delta S°$ for chelation and that for complex formation.

Entropies are experimentally available[4] for the formation of cyclopentane and cyclohexane, but not, regrettably, for higher cycloparaffins. For comparison with solutions, each entropy value has been corrected to a gas pressure such that the concentration is one molar. Then for $n = 3$ (closure of a 5 ring) $\Delta S° = 11.6$ cal./mole °, and for $n = 4$ (closure of a 6 ring) $\Delta S° = 3.7$ cal./mole °.

The analogy between equation 1 and the chemistry of chelation can be illustrated as follows. Provided that $\Delta S°$ is small for reaction 2 (where only one of the nitrogen atoms of ethylenediamine is attached to copper) the difference between the entropy of complex formation and that of chelation is equal to $\Delta S°$ for reaction 3.

$$(H_2O)_2Cu(NH_3)_2^{++} + \text{en} \longrightarrow (H_2O)_2Cu(NH_3)NH_2CH_2CH_2NH_2^{++} + NH_3 \quad (2)$$

$$(H_2O)_2Cu(NH_3)NH_2CH_2CH_2NH_2^{++} \longrightarrow (H_2O)_2Cu(\text{en})^{++} + NH_3 \quad (3)$$

Reaction 3 is analogous to (1) and should, as a first approximation, show a comparable entropy change. In fact, the values for the closure of five- and six-membered rings are very roughly the right size to account for the total chelation effect observed for several metals.[1] The average value of the chelate effect for each ethylenediamine molecule is about 8 e.u. in $Cd(\text{en})_2^{++}$ (Spike and Parry[5a]) or in $Cu(\text{en})_2^{++}$ (Poulson and Bjerrum[5b]). These values are comparable to but somewhat less than the 11.6 e.u. here estimated for the closure of a five-membered ring. The magnitude of the chelate effect, however, is greater for the second than for the first molecule of ethylenediamine.

Of course, as a second approximation, a number of corrections must be considered. These include those for incomplete cancellation of (a) translational entropy, (b) rotational entropy, (c) entropy of solvation.

(a) The over-all equation for chelation (the sum of equations 2 and 3) is shown as (4) below

$$(H_2O)_2Cu(NH_3)_2^{++} + \text{en} \rightleftarrows (H_2O)_2Cu(\text{en})^{++} + 2NH_3 \quad (4)$$

There is one more molecule on the right than on the left-hand side of both (1) and (4). But translational entropy contains a term ($3/2\ R \ln M$) for molecular weight; this term is more important in (4) than in (1). The translational entropy of two moles of ammonia exceeds that for one mole of ethylenediamine by 1.8 e.u. more than the translational entropy of a mole of hydrogen.

(b) Ammonia has three degrees of rotational freedom, hydrogen only two. However, the internal rotation of an ammonia molecule in the complex shown on the left side of eq. 3 should at least approximately take care of this difference. The rotational entropy of an NH_2 group will not exactly cancel that of a CH_3 group.

(c) The most important effect is that of solvation. The entropy of a mole of gaseous ammonia (46.0 e.u.) exceeds that for a one molar solution (26.3 e.u.) by much more than the entropy change (6.4 e.u.) for simple concentration from one atmosphere to one molar. The solvent must then be strongly oriented in the neighborhood of the basic nitrogen atoms. The approximation for the entropy of chelation which is involved in using the entropy of eq. 1 in place of that for eq. 3 or eq. 4 is legitimate only if the entropy of solvation, per amino group, is about the same for ethylenediamine as for ammonia.

The entropy of solution for any compound can readily be calculated from its heat of solution from the vapor phase and the partial pressure over its aqueous solution. The heat of solution[6] for ethylenediamine is 7.5 kcal./mole, and its heat of vaporization[7] 11.20 kcal./mole. The partial pressure of the amine over a one molar solution at 25° (see Experimental) is approximately 0.0013 mm. The entropy of solution from the gas at one atmosphere to one molar solution is then 36 e.u. per mole, or 18 e.u. per amino group. This is close to the value of 19.7 e.u. for ammonia; fortuitously, the small difference is in such a direction as to compensate the correction to the translational entropy.

Such fortuitous cancellation will not always occur. The entropy of solution for methylamine can be calculated from its heats of formation in the gas phase and in solution,[4] and from the partial pressure[8] of the gas above its aqueous solution. These data lead to a value for the entropy of solution of 27 e.u., which is considerably greater than that for either ammonia or for the individual amino groups of ethylenediamine. This large difference in entropy of solution, however, is not appreciably reflected in the entropy of complex formation.[5]

The estimates here involve, of course, the assumption that the various dipositive ions (*e.g.*, $Cu(NH_3)_4^{++}$ and $Cu(\text{en})^{++}$) have the same entropies of solvation. In view of the drastic approximations which are necessary, and in view of the fact that the net entropy of chelation is a small difference between the much larger entropies of translation and cyclization, an estimate based on equation 1 will yield only a crude approximation to the entropy of chelation. This must be true even when the entropy of solvation of the amine is taken explicitly into account. Nevertheless, a consideration of the entropies of translation and of cyclization provides at least an order of magnitude estimate of the chelation effect.

---

[4] National Bureau of Standards, "Selected Values of Chemical Thermodynamic Properties," Washington, D. C., 1952; American Petroleum Institute Research Project 44.

[5] (a) C. G. Spike and R. W. Parry, *J. Am. Chem. Soc.*, **75**, 2726 (1953); (b) I. Poulson and J. Bjerrum, *Acta. Chem. Scand.*, **9**, 1407 (1955).

[6] M. Berthelot, *Ann. chim. phys.*, [7] **20**, 163 (1900).

[7] Landolt-Bornstein, "Physikalisch-Chemische Tabellen," Erg. IIIc, p. 2727.

[8] W. A. Felsing and A. R. Thomas, *Ind. Eng. Chem.*, **21**, 1269 (1929).

Experimental

Ethylenediamine was dried over sodium and fractionated at a 30/1 reflux ratio in a Wheeler all-glass center-rod column protected from moisture and carbon dioxide by soda-lime. The center cut was chosen for the determination of partial pressure.

The partial pressure was measured by a dynamic method. An all-glass train (no ground-glass joints) was constructed as follows: first a wash bottle, second a wash bottle with a medium fritted disc as gas outlet, third a large medium fritted disc as a spray trap, fourth, another wash bottle with a medium fritted disc as gas outlet and fifth an American Meter Co. integrating gas meter. The first two wash bottles were filled with 75 cc. of ethylenediamine solution (about 1.5 M) and the last one with 75 cc. of water; the parts of the apparatus were then sealed together and immersed in a thermostat at 33.0°. Fifty to 100 liters of prepurified nitrogen were passed through the solution at a rate of about 30–70 cc./minute. The solution in the last wash bottle was titrated for ethylenediamine. The average calculated partial pressure at 33° corrected to 1 M ethylenediamine was about 0.003 mm., and the partial pressure over a 1 molar solution at 25° was estimated as 0.0013 mm.

Acknowledgment.—The authors gratefully acknowledge the support of the Guggenheim Memorial Foundation and of the National Science Foundation.

INFRARED ABSORPTION CELL FOR THE STUDY OF HETEROGENEOUS REACTIONS

By Bernard M. Mitzner[1]

Department of Chemistry, Columbia University, New York 25, New York

Received August 23, 1956

The study of heterogeneous reactions between a gas and a solid may be carried out very effectively with the aid of infrared spectroscopy. The solid under investigation can be prepared for infrared study by several procedures such as: (a) evaporating a film of the material on a thin sodium chloride or silver chloride plate (solvent or vacuum evaporation may be employed); (b) rolling a finely powdered sample into a sheet of silver chloride; (c) employing the material under investigation in the form of a sheet or large single crystal (*e.g.*, silver chloride, potassium bromide, etc.). The gas in this study may be contained in a standard gas infrared absorption cell.

If the solid under investigation is placed perpendicular to the infrared beam and is surrounded by a gas, one will obtain both the spectrum of the gas as well as that of the reaction product. (The solid may very well contribute its own infrared absorption spectrum.) Thus, one cannot readily determine whether there is any spectral change as a result of the interaction either on the surface of the solid or in the gas phase. An infrared absorption cell has been devised in our laboratory which is well suited for heterogeneous studies of this nature. This absorption cell solves the problem by both allowing the spectrum of the solid–gas reaction product as well as the gas to be observed, without altering any of the experimental conditions.

The infrared gas absorption cell consists of a 45 mm. glass tube ten cm. long with salt plates affixed to its ends. (The optical path length can be varied according to experimental needs.) A stopcock equipped with a ground glass joint to facilitate filling and emptying of the cell has been fused to the cell body. A 14/35 ground glass joint has been attached directly to the body of the cell as shown. A 14/35 male joint which is equipped with a handle (to facilitate turning) is placed into the female joint. A means of holding the solid sample, such as a needle, is inserted into the male joint. The solid plate can also be attached with bees' wax. An infrared gas cell of the demountable type may be profitably employed in order to facilitate solid sample handling.[2]

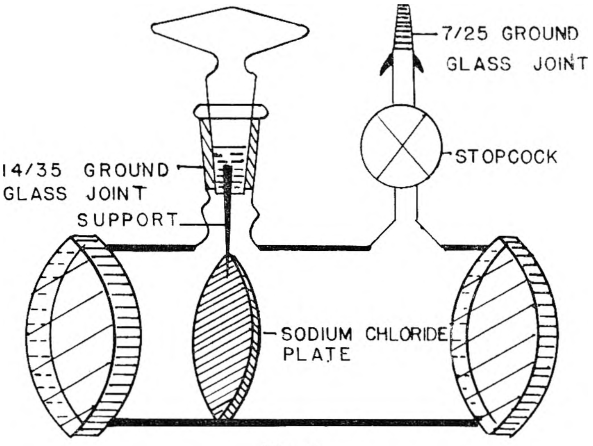

Fig. 1.

Thus, the solid can be rotated in and out of the infrared beam, merely by turning the male ground glass joint 90°, without allowing any pressure change to occur in the absorption cell. When the solid is perpendicular to the infrared beam, the infrared absorption pattern that is obtained is due to the interaction of the gas and the solid. If the solid is rotated 90°, the absorption pattern that is obtained is that of the surrounding gas in the cell which may have undergone some form of reaction.

If a plate is employed that is excessively thick, the entire absorption cell may be rotated 90° (it will then lie upon its side) so that the longer portion of the plate will be perpendicular to the slit of the infrared spectrophotometer (when the plate is "out of the beam") thus minimizing energy losses.

This infrared absorption cell has been successfully employed in studies of surface reactions, chemical absorption and chemical adsorption.

---

(1) Lederle Laboratories Division, American Cyanamid Company, Pearl River, New York.

(2) B. M. Mitzner and S. Z. Lewin, *Anal. Chem.*, **26**, 1254 (1954).

ADDITIONS AND CORRECTIONS

Vol. 57, 1953

Gene P. Rutledge, Roger L. Jarry and Wallace Davis, Jr. Freezing Point Diagram and Liquid–Liquid Solubilities of the System Uranium Hexafluoride–Hydrogen Fluoride.

Page 543. In the footnote of Table I, for "Fig. 1." read "Fig. 2." In col. 2, text line 5 from the end, for "mole" read "weight."

Page 544. In col. 1, line 2, for "formula" read "weight."—Wallace Davis, Jr.

Vol. 58, 1954

Herbert Morawetz and Paula E. Zimmering. Reaction Rates of Polyelectrolyte Derivatives. I. The Solvolysis of Acrylic Acid–*p*-Nitrophenyl Methacrylate Copolymers.

Page 754. The first line of footnote (7a) should read: "First order plots of the methanolysis of similar *p*-nitrophenyl methacrylate copolymers with *methacrylic* acid were strongly concave . . ."—Herbert Morawetz.

H. Rubin and F. C. Collins. Concentration Overpotential at Reversible Electrodes.

Page 958 ff. The authors are grateful to Mr. Fred Anson, Department of Chemistry, Harvard University, for pointing out to us that our statement that, for potentials below saturation potential, the current will converge to the "limiting" current at sufficiently long time is incorrect. The general expression for the current after the short time transient behavior is

$$I\ (t\ \text{large}) = \left[nFAc^\circ{}_1\left(\frac{D}{\pi t}\right)^{1/2}\right]\left[\frac{1 - \dfrac{k_2}{k_1}\left(\dfrac{c^\circ{}_2}{c^\circ{}_1}\right)}{1 + \dfrac{k_2}{k_1}\left(\dfrac{D_1}{D_2}\right)^{1/2}}\right]$$

where the first bracketed term is the limiting current expression and the second term is a constant for any given run. Also Eq. (10) should read $\lim\limits_{x=0} c(x,t) = 0$.—F. C. Collins.

Vol. 60, 1956

P. A. Johnson and A. L. Babb. Self-diffusion in Liquids. I. Concentration Dependence in Ideal and Non-ideal Binary Solutions.

Page 14. The authors report: "In this article an equation was given relating the mutual and self-diffusion coefficients

$$\frac{\mathrm{D}_{12}}{D_{11}} = \frac{D_{12}}{\mathrm{D}_{22}} = \left\{1 + \frac{\partial \ln \gamma_i}{\partial \ln x_i}\right\} \qquad (1)$$

where D_{12} is the mutual diffusion coefficient, and D_{11} and D_{22} are the self-diffusion coefficients at mole fraction x. This equation was ascribed to S. Prager, *J. Chem. Phys.*, 21, 1344 (1953), whereas he actually presented equations first given by L. S. Darken, *Trans. Amer. Inst. Min. Met. Eng.*, 175, 184 (1948), and G. S. Hartley and J. Crank, *Trans. Far. Soc.*, 45, 801 (1949), which lead to a general equation

$$D_{12} = \{x_1D_{22} + x_2D_{11}\}\left\{1 + \frac{\partial \ln \gamma_1}{\partial \ln x_1}\right\} \qquad (2)$$

Equation (2) requires only the assumptions of negligible volume change on mixing, and constant partial molar volumes and was first presented by Darken. Equation (1) requires the added assumption of no net volume flow which limits its application. Equation (2) has been verified by Darken using the data of W. A. Johnson, *Trans. Amer. Inst. Min. Met. Eng.*, 147, 331 (1942), on gold–silver alloys. P. C. Carman and L. H. Stein, *Trans. Far. Soc.*, 52, 619 (1956), recently applied equation (2) to liquid self-diffusion data for the system ethyl iodide–*n*-butyl iodide which behaves nearly ideally. Unfortunately, experimental mutual diffusion data were not available to check the values calculated from equation (2). For non-ideal solutions of the benzene-alcohol type it has been shown by us that the mutual diffusion coefficient corrected for solution activity is not simply related to the self-diffusion coefficients suggested by the general equation (2).

"It appears that for associated systems exhibiting positive vapor pressure deviations a simple activity correction is not sufficient to account for non-ideal diffusion behavior. In view of this, an attempt has been made to assign a diffusion coefficient to the various alcohol "mers" in alcohol–hydrocarbon systems and an expression relating these to the observed diffusivities has been developed. The results of this work will soon be submitted for publication."—A. L. Babb and P. A. Johnson.

H. K. Hall, Jr. Potentiometric Determination of the Base Strengths of Amines in Non-protolytic Solvents.

Page 64. In Fig. 1, the ordinate legend should be "E" instead of "$E_{1/2}$." The abscissa legend should read "log $X/(1 - X)$" instead of "pK."

Page 70. In col. 2, line 24, after "flasks" insert "with ethyl acetate."—H. K. Hall, Jr.

Alfred J. Stamm. Diffusion of Water into Uncoated Cellophane. I. From Rates of Water Vapor Adsorption, and Liquid Water Absorption.

Page 77. In col. 1, Eq. (2), the first term should read "$\bar{D}_d$." Lines 5 and 6 below Eq. (2) insert "differential" before the word "diffusion."

Page 79. In col. 1, Eq. (5) the first term should read "$\bar{D}_a$." and the numerator of the term after the equal sign, "πa_0^2." In line 3 below Eq. (5), after "S," insert the words "beyond the dry thickness, a_0."

Page 80. In Eq. (6) the first term should read "D_a." In col. 2, 6 lines from the end, omit the phrase "where the area above the curve XBY is equal to the area AWYC."

Page 81. In col. 1, line 2, after "0.422" insert "for desorption and $f = 0.578$ for adsorption." In line 4, change "$E_a = (1 - f)^2$" to read "$1 - E_a = f^2$." In lines 9 and 10, omit "or absorbing." In line 13, for "0.333" read "0.667." In col. 2, Fig. 5, on the ordinate, for "$(1 - E_a)$" read "E_a." On the abscissa, after "specimen" add "for desorption, reverse for adsorption." In line 5, for "over-dry" read "oven-dry."

Page 82. In col. 1, the line before Conclusions, for "restraint" read "stress." In col. 2, item (5), line 6, omit the words "lost or." In line 7, for "0.422" read "0.578." In lines 9 and 10, omit the words "of the evaporable or one-third."—Alfred J. Stamm.

Alfred J. Stamm. Diffusion of Water into Uncoated Cellophane. II. From Steady-State Diffusion Measurements.

Page 83. In col. 2, Eq. (1), the first term should be "$\bar{D}_{vp}$." In the next line, add the word "average" before "vapor." Six lines below Eq. (1), for "a" read "an average." In the next line, for "D_{vc}" read "$\bar{D}_{vc}$" and the same correction in the first term of Eq. (2).

Page 84. In col. 2, Eq. (3), the first term should read "D_{vc}."

Page 85. In col. 1, line 1, for "dD_{vc}" read "D_{vc}," and the same change in line 4 below. In line 6, insert the word "average" before "diffusion." In Eq. (4) the first term should be "$\bar{D}_w$." In Eq. (5) the first term should be "D_w," the denominator of the last term "dM," and this same change in the next line of text. Line 11 from the end, for "dM_c" read "dM." In Table I, cols. 9 and 10, omit the "d" from the terms "dD_w" and "dD_{vc}."

Page 86. In col. 2, lines 8 and 6 from the end, omit the letter "d" from "dD_w" and "dD_{vc}."—Alfred J. Stamm.

John T. Neu. Infrared spectrographic studies of preflame reactions of *n*-butane.

Page 323. In Fig. 5, the caption is correct, but the plate is wrong; the correct Fig. 5 is given herewith.—JOHN T. NEU.

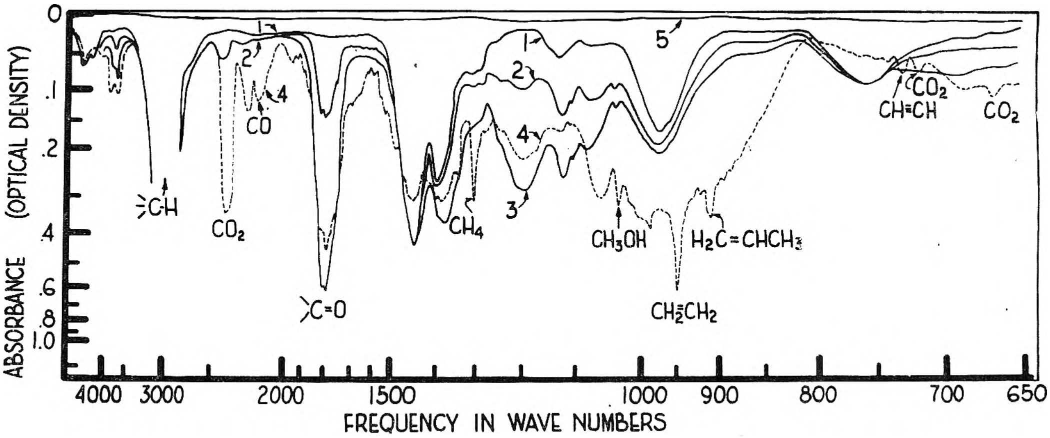

Fig. 5.

A. A. Miller, E. J. Lawton and J. S. Balwit. The Radiation Chemistry of Hydrocarbon Polymers: Polyethylene, Polymethylene and Octacosane.

Page 603. In col. 1, line 20, transpose the words "then the formation" to begin the line below the second formula equation, that is, to precede the words "of *trans*-vinylene."—A. A. MILLER.

Edward F. Casassa. The Conversion of Fibrinogen to Fibrin. XVIII. Light Scattering Studies of the Effect of Hexamethylene Glycol on Thermodynamic Interactions in Fibrinogen Solutions.

Page 927. In section III, line 12, for "A', A'," read "A_2', A_3'," and in line 15 for "A_2 and A_2" read "A_2 and A_2'."

Page 930. In column 2, lines 21–22, read "with $\omega = 1$, $A_2' = A_2$."

Page 932. In column 2, line 35, read "$A_3'/(A_2')^2M' = A_3/A_2{}^2M = 1.0$."—EDWARD F. CASASSA.

M. Spiro. The Transference Numbers of Iodic Acid and the Limiting Mobility of the Iodate Ion in Aqueous Solution at 25°.

Page 977. In col. 1, the equations for ΔV_1, ΔV_2, and ΔV_3 the "$-$" sign should be omitted in all combinations "$+ -$" and "$- -$." Equation (1) should read "$t_{\text{IO}_3}(I = I) - t_{\text{IO}_3}(I = 0) = f(I/\alpha c)$." Two lines above Fig. 1, for "$(I/\alpha c)^{2,7}$" read "$(I/\alpha c)^{2.7}$." The legend for the vertical scale of Fig. 1 should read "$[t_{\text{IO}_3}(I = I) - t_{\text{IO}_3}(I = 0)] \times 10^4$."

Page 978. In the 14th line of the text the factor should read "$1/(t_{\text{H}} + t_{\text{IO}_3})$." Equation (5′) should have a bracket "]" at the end.

Page 980. In the long equation at the bottom, the first term should read "$\frac{1}{1 - \delta}$."—M. SPIRO.

Gert Ehrlich. The Interaction of Nitrogen with a Tungsten Surface.

Page 1390. In col. 1, Eq. (1) the letter "τ" should be above the integral sign. In text line 8 below Fig. 2, insert "τ_D" above the integral sign, substitute τ for λ as the variable of integration, and read "depends only." In Eq. (2) insert "τ_D" over the integral sign and in Eq. (3) "τ_E" similarly. In Eq. (3) omit the $-$ sign before "S_E" and in Eq. (4) and (5) omit the $-$ sign after the equal sign. In col. 2, Eq. (6) after the term "$\mathfrak{F}_A$" the $-$ sign should be $+$. In Eq. (7) after the term "$\mathfrak{F}_F$" the $+$ sign should be $-$, and in the second line of Eq. (8) after "$\mathfrak{F}_A\,dt$" the $-$ sign should be $+$.—GERT EHRLICH.

Author Index to Volume LX, 1956

Ahmann, D. H. See Salmon, O. N., 13.
Alberty, R. A. See Smith, R. M., 180.
Alexander, L. E., and Sommer, E. C. Systematic analysis of C black structures 1646
Allen, E. R. See Woodward, A. E., 939.
Allen, K. A. Equil. between tri-*n*-octylamine and H_2SO_4, 239; equil. between di-*n*-decylamine and H_2SO_4 943
Altman, C. See King, E. L., 1375.
Ames, D. C. See Rush, R. I., 1591.
Amis, E. S. Polar properties of solvent and conductance of electrolytes at infinite dilution, 428; see Cohen, D., 701.
Ammar, I. A., and Awad, S. A. H overpotential at electrodeposited Ni cathodes in HCl solns., 837; effect of some corrosion inhibitors and activators on the H overpotential at Fe cathodes in NaOH solns., 871; H overpotential on Ag in NaOH solns. 1290
Anderson, R. B., Hall, W. K., Lecky, J. A., and Stein, K. C. Sorption studies on American coals 1548
Anderson, R. H. See Woodward, A. E., 939.
Armstrong, A. M., Halpern, J., and Higginson, W. C. E. Reacn. between Hg(I) and Tl(III) in aq. soln.: evidence for dismutation of Hg_2^{++} 1661
Armstrong, D. A., and Winkler, C. A. Comparative production of active N from N, NO and NH_3, and from N at different discharge potentials 1100
Arnett, R. L. See Li, K., 1400.
Asher, D. R., and Simpson, D. W. Glycerol purification by ion exclusion 518
Assarsson, G. O. Equil. in the ternary system $MgCl_2$–$BaCl_2$–H_2O between 18 and 100°, 1436; hydrothermal reacns. between $Ca(OH)_2$ and amorphous silica in atm. of unsatd. steam 1559
Assarsson, G. O., and Rydberg, E. Hydrothermal reacns. between $Ca(OH)_2$ and amorphous silica 397
Augenstine, L. G. See Ray, B. R., 1193.
Awad, S. A. See Ammar, I. A., 837, 871, 1290.

Babb, A. L. See Caldwell, C. S., 51; Johnson, P. A., 14, (corrn.) 1671.
Bacarella, A. L., Finch, A., and Grunwald, E. Vapor pressures and activities in the system dioxane–H_2O—second virial coeffs. in the gaseous system N–dioxane–H_2O 573
Baelor, M. D., Barnum, D., and Gorin, G. Kinetics of thermal decompn. of phenyltrimethylammonium hydroxide in soln. 1004
Baes, C. F., Jr. Redn. of U(VI) by Fe(II) in phosphoric acid soln., 805; a spectrophotometric investigation of uranyl phosphate complex formation in $HClO_4$ soln. 878
Bailey, G. C. See Heckelsberg, L. F., 559.
Bailey, T. L. See Muschlitz, E. E., Jr., 681.
Bak, T. A. A minimum-principle for non-equil. steady states (II) 1611
Baker, A. W. Intermol. assocn. of carbonyl compds. 1660
Baker, F. B. See Newton, T. W., 1417.
Bale, H. D. See Schmidt, P. W., 1580.
Ball, J. S. See Haines, W. E., 549.
Balwit, J. S. See Miller, A. A., 599, (corrn.) 1673.
Bankoff, S. G. Contortional energy requirement in the spreading of large drops 952
Barber, E. J., and Cady, G. H. Vapor pressures of perfluoropentanes, 504; some phys. properties of WF_6 505
Barnett, M. K. See Orban, E., 413.
Barnum, D. See Baelor, M. D., 1004.
Bartell, F. E. See Craig, R. G., 1225.
Bartell, L. S., and Ruch, R. J. Wetting of incomplete monomol. layers 1231
Barton, J. L., and Bloom, H. A b.p. method for detn. of vapor pressures of molten salts 1413
Bartos, H. R., and Margrave, J. L. Thermal decompn. of $NaNO_3$ 256
Bartulovich, J. J. See Ward, W. H., 1208.
Bastian, W. C., and Lapidus, L. Longitudinal diffusion in ion exchange and chromatographic columns—finite column 816
Bauer, S. H., and McCoy, R. E. Energetics of the boranes (III) enthalpy and heat capacity of trimethylamine–trifluoroborane as detd. by the drop method 1529
Bauer, W. H. See Guertin, D. L., 1018; Roth, W., 639; Weber, N., 270.
Beachell, H. C., and Lange, K. R. Sorption of B compds. by Pd and charcoal 307
Beachell, H. C., and Veloric, H. S. Adsorption isotherms, isobars and isosteres of B_2H_6 on BN and Pd on charcoal 102
Becker, W. E. See Mills, A. P., 1644.
Beckmann, C. O. See Winter, S. S., 883.
Begun, G. M., Palko, A. A., and Brown, L. L. NH_3-ammonium carbonate system for the concn. of N-15 48
Bello, J. Protonation of N-methylacetamide 1341
Bello, J., Riese, H. C. A., and Vinograd, J. R. Mechanism of gelation of gelatin—influence of certain electrolytes on m. p. of gels of gelatin and chemically modified gelatins 1299
Bello, J., and Vinograd, J. R. Effect of optical isomers on m.p. of gelatin gels 818
Bennett, R. L., and Scott, J. M. Dipole moments of cyclohexyl azide, cyclopentyl azide and 3-bromocyclohexene 1585
Benson, G. W., and Tompkins, F. C. Sorption of NH_3 by dehydrated potash alum 220
Benson, J. E., and Kwan, T. Kinetics and mechanism of hydrogenation of cyclopropane over a Ni–silica–alumina catalyst 1601
Bent, H. A. Configurational entropy and choice of standard states, entropies of formation of complex ions, and the chelate effect 123
Bent, H. E. See John, H. F., 1524.
Beresniewicz, A. See Wall, F. T., 692.
Bergen, R. L., Jr., and Long, F. A. Salting in of subsd. benzenes by large ion salts 1131
Beringer, F. M., Geering, E. J., Kuntz, I., and Mausner, M. Diaryliodonium salts (IV) ion-pairs and Cu catalysis in reacns. of diphenyliodonium ions with halide ions and hydroxylic solvents 141
Berlad, A. L. See Potter, A. E., Jr., 97.
Bernstein, F. See Gregor, H. P., 263.
Bertsch, C. R., Fernelius, W. C., and Block, B. P. Molarity quotients for formation of complexes between Cd ions and amines containing S 384
Binford, J. S., Jr., and Eyring, H. Kinetics of the steam–C reacn. 486
Bitler, P. L. See Li, K., 1400.
Bhatnagar, R. P. See Shukla, R. P., 809.
Block, B. P. See Bertsch, C. R., 384.
Bloom, H. See Barton, J. L., 1413.
Bloom, H., and Doull, N. J. Transport no. measurements in pure fused salts 620
Bloom, H., and Rhodes, D. C. Molten salt mixts. (Part 2) refractive index of molten nitrate mixts. and their molar refractivities 791
Bockris, J. O'M., and Mellors, G. W. Elec. conductance in liq. Pb silicates and borates 1321
Bohmfalk, E. See Lacher, J. R., 492.
Bond, G. C. Adsorption of D by a Pt catalyst 702
Bondi, A., and Parry, H. L. Phys. properties of 2,4,6-tri-dimethylaminomethyl-phenol triacetate 1406
Bonilla, C. F. See Makansi, M. M., 128.
Bonner, O. D., Holland, V. F., and Smith, L. L. Osmotic and activity coeffs. of some sulfonic acids and their relationship to ion exchange equil. 1102
Bonner, O. D., and Livingston, F. L. Cation-exchange equil. involving some divalent ions 530
Boocock, G., and Pritchard, H. O. Some kinetics studies with parahydrogen 1329
Bornong, B. See Duke, F. R., 1015.
Boyars, C. See Wood, R. E., 1584.
Boyd, G. E. See Myers, G. E., 521.
Boyd, G. E., and Larson, Q. V. Report on the occurrence of Tc on the earth's crust 707
Boyle, J. S. See Orban, E., 413.

Bradley, R. S. Energetics and statistical mechanics of the kinetics of solid→solid reacns 1347
Bragg, R. H. See Brunauer, S., 112, 116.
Brewer, L. See Hultgren, N., 947.
Bril, K., Bril, S., and Krumholz, P. Kinetics of displacement reacns. involving metal complexes of ethylenediaminetetraacetic acid (II) 251
Bril, S. See Bril, K., 251.
Brody, O. V., and Fuoss, R. M. Bolaform electrolytes (V) conductance of some bisquaternary salts in MeOH and in EtOH, 156; dipping electrodes for precision conductimetry 177
Brown, C. T. See Gardner, H. J., 1458.
Brown, L. L. See Begun, G. M., 48.
Browning, L. C. See Gelernter, G., 1260.
Brunauer, S., Copeland, L. E., and Bragg, R. H. Stoichiometry of hydration of tricalcium silicate at room temp. (I) hydration in a ball mill, 112; (II) hydration in paste form 116
Brunauer, S., Kantro, D. L., and Weise, C. H. Heat of decompn. of tricalcium silicate into β-dicalcium silicate and CaO 771
Bryant, J. M. See Wendlandt, W. W., 1145.
Burkardt, L. A., and Moore, D. W. F.p. diagrams of some systems containing TNT (II) 1136
Burwasser, H., and Pease, R. N. Preliminary study of photolysis of pentaborane vapor 1589
Burwell, R. L., Jr., and Tuxworth, R. H. Isotopic exchange between D and hydrocarbons on Ni--silica catalysts 1043
Butler, J. N. See Ross, S., 1255.
Buzzell, J. G. See Tanford, C., 225.
Buzzell, J. G., and Tanford, C. Effect of charge and ionic strength on the viscosity of ribonuclease. 1204

CADY, G. H. See Barber, E. J., 504, 505.
Calderbank, P. H., and Nikolov, N. S. Urea–hydrocarbon adducts 1
Caldwell, C. S., and Babb, A. L. Diffusion in ideal binary liq. mixts. 51
Calvert, J. G. See Ritchey, W. M., 1465.
Camin, D. L., and Rossini, F. D. Phys. properties of the 17 isomeric hexenes of the API research series 1446
Campbell, D. E. See Laurene, A. H., 901.
Campbell, G. M. A detn. of thermodynamic properties of liq. 3-methylthiophene by the ultrasonic method 1147
Capps, R. H., and Jackson, W. M. D., vapor pressure and heat of vaporization of 2,2,3-trichloroheptafluorobutane 811
Carpenter, D. K. See Newman, S., 648.
Carr, C. W. See Klevens, H. B., 1245.
Cartledge, G. H. Mechanism of inhibition of corrosion by the pertechnetate ion (II) reversibility of the inhibiting mechanism, 28; (III) studies on the perrhenate ion, 32; electrode potential of the OsO$_2$–OsO$_4$ couple, 1468; passivation of Fe by Os(VIII) oxide and origin of the flade potential, 1571; see Sympson, R. F., 1037.
Casali, L. See Lacher, J. R., 608.
Casassa, E. F. Conversion of fibrinogen to fibrin (XVIII) light scattering studies of the effect of hexamethylene glycol on thermodynamic interacns. in fibrinogen solns., 926, (corrn.) 1673
Chadwell, A. J., Jr., and Smith, H. A. Studies with Raney Co catalyst 1339
Chambers, J. F., Stokes, J. M., and Stokes, R. H. Conductances of concd. aq. NaCl and KCl solns. at 25° 985
Champion, W. M. See Karasz, F. E., 376.
Chang, S.-Y., and Morawetz, H. Polymer assocn. (III) mol. aggregation and intramol. group assocn. in dil. solns. of styrene-methacrylic acid copolymers 782
Chasanov, M. G., and Lynch, C. C. Polarographic thiourea–formaldehyde kinetic studies 1151
Chepeswick, C. See Goring, D. A. I., 506.
Chessick, J. J. See Healey, F. H., 1001; Young, G. J., 394.
Chessick, J. J., Healey, F. H., and Zettlemoyer, A. C. Adsorption and heat of wetting studies of Teflon 1345
Chessick, J. J., and Zettlemoyer, A. C. Studies of the surface chemistry of silicate minerals (IV) adsorption and heat of wetting measurements of attapulgite 1181
Chipman, J. Note on the producer gas equil. and the entropy of graphite 1467
Chou, A., and Kerker, M. Refractive index of colloidal sols 562
Chu, T. L., and Weismann, T. J. Triarylboron anions (III) dissocn. const. of Na trimesitylboron in tetrahydrofuran 1020
Clark, A. See Heckelsberg, L. F., 559.
Clark, H. M. See Laurene, A. H., 901.
Clark, L. W. Decompn. of malonic acid in glycerol and in dimethyl sulfoxide, 825; decarboxylation of malonic acid in triethyl phosphate, 1150; kinetics of decompn. of malonic acid in aromatic amines, 1340; effect of picolines on malonic acid 1583
Clifton, D. G., and MacWood, G. E. Thermodynamics of the Ti chlorides (I) heat of formation of TiCl$_3$, 309; (II) heat of formation of TiCl$_2$ 311
Cohen, D., Amis, E. S., Sullivan, J. C., and Hindman, J. C. Kinetics of reacn. between Np(IV) and Np(VI) in a mixed solvent 701
Collins, F. C. See Rubin, H., (corrn.) 1671.
Collins, F. C., and Leineweber, J. P. Kinetics of homogeneous pptn. of BaSO$_4$ 389
Cook, G. L. See Haines, W. E., 549.
Cook, H. D., and Ries, H. E., Jr. Effects of spreading solvent on monolayers as detd. by pressure–area and radioactivity–area isotherms 1533
Cooper, J. A. See Linke, W. F., 1662.
Copeland, L. E. See Brunauer, S., 112, 116.
Coryell, C. D. See Tuck, D. G., 378.
Cosgrove, L. A. Porosity of anodic oxide coatings on Al—comparison of *n*-butane and krypton sorption 385
Cotton, F. A., and Harris, F. E. Thermodynamics of chelate formation (II) a Monte Carlo study of the distribution of configurations in short chains... 1451
Courtney, W. G. Nucleation of Cu metal from aq. soln. 1461
Craig, R. G., Van Voorhis, J. J., and Bartell, F. E. Free energy of immersion of compressed powders with different liqs. (I) graphite powders.. 1225
Crespi, H. L., Uphaus, R. A., and Katz, J. J. Ultracentrifugal behavior of some proteins in non-aq. solvents 1190
Crook, E. H. See Strauss, U. P., 577.

D'AGOSTINO, C., Jr. See Schufle, J. A., 1623.
Dalton, R. L. See Iler, R. K., 955.
Danforth, J. D., and Martin, D. F. Effect of alkali metal ions on activity of cracking catalysts.. 422
Daniels, F. Phys. chemistry in geochemistry 705
Darby, P. W. See Gray, T. J., 201, 209.
Dauben, C. H., Templeton, D. H., and Myers, C. E. Crystal structure of Cr$_5$Si$_3$ 443
Davies, M., and Thomas, D. K. Isopiestic studies of aq. dicarboxylic acid solns., 41; energies and entropies of assocn. for amides in benzene solns. (Part I) 763; (Part II) 767
Davis, W., Jr. See Rutledge, G. P. (corrn.), 1671.
Dawson, L. R. See Sears, P. G., 169, 1433.
DeGeiso, R. C., and Hume, D. N. Basicity of the silver bromide complex ion 255
Dekker, A. O. See Schultz, R. D., 1095.
Dell, R. M., Klemperer, D. F., and Stone, F. S. Thermal effects in chemisorption of O on Ni—a comparative investigation using powders and evaporated films 1586
De Vries, T. See Vanderkooi, W. N., 636.
Dodgen, H. W., and Ragle, J. L. Nuclear spin contribution to low temp. thermodynamic properties of I, Br and Cl 909
Doran, M. See Miller, M. L., 186.
Dorfman, L. M. Radiolysis of ethane: mol. detachment of H 826
Douglas, D. L. See Shipko, F. J., 1519.
Doull, N. J. See Bloom, H., 620.
Downing, J. H. See Edwards, R. K., 108.
Doyle, G. J. See Gucker, F. T., 989.
Drago, R. S., and Sisler, H. H. Liquid–vapor

equil. in the system NH_3–hydrazine at elevated temps. 245
Drickamer, H. G. See Tichacek, L. J., 660, 820.
Droege, J. W. See Wirth, H. E., 917.
Duffield, J. See Smith, R. N., 495.
Duke, F. R., and Bornong, B. The Fe(II)–Tl(III) reacn. at high chloride concn. 1015
Dunlop, P. J. Concn. dependence of the diffusion coeff. of raffinose in dil. aq. soln. at 25° 1464
Dunning, H. N. See Hsiao, L., 657.
Dwyer, F. P., and Sargeson, A. M. Resolution of tris-oxalato metal complexes 1331

Edwards, R. K., and Downing, J. H. Thermodynamics of the liq. solns. in the triad Cu–Ag–Au (I) the Cu–Ag system 108
Egan, E. P., Jr. Extrapolation of cooling curves in measurements of heat capacity 1344
Ehrlich, G. Interacn. of N with a W surface, 1388, (corrn.) 1673
Eigner, J. See Wolfgang, R., 1137.
Eischens, R. P., Francis, S. A., and Pliskin, W. A. Effect of surface coverage on spectra of chemisorbed CO 194
von Elbe, G. See Roth, W., 512.
Elias, L., and Schiff, H. I. A modified direct current conductance method for general application 595
Ellison, A. H., and Zisman, W. A. Surface activity at the org. liquid/air interface 416
Elmore, G. V., and Tanner, H. A. Photochem. properties of ZnO 1328
Elverum, G. W., Jr., and Mason, D. M. M. p. measurements of the system HNO_3–N_2O_4–H_2O 104
Emery, E. See Lacher, J. R., 492.
Emmett, P. H. See MacIver, D. S., 824.
Endo, R. See Takeda, M., 1202.
Epstein, J. See Rosenthal, R. W., 1596.
Epstein, M. B. See Li, K., 1400.
Epstein, M. B., Wilson, A., Gershman, J., and Ross, J. Film drainage transition temps.–salt effect 1051
Ergun, S. Kinetics of reacn. of CO_2 with C 480
Estok, G. K. Obviation of soln. d. measurements in elec. moment detns. 1336
Eyring, H. See Binford, J. S., Jr., 486; Fava, A., 890; Kato, H. P., 404.

Fava, A., and Eyring, H. Equil. and kinetics of detergent adsorption—a generalized equilibration theory 890
Ferguson, R. See Winger, A. G., 556.
Fernelius, W. C. See Bertsch, C. R., 384; Irving, R. J., 1427.
Ferraro, C. F., and Maurer, J. J. Dielec. dispersion behavior of amylopectin acetate–tricresyl phosphate systems 382
Ferroni, E., and Gabrielli, G. Detn. of the equil. const. by means of surface tension measurements 1258
Ferry, J. D. See Helders, F. E., 1536, 1575; Landel, R. F., 294; Plazek, D. J., 289; Udy, D. C., 123.
Finch, A. See Bacarella, A. L., 573.
Fineman, M. A. See Kolthoff, I. M., 1383.
Fink, R. W., and Westrum, E. F., Jr. Thermal expansion of crystalline KHF_2 800
Fisher, S., and Kunin, R. Effect of cross-linking on properties of carboxylic polymers (I) apparent dissocn. consts. of acrylic and methacrylic acid polymers 1030
Flajšman, F. See Mirnik, M., 1473.
Flanagan, T. B., and Rabinovitch, B. S. Exchange and isomn. of *trans*-ethylene-d_2 on Ni—kinetic studies, 724; exchange and isomn. of deuteroethylenes on Ni equilibration 730
Flory, P. J. See Hunt, M. L., 1278.
Flynn, J. H. A method for detg. rate equations for reacns. in which the concn. of the reactant is unknown 1332
Folman, M. See Garbatski, U., 793.
Forst, W., and Winkler, C. A. Reacn. of active N with MeCN 1424
Foss, J. Intermediate order heterogeneous catalysis and heats of adsorption 1012
Foster, K. W., and Stites, J. G., Jr. Neutron emission from actinium fluoride 1017
Fowkes, F. M. See Sawyer, W. M., 1235.
Fraioli, A. V. See Healey, F. H., 1001.
Francis, A. W. Ternary systems with 3 separate binodal curves 20
Francis, S. A. See Eischens, R. P., 194.
Francois, E. E. See Law, J. T., 353.
Franklin, J. L., and Nicholson, D. E. A kinetic study of decompn. of hydrocarbons by silica–alumina catalysts 59
Freeman, E. S. Kinetics of thermal decompn. of $NaNO_3$ and of the reacn. between $NaNO_2$ and O_2 1487
Freeman, E. S., and Gordon, S. Application of the absolute rate theory to the ignition of propagatively reacting systems—thermal ignition of the systems $LiNO_3$–Mg, $NaNO_3$–Mg 867
Freeman, M. P., and Halsey, G. D., Jr. Solid soln. Kr–Xe from 90 to 120°K., the vapor pressures of A, Kr, and Xe 1119
Freeman, R. D. Crystallographic evidence for the trihydrate of AlF_3 1152
Friedland, S. S., and Strakna, R. E. Appearance potential studies (I) 815
Friedman, H. L. See Haugen, G. R., 1363.
Frilette, V. J. Prepn. and characterization of bipolar ion-exchange membranes 435
Frisch, H. L. Turbulent coagulation of colloids, 463; gas permeation through membranes due to simultaneous diffusion and convection 1177
Fritz, J. J. Vapor pressure of HCl above non-aq. solns. 1461
Fromm, F., and Loeffler, M. C. Vapor pressure of Et *trans*-β-(2-furyl)-acrylate 252
Fuerstenau, D. W. Streaming potential studies on quartz in solns. of aminium acetates in relation to the formation of hemimicelles at the quartz–soln. interface 981
Funt, B. L., and Neparko, E. Kinetics of luminescence quenching in liq. scintillators 267
Fuoss, R. M. See Brody, O. V., 156, 177; Gross, B., 474.

Gable, R. W., and Strobel, H. A. Non-aq. ion exchange (I) some cation equil. studies in MeOH 513
Gabrielli, G. See Ferroni, E., 1258.
Garbatski, U., and Folman, M. Multilayer adsorption on plane surfaces by capacity measurements (I) adsorption on glass at high relative pressures 793
Gardner, H. J., Brown, C. T., and Janz, G. J. Prepn. of dry alkali chlorides for solutes and solvents in conductance studies 1458
Garrett, A. B. See Haseley, E. A., 1136.
Garvin, D., and Schubert, C. Vapor phase infrared spectra of ozonides of ethylene, propylene and isobutylene 807
Gayer, K. H., and Woontner, L. Soly. of $Fe(OH)_2$ and $Fe(OH)_3$ in acidic and basic media at 25° 1569
Geering, E. J. See Beringer, F. M., 141.
Gelernter, G., Browning, L. C., Harris, S. R., and Mason, C. M. Slow thermal decompn. of cellulose nitrate 1260
Gershfeld, N. L. See Strauss, U. P., 577.
Gershman, J. See Epstein, M. B., 1051.
Gibb, T. R. P., Jr. See Libowitz, G. G., 510.
Gilbert, J. W., and Lagemann, R. T. Some thermodynamic properties of liq. chloroethane 804
Gilkerson, W. R. Kinetics of reacn. of EtOH with *p*-nitrobenzoyl chloride in nitrobenzene at 7.38° 1142
Gilles, P. W., and Margrave, J. L. Heats of formation of Na_2O_2, NaO_2 and KO_2 1333
Glew, D. N. See Hildebrand, J. H., 618.
Glew, D. N., and Hildebrand, J. H. Soly. and partial molal vol. of I in perfluoro-*n*-heptane 616
Glew, D. N., and Reeves, L. W. Purif. of perfluoro-*n*-heptane and perfluoromethylcyclohexane 615
Glew, D. N., and Robertson, R. E. Spectrophotometric detn. of soly. of cumene in H_2O by a kinetic method 332
Gokcen, N. A. See Kemppinen, A. I., 126.
Goldblatt, M., and Robinson, E. S. D. of liq. DBr 1588

Goldenson, J. See Guertin, D. L., 1018; Halpern, E., 1372.

Golub, M. A. Viscosity of alfin polyisoprene at very small and quite high rates of shear 431

Good, R. J. See Ross, J. W., 1167.

Good, W. D. See Scott, D. W., 1090.

Good, W. D., Scott, D. W., and Waddington, G. Combustion calorimetry of org. F compds. by a rotating-bomb method 1080

Goodrich, R. W. See Moore, T. E., 564.

Gootman, E. A. See Moore, T. E., 564.

Gordon, A. S. See Heller, C. A., 1315; Smith, S. R., 759, 1059.

Gordon, A. S., and Knipe, R. H. Second explosion limits of CO-O_2 mixts., 1023; second explosion limits of CO-O mixts 1344

Gordon, S. See Freeman, E. S., 867.

Gorin, G. See Baelor, M. D., 1004.

Goring, D. A. I., and Chepeswick, C. Variation of sedimentation const. with field and temp. for naturally occurring polyelectrolytes 506

Goto, K. Effect of pH on polymn. of silicic acid 1007

Gover, T. A. See Lester, G. R., 1076.

Gover, T. A., and Sears, P. G. Conductances of some electrolytes in 1-propanol at 25° 330

Graham, D. Negative "net" heats of adsorption 1022

Graham, D., and Hansen, R. S. Structures of adsorbed monolayers (I) normal aliphatic alcs. and carboxylic acids adsorbed from aq. solns. on graphon 1153

Grand, J. A. See Walker, B. E., 231.

Gray, T. J., and Darby, P. W. Relationship between adsorption kinetics and the defect solid state, 201; semi-conductivity and catalysis in the NiO system 209

Graydon, W. F. See Stewart, R. J., 750.

Greenberg, S. A. Chemisorption of $Ca(OH)_2$ by silica 325

Greene-Kelly, R. Montmorillonite complexes with satd. ring compds 808

Gregor, H. P. See Lazare, L., 641.

Gregor, H. P., Hamilton, M. J., Oza, R. J., and Bernstein, F. Studies on ion exchange resins (XV) selectivity coeffs. of methacrylic acid resins toward alkali metal cations 263

Gross, B., and Fuoss, R. M. Elec. props. of solids (XIX) C black in polar and non-polar polymers 474

Grunwald, E. See Bacarella, A. L., 573.

Gucker, F. T., and Doyle, G. J. Amplitude of vibration of aerosol droplets in a sonic field 989

Guertin, D. L., Wiberley, S. E., Bauer, W. H., and Goldenson, J. Infrared spectra of three Al alkoxides 1018

HAINES, W. E., Helm, R. V., Cook, G. L., and Ball, J. S. Purification and properties of ten org. S compds.–second series 549

Hall, H. K., Jr. Potentiometric detn. of base strengths of amines in non-protolytic solvents, 63, (corrn.) 1671

Hall, W. K. See Anderson, R. B., 1548.

Halpern, E., and Goldenson, J. Infrared spectra of some reacn. products of octafluoroisobutene 1372

Halpern, J. See Armstrong, A. M., 1661; Korinek, G. J., 285; Webster, A. H., 280.

Halpern, J., MacGregor, E. R., and Peters, E. Nature of the activated intermediate in the homogeneous catalytic activation of H by cupric salts 1455

Halsey, G. D., Jr. See Freeman, M. P., 1119; Karasz, F. E., 376.

Hamill, W. H. See Nash, J. R., 823.

Hamilton, L. S. See Luder, W. F., 1470.

Hamilton, M. J. See Gregor, H. P., 263.

Hammerle, W. G. See Tinoco, I., Jr., 1619.

Hanai, T. See Koizumi, N., 1496.

Hansen, R. S. See Graham, D., 1153.

Hansen, R. S., Minturn, R. E., and Hickson, D. A. Inference of adsorption from differential double layer capacitance measurements 1185

Hanson, H. P., and Milligan, W. C. The Ni K absorption edges of oxides of Ni 1144

Harris, F. E. See Cotton, F. A., 1451.

Harris, P. M. See Tsai, K-R., 338, 345.

Harris, S. R. See Gelernter, G., 1260.

Harris, W. F., and Sweet, T. R. Stability of metal chelates of subsd. anthranilic acids 509

Harvey, M. R. See Wall, L. A., 1306.

Harwood, H. J. See Hoerr, C. W., 1265.

Haseley, E. A., Garrett, A. B., and Sisler, H. H. Heat of combustion of tri-*sec*-butylborane 1136

Hatfield, M. R., and Rathmann, G. B. Application of the absolute rate theory to adhesion 957

Haugen, G. R., and Friedman, H. L. Partition of electrolytes between aq. and org. phases (II) free energy of transfer from pure H_2O to H_2O satd. with nitromethane 1363

Head, E. L. See Huber, E. J., Jr., 1457, 1582.

Healey, F. H. See Chessick, J. J., 1345; Young, G. J., 394.

Healey, F. H., Chessick, J. J., and Fraioli, A. V. Adsorption and heat of immersion studies of Fe oxide 1001

Heckelsberg, L. F., Clark, A., and Bailey, G. C. Elec. conductivity and catalytic activity of ZnO 559

Heiks, J. R. See Orban, E., 413.

Heiks, J. R., and Orban, E. Liq. viscosities at elevated temps. and pressures: viscosity of benzene from 90° to its critical temp 1025

Helders, F. E., and Ferry, J. D. Non-Newtonian flow in concd. solns. of Na desoxyribonucleate 1536

Heller, C. A., and Gordon, A. S. Isopropyl radical reacns. (I) photolysis of diisopropyl ketone 1315

Helm, R. V. See Haines, W. E., 549.

Henderson, H. T., and Hill, G. R. A kinetic study of CH_3Cl combustion 874

Herman, R. See Moore, G. E., 813.

Hickmott, T. W., and Selwood, P. W. Proton relaxation on catalytic solids 452

Hickson, D. A. See Hansen, R. S., 1185.

Higginson, W. C. E. See Armstrong, A. M., 1661.

Higuchi, W. I. See O'Konski, C. T., 1598.

Hildebrand, J. H. See Glew, D. N., 616; Reeves, L. W., 949.

Hildebrand, J. H., and Glew, D. N. Entropy of soln. of I 618

Hill, G. R. See Henderson, H. T., 874.

Hill, K. J., and Winter, E. R. S. Thermal dissocn. pressure of $CaCO_3$ 1361

Hill, T. L. Influence of electrolyte on effective dielec. consts. in enzymes, proteins and other mols., 253; swelling of protein mols. in soln. and the α-β transformation, 358; swelling of protein mols. in solns. (II) 1593

Hillig, W. B. Nucleation frequencies for crystallization of Se glass 65

Hindin, S. G. See Weller, S. W. 1506.

Hindin, S. G., and Weller, S. W. Effect of pretreatment on activity of γ-alumina (I) ethylene hydrogenation 1591

Hindman, J. C. See Cohen, D., 701.

Hirst, R. G., King, A. J., and Kanda, F. A. The Ba–Sr eq. system 302

Hobbs, M. E. See Morin, M. G., 1594.

Hoerr, C. W., and Harwood, H. J. Soly. of tristearin in org. solvents 1265

van der Hoff, B. M. E. On the mechanism of emulsion polymn. of styrene 1250

Holland, V. F. See Bonner, O. D., 1102.

Holley, C. E., Jr. See Huber, E. J., Jr., 498, 1457, 1582.

Holmes, B. G. See Zimmerman, J. R., 1157.

Honig, J. G., and Singleterry, C. R. Phys.-chem. behavior of oil-dispersible soap solns. (II) alkali and alkaline earth phenylstearates in benzene, 1108; (III) colloid structure in dil. arylstearate-benzene systems 1114

Horst, R. W. See Rush, R. I., 1591.

Hougen, J. O. See Mannella, G., 1148.

Hovermale, R. A., and Sears, P. G. Dipolar ions in non-aq. solvents (I) dielec. increments as supporting evidence for dipolar structure of sulfamic acid 1579

Hoyer, H. W. H^+ coulometer 372

Hsiao, L., Dunning, H. N., and Lorenz, P. B. Crit. micelle concns. of polyoxyethylated nonionic detergents 657

Hu, J-H., and MacWood, G. E. Soly. of H in diborane 1483

Huber, E. J., Jr., Head, E. L., and Holley, C. E., Jr. Heats of combustion of Dy and Yb, 1457; heat of combustion of Er 1582

Huber, E. J., Jr., and Holley, C. E., Jr. Heat of combustion of Ca 498

Huggins, C. M., and Pimentel, G. C. Systematics of infrared spectral properties of H bonding systems: frequency shift, half width and intensity 1615

Huggins, C. M., Pimentel, G. C., and Shoolery, J. N. Proton magnetic resonance studies of the H bonding of phenol, subsd. phenols and AcOH 1311

Hultgren, N., and Brewer, L. Gaseous Mo oxychloride 947

Hume, D. N. See DeGeiso, R. C., 255; Leonard, G. W., 1493.

Hunt, H. See Marshall, P., 121, 732,

Hunt, M. L., Newman, S., Scheraga, H. A., and Flory, P. J. Dimensions and hydrodynamic properties of cellulose trinitrate mols. in dil solns 1278

Husney, R. M. See Pontius, R. B., 9.

Hutchinson, E., and Winslow, L. Heats of micelle formation 122

ILER, R. K., and Dalton, R. L. Degree of hydration of particles of colloidal silica in aq. soln 955

Imperante, J. See Sheppard, E., 584.

Ingraham, L. L. See Westheimer, F. H., 1668.

Innes, K. K. Temp. dependence of viscosity of liqs 817

Irvine, J. W., Jr. See Tuck, D. G., 378.

Irving, R. J., and Fernelius, W. C. Formation consts. of some metal derivs.: *S*-alkyl carboxylic acids 1427

JACKSON, W. M. Viscosities of the binary gas mixts., CH_4-CO_2 and ethylene-A, 789; see Capps, R. H., 811.

Jacobson, H. W. See Smith, G. W., 1008.

Jamieson, J. W. S., and Winkler, C. A. Reacns. of ethylenimine and N-methylethylenimine with at. H and their relation to complexes in active N reacns 1542

Janz, G. J. See Gardner, H. J., 1458; Jarvie, J. M. S., 1430.

Jarry, R. L. See Rutledge, G. P., (corrn.) 1671.

Jarry, R. L., and Miller, H. C. Liq. density, vapor pressure and crit. temp. and pressure of NF_3 1412

Jarvie, J. M. S., and Janz, G. J. Kinetic study of the trifluoroacetonitrile-butadiene cyclization 1430

Jasper, J. J., and Wood, T. D. Surface pressure of soluble benzoic acid films at H_2O-halobenzene interfaces 1625

John, H. F., and Bent, H. E. Sepn. of org. solns. by thermal diffusion 1524

Johnson, P. A., and Babb, A. L. Self-diffusion in liqs. (I) concn. dependence in ideal and non-ideal binary solns. 14, (corrn.) 1671

Jolly, W. L. Thermodynamic properties of chloramine, dichloramine and NCl_3 507

Jones, L. V. See Orban, E., 413.

KAKIHANA, H., Maruichi, N., and Yamasaki, K. Ion exchange in concd. solns., NaCl-HCl and LiCl-HCl systems 36

Kanda, F. A. See Hirst, R. G., 302.

Kaneko, T. M., and Wadsworth, M. E. Catalytic redn. of Co from ammoniacal $CoSO_4$ solns 457

Kantro, D. L. See Brunauer, S., 771.

Kaplan, M. L. See Pontius, R. B., 9.

Karasz, F. E., Champion, W. M., and Halsey, G. D., Jr. Growth of ice layers on surfaces of anatase and AgI 376

Karl-kroupa, E. See Langguth, R. P., 1335.

Kato, H. P., Zwolinski, B. J., and Eyring, H. Na transport in isolated frog skin 404

Katz, J. J. See Crespi, H. L., 1190.

Katz, M. J. Some adsorption data on acetylene black 1338

Kay, R. L. See Shedlovsky, T., 151.

Keenan, A. G. Cryoscopic heat of fusion of ammonium nitrate 1356

Kemppinen, A. I., and Gokcen, N. A. D. of dibutyl phthalate 126

Kerker, M. See Chou, A., 562.

Kianpour, A. See Lacher, J. R., 1454.

King, A. J. See Hirst, R. G., 302.

King, C. V., and Levy, B. Exchange between adsorbed and dissolved sulfate ions 374

King, E. G. Heat capacities at low temps. and entropies of five spinel minerals 410

King, E. L. Unusual kinetic consequences of certain enzyme catalysis mechanisms 1378

King, E. L., and Altman, C. A schematic method of deriving the rate laws for enzyme-catalyzed reacns 1375

Kingery, W. D. See Kurkjian, C. R., 961.

Klemperer, D. F. See Dell, R. M., 1586.

Kleppa, O. J. Thermodynamic properties of the moderately dil. liq. solns. of Cu, Ag and Au in Tl, Pb and Bi, 446; calorimetric investigation of some binary and ternary liq. alloys rich in Sn, 842; heat of formation of solid and liq. alloys in the systems Ag-Cd, Ag-In and Ag-Sb at 450°, 846; heat of formation of solid and liq. binary alloys of Cu with Cd, In, Sn and Sb at 450°, 852; heat of formation of some solid and liq. binary alloys of Au with Cd, In, Sn and Sb 858

Klevens, H. B., and Carr, C. W. Equil. dialysis of soap and detergent solns 1245

Kmak, W. S. See Tichacek L. J., 660.

Knipe, R. H. See Gordon, A. S., 1023, 1344.

Knox, J. H., and Trotman-Dickenson, A. F. Reacns. of Cl atoms—a test of the transition state theory 1367

Koizumi, N., and Hanai, T. Dielec. properties of lower membered polyethylene glycols at low frequencies 1496

Kolthoff, I. M. See Reynolds, W. L., 969, 996.

Kolthoff, I. M., and Fineman, M. A. Kinetics of the reacn. between chromate and As_2O_3 in alkaline medium—induced redn. of O by this couple 1383

Kolthoff, I. M., and Shams El Din, A. M. Redn. of hexavalent Cr at the rotated Pt electrode-permeability of the film formed 1564

Korinek, G. J., and Halpern, J. Kinetics of reacn. of mol. H with mercuric and mercurous perchlorates in aq. soln 285

Korst, W. L. See Warf, J. C., 1590.

Kosiba, W. L. See Wirth, H. E., 923.

Kottle, S., and Morgan, L. O. Interacn. of Cr(VI) anions with Cr metal surfaces 738

Kraus, C. A. The ion-pair concept: its evolution and some applications 129

Krieve, W. F., and Mason, D. M. Soly. of Cl in $TiCl_4$ and of CO_2 and O_2 in Cl 374

Krigbaum, W. R. See Newman, S., 648.

Krogh-Moe, J. See Schmidt, P. W., 1580.

Kronman, M. J., Stern, M. D., and Timasheff, S. N. On the aggregation of bovine serum albumin in acid *p*H 829

Krumholz, P. Studies on the coördinate bond (IV) mechanism of formation and of dissocn. of the tris-(2,2′-dipyridyl)-Fe(II) complex, 87; see Bril, K., 251.

Kubokawa, Y., and Toyama, O. Elec. conductivity change caused by the chemisorption of H on ZnO, ZnO-Cr_2O_3 and ZnO-MoO_3 833

Kummer, J. T. Catalytic oxidn. of ethylene to ethylene oxide over single crystals of Ag 666

Kunin, R. See Fisher, S., 1030; Winger, A. G., 556.

Kuntz, I. See Beringer, F. M., 141.

Kurkjian, C. R., and Kingery, W. D. Surface tension at elevated temps. (III) effect of Cr, In, Sn and Ti on liq. Ni surface tension and interfacial energy with Al_2O_3 961

Kwan, T. Power rate law in heterogeneous catalysis, 1033; see Benson, J. E., 1601.

LACHER, J. R., Casali, L., and Park, J. D. Reacn. heats of org. halogen compds. (V) vapor phase bromination of tetrafluoroethylene and trifluorochloroethylene 608

Lacher, J. R., Emery, E., Bohmfalk, E., and Park, J. D. Reacn. heats of org. compds. (IV) a high

temp. calorimeter and the hydrogenation of Me, Et and vinyl chlorides........ 492
Lacher, J. R., Kianpour, A., and Park, J. D. Reacn. heats of org. halogen compds. (VI) catalytic hydrogenation of some alkyl fluorides....... 1454
Lad, R. A. See Metz, F. I., 277.
Lagemann, R. T. See Gilbert, J. W., 804.
LaMer, V. K. See Rosano, H. L., 348.
Landel, R. F., and Ferry, J. D. Dynamic mechanical properties of the system cellulose tributyrate–dimethyl phthalate........ 294
Lange, K. R. See Beachell, H. C., 307.
Langguth, R. P., Osterheld, R. K., and Karl-kroupa, E. Verification by chromatography of the thermal formation of V and Pb tetrapolyphosphates........ 1335
Lapidus, L. See Bastian, W. C., 816.
Larach, S., McCarroll, W. H., and Shrader, R. E. Luminescence properties of Zn–inter-chalcogenides (I) Zn sulfo-telluride phosphors........ 604
Larach, S., and Turkevich, J. Magnetic properties of ZnS phosphors with Mn activator........ 1598
Larson, Q. V. See Boyd, G. E., 707.
Lasater, J. A. See Zimmerman, J. R., 1157.
Lassettre, E. N. See Tsai, K-R., 338, 345.
Laurene, A. H., Campbell, D. E., Wiberley, S. E., and Clark, H. M. Extraction of $FeCl_3$ by isopropyl ether (Part I) significance of H_2O in the extracted Fe complex........ 901
Law, J. T., and Francois, E. E. Adsorption of gases on a Si surface........ 353
Lawton, E. J. See Miller, A. A., 599, (corrn.) 1673.
Lazare, L., Sundheim, B. R., and Gregor, H. P. A model for cross-linked polyelectrolytes........ 641
Lecky, J. A. See Anderson, R. B., 1548.
Leftin, H. P. See Lichtin, N. N., 160, 164.
Leineweber, J. P. See Collins, F. C., 389.
Leonard, G. W., Smith, M. E., and Hume, D. N. Thiocyanate complexes of Pb and Tl in soln........ 1493
Lesnini, D. See Smith, R. N., 1063.
Lester, G. R. See Sears, P. G., 1433.
Lester, G. R., Gover, T. A., and Sears, P. G. A study of conductances of some uni-univalent electrolytes in N,N-dimethylacetamide at 25°........ 1076
Leung, Y. C., and Waser, J. Crystal structure of phosphorus diiodide, P_2I_4........ 539
Levy, B. See King, C. V., 374.
Lewis, B. See Roth, W., 512.
Lewis, D. R. Thermoluminescence of dolomite and calcite........ 698
Li, J. C. M., and Pitzer, K. S. Energy levels and thermodynamic functions for mols. with internal rotation (IV) extended tables for mols. with small moments of inertia........ 466
Li, K., Arnett, R. L., Epstein, M. B., Ries, R. B., Bitler, P. L., Lynch, J. M., and Rossini, F. D. Correlation of phys. properties of normal alkyl series of compds........ 1400
Libowitz, G. G., and Gibb, T. R. P., Jr. Ionic character of transition metal hydrides........ 510
Lichtin, N. N., and Leftin, H. P. Ionization and dissocn. equil. in liq. SO_2 (III) dissocn. of spherical ions, 160; (IV) alkyl and aryl derivs. of triphenylchloromethane at 0 and −8.9°........ 164
Lindenbaum, A., and Schubert, J. Binding of org. anions by serum albumin........ 1663
Linke, W. F. $FeCl_3$-$10H_2O$; the systems $FeCl_3$–H_2O and $FeCl_3$–HCl–H_2O below 0°........ 91
Linke, W. F., and Cooper, J. A. System Na_2SO_4–Na_2MoO_4–H_2O at 35 and 100°........ 1662
Livingston, F. L. See Bonner, O. D., 530.
Loeb, G. I., and Scheraga, H. A. Hydrodynamic and thermodynamic properties of bovine serum albumin at low *p*H........ 1633
Loeffler, M. C. See Fromm, F., 252.
Logan, R. A. See Thurmond, C. D., 591.
Long, F. A. See Bergen, R. L., Jr., 1131.
Lorenz, P. B. See Hsiao, L., 657.
Low, M. J. D. See Sarmousakis, J. N., 1139.
Luder, W. F., and Hamilton, L. S. Acids and bases (X) conductances of $SbBr_3$ and $SnCl_2$ in dimethylformamide on addn. of piperidine........ 1470
Ludlum, D. B. Micelle formation in solns. of some isomeric detergents........ 1240
Lundberg, J. L. See Zimm, B. H., 425.
Lynch, C. C. See Chasanov, M. G., 1151.
Lynch, J. M. See Li, K., 1400.
Lyons, P. A. See Tinoco, I., Jr., 1342.
MACGREGOR, E. R. See Halpern, J., 1455.
MacIver, D. S., and Emmett, P. H. Adsorption of N on pure NaCl........ 824
MacKay, J. R. See Rush, R. I., 1591.
MacWood, G. E. See Clifton, D. G., 309, 311; Hu, J.-H., 1483; Sanderson, B. S., 314, 316.
Madsen, M. See Makansi, M. M., 128.
Magne, F. C. See Mod, R. R., 1651.
Magnuson, J. A., and Wolfenden, J. H. HI_3........ 1665
Makansi, M. M., Madsen, M., Selke, W. A., and Bonilla, C. F. Vapor pressure of K........ 128
Mannella, G., and Hougen, J. O. "β-Tungsten" as a product of oxide redn........ 1148
Manson, J. E. Effect of I vapor on AgI........ 806
Margrave, J. L. Gaseous mols. of geochem. significance, 715; see Bartos, H. R., 256; Gilles, P. W., 1333; Neugebauer, C. A., 1318; Sime, R. J., 810; Sthapitanonda, P., 1628.
Markovitz, H. See Helders, F. E., 1575.
Markowitz, M. M. See Osterheld, R. K., 863.
Marshall, P. R., and Hunt, H. Liq. NH_3 as a solvent (XI) conductivity of metal-NH_3 solns., 121; (XII) an investigation of metal–NH_3 systems by means of their vapor pressures........ 732
Martell, A. E. See Ueno, K., 934, 1270.
Martin, D. F. See Danforth, J. D., 422.
Martin, R. B., and Tashdjian, M. O. Polarographic redn. of N-nitrosamines........ 1028
Maruichi, N. See Kakihana, H., 36.
Maslan, F. D., and Stoddart, E. A., Jr. Acetonitrile–H_2O liquid–vapor equil........ 1146
Mason, C. M. See Gelernter, G., 1260.
Mason, D. M. See Elverum, G. W., Jr., 104; Krieve, W. F., 374.
Mason, D. M., and Vango, S. P. Measurement of optical absorbancy of $TiCl_4$(g) in the ultraviolet region........ 622
Maurer, J. J. See Ferraro, C. F., 382.
Mausner, M. See Beringer, F. M., 141.
McAtee, J. L. See Milligan, W. O., 273.
McCarroll, W. H. See Larach, S., 604.
McCormack, J. B., Walkup, J. H., and Rush, R. I. B.p.–compn. diagram for the system 1,4-dioxane–*n*-BuOH........ 826
McCoy, R. E. See Bauer, S. H., 1529.
McDaniel, D. H., and Smoot, C. R. Approximations in the kinetics of consecutive reacns........ 966
McGarvey, B. R. Paramagnetic resonance in Cu chelates........ 71
McLaughlin, E. P., and Scott, R. L. Soly. of I and phenanthrene in hydrofluorocarbons........ 674
Mellors, G. W. See Bockris, J. O'M., 1321.
Merriam, C. N., Jr. See Thomas, H. C., 249.
Metz, F. I., and Lad, R. A. Effect of substrate on crystallization of metallic films........ 277
Metzner, B. M. Infrared absorption cell for study of heterogeneous reacns........ 1670
Miller, A. A., Lawton, E. J., and Balwit, J. S. Radiation chemistry of hydrocarbon polymers: polyethylene, polymethylene and octacosane, 599, (corrn.)........ 1673
Miller, D. G. An anal. proof that the extremum of the thermodynamic probability is a maximum, 536; on the Stokes–Robinson hydration model for solns........ 1296
Miller, H. C. See Jarry, R. L., 1412.
Miller, M. L. Concd. salt solns. (III) elec. conductance of solns. of NaSCN, NaI and $NaClO_4$........ 189
Miller, M. L., and Doran, M. Concd. salt solns. (II) viscosity and d. of NaSCN, $NaClO_4$ and NaI........ 186
Miller, M. L., and Sheridan, C. L. Concd. salt solns. (I) activity coeffs. of NaSCN, NaI and $NaClO_4$........ 184
Miller, R. C., and Smyth, C. P. Microwave absorption and mol. structure in liqs. (XVI) dipole direction and relaxation time in pyridine, trioxane and their sym. trimethyl derivs........ 1354
Miller, R. R. See Walker, B. E., 231.

Milligan, W. O. See Hanson, H. P., 1144; Richardson, J. T., 1223.
Milligan, W. O., and McAtee, J. L. Crystal structure of γ-AlOOH and γ-ScOOH 273
Mills, A. P., and Becker, W. E. Si–Br and Si–C (aryl) bond parachors and the Si–Br bond refrac. 1644
Minturn, R. E. See Hansen, R. S., 1185.
Mirnik, M., Flajšman, Schulz, K. F., and Težak, B. Negative activity limit of stability and coagulation values of Ag halides 1473
Mitzner, B. M. Infrared absorption cell for study of heterogeneous reactions 1670
Mod, R. R., Magne, F. C., and Skau, E. L. Binary f.p. diagrams for palmitic acid with a series of subsd. 2-aminopyridines 1651
Mod, R. R., and Skau, E. L. Binary f.p. diagrams for 2-aminopyridine with satd. and unsatd. long chain fatty acids 963
Monger, J. M., and Redlich, O. Peroxysulfuric acid and peroxyformic acid—equil. and formation rate 797
Mooi, J. See Smith, R. N., 495, 1063.
Moon, K. A. Pressure–compn.–temp. relations in the Pd–H system 502
Moore, D. W. See Burkardt, L. A., 1136.
Moore, G. E., Shuler, K. E., Silverman, S., and Herman, R. Reacns. of NH_3 and hydrazine with O atoms and H atoms in atomic flames 813
Moore, T. E., Goodrich, R. W., Gootman, E. A., Slezak, B. S., and Yates, P. C. Extraction of inorg. salts by 2-octanol (II) Co(II) and Ni(II) chlorides and bromides—effect of electrolytes 564
Moran, H. E., Jr. System LiCl–H_2O 1666
Morawetz, H. See Chang, S.-Y., 782.
Morawetz, H., and Zimmering, P. E. Reacn. rates of polyelectrolyte derivs. (I) solvolysis of acrylic acid–nitrophenyl methacrylate copolymers (corrn.) 1671
Morey, G. W. Exptl. geology 718
Morgan, L. O. See Kottle, S., 739.
Morin, M. G., Paulett, G., and Hobbs, M. E. Nuclear magnetic resonance chem. shift detns. by means of a concentric cylinder sample cell 1594
Morrow, J. C. X-Ray powder pattern and unit cell dimensions of K_2ReI_6 19
Mukherjee, L. M. Standard potential of the Ag–Ag halide electrodes in EtOH and the free energy change in the transfer of HCl, HBr and HI from EtOH to H_2O, 974; on the detn. of the autoprotolysis const. of EtOH 1019
Muschlitz, E. E., Jr., and Bailey, T. L. Negative ion formation in H_2O_2 and H_2O vapor—perhydroxide ion 681
Myers, C. E. See Dauben, C. H., 443.
Myers, G. E., and Boyd, G. E. A thermodynamic calcn. of cation exchange selectivities 521

NARSIMHAN, G. On the eq. of motion of a spherical particle in a centrifugal field 1476
Nash, J. R., Hamill, W. H., and Williams, R. R., Jr. Diffusion–recombination in decompn. of acetyl peroxide 823
Neale, S. M., and Williamson, G. R. Cellulose–H_2O–salt system 741
Neparko, E. See Funt, B. L., 267.
Neu, J. T. Infrared spectrographic studies of preflame reacns. of *n*-butane, 320, (corrn.) 1673
Neugebauer, C. A., and Margrave, J. L. Heats of formation of tetrafluoroethylene, tetrafluoromethane and 1,1-difluoroethylene 1318
Newman, S. See Hunt, M. L., 1278.
Newman, S., Krigbaum, W. R., and Carpenter, D. K. Reversible assocn. of cellulose nitrate in EtOH 648
Newton, T. W., and Baker, F. B. Reacn. between Pu(III) and O in aq. sulfate solns. 1417
Nicholson, D. E. See Franklin, J. L., 59.
Nikolov, N. S. See Calderbank, P. H., 1.
Nixon, A. C., and Smith, R. E. Phase relations in the system $CaBr_2$, CaO and H_2O 1422
Nixon, E. R. Infrared spectrum of biphosphine 1054
Nowotny, H., Searcy, A. W., and Orr, J. E. Structures of some germanides of formula M_5Ge_3 677

OGARD, A. E., and Rabideau, S. W. Kinetics of reacn. between Pu^{+3} and PuO_2^{+2} 812
Ogg, R. A., Jr. See Ray, J. D., 1460, 1599.
Oiwa, I. T. Activity coeffs. of HCl in MeOH–H_2O mixts. 754
O'Konski, C. T., and Higuchi, W. I. Kinetics of nucleation in turbulent jets 1598
Orban, E. See Heiks, J. R., 1025.
Orban, E., Barnett, M. K., Boyle, J. S., Heiks, J. R., and Jones, L. V. Phys. properties of aq. uranyl sulfate solns. from 20 to 90° 413
Orr, J. E. See Nowotny, H., 677.
Osterheld, R. K. See Langguth, R. P., 1335.
Osterheld, R. K., and Markowitz, M. M. Polymn. and depolymn. phenomena in phosphate-metaphosphate systems at higher temps. (IV) condensation reacns. of alkali metal H phosphates 863
Oza, R. J. See Gregor, H. P., 263.
Oza, T. M., and Oza, V. T. Decompn. of hyponitrites of Ca and Sr 192
Oza, V. T. See Oza, T. M., 192.

PACE, E. L. See Siebert, A. R., 828.
Palko, A. A. See Begun, G. M., 48.
Palmer, E. D. See Wirth, H. E., 911, 914.
Park, J. D. See Lacher, J. R., 492, 608, 1454.
Parry, H. L. See Bondi, A., 1406.
Paulett, G. See Morin, M. G., 1594.
Pease, R. N. See Burwasser, H., 1589.
Peters, E. See Halpern, J., 1455.
Peterson, L. E. See Reyerson, L. H., 1172.
Phillips, L. R. See Schreyer, J. M., 588.
Pierotti, R. A. See Smith, R. N., 495.
Pilpel, N. Viscoelasticity in aq. soap solns. 779
Pimentel, G. C. See Huggins, C. M., 1311, 1615.
Pitzer, K. S. See Li, J. C. M., 466.
Pitzer, K. S., and Polissar, J. Order–disorder problem for ice 1140
Plazek, D. J., and Ferry, J. D. Viscosities and dynamic mechanical properties of the system cellulose trinitrate–isophorone 289
Pliskin, W. A. See Eischens, R. P., 194.
Polestak, W. J., and Zimmerman, H. K., Jr. Ultraviolet absorption study of protolysis consts. of some *p*-subsd. phenylphosphonic acids in H_2O 787
Polissar, J. See Pitzer, K. S., 1140.
Polley, M. H. See Smith, W. R., 689.
Pontius, R. B., Kaplan, M. L., and Husney, R. M. Effect of buffer and electrolyte on diffusion of an acid dye in gelatin 9
Potter, A. E., Jr., and Berlad, A. L. Quenching of flames of propane–O–A and propane–O_2–He mixts. 97
Pritchard, H. O. See Boocock, G., 1329.
Proper, R. See Rosenthal, R. W., 1596.
Pundsack, F. L. Properties of asbestos (II) d. and structure of chrysotile 361
Pundsack, F. L., and Reimschussel, G. Properties of asbestos (III) basicity of chrysotile suspensions 1218

RAATS, E. See Walker, P. L., Jr., 364, 370.
Rabideau, S. W. See Ogard, A. E., 812.
Rabinovitch, B. S. See Flanagan, T. B., 724, 730.
Rabinovitch, B. See Yudelson, J., 1512.
Ragle, J. L. See Dodgen, H. W., 909.
Ramsey, W. J. See Zalkin, A., 234, 1275.
Rathmann, G. B. See Hatfield, M. R., 957.
Rautenberg, T. H. See Roth, W., 379.
Ray, B. R., and Augenstine, L. G. Trypsin monolayers at the H_2O–air interface (I) film characteristics and the recovery of enzymatic activity 1193
Ray, J. D., and Ogg, R. A., Jr. Heat of formation of nitramide, 1460; anomalous entropy of KNO_2 1599
Redlich, O. See Monger, J. M., 797.
Reed, S. F. See Wiley, R. H., 533.
Reeves, L. W. See Glew, D. N., 615.
Reeves, L. W., and Hildebrand, J. H. Entropy of soln. of Br in perfluoro-*n*-heptane 949
Reich, I. Factors responsible for stability of detergent micelles 257
Reichmann, M. E. A preliminary light scattering study of enzymatic degradation of desoxyribose nucleic acid 831

Reimschussel, G. See Pundsack, F. L., 1218.
Reyerson, L. H., and Peterson, L. E. Sorption of gases by solid polymers (I) sorption of NH_3 by nylon (II) sorption of HCl by nylon 1172
Reynolds, W. L., and Kolthoff, I. M. Reacn. between aquo ferrous Fe and cumene hydroperoxide, 969; reacns. of ferrous versenate and ferrous pyrophosphate with cumene hydroperoxide 996
Rhodes, D. C. See Bloom, H., 791.
Richardson, J. T., and Milligan, W. O. Magnetic susceptibility studies in the system NiO–Al_2O_3.... 1223
Richman, D., and Thomas, H. C. Self-diffusion of Na^+ in a cation-exchange resin 237
Rieman, W., III. See Sargent, R., 1370.
Ries, H. E., Jr. See Cook, H. D., 1533.
Ries, R. B. See Li, K., 1400.
Riese, H. C. A. See Bello, J., 1299.
Ritchey, W. M., and Calvert, J. G. Photosensitized oxidn. of CO on Cu_2O 1465
Robertson, R. E. See Glew, D. N., 332.
Robinson, E. S. See Goldblatt, M., 1588.
Robinson, R. A. Note on osmotic coeffs. of aq. KCl solns. at 25° 501
Rogers, M. T. Elec. moments of some derivs. of pyridine and quinoline 125
Rogers, M. T., and Speirs, J. L. BrF_5—freezing and boiling points, heat of vaporization and vapor pressure–temp. relations 1462
Romo, L. A. Exchange of H by D in hydroxyls of kaolinite, 987; phase equil. in the system NiO–H_2O 1021
Rosano, H. L., and LaMer, V. K. Rate of evaporation of H_2O through monolayers of esters, acids and alcs 348
Rosen, J. S. Vols. of solute in soln 7
Rosenthal, R. W., Proper, R., and Epstein, J. Distribution of some phosphonofluoridates between org. solvents and H_2O 1596
Ross, J. See Epstein, M. B., 1051.
Ross, J. W., and Good, R. J. Adsorption and surface diffusion of *n*-butane on spheron 6 (2700°) C black 1167
Ross, S., and Butler, J. N. Inhibition of foaming (VII) effects of antifoaming agents on surface-plastic solns 1255
Rossini, F. D. See Camin, D. L., 1446; Li, K., 1400.
Roth, W., and Bauer, W. H. Explosive oxidn. of diborane 639
Roth, W., von Elbe, G., and Lewis, B. Second explosion limits of CO–O_2 mixts 512
Roth, W., and Rautenberg, T. H. Kinetics of the CS_2–NO reacn. and the mechanism of light emission in the explosive reacn 379
Rowland, F. S. See Wolfgang, R., 1137.
Rubin, H., and Collins, F. C. Concn. overpotential at reversible electrodes, (corrn.) 1671
Ruch, R. J. See Bartell, L. S., 1231.
Rundle, R. E. Me compds. of the elements 1659
Russell, E. R. See Shereshefsky, J. L., 1164.
Rush, R. I. See McCormack, J. B., 826.
Rush, R. I., Ames, D. C., Horst, R. W., and McKay, J. R. Some properties of the systems dioxane–Bu alcs 1591
Rust, P. M. See Whittaker, A. G., 904.
Rutledge, G. P., Jarry, R. L., and Davis, W., Jr. F.p. diagram and liquid–liquid solys. of system UF_6-HF (corrn.) 1671
Ryan, J. P. See Shepard, J. W., 127.
Rydberg, E. See Assarsson, G. O., 397.

SALDICK, J. Concn. effects on solvent extraction coeffs. of some trivalent metal halides 500
Salmon, O. N., and Ahmann, D. H. Li–Na liq. metal system 13
Sanderson, B. S., and MacWood, G. E. Thermodynamics of the Ti chlorides (III) sublimation pressure of $TiCl_3$, 314; (IV) disproportionation of Ti trichlorides 316
Sandus, O. See Wood, S. E., 801.
Sargent, R., and Rieman, W., III. Application of the plate theory to anion-exchange chromatography of glycols 1370
Sargeson, A. M. See Dwyer, F. P., 1331.
Sarmousakis, J. N., and Low, M. J. D. Activity coeffs. of benzoic acid in some aq. salt solns 1139
Sawyer, W. M., and Fowkes, F. M. Monolayers in equil. with lenses of oil on H_2O (I) octadecanol and tetradecanoic acid in white oil 1235
Scheraga, H. A. See Hunt, M. L., 1278; Loeb, G. I., 1633; Wagner, M. L., 1066.
Schiff, H. I. See Elias, L., 595.
Schilt, A. A., and Smith, G. F. Acid dissocn. consts. of subsd. 1,10-phenanthrolines 1546
Schmidt, P. W., Krogh-Moe, J., and Bale, H. D. Small angle X-ray scattering by $Al(OH)_3$ gel 1580
Schreyer, J. M., and Phillips, L. R. Soly. of U(IV) orthophosphates in $HClO_4$ solns 588
Schubert, C. See Garvin, D., 807.
Schubert, J. See Lindenbaum, A., 1663.
Schufle, J. A., and D'Agostino, C., Jr. Stability of Tl(I) citrate complex 1623
Schuler, R. H. Effect of I on radiolysis of benzene. 381
Schultz, R. D., and Dekker, A. O. Effect of phys. sorption on the absolute decompn. rates of crystalline NH_4Cl and $CuSO_4{\cdot}3H_2O$ 1095
Schulz, K. F. See Mirnik, M., 1473.
Scott, D. W. See Good, W. D., 1080.
Scott, D. W., Good, W. D., and Waddington, G. Tetraethyllead: heat of formation by rotating-bomb calorimetry 1090
Scott, J. M. See Bennett, R. L., 1585.
Scott, R. L. See McLaughlin, E. P., 674; Thorp, N., 670, 1441.
Searcy, A. W. See Nowotny, H., 677.
Sears, P. G. See Gover, T. A., 330; Hovermale, R. A., 1579; Lester, G. R., 1076.
Sears, P. G., Lester, G. R., and Dawson, L. R. A study of conductance behavior of some uni-univalent electrolytes in dimethyl sulfoxide at 25° 1433
Sears, P. G., Wilhoit, E. D., and Dawson, L. R. Conductances of K thiocyanate and tetra-*n*-butylammonium iodide in acetone at several temps. within the range 25 to −50° 169
Selke, W. A. See Makansi, M. M., 128.
Selwood, P. W. See Hickmott, T. W., 452.
Shams El Din, A. M. See Kolthoff, I. M., 1564.
Shedlovsky, T., and Kay, R. L. Ionization const. of AcOH in H_2O–MeOH mixts. at 25° from conductance measurements 151
Shepard, J. W., and Ryan, J. P. Use of C-14 labeled perfluorooctanoic acid in study of adhesion and other surface phenomena 127
Sheppard, E., Imperante, J., and Wright, I. S. Action of heparin on polymn. of fibrinogen 584
Shereshefsky, J. L., and Russell, E. R. Activated adsorption of O on glass 1164
Shereshefsky, J. L., and Weir, C. E. Adsorption of gases and vapors on glass spheres (II) two-dimensional condensations of O 1162
Sheridan, C. L. See Miller, M. L., 184.
Shiio, H., and Yoshihashi, H. Measurement of the amount of bound H_2O by ultrasonic interferometer (II) polyvinyl alc. and its partially subsd. acetates 1049
Shinoda, K. Crit. micelle concns. in aq. solns. of K alkane tricarboxylates 1439
Shipko, F. J., and Douglas, D. L. Stability of $Fe(OH)_2$ ppts 1519
Shoolery, J. N. See Huggins, C. M., 1311.
Shrader, R. E. See Larach, S., 604.
Shukla, R. P., and Bhatnagar, R. P. Note on viscosity of mixts. (II) liquid–liquid ternary mixts... 809
Shuler, K. E. See Moore, G. E., 813.
Siebert, A. R., and Pace, E. L. Heat capacities of multimol. layers of NF_3 adsorbed on anatase 828
Siegel, R. H. See Slabaugh, W. H., 1105.
Silverman, S. See Moore, G. E., 813.
Sime, R. J., and Margrave, J. L. Gaseous metal nitrides (II) vapor pressure of GaN(s) and evidence for a complex gaseous nitride 810
Simpson, D. W. See Asher, D. R., 518.
Singleterry, C. R. See Honig, J. G., 1108, 1114.
Singleton, J. H. H sorption and the parahydrogen conversion on evaporated Ni films 1606
Sisler, H. H. See Drago, R. S., 245; Haseley, E. A., 1136.

Skau, E. L. See Mod, R. R., 963, 1651.
Slabaugh, W. H., and Siegel, R. H. Sorption of NH_3 by homoionic bentonites 1105
Slezak, B. S. See Moore, T. E., 564.
Smyth, C. P. See Miller, R. C., 1354.
Smith, G. F. See Schilt, A. A., 1546.
Smith, G. W., and Jacobson, H. W. Characteristics of adsorption of complex metal-ammines and other complex ions of Zn, Cu, Co, Ni and Ag on silica gel 1008
Smith, H. A. See Chadwell, A. J., Jr., 1339.
Smith, L. L. See Bonner, O. D., 1102.
Smith, M. E. See Leonard, G. W., 1493.
Smith, P. Estimate of the size and shape of the O_3^- ion 1471
Smith, R. E. See Nixon, A. C., 1422.
Smith, R. M., and Alberty, R. A. Apparent stability consts. of ionic complexes of various adenosine phosphates with monovalent cations 180
Smith, R. N., Duffield, J., Pierotti, R. A., and Mooi, J. C-O and C-H surface complexes 495
Smith, R. N., Lesnini, D., and Mooi, J. Anomalous adsorptive properties of NO 1063
Smith, R. P. Relationship of force const. and bond length 1293
Smith, S. R., and Gordon, A. S. Studies of diffusion flames (I) CH_4 diffusion flame, 759; (II) diffusion flames of some simple alcs 1059
Smith, W. R., and Polley, M. H. Oxidn. of graphitized C black 689
Smoot, C. R. See McDaniel, D. H., 966.
Sommer, E. C. See Alexander, L. E., 1646.
Sone, K. See Yasuda, M., 1667.
Spalaris, C. N. Micropore structure of artificial graphite 1480
Speirs, J. L. See Rogers, M. T., 1462.
Spernol, A. Correction of Stokes' laws of friction for particles of mol. size 703
Spiro, M. Transference nos. of HIO_3 and the limiting mobility of the iodate ion in aq. soln. at 25°, 976, (corrn.) 1673
Stahmann, M. A. See Van Kley, H., 1200.
Stamm, A. J. Diffusion of H_2O into uncoated cellophane (I) from rates of H_2O vapor adsorption, and liq. H_2O absorption, 76, (corrn.) 1671; (II) from steady-state diffusion measurements 83, (corrn.) 1671
Stein, K. C. See Anderson, R. B., 1548.
Stern, K. H. Electrode potentials in fused systems (II) a study of the AgCl-KCl system, 679; (III) Pt electrode in some halide melts 1443
Stern, M. D. See Kronman, M. J., 829.
Stewart, R. J., and Graydon, W. F. Ion-exchange membranes (II) ion transfer rates 750
Sthapitanonda, P., and Margrave, J. L. Kinetics of nitridation of Mg and Al 1628
Stirton, A. J. See Weil, J. K., 899.
Stites, J. G., Jr. See Foster, K. W., 1017.
Stoddard, E. A., Jr. See Maslan, F. D., 1146.
Stokes, J. M. See Chambers, J. F., 985.
Stokes, J. M., and Stokes, R. H. Conductances of some simple electrolytes in aq. sucrose solns. at 25° 217
Stokes, R. H. See Chambers, J. F., 985; Stokes, J. M., 217.
Stone, F. S. See Dell, R. M., 1586.
Strakna, R. E. See Friedland, S. S., 815.
Strauss, U. P., Gershfeld, N. L., and Crook, E. H. Transition from typical polyelectrolyte to poly-soap (II) viscosity studies of poly-4-vinylpyridine derivs. in aq. KBr solns 577
Strobel, H. A. See Gable, R. W., 513.
Sullivan, J. C. See Cohen, D., 701.
Sundheim, B. R. Transference numbers in molten salts, 1381; see Lazare, L., 641.
Suryanarayana, C. V. See Venkatesan, V. K., 775, 777.
Suzuki, K. See Yasuda, M., 1649.
Sweet, T. R. See Harris, W. F., 509.
Sympson, R. F., and Cartledge, G. H. Mechanism of inhibition of corrosion by the pertechnetate ion (IV) comparison with other XO_4-inhibitors ... 1037

TAKEDA, M., and Endo, R. Viscosity of dil. polyvinyl chloride soln 1202
Tamaru, K. Thermal decompn. of SnH_4, 610; decompn. of NH_3 on Ge 612
Tanford, C. See Buzzell, J. G., 1204.
Tanford, C., and Buzzell, J. G. Viscosity of aq. solns. of bovine serum albumin between *p*H 4.3 and 10.5 225
Tanner, H. A. See Elmore, G. V., 1328.
Tashdjian, M. O. See Martin, R. B., 1028.
Templeton, D. H. See Dauben, C. H., 443; Zalkin, A., 821, 1275.
Težak, B. See Mirnik, M., 1473.
Thomas, D. K. See Davies, M., 41, 763, 767.
Thomas, H. C. See Richman, D., 237.
Thomas, H. C., and Merriam, C. N., Jr. Kinetics of chromatography on clays 249
Thorp, N., and Scott, R. L. Fluorocarbon solns. at low temps. (I) liq. mixts. CF_4-CHF_3, CF_4-CH_4, CF_4-Kr, CH_4-Kr, 670; (II) liq. mixts. C_2H_6-C_2F_6, C_2F_6-CHF_3, CH_2F_2-CHF_3, C_2H_6-CHF_3 and Xe-CHF_3 1441
Thurmond, C. D., and Logan, R. A. Distribution of Cu between Ge and ternary melts satd. with Ge. 591
Tichacek, L. J., and Drickamer, H. G. Thermal diffusion near the crit. soln. temp 820
Tichacek, L. J., Kmak, W. S., and Drickamer, H. G. Thermal diffusion in liqs.; effect of nonideality and assocn 660
Timasheff, S. N. See Kronman, M. J., 829.
Tinoco, I., Jr., and Hammerle, W. G. Influence of an external elec. field on optical activity of fluids .. 1619
Tinoco, I., Jr., and Lyons, P. A. Diffusion of isoionic, salt-free bovine serum albumin 1342
Tompkins, F. C. See Benson, G. W., 220.
Toops, E. E., Jr. Phys. properties of eight high-purity nitroparaffins 304
Toyama, O. See Kubokawa, Y., 833.
Trautman, R. Operating and comparating procedures facilitating Schlieren pattern analysis in an ultracentrifugation 1211
Trotman-Dickenson, A. F. See Knox, J. H., 1367.
Tryon, M. See Wall, L. A., 1306.
Tsai, K-R., Harris, P. M., and Lassettre, E. N. Crystal structure of Cs_2O, 338; crystal structure of Cs_3O 345
Tuck, D. G., Coryell, C. D., and Irvine, J. W., Jr. Fast chloride exchange between HCl and chloroauric acid in β,β'-dichlorodiethyl ether 378
Turkevich, J. See Larach, S., 1598.
Tuxworth, R. H. See Burwell, R. L., Jr., 1043.

UDY, D. C., and Ferry, J. D. Interacns. in polymer solns. obsd. by equilibrations across membranes 123
Ueno, K., and Martell, A. E. Vanadyl chelates of tetraphenylporphine and its *p*-subsd. derivs., 934; infrared studies on synthetic O carriers 1270
Uphaus, R. A. See Crespi, H. L., 1190.

VAN ARTSDALEN, E. R. Complex ions in molten salts—ionic assocn. and common ion effect, 172; see Yaffe, I. S., 1125.
Vanderkooi, W. N., and DeVries, T. Heat capacity of gases at low pressure using a wire-ribbon method 636
Vango, S. P. See Mason, D. M., 622.
Van Kley, H., and Stahmann, M. A. Electrophoresis of polypeptidyl proteins 1200
Van Voorhis, J. J. See Craig, R. G., 1225.
Veloric, H. S. See Beachell, H. C., 102.
Venkatesan, V. K., and Suryanarayana, C. V. Conductance and other phys. properties of urea solns., 775; a physico-chem. study of pyridine-acetic acid system 777
Vinograd, J. R. See Bello, J., 818, 1299.
Vold, M. J. Colloidal structure in Li stearate greases 439

WADDINGTON, G. See Good, W. D., 1080; Scott, D. W., 1090.
Wadsworth, M. E. See Kaneko, T. M., 457.
Wagener, S. Adsorption measurements at very low pressures 567

Wagner, M. L., and Scheraga, H. A. Gouy diffusion studies of bovine serum albumin 1066
Walker, B. E., Grand, J. A., and Miller, R. R. High temp. heat content and heat capacity of Al_2O_3 and $MoSi_2$ 231
Walker, P. L., Jr., and Raats, E. Changes in phys. properties of graphitized C rods upon gasification with CO_2, 364; effect of gas diffusion in graphitized C rods on their gasification rate with CO_2. 370
Walkup, J. H. See McCormack, J. B., 826.
Wall, F. T., and Beresniewicz, A. Electrolytic interacn. of nylon with aq. solns. of HCl 692
Wall, L. A., Harvey, M. R., and Tryon, M. Oxidative degradation of styrene and α-deuterostyrene polymers 1306
Wallace, W. E. See Wollam, J. S., 1654.
Wang, P. Molten cyanide process of purifying Ge from Cu contamination 45
Ward, W. H., and Bartulovich, J. J. Mol. kinetic and chem. properties of wool cortical cell fractions 1208
Warf, J. C., and Korst, W. L. Solns. of Eu and Yb metals in liq. NH_3 1590
Waser, J. See Leung, Y. C., 539.
Waugh, D. F. See Yphantis, D. A., 623, 630.
Weber, N., and Bauer, W. H. Flow properties of Al dilaurate–toluene gels 270
Webster, A. H., and Halpern, J. Homogeneous catalytic activation of mol. H in aq. soln. by Ag salts 280
Weil, J. K., and Stirton, A. J. Crit. micelle concns. of α-sulfonated fatty acids and their esters 899
Weir, C. E. See Shereshefsky, J. L., 1162.
Weise, C. H. See Brunauer, S., 771.
Weismann, T. J. See Chu, T. L., 1020.
Weller, S. W. See Hindin, S. G., 1501.
Weller, S. W., and Hindin, S. G. Effect of pretreatment on activity of γ-alumina (II) H–D exchange 1506
Wellman, W. W. See Wirth, H. E., 919, 921.
Wendlandt, W. W., and Bryant, J. M. Solys. of some metal nitrate salts in tri-*n*-butyl phosphate 1145
Westheimer, F. H., and Ingraham, L. L. Entropy of chelation 1668
Westrum, E. F., Jr. See Fink, R. W., 800.
Whittaker, A. G., Williams, H. and Rust, P. M. Burning rate studies (IV) effect of exptl. conditions on consumption rate of the liq. system 2-nitropropane–HNO_3 904
Wiberley, S. E. See Guertin, D. L., 1018; Laurene, A. H., 901.
Wiebe, A. K. Elution time and resolution in vapor chromatography 685
Wiley, R. H., and Reed, S. F. Sulfostyrenes—prepn. of variable capacity sulfostyrene cation exchange polymers from styrene sulfonamidostyrene copolymers 533
Wilhoit, E. D. See Sears, P. G., 169.
Williams, H. See Whittaker, A. G., 904.
Williams, R. L. Relation of force const. to electronegativity and covalent radius 1016
Williams, R. R., Jr. See Nash, J. R., 823.
Williamson, G. R. See Neale, S. M., 741.
Wilson, A. See Epstein, M. B., 1051.
Winger, A. G., Ferguson, R., and Kunin, R. Electroösmotic transport of H_2O across permselective membranes 556
Winkler, C. A. See Armstrong, D. A., 1100; Forst, W., 1424; Jamieson, J. W. S., 1542.
Winkler, M. H. Exptl. investigation of some models for optical activity 1656
Winslow, L. See Hutchinson, E., 122.
Winter, E. R. S. See Hill, K. J., 1361.
Winter, S. S., and Beckmann, C. O. Influence of structure upon the viscous behavior of some carboxymethyl polysaccharides 883
Wirth, H. E., Droege, J. W., and Wood, J. H. Low temp. heat capacity of palmitic acid and Me palmitate 917
Wirth, H. E., and Kosiba, W. L. Isothermal dehydration of hydr. Na palmitate 923
Wirth, H. E., and Palmer, E. D. Vapor pressure and dielec. const. of diborane, 911; dielec. const. and vapor pressure of pentaborane 914
Wirth, H. E., and Wellman, W. W. Dielec. const. of hydr. Na palmitate, 919; phase transitions in Na palmitate by dielec. const. measurements 921
Wolfenden, J. H. See Magnuson, J. A., 1665.
Wolfgang, R., Eigner, J., and Rowland, F. S. Studies of the recoil tritium labeling reacn. (II) CH_4 and C_2H_6 1137
Wollam, J. S., and Wallace, W. E. Comparison of pycnometric and X-ray densities for NaCl–NaBr and KCl–KBr systems 1654
Wood, E. A. Question of a phase transition in Si 508
Wood, J. H. See Wirth, H. E., 917.
Wood, R. E., and Boyars, C. Dielec. properties of solid nitrodichloro-*o*-xylenes 1584
Wood, S. E., and Sandus, O. Vol. of mixing of binary mixts. (IV) benzene-2,2,4-trimethylpentane (isoöctane) 801
Wood, T. D. See Jasper, J. J., 1625.
Woodward, A. E., Allen, E. R., and Anderson, R. H. A phase rule study of the system ZnO–CrO_3-H_2O at 25° 939
Woontner, L. See Gayer, K. H., 1569.
Wright, I. S. See Sheppard, E., 584.

YAFFE, I. S., and Van Artsdalen, E. R. Elec. conductance and d. of pure molten alkali halides 1125
Yamasaki, K. See Kakihana, H., 36; Yasuda, M., 1649, 1667.
Yasuda, M., Sone, K., and Yamasaki, K. Stability of Zn and Cd complexes with some Xe derivs. of 1,10-phenanthroline and 2,2′-bipyridine 1667
Yasuda, M., Suzuki, K., and Yamasaki, K. Stability of Cu and Ni chelates of some phthalic acid derivs 1649
Yates, D. J. C. Influence of the polar nature of the adsorbate on adsorption expansion 543
Yates, P. C. See Moore, T. E., 564.
Yoshihashi, H. See Shiio, H., 1049.
Young, G. J., Chessick, J. J., and Healey, F. H. Heats of adsorption from soln. from heat of immersion data 394
Yphantis, D. A., and Waugh, D. F. Ultracentrifugal characterization by direct measurement of activity (I) theoretical, 623; (II) exptl. 630
Yudelson, J., and Rabinovitch, B. Light scattering behavior of 3-dimensional network gels 1512

ZALKIN, A., and Ramsey, W. J. Intermetallic compds. between Li and Pb (I) structures of Li_3Pb and Li_7Pb_2 234
Zalkin, A., Ramsey, W. J., and Templeton, D. H. Intermetallic compds. between Li and Pb (II) crystal structure of Li_8Pb_3 1275
Zalkin, A., and Templeton, D. H. Crystal structure of Na amide 821
Zapas, L. J. See Helders, F. E., 1575.
Zettlemoyer, A. C. See Chessick, J. J., 1181, 1345.
Zimm, B. H., and Lundberg, J. L. Sorption of vapors by high polymers 425
Zimmering, P. E. See Morawetz, H. (corrn.) 1671
Zimmerman, H. K., Jr. See Polestak, W. J., 787.
Zimmerman, J. R., Holmes, B. G., and Lasater, J. A. A study of adsorbed H_2O on silica gel by nuclear resonance techniques 1157
Zisman, W. A. See Ellison, A. H., 416.
Zwolinski, B. J. See Kato, H. P., 404.

Subject Index to Volume LX, 1956

ABSORPTION cell, infrared, for study of heterogeneous reacns.................................. 1670
Acetamide, conductances of uni-univalent electrolytes in N,N-Me_2-, 1076; protonation of N-Me-.... 1341
Acetanilide, energies and entropies of assocn. for amides in benzene solns........................763, 767
Acetic acid, ionization const. in H_2O–MeOH, 151; physico-chem. study of pyridine–, system.......... 777
Acetone, conductances of K thiocyanate and tetra-*n*-butyl-ammonium iodide in.................... 169
Acetonitrile, –H_2O liquid–vapor equil., 1146; kinetic study of trifluoro-, –butadiene cyclization.......... 1430
Acetyl peroxide, diffusion–recombination in decompn. of.. 823
Acrylic acid, vapor pressure of ethyl *trans*-β-(2-furyl)-acrylate, 252; apparent dissocn. consts. of, polymers, 1030; solvolysis of *p*-nitrophenyl methacrylate–, copolymers (corrn.).................. 1671
Actinium, neutron emission from, fluoride........... 1017
Activity coefficients, of concd. salt solns., 184; of HCl in MeOH–H_2O mixts., 754; of benzoic acid in aq. salt solns.. 1139
Adenosine phosphates, stability consts. of ionic complexes of.. 180
Adhesion, application of the absolute rate theory to.. 957
Adsorption, measurements at very low pressures, 567; of N on pure NaCl, 824; studies of Fe oxides, 1001; of complex metal–ammines and other complex ions, 1008; structures of adsorbed monolayers, 1153; adsorbed H_2O on silica gel by nuclear resonance techniques, 1157; of gases and vapors on glass spheres, 1162; activated, of O on glass, 1164; of *n*-butane on C, 1167; measurements of attapulgite, 1181; from differential capacitance measurements, 1185; data on acetylene black............. 1338
Aerosol droplets, amplitude of vibration of, in a sonic field.. 989
Alum, sorption of NH_3 by dehydrated potash........ 220
Alumina, pretreatment effect on activity of γ-....1501, 1506
Aluminum, heat capacity and content of Al_2O_3, 231; crystal structure of γ-AlOOH, 273; porosity of anodic oxide coatings on, 385; heat capacity and entropy of, 410; infrared spectra of three, alkoxides, 1018; crystallographic evidence for the trihydrate of AlF_3, 1152; magnetic susceptibility studies in system NiO–Al_2O_3, 1223; small angle X-ray scattering by $Al(OH)_3$ gel, 1580; kinetics of nitridation of.. 1628
Amines, base strengths of, in non-protolytic solvents, 63; (corrn.) 1671; molarity quotients for formation of complexes between Cd ions and, containing S.. 384
Ammonia, liq., as a solvent, conductivity, 121; sorption by dehydrated potash alum, 220; liquid–vapor equil. in the system NH_3–hydrazine, 245; decompn. on Ge, 612; investigation of metal–NH_3 systems by vapor pressures, 732; production of active N from N, NO and, 1100; sorption by homoionic bentonites, 1105; sorption by nylon.... 1172
Ammonium chloride, linear decompn. rates of........ 1095
Ammonium nitrate, cryoscopic heat of fusion of...... 1356
Amylopectin, dielec. dispersion behavior of, acetate–tricresyl phosphate systems.................... 382
Amylose, viscous behavior of carboxymethyl polysaccharides.. 883
Anatase, ice layers on the surfaces of.............. 376
Anthranilic acid, stability of metal chelates of subsd. 509
Antimony, conductances of $SbBr_3$ and $SnCl_2$ in dimethylformamide on addn. of piperidine.......... 1470
Argon, quenching of flames of propane–O_2–, mixts., 97; adsorption on a Si surface, 353; viscosity of mixt., ethylene–, 789; vapor pressures of......... 1119
Arsenic, reacn. between chromate and As_2O_3......... 1383
Asbestos, properties of..........................361, 1218
Association, energies and entropies of amides in benzene solns..763, 767
Attapulgite, adsorption and heat of wetting measurements of.. 1181
Autoprotolysis constant, detn. of, of EtOH.......... 1019

BARIUM, Ba–Sr equil. system, 302; kinetics of homogeneous pptn. of $BaSO_4$, 389; chromatography of thermal formation of, tetrapolyphosphates, 1335; the ternary system $MgCl_2$–$BaCl_2$–H_2O between 18 and 100°.......................... 1436
Bentonites, sorption of NH_3 by homoionic........... 1105
Benzene, self-diffusion in, 14; diffusion in ideal binary liq. mixts., 51; effect of I on radiolysis of, 381; sorption of vapors by high polymers, 425; energies of amides in, solns., 763, 767; viscosity of liquid–liquid ternary mixts., 809; viscosity from 90° to critical temp., 1025; salting in of subsd., by large ion salts, 1131; sepn. of org. solns. by thermal diffusion, 1524; effects of spreading solvent on monolayers as detd. by pressure–area isotherms......... 1533
Benzoic acid, activity coeffs. of, in aq. salt solns., 1139; surface pressure of soluble, films at H_2O–halobenzene interfaces.......................... 1625
Biphenyl, sepn. of org. solns. by thermal diffusion.... 1524
Bipolar ion-exchange membranes, prepn. and characterization of.. 435
Bismuth, heats of soln. of Cu, Ag and Au in liq....... 446
Bolaform electrolytes, conductance of bisquaternary salts in alc.. 156
Bond length, relationship of force const. and......... 1293
Borane, adsorption of di-, on BN, 102; explosive oxidn. of di-, 639; vapor pressure and dielec. constant of di-, 911, and penta-, 914; heat of combustion of tri-*s*-Bu, 1136; soly. of H in di-, 1483; energetics of the, 1529; photolysis of penta-, vapor 1589
Boric acid, elec. conductance in liq. borates.......... 1321
Boron, sorption of, compds. by Pd and charcoal, 307; gaseous mols. of geochem. significance, 715; triaryl-, anions (dissocn. const. of Na trimesityl-, in tetrahydrofuran).......................... 1020
Bovine serum albumin, viscosity of aq. solns. of, 225; aggregation of, in acid *p*H.......................... 829
Bromine, nuclear spin contribution to low temp. thermodynamic properties of, 909; entropy of soln. of Br in perfluoro-*n*-heptane, 949; f.p. and b.p., heat of vaporization and vapor pressure–temp. relations of BrF_5, 1462; Si–, bond parachors and Si–, bond refraction.......................... 1644
Butane, d., vapor pressure and heat of vaporization of 2,2,3-trichloroheptafluoro-.......................... 811
n-Butane, spectra studies of preflame reacns. of, 320, (corrn.), 1673; comparison of, and krypton sorption, 385; adsorption and surface diffusion on C.... 1167
Butyl alcohols, properties of dioxane–, systems...... 1591
n-Butyl alcohol, heats of adsorption on C, 394; b.p.–compn. diagram for system 1,4-dioxane–, 826; solys. of some metal nitrate salts in tri-*n*-butyl phosphate.. 1145

CADMIUM, molarity quotients for formation of complexes between Cd ions and amines containing S, 384; stability of, complexes with Me derivs. of 1,10-phenanthroline and 2,2′-bipyridine.......... 1667
Calcite, thermoluminescence of.......................... 698
Calcium, heat of combustion of, 498; investigation of metal–NH_3 systems by vapor pressures......... 732
Calcium compounds, hydration of tricalcium silicate in a ball mill, 112; hydration of tricalcium silicate in paste form, 116; decompn. of hyponitrites of, 192; chemisorption of $Ca(OH)_2$ by silica, 325; hydrothermal reacns. of amorphous silica and $Ca(OH)_2$, 397; heat of decompn. of tricalcium silicate, 771; thermal dissocn. pressure of $CaCO_3$, 1361; phase relations in system $CaBr_2$, CaO and H_2O, 1422; hydrothermal reacns. between $Ca(OH)_2$ and amorphous silica.......................... 1559
Calorimeter, high temp., and hydrogenation of Me, Et and vinyl chlorides.......................... 492
Carbon, change of graphitized C after gasification, 364; gasification rates of graphitized C rods, 370; kinetics of CS_2–NO reacn. and mechanism of light

emission in the explosive reacn., 379; heats of adsorption of *n*-BuOH on, 394; black in polar and non-polar polymers, 474; kinetics of reacn. of CO_2 with, 480; kinetics of the steam–C reacn., 486; C–O and C–H surface complexes, 495; oxidn. of graphitized C black, 689; structures of adsorbed monolayers, 1153; adsorption and surface diffusion of *n*-butane on, 1167; free energy of immersion of compressed powders with liqs., graphite, 1225; adsorption data on acetylene black, 1338; producer gas equil. and entropy of graphite, 1467; micropore structure of artificial graphite, 1480; systematic analysis of, black structures 1646
Carbon, C^{12}, effect of surface coverage on spectra of chemisorbed CO 194
Carbon, C^{14}, self-diffusion in liqs., 14; labeled perfluoroöctanoic acid in study of adhesion and other surface phenomena 127
Carbon dioxide, soly. in Cl, 374; viscosity of mixt. CH_4–CO_2 789
Carbon monoxide, effect of surface coverage on spectra of chemisorbed, 194; influence of the polar nature of the adsorbate on adsorption expansion, 543; adsorption measurements at very low pressures, 567; second explosion limits of CO–O_2 mixts., 512, 1023, 1344; photosensitized oxidn. of, on Cu_2O 1465
Carbonyl compounds, intermol. assocn. of 1660
Carrageen, variation of sedimentation const. with field and temp. for naturally occurring polyelectrolytes 506
Catalysis, intermediate order heterogeneous, and heats of adsorption, 1012; power rate law in heterogeneous 1033
Cation exchange selectivities, thermodynamic calcn. of 521
Cell, infrared absorption 1670
Cellophane, diffusion of H_2O into uncoated, 76, 83 (corrns.) 1671
Cellulose, properties of the system, trinitrate–isophorone, 289; system, tributyrate–dimethyl phthalate, 294; reversible assocn. of, nitrate in EtOH, 648; –H_2O–salt system, 741; slow thermal decompn. of, nitrate, 1260; dimensions and hydrodynamic properties of, trinitrate mols. in dil. solns 1278
Centrifugal field, eq. of motion of a spherical particle in 1476
Cerium, ionic character of transition metal hydrides 510
Cesium, crystal structure of Cs_2O, 338; crystal structure of Cs_3O 345
Cetane, effect of alkali metal ions on activity of cracking catalysts 422
Cetyl alcohol, rate of evaporation of H_2O through 348
Chelates, paramagnetic resonance in Cu, 71; mechanism of formation of tris-(2,2′-dipyridyl)-Fe(II) complex, 87; effect, entropies of formation of complex ions, 123; stability of metal, of subsd. anthranilic acids, 509; infrared studies on synthetic O carriers, 1270; thermodynamics of, formation, 1451; stability of Cu and Ni, of phthalic acid derivs., 1649; entropy of chelation 1668
Chloramine, thermodynamic properties of 507
Chlorine, soly. in $TiCl_4$, 374; nuclear spin contribution to low temp. thermodynamic properties of, 909; reacns. of, atoms 1367
Chloroauric acid, fast chloride exchange between HCl and, in β,β'-dichlorodiethyl ether 378
Chromatography, kinetics on clays, 249; vapor phase, 685; longitudinal diffusion in, columns, 816; of thermal formation of Ba and Pb tetrapolyphosphates, 1335; application of plate theory to anion-exchange, of glycols 1370
Chromium, crystal structure of Cr_5Si_3, 443; interacn. of Cr(VI) anions with metal surfaces, 738; phase rule study of the system ZnO–CrO_3–H_2O, 939; reacn. between chromate and As_2O_3, 1383; redn. of Cr(VI), at rotated Pt electrode 1564
Chrysotile, d. and structure of, 361; basicity of, suspensions 1218
Citric acid, stability of Tl(I) citrate complex 1623
Clays, kinetics of chromatography on 249
Coagulation values, negative activity limit of stability and, of Ag halides 1473
Coal, sorption studies on American 1548
Cobalt, heat capacity and entropy of, 410; catalytic redn. of, 457; extraction of Co(II) salts by 2-octanol, 564; adsorption of complex metal–ammines and other complex ions of, on silica gel, 1008; studies with Raney, catalyst 1339
Collagen, sorption of vapors by high polymers 425
Colloids, turbulent coagulation of 463
Complex ions, in molten salts 172
Concentration overpotential, at reversible electrodes (corrn.) 1671
Conductance, ionization const. of AcOH in H_2O–MeOH mixts. from, 151; of bisquaternary salts in alc., 156; dissocn. of spherical ions, 160; of alkyl and aryl derivs. of triphenylchloromethane, 164; of K thiocyanate in acetone, 169; dipping electrodes for precision conductimetry, 177; elec., of solns. of NaSCN, NaI and $NaClO_4$, 189; of simple electrolytes in aq. sucrose solns., 217; of electrolytes in 1-propanol, 330; of electrolytes at infinite dilution, 428; C black in polar and non-polar polymers, 474; a modified direct current, method for general application, 595; of urea solns., 775; of aq. NaCl and KCl solns., 985; of uni-univalent electrolytes in N,N-dimethylacetamide, 1076; elec., of pure molten alkali halides, 1125; elec., in liq. Pb silicates and borates, 1321; of 2,4,6-tri-dimethylaminomethyl-phenol triacetate, 1406; behavior of some uni-univalent electrolytes in dimethyl sulfoxide 1433
Consecutive reactions, approximations in kinetics of 966
Contortional energy, requirement in spreading of large drops 952
Copper, paramagnetic resonance in, chelates, 71; thermodynamics of liq. solns. in the Cu–Ag system, 108; heats of soln. in liq. Tl, Pb and Bi, 446; solys. in solid Ge, 591; heat of formation of solid and liq. binary alloys of Cu with Cd, In, Sn and Sb, 852; linear decompn. rates of $CuSO_4 \cdot 3H_2O$, 1095; formation consts. of, derivs. of S-alkyl carboxylic acids, 1427; catalytic activation of H by cupric salts, 1455; nucleation of, metal from aq. soln., 1461; stability of, chelates of phthalic acid derivs. 1649
Corrosion, inhibition by the pertechnetate ion, 28, 1037; inhibition by the perrhenate ion 32
Cresyl phosphate, systems, dielec. dispersion behavior of amylopectin acetate–tri- 382
Critical solution temperature, thermal diffusion near 820
Crystal structure, of Cs_2O, 338; of Cs_3O, 345; of Cr_5Si_3 443
Cumene, soly. in H_2O 332
Cumene hydroperoxide, reacn. of aquo ferrous Fe with, 969; reacn. of ferrous versenate with 996
Cyclohexane, decompn. of hydrocarbons by silica–alumina catalysts, 59; purification of perfluoromethyl-, 615; isotopic exchange between D and hydrocarbons on Ni–silica catalysts, 1043; dipole moments of cyclohexyl azide, cyclopentyl azide and 3-bromocyclohexene 1585
Cyclopropane, kinetics and mechanism of hydrogenation over a Ni–silica–alumina catalyst 1601

DECANE, critical micelle concns. in aq. solns. of K alkane tricarboxylates 1439
n-Decylamine, equil. between H_2SO_4 and 943
Density, of normal alkyl series of compds., 1400; liq., of NF_3 1412
Desoxyribonucleic acid, non-Newtonian flow in concd. solns. of Na salt of, 1536; dynamic mechanical properties of concd. solns. of Na salt of 1575
Detergents, equil. and kinetics of, adsorption, 890; micelle formation in solns. of some isomeric, 1240; equil. dialysis of, solns 1245
Deuterium, adsorption by a Pt catalyst, 702; exchange and isomn. of *trans*-ethylene-d_2 on Ni, 724; exchange and isomn. of deuteroethylenes on Ni, 730; exchange of H by, in hydroxyls of kaolinite, 987; isotopic exchange between D and hydrocarbons on Ni–silica catalysts, 1043; oxidative degradation of styrene and α-deuterostyrene polymers, 1306; effect of γ-alumina on H–, exchange, 1506; d. of liq. DBr 1588

Dialysis, equil. of soap and detergent solns........... 1245

Diborane, adsorption on BN, 102; explosive oxidn. of, 639; vapor pressure and dielec. const. of, 911; soly. of H in.. 1183

Dielectric constants, in enzymes, proteins and other mols., 253; of hydr. Na palmitate, 919; phase transitions in Na palmitate by, measurements..... 921

Dielectric properties, of lower membered polyethylene glycols.. 1496

Diffusion, of acid dye in gelatin, 9; self-, in liqs., 14, (corrn.)1671; in ideal binary liq. mixts., 51; of H_2O into uncoated cellophane, 76, 83, (corrn.) 1671; thermal, in liqs., 660; longitudinal, in ion exchange and chromatographic columns, 816; flames of simple alcs., 1059; Gouy, studies of bovine serum albumin, 1066; gas permeation through membranes by, 1177; concn. dependence of, coeff. of raffinose in dil. aq. soln........................... 1464

Dioxane, vapor pressures and activities in the system dioxane–H_2O, 573; b.p.-compn. diagram for system *n*-BuOH–1,4-dioxane, 826; properties of Bu alcs.–, systems.............................. 1591

Dissociation constant, base strengths of amines in non-protolytic solvents, 63; of Na trimesitylboron in tetrahydrofuran, 1020; of acrylic and methacrylic acid polymers, 1030; acid, of subsd. 1,10-phenanthrolines.......................... 1546

Dolomite, thermoluminescence of.................. 698

Dye, diffusion in gelatin of an acid................. 9

Dysprosium, heats of combustion of.............. 1457

ELECTRIC field, influence of an external, on optical activity of fluids.............................. 1619

Electric moments, of derivs. of pyridine and quinoline, 125; obviation of soln. density measurements detns. in, 1336; of cyclohexyl azide, cyclopentyl azide and 3-bromo-cyclohexene.................. 1585

Electrode potentials, in fused systems, study of AgCl–KCl system............................. 679

Electrolytes, partition of, between aq. and org. phases.. 1363

Electrophoresis, of polypeptidyl proteins............ 1200

Energy levels, for mols. with internal rotation........ 466

Entropy, configurational and choice of standard states, formation of complex ions and chelate effect. 123

Entropy of chelation.................................. 1668

Entropy of solution, of I................................ 618

Enzymes, electrolyte influence on effective dielec. consts. in, 253; schematic method of deriving rate laws for -catalyzed reacns., 1375; unusual kinetic consequences of, catalysis mechanisms............ 1378

Erbium, heat of combustion of..................... 1582

Ethane, thermodynamic properties of liq. chloro-, 804; radiolysis of, mol. detachment of H.......... 826

Ethane, liq. mixts. C_2H_6–C_2F_6, C_2F_6–CHF_3, CH_2F_2–CHF_3, C_2H_6–CHF_3 and Xe–CHF_3................ 1441

Ethanol, detn. of autoprotolysis const. of, 1019; kinetics of reacn. of, with *p*-nitrobenzoyl chloride.. 1142

Ethylene, vapor phase bromination of tetrafluoro-, 608; catalytic oxidn. to, oxide, 666; exchange and isomn. of *trans*-ethylene-d_2 on Ni, 724; exchange and isomn. of deutero-, on Ni, 730; viscosity of A–, mixt., 789; vapor phase infrared spectra of the ozonides of, 807; heats of formation of tetrafluoro-, and -methane, 1318; dielec. properties of lower membered poly-, glycols, 1496; effect of γ-alumina in, hydrogenation..................... 1501

Ethylenediaminetetraacetic acid, kinetics of displacement reacns. of metal complexes of........... 251

Ethylenimine, reacns. with at. H.................... 1542

Europium, solns. of Yb and, metals in liq. NH_3....... 1590

Extraction coefficients, concn. effects on solvent, of some trivalent metal halides...................... 500

FIBRIN, conversion of fibrinogen to, 926, (corrn.).... 1673

Fibrinogen, action of heparin on polymn. of.......... 584

Flame, MH_4 diffusion, 759; reacns. of NH_3 and hydrazine with O atoms and H atoms in atomic...... 813

Fluorine, C-14 labeled perfluoroöctanoic acid in study of adhesion and other surface phenomena, 127; vapor phase bromination of tetrafluoroethylene, 608; purification of perfluoro-*n*-heptane, 615; fluorocarbon solns. at low temp., 670; soly. of I and phenanthrene in hydrofluorocarbons, 674; thermal expansion of crystalline KHF_2, 800; d., vapor pressure and heat of vaporization of 2,2,3-trichloroheptafluorobutane, 811; entropy of soln. of Br in perfluoro-*n*-heptane, 949; combustion calorimetry of org. F compds. by a rotating-bomb method, 1080; heats of formation of tetrafluoroethylene and -methane, 1318; liq. mixts. C_2H_6–C_2F_6, C_2F_6–CHF_3, CH_2F_2–CHF_3, C_2H_6–CHF_3 and Xe–CHF_3, 1441; f.p. and b.p., heat of vaporization and vapor pressure–temp. relations of BrF_5................ 1462

Fluoroform, heat capacity of gases at low pressure.... 636

Foaming, inhibition of.............................. 1255

Force constant, relation to electronegativity and covalent radius, 1016; relationship with bond length.. 1293

Free energy, thermodynamic properties of chloramine, dichloramine and NCl_3.................. 507

Free energy of immersion, of compressed powders with liqs.. 1225

Friction law, correction of Stokes', for particles of mol. size.. 703

Frog skin, Na transport in isolated.................. 404

GALLIUM, gaseous mols. of geochem. significance, 715; gaseous metal nitrides, vapor pressure of GaN(s).. 810

Gas permeation, through membranes............... 1177

Gelatin, diffusion of an acid dye in, 9; effect of optical isomers on m.p. of, gels, 818; mechanism of gelation of.. 1299

Geochemistry, phys. chemistry in, 705; occurrence of Tc on the earth's crust, 707; gaseous mols. of, significance, 715; exptl. geology...................... 718

Germanium, a molten cyanide process of purifying, 45; solys. of Cu in solid, 591; decompn. of NH_3 on, 612; structure of germanides of formula M_5Ge_3.... 677

Glass, influence of the polar nature of the adsorbate on adsorption expansion. 543; adsorption on, at high relative pressures, 793; adsorption of gases and vapors on, spheres, 1162; activated adsorption of O on.. 1164

Glycerol, purification by ion exclusion, 518; light scattering behavior of 3-dimensional network gels.. 1512

Glycols, application of plate theory to anion-exchange chromatography of.............................. 1370

Gold, crystallization of metallic films, 277; heat of formation of some solid and liq. binary alloys of Au with Cd, In, Sn and Sb........................ 858

HEAT capacity, of five spinel minerals, 410; of gases at low pressure, 636; low temp., of palmitic acid and Me palmitate, 917; extrapolation of cooling curves in measurements of, 1344; of trimethylamine–trifluoroborane........................ 1529

Heat of adsorption, intermediate order heterogeneous catalysis and, 1012; negative "net"............... 1022

Heat of combustion, of Ca, 498; of org. F compds. by a rotating-bomb method, 1080; of tri-*s*-butylborane, 1136; of Dy and Yb, 1457; of Er......... 1582

Heat of formation, of $TiCl_3$, 309; of $TiCl_2$, 311; of tetrafluoroethylene and trifluorochloroethylene, 608; of solid and liq. alloys in systems Ag–Cd, Ag–In and Ag–Sb, 846; of solid and liq. binary alloys of Cu with Cd, In, Sn and Sb, 852; of some solid and liq. binary alloys of Au with Cd, In, Sn and Sb, 858; of tetraethyllead by rotating bomb method, 1090; of Na_2C_2, NaO_2 and KO_2, 1333; of nitramide.. 1460

Heat of fusion, cryoscopic, of ammonium nitrate..... 1356

Heat of hydrogenation, of some alkyl fluorides....... 1454

Heat of reaction, of org. halogen compds............. 1454

Heat of solution, of binary and ternary liq. alloys rich in Sn.. 842

Heat of wetting, studies of teflon.................... 1345

Helium, quenching of flames of propane–O_2–, mixts... 97

Heparin, action on polymn. of fibrinogen............ 584

n-Heptane, purification of perfluoro-, 615; soly. and partial molal vol. of I in perfluoro-, 616; entropy of soln. of Br in perfluoro-.......................... 949

Heptane, critical micelle concns. in aq. solns. of K alkane tricarboxylates............................ 1439

Hexenes, phys. properties of the 17 isomeric, of the

API research series ... 1446

Hydrazine, liquid–vapor equil. in the system NH_3–, 245; reacns. of NH_3 and, with O atoms and H atoms in atomic flames ... 813

Hydrocarbons, phys. properties of eight high-purity nitroparaffins ... 304

Hydrochloric acid, fast chloride exchange between, and chloroauric acid in β,β'-dichlorodiethyl ether, 378; activity coeffs. in MeOH–H_2O mixts., 754; vapor pressure of, above non-aq. solns ... 1461

Hydrogen, activation of mol., by Ag salts, 280; redn. of Hg^{++} and Hg_2^{++} with mol., 285; C–O and C–H surface complexes, 495; pressure–compn.–temp. relations in the Pd–H system, 502; chemisorption, on ZnO, 833; overpotential at electrodeposited Ni cathodes in HCl solns., 837; overpotential at Fe cathodes in NaOH solns., 871; overpotential on Ag in NaOH solns., 1290; kinetics studies with para-, 1329; catalytic activation of, by cupric salts, 1455; soly. in diborane, 1483; effect of γ-alumina on D–, exchange, 1506; reacns. of ethylenimine with at., 1542; sorption and para-, conversion on evaporated Ni films, 1606; spectral properties of, bonding systems ... 1615

Hydrogen ion coulometer ... 372

Hydrogen peroxide, negative ion formation in, and H_2O vapor, the perhydroxide ion ... 681

Hyponitrites, of Ca and Sr, decompn. of ... 192

ICE, layers on surfaces of anatase and AgI, 376; order–disorder problem for ... 1140

Infrared absorption cell, for study of heterogeneous reacns ... 1670

Internal rotation, energy levels and thermodynamic functions for mols. with ... 466

Iodic acid, transference nos. of, 976, (corrn.) ... 1673

Iodine, diaryliodonium salts, 141; effect on radiolysis of benzene, 381; crystal structure of P_2I_4, 539; soly. and partial molal vol., in perfluoro-n-heptane, 616; entropy of soln. of, 618; soly. in hydrofluorocarbons, 674; effect of vapor on AgI, 806; nuclear spin contribution to low temp. thermodynamic properties of, 909; detn. of equil. const. by surface tension measurements, 1258; HI_3 ... 1665

Ionization constant, of AcOH in H_2O–MeOH ... 151

Ion-pairs, evolution and applications of, concept, 129; Cu catalysis in reacns. of diphenyliodonium ions with halide ions and hydroxylic solvents ... 141

Iron, mechanism of formation of tris-(2,2'-dipyridyl)-Fe(II) complex, 87; $FeCl_3 \cdot 10H_2O$, systems $FeCl_3$–H_2O and $FeCl_3$–HCl–H_2O, 91; heat capacity and entropy of, 410; H overpotential at, cathodes in NaOH solns., 871; extraction of $FeCl_3$ by isopropyl ether, 901; reacn. between aquo ferrous Fe and cumene hydroperoxide, 969; reacn. of ferrous versenate with cumene hydroperoxide, 996; adsorption and heat of immersion studies on oxide, 1001; Fe(II)–Tl(III) reacn. at high chloride concn., 1015; stability of $Fe(OH)_2$ ppts., 1519; soly. of $Fe(OH)_2$ and $Fe(OH)_3$ in acidic and basic media, 1569; passivation by Os(VIII) oxide ... 1571

Isobutene, infrared spectra of some reacn. products of octafluoro- ... 1372

Isoöctane, benzene-2,2,4-trimethylpentane ... 801

Isophorone, properties of the system cellulose trinitrate– ... 289

Isoprene, viscosity of alfin poly- ... 431

Isopropyl alcohol, photolysis of diisopropyl ketone ... 1315

Isopropyl ether, extraction of $FeCl_3$ by ... 901

KAOLINITE, exchange of H by D in hydroxyls of ... 987

Krypton, comparison of n-butane and, sorption, 385; fluorocarbon solns. at low temps., 670; vapor pressures of ... 1119

LAURIC acid, heats of micelle formation, 122; flow properties of Al dilaurate–toluene gels, 270; film drainage transition temps., 1051; effects of antifoaming agents on surface-plastic solns ... 1255

Lauryl alcohol, ternary systems with three separate binodal curves ... 20

Lead, intermetallic compds. between Li and, 234, 1275; transport no. measurements in pure fused salts, 620; heat of formation of tetraethyl-, by rotating-bomb method, 1090; chromatography of thermal formation of, tetrapolyphosphates, 1335; thiocyanate complexes in soln ... 1493

Light scattering, effect of hexamethylene glycol on thermodynamic interacns. in fibrinogen solns., 926; behavior of 3-dimensional network gels ... 1512

Lithium, Li–Na liq. metal system, 13; ion exchange in concd. solns., LiCl–HCl, 36; intermetallic compds. between Pb and, 234, 1275; effect of alkali metal ions on activity of cracking catalysts, 422; colloidal structure in, stearate greases, 439; elec. conductance and d. of pure molten alkali halides, 1125; system LiCl–H_2O ... 1666

MAGNESIUM, thermal ignition of systems $LiNO_3$–Mg and $NaNO_3$–Mg, 867; ternary system $MgCl_2$–$BaCl_2$–H_2O between 18 and 100°, 1436; kinetics of nitridation of ... 1628

Magnetic susceptibility, studies in system NiO–Al_2O_3 ... 1223

Malonic acid, isopiestic studies of dicarboxylic acid solns., 41; decompn. in glycerol and in dimethyl sulfoxide, 825; decarboxylation in triethyl phosphate, 1150; kinetics of decompn. of, in aromatic amines, 1340; effect of picolines on ... 1583

Manganese, magnetic properties of ZnS phosphors with, activator ... 1598

Mercury, reduction of Hg^{++} and Hg_2^{++} with mol. H, 285; reacn. between Hg(I) and Tl(III) ... 1661

Methacrylic acid, selectivity coeffs. of, resins toward alkali metal cations, 263; mol. assocn. in styrene–, copolymers ... 782

Methane, fluorocarbon solns. at low temps., 670; diffusion flame, 759; viscosity of mixt. CH_4–CO_2, 789; studies of recoil tritium labeling reacn ... 1137

Methanol, some cation equil. studies in, 513; activity coeffs. of HCl in MeOH–H_2O mixts., 754; viscosity of liquid–liquid ternary mixts., 809; diffusion flames of ... 1059

Methylamine, heat capacity of trifluoroborane–tri- ... 1529

Methylammonium hydroxide, thermal decompn. of phenyltri- ... 1004

Methyl chloride, kinetic study of, combustion ... 874

Methyl compounds, of the elements ... 1659

Methyl cyanide, reacn. of active N with ... 1424

Micelle, heats of formation, 122; factors responsible for stability of detergent, 257; critical, concns. of polyethylated non-ionic detergents, 657; crit., concns. of α-sulfonated fatty acids and their esters, 899; streaming potential studies on quartz in solns. of aminium acetates in relation to formation of hemi-, 981; alkali and alkaline earth phenylstearates in benzene, 1108; colloid structure in dil. arylstearate–benzene systems, 1114; formation in solns. of some isomeric detergents, 1240; critical, concns. in aq. solns. of K alkane tricarboxylates ... 1439

Micropore structure, of artificial graphite ... 1480

Microwave absorption, in liqs ... 1354

Minimum-principle, for non-equil. steady states ... 1611

Molal activity coefficients, Stokes–Robinson hydration model for solns ... 1296

Molybdenum, heat capacity and content of $MoSi_2$, 231; gaseous, oxychloride, 947; system Na_2SO_4–Na_2MoO_4–H_2O ... 1662

Montmorillonite, complexes with satd. ring compds. ... 808

Motion, eq. of, of a spherical particle in a centrifugal field ... 1476

NEPTUNIUM, kinetics of reacn. between Np(IV) and Np(VI) in a mixed solvent ... 701

Neutron, emission from actinium fluoride ... 1017

Nitramide, heat of formation of ... 1460

Nickel, semi-conductivity and catalysis in the NiO system, 209; extraction of Ni(II) salts by 2-octanol, 564; H overpotential at electrodeposited, cathodes in HCl acid solns., 837; surface tension at elevated temps., 961; phase equil. in system NiO–H_2O, 1021; isotopic exchange between D and hydrocarbons on Ni-silica catalysts, 1043; Ni K absorption edges of oxides of, 1144; magnetic susceptibility studies in system NiO–Al_2O_3, 1223; resolution of tris-oxalato metal complexes, 1331;

thermal effects in chemisorption of O on, 1586; hydrogenation of cyclopropane over a silica-alumina–, catalyst, 1601; H sorption and para-hydrogen conversion on evaporated, films, 1606; stability of, chelates of phthalic acid derivs. 1649
Nitric acid, melting point measurements of the system HNO_3–N_2O_4–H_2O, 104; refractive index of molten nitrate mixts., 791; thermal ignition of system $LiNO_3$–Mg, 867; consumption rate of liq. system 2-nitropropane–, 904; thermal decompn. of $NaNO_3$ and reacn. between $NaNO_2$ and O_2 1487
Nitrogen, second virial coeffs. in gaseous system N–dioxane–H_2O, 573; adsorption on pure NaCl, 824; heat capacities of multimol. layers of NF_3 adsorbed on anatase, 828; anomalous adsorptive properties of NO, 1063; production of active, from N, NO and NH_3, 1100; interacn. with a W surface, 1388, (corrn.) 1673; liq. density, vapor pressure and crit. temp. and pressure of NF_3, 1412; reacn. of active N with MeCN, 1424; kinetics of nitridation of Mg and Al 1628
Nitrogen, N^{16}, NH_3-ammonium carbonate system 48
Nitromethane, free energy of transfer from pure H_2O to H_2O satd. with 1363
Nitroparaffins, phys. properties of eight high-purity 304
N-Nitrosamines, polarographic redn. of 1028
Nitrous acid, anomalous entropy of KNO_2 1599
Nuclear magnetic resonance, chem. shift detns. by means of a concentric cylinder sample cell 1594
Nucleation, frequencies for crystallization of Se glass, 56; kinetics of, in turbulent jets 1598
Nucleic acid, light scattering study of enzymatic degradation of desoxyribose- 831
Nylon, electrolytic interacn. with aq. solns. of HCl, 692; sorption of NH_3 by 1172

OCTACOSANE, radiation chemistry of 599, (corrn.) 1673
Octadecanol, monolayers in white oil 1235
n-Octadecylamine, wetting of incomplete monomol. layers 1231
Octafluoroisobutene, infrared spectra of some reacn. products of 1372
n-Octane, urea–hydrocarbon adducts 1
Octanoic acid, C-14 labeled perfluoro-, in study of adhesion and other surface phenomena 127
2-Octanol, extraction of inorg. salts by 564
n-Octylamine, equil. between H_2SO_4 and tri- 239
Oleic acid, viscoelasticity in aq. soap solns. 779
Optical activity, exptl. investigation of models for 1656
Osmium, electrode potential of the OsO_2–OsO_4 couple, 1468; passivation of Fe by Os(VIII) oxide 1571
Osmotic coefficients, of aq. KCl solns., 501; of sulfonic acids 1102
Oxygen, quenching of flames of propane–O_2–A and propane–O_2–He mixts, 97; relationship between adsorption kinetics and the defect solid state, 201; C–O and C–H surface complexes, 495; second explosion limits of CO–O_2 mixts., 512, 1023, 1344; reacns. of NH_3 and hydrazine with O atoms and H atoms in atomic flames, 813; two-dimensional condensation of, 1162; activated adsorption on glass, 1164; estimate of the size and shape of the O_3^- ion, 1471; thermal effects in chemisorption of, on Ni 1586
Ozone, vapor phase infrared spectra of the ozonides of ethylene, propylene and isobutylene 807

PALLADIUM, adsorption on charcoal, 102; sorption of B compds. by charcoal and, 307; pressure–compn.–temp. relations in the Pd–H system 502
Palmitic acid, low temp. heat capacity of, 917; dielec. const. of hydr. Na palmitate, 919; phase transitions in Na palmitate by dielec. const. measurements, 921; isothermal dehydration of hydr. Na palmitate, 923; binary f.p. diagrams for, with a series of subsd. 2-aminopyridines 1651
Parachors, Si–Br bond 1644
Pentaborane, dielec. const. and vapor pressure of 914
Pentane, vapor pressures of perfluoro-, 504; study of distribution of configurations in short chains 1451
Permselective membranes, electroösmotic transport of H_2O across 556
Peroxysulfuric acid, equil. and formation rate 797
Phase rule, urea–hydrocarbon adducts, 1; Li–Na liq. metal system, 13; ternary systems with three separate binodal curves, 20; systems $FeCl_3$–H_2O and $FeCl_3$–HCl–H_2O, 91; Ba–Sr equil. systems, 302; solys. of Cu in solid Ge, 591; exptl. geology, 718; study of the system ZnO–CrO_3–H_2O, 939; system $CaBr_2$, CaO and H_2O, 1422; ternary system $MgCl_2$–$BaCl_2$–H_2O between 18 and 100° 1436
Phenanthrene, solv. in hydrofluorocarbons 674
1,10-Phenanthroline, acid dissocn. consts. of subsd., 1546; stability of Zn and Cd complexes with Me derivs. of 1667
Phenol, proton magnetic resonance studies of H bonding of, 1311; phys. properties of 2,4,6-tri-dimethylaminomethyl-, triacetate 1406
Phosphonic acid, protolysis consts. of *p*-subsd. Ph 787
Phosphonofluoridates, distribution between org. solvents and H_2O 1596
Phosphoric acid, condensation reacns. of alkali metal H phosphates, 863; uranyl phosphate complex formation in $HClO_4$ soln., 878; verification by chromatography of the thermal formation of Ba and Pb tetrapolyphosphates 1335
Phosphors, magnetic properties of ZnS, with Mn activator 1598
Phosphorus, crystal structure of P_2I_4, 539; infrared spectrum of biphosphine 1054
Photolysis, of diisopropyl ketone, 1315; of pentaborane vapor 1589
Phthalic acid, d. of dibutyl phthalate, 126; system cellulose tributyrate–dimethyl phthalate, 294; stability of Cu and Ni chelates of, derivs. 1649
Picolines, effect on malonic acid 1583
Platinum, adsorption of D by, catalyst, 702; electrode in some halide melts 1443
Plutonium, kinetics of reacn. between Pu^{+3} and PuO_2^{+2}, 812; reacn. between Pu(III) and O in aq. sulfate solns. 1417
Polarography, redn. of N-nitrosamines, 1028; thiourea–formaldehyde kinetic studies 1151
Polyelectrolytes, model for cross-linked 641
Porphine, vanadyl chelates of Ph_4- 934
Potassium, liq. NH_3 as a solvent, conductivity of metal-NH_3 solns., 121; vapor pressure of, 128; dissocn. of spherical ions of, salts, 160; conductance of, thiocyanate in acetone, 169; osmotic coeffs. of KCl solns., 501; study of the AgCl–KCl system, electrode potentials, 679; conductances of KCl solns., 985; elec. conductance and d. of pure molten alkali halides, 1125; prepn. of dry alkali chlorides for solutes and solvents in conductance studies, 1458; anomalous entropy of KNO_2, 1599; comparison of pycnometric and X-ray densities for NaCl–NaBr and KCl–KBr systems 1654
Potential, appearance studies, 815; of Ag–Ag halide electrodes in EtOH, 974; electrode, of the OsO_2–OsO_4 couple 1468
Propane, decompn. of hydrocarbons by silica–alumina catalysts, 59; quenching of flames of mixts. of O_2–A–, and O_2–He–, 97; consumption rate of liq. system HNO_3–2-nitro-, 904; catalytic hydrogenation of alkyl fluorides 1454
1-Propanol, conductances of electrolytes in 330
Protein, mols., swelling in soln., 358; ultracentrifugal behavior of, in non-aq. solvents, 1190; electrophoresis of polypeptidyl, 1200; mol. kinetic and chem. properties of wool cortical cell fractions, 1208; swelling of, mols. in soln. 1593
Proton, magnetic resonance studies of H bonding of phenol 1311
Proton relaxation, on catalytic solids 452
Pyridine, mechanism of formation of tris-(2,2′-dipyridyl)–Fe(II) complex, 87; elec. moments of, derivs. 125; physico-chem. study of AcOH–, system, 777; binary f.p. diagram for 2-amino-, 963; dipole direction and relaxation time in, 1354; binary f.p. diagrams for palmitic acid with a series of subsd. 2-amino-, 1651; stability of Zn and Cd complexes with Me derivs. of 2,2′-bi- 1667

RADIATION chemistry, of hydrocarbon polymers, 599, (corrn.) 1673

Raffinose, concn. dependence of diffusion coeff. of 1464

X-Ray, small angle, scattering by $Al(OH)_3$ gel 1580

Reaction velocity, decompn. of hydrocarbons by silica–alumina catalysts, 59; relationship between adsorption kinetics and the defect solid state, 201; of metal complexes of ethylenediaminetetraacetic acid, 251; of luminescence quenching in liq. scintillators, 267; redn. of Hg^{++} and Hg_2^{++} with mol. H, 285; of CS_2–NO reacn. and mechanism of light emission in the explosive reacn., 379; homogeneous pptn. of $BaSO_4$, 389; reacn. of CO_2 with C, 480; of the steam–C reacn., 486; between Np(IV) and Np(VI) in mixed solvent, 701; exchange and isomn. of *trans*-ethylene-d_2 on Ni, 724; exchange and isomn. of deuteroethylenes on Ni, 730; kinetic study of CH_3Cl combustion, 874; equil. and kinetics of detergent adsorption, 890; approximations in kinetics of consecutive reacns., 966; thermal decompn. of phenyltrimethylammonium hydroxide, 1004; linear decompn. rates of NH_4Cl, 1095; of EtOH with *p*-nitrobenzoyl chloride in nitrobenzene, 1142; mechanism of emulsion polymn. of styrene, 1250; detg. rate equations with concn. of the reactant unknown, 1332; decompn. of malonic acid in aromatic amines, 1340; kinetics of solid → solid reacns., 1347; schematic method of deriving rate laws for enzyme-catalyzed reacns., 1375; kinetic consequences of certain enzyme catalysis mechanisms, 1378; oxidn. of As_2O_3, 1383; kinetic study of trifluoroacetonitrile–butadiene cyclization, 1430; of thermal decompn. of $NaNO_3$, 1487; of hydrogenation of cyclopropane over a Ni-silica–alumina catalyst, 1601; of nitridation of Mg and Al 1628

Refractive index, of colloidal sols, 562; of molten nitrate mixts 791

Resin, ion exchange, in concd. solns., 36; self-diffusion of Na^+ in a cation-exchange, 237; studies on, 263; cation equil. studies in MeOH, 513; thermodynamic calcn. of cation exchange selectivities, 521; cation-exchange equil. involving some divalent ions, 530; prepn. of sulfostyrene cation exchange, 533; membranes, ion transfer rates 750

Rhenium, crystal structure of K_2ReI_6, 19; inhibition of corrosion by the perrhenate ion 32

Ribonuclease, effect of charge and ionic strength on viscosity of 1204

SCANDIUM, crystal structure of γ-ScOOH 273

Scintillators, kinetics of luminescence quenching in liq 267

Sebacic acid, light scattering behavior of 3-dimensional network gels 1512

Sedimentation constant, variation of, with field and temp. for naturally occurring polyelectrolytes, 506; ultracentrifugal characterization by measurement of activity, 623; ultracentrifugal characterization by direct measurement of activity 630

Selenium, glass, nucleation frequencies for crystallization of 56

Serum albumin, ultracentrifugal characterization by direct measurement of activity, 630; Gouy diffusion studies of bovine, 1066; diffusion of isoionic, salt-free bovine, 1342; hydrodynamic and thermodynamic properties of bovine, 1633; binding of org. anions by 1663

Silica, chemisorption of $Ca(OH)_2$ by, 325; hydrothermal reacns. between $Ca(OH)_2$ and amorphous, 397; effect of alkali metal ions on activity of cracking catalysts, 422; hydration of particles of colloidal, in aq. soln., 955; streaming potential studies on quartz, 981; adsorption of complex metal–ammines and other complex ions of Zn, Cu, Co, Ni and Ag on, gel, 1008; adsorbed H_2O on, gel by nuclear resonance techniques, 1157; surface chemistry of silicate minerals, 1181; hydrothermal reacns. between $Ca(OH)_2$ and amorphous 1559

Silicic acid, hydration of tricalcium silicate in a ball mill, 112; hydration of tricalcium silicate in paste form, 116; heat of decompn. of tricalcium silicate, 771; effect of *p*H on polymn. of, 1007; elec. conductance in Pb silicates 1321

Silicon, adsorption of gases on, surface, 353; question of a phase transition in, 508; Br–, and C–, bond parachors and Br–, bond refraction 1644

Siloxane, surface activity at org. liquid/air interface . . 416

Silver, thermodynamics of liq. solns. in the Cu–Ag system, 108; basicity of the, bromide complex ion, 255; crystallization of metallic films, 277; activation of mol. H by, salts, 280; heats of soln. in liq. Tl, Pb and Bi, 446; catalytic oxidn. of ethylene to oxide over, crystals, 666; study of AgCl–KCl system, electrode potentials, 679; heat of formation of solid and liq. alloys in the systems Ag–Cd, Ag–In and Ag–Sb, 846; potential of Ag–Ag halide electrodes in EtOH, 974; H overpotential on, in NaOH solns., 1290; the Pt electrode in halide melts, 1443; negative activity limit of stability and coagulation values of, halides 1473

Soap solutions, phys.-chem. behavior of oil-dispersible, ... 1108, 1114

Sodium, Li–Na liq. metal system, 13; liq. NH_3 as a solvent, conductivity of metal-NH_3 solns., 121; complex ions in molten $NaNO_3$, 172; activity coeffs. of NaSCN, 184; viscosity and d. of NaSCN, 186; elec. conductance of, NaSCN solns., 189; self-diffusion of Na^+ in cation-exchange resin, 237; thermal decompn. of $NaNO_3$, 256; transport in isolated frog skin, 404; ion-exchange membranes, ion transfer rates, 750; crystal structure of, amide, 821; conductances of aq. NaCl solns., 985; heats of formation of Na_2O_2 and NaO_2, 1333; a b.p. method for detn. of vapor pressures of molten, 1413; comparison of pycnometric and X-ray densities for NaCl–NaBr and KCl–KBr systems, 1654; system Na_2SO_4–Na_2MoO_4–H_2O 1662

Solute, vols. in soln 7

Sonic studies, amplitude of vibration of aerosol droplets, 989; measurement of bound H_2O by ultrasonic interferometer, 1049; detn. of thermodynamic properties of liq. 3-methylthiophene by the ultrasonic method 1147

Sorption, of gases by solid polymers, 1172; studies on American coals 1548

Spectra, infrared, of reacn. products of octafluoroisobutene, 1372; frequency shift, half width and intensity measurements of H bonding systems 1615

Spherical particles, eq. of motion of, in a centrifugal field 1476

Stability constants, of ionic complexes 180

Starch, viscous behavior of carboxymethyl polysaccharides 883

Statistical mechanics, of kinetics of solid → solid reacns 1347

Steady states, a minimum principle for non-equil 1611

Stearic acid, rate of evaporation of H_2O through, 348; colloidal structure in Li stearate greases, 439; critical micelle concns. of α-sulfonated fatty acids and their esters, 899; binary f.p. diagram for 2-aminopyridine, 963; alkali and alkaline earth phenylstearates in benzene, 1108; colloid structure in dil. arylstearate–benzene systems, 1114; solv. of tristearin in org. solvents, 1265; effects of spreading solvent on monolayers as detd. by pressure–area isotherms 1533

Strontium, decompn. of hyponitrites of, 192; Ba–Sr equil. system 302

Styrene, interacns. in polymer solns. obsd. by equilibrations across membranes, 123; sorption of vapors by high polymers, 425; prepn. of sulfo-, cation exchange resins, 533; mol. assocn. in methacrylic acid-, copolymers, 782; mechanism of emulsion polymn. of, 1250; oxidative degradation of, polymers 1306

Sublimation pressure, of $TiCl_3$ 314

Sucrose, conductances of simple electrolytes in aq., solns 217

Sulfamic acid, dielec. increments as supporting evidence for dipolar structure of 1579

Sulfate ions, exchange between adsorbed and dissolved 374

Sulfonic acids, osmotic and activity coeffs. of 1102

Sulfostyrenes, prepn. of, cation exchange resins 533

Sulfoxide, conductance behavior of some uni-univalent electrolytes in dimethyl 1433

Sulfur compounds, purification and properties of org.,

549; refractive index of S hydrosols, 562; luminescence properties of Zn–sulfo-telluride, phosphors, 604; formation consts. of some metal derivs. of *S*-alkyl carboxylic acids 1427
Sulfur dioxide, ionization and dissocn. equil. in 160, 164
Sulfuric acid, equil. between tri-*n*-octylamine and, 239; equil. between di-*n*-decylamine and 943
Surface, activity at org. liquid/air interface, 416; contortional energy requirement in the spreading of large drops, 952; trypsin monolayers at H_2O–air interface, 1193; wetting of incomplete monomol. layers, 1231; monolayers in equil. with lenses of oil on H_2O 1235
Surface tension, at elevated temps., 961; detn. of equil. const. by, measurements 1258

TECHNETIUM, reversibility of the pertechnetate ion inhibiting mechanism, 28; occurrence on the earth's crust, 707; inhibition of corrosion by the pertechnetate ion 1037
Teflon, adsorption and heat of wetting of 1345
Tellurium, luminescence properties of N sulfo-telluride phosphors 604
Tetradecanoic acid, monolayers in white oil 1235
Thallium, heats of soln. of Cu, Ag and Au in liq., 446; Fe(II)–Tl(III) reacn. at high chloride concn., 1015; thiocyanate complexes in soln., 1493; stability of Tl(I) citrate complex, 1623; reacn. between Hg(I) and Tl(III) 1661
Thermal diffusion, sepn. of org. solns. by 1524
Thermodynamic probability, proof that extremum of, is a maximum 536
Thiocyanate, complexes of Pb and Tl in soln 1493
Thiophene, detn. of thermodynamic properties of liq. 3-Me, by the ultrasonic method 1147
Thiourea, –formaldehyde kinetic studies, polarographic 1151
Thorium, solys. of metal nitrate salts in tri-*n*-Bu phosphate 1145
Tin, thermal decompn. of SnH_4, 610; calorimetric study of binary and ternary liq. alloys rich in, 842; conductances of $SbBr_3$ and $SnCl_2$ in dimethylformamide on addn. of piperidine 1470
Titanium, thermodynamics of, chlorides, 309; heat of formation of $TiCl_2$, 311; sublimation pressure of $TiCl_3$, 314; disproportionation of, trichlorides, 316; soly. of Cl in $TiCl_4$, 374; ionic character of transition metal hydrides, 510; measurement of optical absorbancy of $TiCl_4(g)$ in ultraviolet region 622
TNT, f. p. diagrams of some systems containing 1136
Toluene, flow properties of Al dilaurate–, gels 270
Toluenesulfonic acid, salting in of subsd. benzenes by large ion salts 1131
Transference number, measurements in pure fused salts, 620; of HIO_3, 976; in molten salts 1381
Trioxane, dipole direction and relaxation time in 1354
Triphenylchloromethane, conductance of alkyl and aryl derivs. of 164
Tritium, studies of recoil, labeling reacn 1137
Trypsin, monolayers at H_2O–air interface 1193
Tungsten, phys. properties of WF_6, 505; "β-tungsten," as a product of oxide redn., 1148; interacn. of N with a surface, 1388, (corrn.) 1673

ULTRACENTRIFUGE, characterization by measurement of activity, 623, 630; behavior of proteins in non-aq. solvents, 1190; operating and comparating procedures in anal 1211
Unit cell, dimensions of K_2ReI_6 19
Uranium, phys. properties of aq. uranyl sulfate, 413; ionic character of transition metal hydrides, 510; soly. of U(IV) orthophosphates in $HClO_4$ solns., 588; redn. of U(VI) by Fe(II) in phosphoric acid soln., 805; uranyl phosphate complex formation in $HClO_4$ soln., 878; liq.–liq. solys. of system UF_6–HF, (corrn.) 1671
Urea, –hydrocarbon adducts, 1; conductance and phys. properties of, solns 775

VANADIUM, vanadyl chelates of tetraphenylporphine 934
Vapor pressure, isopiestic studies of aq. dicarboxylic acid solns., 41; of Et *trans*-β-(2-furyl)-acrylate, 252; of perfluoropentanes, 504; in the system dioxane–H_2O, 573; of diborane, 911; of pentaborane, 914; a b.p. method for detn. of, of molten salts, 1413; of HCl above non-aq. solns 1461
Vinyl acetate, interacns. in polymer solns. obsd. by equilibrations across membranes 123
Vinyl compounds, high temp. calorimeter and hydrogenation of Me, Et and, 492; viscosity studies of poly-4-vinylpyridine derivs. in aq. KBr solns., 577; polyvinyl alcohol, and its partially subsd. acetates, 1049; viscosity of dil. polyvinyl chloride soln 1202
Viscoelasticity, in aq. soap solns 779
Viscosity, of NaSCN, $NaClO_4$ and NaI, 186; of aq. solns. of bovine serum albumin, 225; of alfin polyisoprene, 431; studies of poly-4-vinylpyridine derivs. in aq. KBr solns., 577; of gas mixts. CH_4–CO_2 and ethylene–A, 789; temp. dependence of, of liqs., 817; viscous behavior of carboxymethyl polysaccharides, 883; of benzene from 90° to critical temp., 1025; of dil. polyvinyl chloride soln., 1202; effect of charge and ionic strength on, of ribonuclease 1204
Volumes, of solute in soln 7

WATER, rate of evaporation through monolayers of esters, acids and alcs., 348; electroösmotic transport across permselective membranes, 556; adsorption on glass at high relative pressures, 793; adsorbed H_2O on silica gel by nuclear resonance techniques 1157
Wool cortical cell fractions, mol. kinetic and chem. properties of 1208

XENON, vapor pressures of 1119
Xylene, dielec. properties of solid nitrodichloro-*o*- 1584

YTTERBIUM, heats of combustion of, 1457; solns. of Eu and, metals in liq. NH_3 1590

ZINC, crystallization of metallic films, 277; elec. conductivity and catalytic activity of ZnO, 559; luminescence properties of Zn-interchalcogenides, 604; chemisorption of H on ZnO, 833; phase rule study of the system ZnO–CrO_3–H_2O, 939; adsorption of complex metal–ammines and other complex ions of, on silica gel, 1008; photochem. properties of ZnO, 1328; magnetic properties of ZnS phosphors with Mn activator, 1598; stability of, complexes with Me derivs. of 1,10-phenanthroline and 2,2′-bipyridine 1667

Literature Resources for Chemical Process Industries

Designed To Help Both The *New* And The *Experienced* Searcher Of Literature Find What He Wants

Discusses various information sources with 13 articles on market research, 7 on resins and plastics, 6 on textile chemistry, 10 on the food industry, 10 on petroleum, and 13 on general topics, plus 34 pages of index.

order from:

Special Publications Department
American Chemical Society
1155 Sixteenth Street, N.W.
Washington 6, D.C.

Number 10 in
Advances in Chemistry Series

edited by the staff of
Industrial and Engineering Chemistry

582 pages—paper bound—$6.50 per copy

CHEMICAL NOMENCLATURE

Number eight of the Advances in Chemistry Series
Edited by the staff of *Industrial and Engineering Chemistry*

A collection of papers comprising the Symposium on Chemical Nomenclature, presented before the Division of Chemical Literature at the 120th meeting—Diamond Jubilee—of the American Chemical Society, New York, N. Y., September 1951

Paper bound $2.50

Published August 15, 1953, by
AMERICAN CHEMICAL SOCIETY
1155 Sixteenth Street, N.W.
Washington, D. C.

CONTENTS

Introduction 1
Letter of Greeting 3
Some General Principles of Inorganic Chemical Nomenclature 5
Nomenclature of Coordination Compounds and Its Relation to General Inorganic Nomenclature 9
Problems of an International Chemical Nomenclature 38
Chemical Nomenclature in Britain Today 49
Chemical Nomenclature in the United States 55
Basic Features of Nomenclature in Organic Chemistry 65
Organic Chemical Nomenclature, Past, Present, and Future 75
Work of Commission on Nomenclature of Biological Chemistry 83
Nomenclature in Industry 95
Development of Chemical Symbols and Their Relation to Nomenclature 99
The Role of Terminology in Indexing, Classifying, and Coding 106

Collectors' Items
Now Available at Special Reduced Rates

Chemistry—
Key To Better Living

and

Seventy-Five Eventful Years

by Charles Edward Browne and Mary Elvira Weeks

These two volumes—unique in their contribution to chemical literature—are now available for only $7.50 when purchased together.

CHEMISTRY—KEY TO BETTER LIVING is a profusely illustrated history of chemical developments in the United States. It includes accounts of the activities of the Divisions of the Society and their influence on the progress of science and industry.

SEVENTY-FIVE EVENTFUL YEARS is the official history of the American Chemical Society. This book traces the growth of the Society, describes its manifold activities, relates the part it has played in affairs of national importance, and culminates with a description of the Diamond Jubilee.

Chemistry—Key To Better Living	$4.00
Seventy-Five Eventful Years	5.00
Chemistry—Key To Better Living and Seventy-Five Eventful Years	$7.50

order from:

Special Publications Department
American Chemical Society
1155 Sixteenth Street, N.W.
Washington 6, D.C.